

**DEVELOPMENT AND APPLICATION OF DISJUNCT
EDDY COVARIANCE TECHNIQUES FOR THE
MEASUREMENT AND INTERPRETATION OF FLUXES
OF VOLATILE ORGANIC COMPOUNDS FROM URBAN
AND RURAL CANOPIES**

Ben Langford BSc. (Hons.)

A thesis submitted for the degree of
Doctor of Philosophy,
Lancaster University.

Faculty of Science
Environmental Science Department
Lancaster University

May 2008

ProQuest Number: 11003731

All rights reserved

INFORMATION TO ALL USERS

The quality of this reproduction is dependent upon the quality of the copy submitted.

In the unlikely event that the author did not send a complete manuscript and there are missing pages, these will be noted. Also, if material had to be removed, a note will indicate the deletion.



ProQuest 11003731

Published by ProQuest LLC (2018). Copyright of the Dissertation is held by the Author.

All rights reserved.

This work is protected against unauthorized copying under Title 17, United States Code
Microform Edition © ProQuest LLC.

ProQuest LLC.
789 East Eisenhower Parkway
P.O. Box 1346
Ann Arbor, MI 48106 – 1346

Acknowledgements

I offer my sincere gratitude to my supervisors here at Lancaster University, Professor Nick Hewitt and Dr Brian Davison without whose support, guidance and patience none of this work would have been possible.

I would also like to pay special tribute to Dr Eiko Nemitz (CEH, Edinburgh), not only for his supervision, but for sharing his knowledge and enthusiasm for the subject and for offering up his valuable time to answer my many questions.

I offer my gratitude to Dr Malcolm Possell and Dr Mick Wilkinson for their continued support and advice, as well as to Annette Ryan and Jullada Laothawornkitkul who provided a welcome distraction whenever needed.

I also thank my colleagues at CEH Edinburgh, Dr Gavin Phillips, Dr Daniela Famulari, Dr Claire Campbell, Pawel Misztal and Emily House without whose sense of fun, the days spent in the field would have felt much longer.

I would like to acknowledge the technical skills of both Geoff Johnson and Ian Edmondson which were invaluable to this project.

I am indebted to the Natural Environmental Research Council for financing this studentship and supplying funds for conferences and research meetings.

Finally, for her patience, support, understanding and brew making skills, I owe my partner, Jen, a huge debt of gratitude.

Development and application of disjunct eddy covariance techniques for the measurement and interpretation of fluxes of volatile organic compound from urban and rural canopies

Ben Langford BSc. (Hons.)

This thesis is submitted for the degree of Doctor of Philosophy and is the work of the above author. It has not been submitted for a higher degree elsewhere.

May 2008

Abstract

Two disjunct eddy covariance systems for the measurement of volatile organic compound (VOC) fluxes were developed. The first, disjunct eddy covariance (DEC), was validated against the standard eddy covariance (EC) technique, in a study of CO₂ and H₂O fluxes from a grassland field (Easter Bush, Edinburgh, Scotland). The comparison convincingly showed fluxes measured by the DEC technique to be comparable to those measured using the EC technique. A second, simplified approach, virtual disjunct eddy covariance (vDEC), was developed and compared against standard DEC during the CityFlux project, where measurements of VOC fluxes were made from Portland Tower in Manchester. Averaged daily fluxes measured by the vDEC system typically ranged between 19 and 90 $\mu\text{g m}^{-2} \text{h}^{-1}$ for individual VOC species and were comparable to those measured by the DEC system, but were typically 19% higher than the latter. The discrepancies between the two methods were thought to relate to both the reduced response time of the DEC system which attenuated higher frequency flux contributions

and the high level of noise in the covariance function which may have led to a systematic overestimation of the flux. The vDEC technique was subsequently deployed on the Telecom Tower in central London to give very detailed flux information on seven VOC species. Individual average fluxes ranged between 5 and 100 $\mu\text{g m}^{-2} \text{h}^{-1}$ and were well correlated with traffic density. Fluxes of benzene were extrapolated to give an annual emission estimate for the city, which was found to be 1.8 times lower than that suggested by the National Atmospheric Emission Inventory. Finally, two vDEC systems, one using a high sensitivity (HS) proton transfer reaction mass spectrometer (PTR-MS) and the other a standard model (Std), were used alongside each other to measure biogenic VOC fluxes from macchia vegetation at the Castelporziano nature reserve near Rome, Italy. The two systems compared well, although the HS system appeared to give fluxes with greater amplitude than the Std model. This highlighted the importance of the allocation of correct lag times when using vDEC, particularly at night. Fluxes of isoprene and monoterpenes were compared with the Guenther algorithm of 1995 and showed excellent agreement between the modelled and measured values.

The results presented in this study have convincingly demonstrated the capacity of the DEC and vDEC techniques to give very detailed VOC flux information over a range of non-ideal canopies, which can be used to both validate and constrain “bottom-up” style emission inventories.

Table of Contents

Acknowledgements	ii
Abstract	iii
Table of contents	v
List of figures	x
List of tables	vi
Nomenclature	xiii

Chapter I

I. Introduction	1
1.1 Biosphere /Atmosphere interactions	1
1.2 Bottom up approach to quantifying trace gas exchange ..	4
1.3 Top up approach to quantifying trace gas exchange	7
1.4 Atmospheric transport processes	8
1.5 The conservation equation	9
1.6 Enclosure techniques (non aerodynamic technique)	11
1.7 Micrometeorological approaches (aerodynamic)	13
1.8 Eddy Covariance	16
<i>1.8.1 Theoretical requirements</i>	18
<i>1.8.2 Coordinate rotation</i>	18
<i>1.8.3 Sensor requirements</i>	19
1.9 Eddy Accumulation	21
1.10 Relaxed Eddy Accumulation	22
1.11 Disjunct Eddy Covariance	24
1.12 Aims and objectives	27

Chapter II

II. Methods	29
2.1 The proton transfer reaction – mass spectrometer	29
<i>2.1.1 Mass detection</i>	32
<i>2.1.2 Instrument background</i>	33
<i>2.1.3 The PTR-MS control software</i>	37
<i>2.1.4 Maintaining optimum SEM operating voltage</i>	39
2.2 Disjunct eddy covariance – concept and design	40
<i>2.2.1 Theoretical testing of DEC concept</i>	41
2.3 The disjunct flux sampler	46
2.4 Laboratory testing	47
<i>2.4.1 Effects of changing drift tube pressure</i>	49

2.4.2	<i>Correction for sample carryover</i>	51
2.5	Field testing – evaluation against EC	52
2.5.1	<i>Field experiment and setup</i>	53
2.5.2	<i>Disjunct flux sampler – setup</i>	54
2.5.3	<i>Eddy covariance – setup</i>	56
2.5.4	<i>Results and discussion</i>	56
2.5.5	<i>Concentrations</i>	56
2.5.6	<i>Comparison of sensible heat fluxes</i>	57
2.5.7	<i>Comparison of CO₂ & H₂O fluxes</i>	60
2.5.8	<i>Potential experiment improvements</i>	61
2.5.9	<i>Conclusions</i>	62
2.6	Virtual disjunct eddy covariance (vDEC)	63
2.7	Post processing of data	66

Chapter III

III. Mixing ratios and eddy covariance flux measurements of volatile organic compounds from an urban canopy (Manchester, U.K.)..... 70

	Abstract	72
3.1	Introduction	76
3.2	Methods	76
3.2.1	<i>Measurement site and general setup</i>	76
3.2.2	<i>The proton transfer reaction mass spectrometer (PTR-MS)</i> . 78	
3.2.3	<i>Flux measurements</i>	79
3.2.3.1	<i>Virtual disjunct eddy covariance sampling system (vDEC)</i> ..	80
3.2.3.2	<i>Disjunct flux sampling system (DFS)</i>	81
3.2.3.3	<i>Flux calculations</i>	83
3.3	Results & discussion	86
3.3.1	<i>VOC concentrations</i>	86
3.3.2	<i>VOC fluxes</i>	96
3.3.3	<i>Comparison of measured benzene fluxes with NAEI estimates</i>	101
3.4	Conclusions	105
3.5	Acknowledgements	106

Chapter IV

IV.	Emission estimates and concentrations of volatile organic compounds from central London based on eddy covariance flux measurements.....	107
	Abstract.....	109
4.1	Introduction.....	110
4.2	Experimental.....	112
4.2.1	<i>Measurement site.....</i>	<i>112</i>
4.2.2	<i>VOC sampling.....</i>	<i>114</i>
4.2.3	<i>Data acquisition.....</i>	<i>115</i>
4.2.4	<i>Calculation of fluxes.....</i>	<i>116</i>
4.2.5	<i>Quality assessment of fluxes.....</i>	<i>117</i>
4.2.6	<i>NAEI emission estimates.....</i>	<i>119</i>
4.2.7	<i>Calculation of the flux footprint.....</i>	<i>121</i>
4.3	Results and discussion.....	121
4.3.1	<i>Concentration measurements.....</i>	<i>121</i>
4.3.1.1	<i>Trends in VOC concentration.....</i>	<i>121</i>
4.3.1.2	<i>Comparison with GC-MS and national monitoring network data.....</i>	<i>126</i>
4.3.1.3	<i>Temporal trends in VOC concentrations in London from 2001-2006.....</i>	<i>128</i>
4.3.2	<i>VOC fluxes.....</i>	<i>132</i>
4.3.2.1	<i>Trends in VOC fluxes.....</i>	<i>132</i>
4.3.3	<i>Comparison of VOC and CO concentrations.....</i>	<i>138</i>
4.3.4	<i>Comparison of VOC and CO fluxes.....</i>	<i>141</i>
4.3.5	<i>Ratios of CO to VOC – Concentrations and fluxes.....</i>	<i>142</i>
4.3.6	<i>VOC flux dependence on traffic activity.....</i>	<i>144</i>
4.3.7	<i>Comparison of measured fluxes with NAEI emission estimates.....</i>	<i>147</i>
4.5	Conclusions.....	150
4.6	Acknowledgements.....	150

Chapter V

v.	Mixing ratios and fluxes of volatile organic compounds above Mediterranean macchia vegetation (Castelporziano, Italy).....	152
5.1	Introduction.....	153
5.2	Method.....	155
5.2.1	<i>Site description.....</i>	<i>155</i>
5.2.2	<i>Climate and meteorology.....</i>	<i>156</i>
5.2.3	<i>Instrumentation.....</i>	<i>157</i>
5.2.4	<i>VOC sampling.....</i>	<i>158</i>

5.2.5	<i>Calibration</i>	160
5.2.6	<i>Data logging</i>	161
5.2.7	<i>Flux calculation</i>	161
5.2.8	<i>Post-processing of data</i>	162
5.2.9	<i>Modelling of isoprene and monoterpene fluxes</i>	162
5.3	Results and discussion	164
5.3.1	<i>Summary of weather and meteorology</i>	164
5.3.2	<i>Measurements of VOC concentrations</i>	165
5.3.3	<i>Fluxes of VOCs from the macchia</i>	168
5.3.4	<i>Comparison of VOC fluxes</i>	173
5.3.5	<i>Wind sector dependence – concentrations and fluxes</i>	175
5.3.6	<i>Comparison of measured and modelled fluxes</i>	178
5.4	Conclusions	181

Chapter VI

VI.	Analysis of uncertainty and errors	183
6.1	Systematic and random errors	183
6.2	Potential systematic errors in the DEC systems	184
6.2.1	<i>Transmission numbers and calibration</i>	184
6.2.2	<i>Disjunct sampling intervals and attenuation</i>	186
6.2.3	<i>Attenuation of low frequency flux contributions</i>	188
6.3	Potential random errors in the DEC systems	190
6.4	Measurement precision and detection limits	194
6.5	Measurement site and the effect of wake turbulence	196
6.6	Errors due to geophysical variability	203
6.7	The Representativeness of flux measurements made over urban canopies	204
6.8	Conclusions	205

Chapter VII

VII.	Discussion and conclusions	207
7.	Discussion and conclusions	207
7.1	Disjunct eddy covariance	207
7.2	Virtual disjunct eddy covariance	209
7.3	System improvements	210
7.3.1	<i>Compound identification</i>	210
7.3.2	<i>Online calibration</i>	211
7.3.3	<i>Padding of disjunct data</i>	212
7.3.4	<i>Improvements to logging software</i>	215
7.4	“Top down” versus “Bottom up” emission inventory approach	216
7.5	Future work	220

7.6	Final remarks.....	219
	References.....	221
	Appendix I.....	235
	Appendix II.....	240
	Appendix III.....	246
	Appendix IV.....	247

Tables and Figures

Figure 1.1	Role of VOCs in the global climate system.....	3
Figure 1.2	Diagram of planetary boundary structure and transport processes.....	9
Figure 1.3	Schematic of wake effects in stable and unstable atmospheric conditions.....	15
Figure 1.4	Cartesian coordinate frame and tilt errors.....	19
Figure 1.5	Graph of a continuous (EC) time series of temperature and vertical wind speed, and the concept of disjunct sampling.....	25
Figure 2.1	Schematic of PTR-MS instrument.....	31
Figure 2.2	Graph of PTR-MS background measured using a charcoal filter.....	34
Figure 2.3	Graph of PTR-MS background measured using a silica gel filter.....	35
Figure 2.4	Graph of PTR-MS background measured using a drierite filter.....	35
Figure 2.5	Graph of PTR-MS background measured using a molecular sieve.....	36
Figure 2.6	Graph of PTR-MS background measured using a platinum catalyst.....	37
Figure 2.7	Screen shot of LabVIEW programme used to calculate optimum SEM voltages.....	40
Figure 2.8	Graph illustrating the agreement between EC heat fluxes and simulated DEC heat fluxes.....	43
Figure 2.9	Graph showing the increase in standard deviation with longer DEC sampling intervals.....	43
Figure 2.10	Graph showing the bias between EC and DEC calculated fluxes at differing sampling times at a height of 5 m.....	45
Figure 2.11	Graph showing the bias between EC and DEC calculated fluxes at differing sampling times at a height of 80 m.....	46
Figure 2.12	Schematic of the disjunct flux sampler and experimental setup.....	48
Figure 2.13	Channel 2 isoprene concentrations after reorientation of valve 6.....	49
Figure 2.14	Graph illustrating the effect of the DFS on PTR-MS drift tube pressures.....	50
Figure 2.15	Fluctuations in E/N ratio caused by backpressure in ISRs.....	51
Figure 2.16	Diagram of the Easter Bush field measurement site.....	54
Figure 2.17	Schematic of the DFS setup at Easter Bush.....	55
Figure 2.18	CO_2 and H_2O concentrations measured by the EC and DEC systems.....	58
Figure 2.19	Diurnal profile of CO_2 and H_2O fluxes measured by the EC and DEC techniques.....	61
Figure 2.20	Cross correlation function used to realign PTR-MS data with the corresponding vertical wind velocities.....	65
Figure 3.1	Representation of PTR-MS measurement sequence and duty cycles used at Portland tower.....	80
Figure 3.2	Schematic of experimental setup used at Portland tower.....	82
Figure 3.3	Graph showing average VOC concentrations, wind direction and temperatures.....	88
Figure 3.4	Scatter plots of VOC concentrations measured at Portland tower....	90
Figure 3.5	Plot of isoprene and benzene concentrations measured at Portland tower in relation to temperature.....	92
Figure 3.6	Graph showing the temperature-dependant fraction of isoprene measured at Portland tower.....	93

Figure 3.7	Graph showing the ratio of benzene to toluene concentrations and average wind speeds.....	95
Figure 3.8	Averaged diurnal flux profiles of VOCs measured at Portland tower using the DEC and vDEC techniques.....	97
Figure 3.9	Predicted one-dimensional flux footprint from Portland tower for a range of u^* values.....	102
Figure 3.10	Analysis of benzene wind sector dependence.....	103
Figure 4.1	NAEI emission estimates for central London.....	120
Figure 4.2	Average diurnal concentration profiles for 8 VOCs measured above central London.....	122
Figure 4.3	Comparison of VOC mixing ratios measured by the PTR-MS and GC-MS at the Telecom Tower.....	127
Figure 4.4	Graph showing the seasonality in the ratio of benzene to toluene over a five year period.....	130
Figure 4.5	Plot showing the temperature dependency of isoprene, toluene and isopentane concentrations measured in central London.....	131
Figure 4.6	Time series of VOC and CO fluxes measured at the BT tower between the (01/10/06 – 30/10/06).....	133
Figure 4.7	Average diurnal profiles of VOC fluxes measured above central London.....	134
Figure 4.8	Graph of acetone fluxes, traffic counts and mixed layer depth.....	136
Figure 4.9	Time series of VOC concentrations measured above central London.....	140
Figure 4.10	Typical daily ratios of CO to VOC concentrations and fluxes measured above central London from the BT tower.....	143
Figure 4.11	Correlations between traffic activity and VOC fluxes.....	146
Figure 4.12	Relationship between traffic density and average vehicle speed.....	147
Figure 4.13	Annual VOC emission estimates for central London based on flux measurements.....	149
Figure 5.1	Sketch of the terrain topography at the Castelporziano nature reserve.....	156
Figure 5.2	Instrument setup at the Castelporziano field site.....	159
Figure 5.3	VOC concentrations measured by the HS and Std PTR-MS instruments at the Castelporziano field site.....	166
Figure 5.4	Regressions analysis of VOCs measured by the HS and Std PTR-MS instruments.....	168
Figure 5.5	Time series of measured VOC fluxes at the Castelporziano field site.....	170
Figure 5.6	Average diurnal flux profiles.....	172
Figure 5.6	Comparison of isoprene and methanol fluxes measured by two different PTR-MS instruments.....	174
Figure 5.7	Wind roses of fluxes and concentrations measured at the Castelporziano field site.....	176
Figure 5.8	Wind rose showing the advection of anthropogenic compounds over the nature reserve at night.....	178
Figure 5.9	Comparison of measured and modelled isoprene and monoterpene fluxes.....	179
Figure 5.10	Plots showing the temperature dependence of BVOC emissions from maquis vegetation.....	181

Figure 6.1	Potential error incurred at the Telecom Tower due to the choice of averaging period.....	190
Figure 6.2	Determination of lag times and measurement precision.....	195
Figure 6.3	Satellite image of Manchester city centre and Portland Tower rooftop.....	197
Figure 6.4	Satellite image of London city centre and the Telecom Tower rooftop.....	198
Figure 6.5	Rotation angles as a function of wind direction during the CityFlux and REPARTEE measurent campaigns.....	199
Figure 6.6	Quality assessment of measured fluxes based on the integral turbulence statistics.....	202
Figure 7.1	Graph showing various methods for padding disjunct data sets.....	213
Figure 7.2	Underestimation of fluxes due to the attenuation of high frequency flux contributions by the padding methods.....	214

* * *

Table 2.1	Comparison of sensible heat fluxes calculated by the EC and DEC flux measurement techniques.....	42
Table 3.1	Summary of VOC concentrations and fluxes measured at Portland Tower.....	87
Table 3.2	List of biogenic and anthropogenic sources including atmospheric lifetimes.....	91
Table 3.3	Estimates of VOC emissions from Manchester city centre based of micrometeorological flux measurements.....	104
Table 4.1	List of VOC flux measurements above urban canopies.....	137
Table 4.2	List of typical VOC/CO ratios during the REPARTEE campaign....	144
Table 5.1	Summary of VOC fluxes and concentrations measured at the Castelporziano field site.....	167
Table 6.1	Uncertainty in the flux measurements due to disjunct sampling intervals and flux attenuation.....	187
Table 6.2	Uncertainty in individual PTR-MS count rates due to counting statistic.....	192
Table 6.3	Parameters used for the analysis of turbulence statistics.....	201
Table 6.4	Uncertainty in flux measurements due to geophysical variability.....	204

Nomenclature

LATIN ALPHABET

C_p	Specific heat capacity of air	1246 J Kg ⁻¹ K ⁻¹
F_χ	Flux	μg m ⁻² s ⁻¹
g	Acceleration due to gravity	m s ⁻²
h	Tree or boundary layer height	m
H	Sensible heat flux	W m ⁻²
LE	Latent heat flux	W m ⁻²
t	Time	s
T	Temperature	°C, K
T_{sonic}	Temperature measured by sonic anemometer	°C
T_L	Leaf temperature	°C, K
T_s	Leaf temperature at standard conditions	303 K
T_{std}	Absolute zero	273.15 K
U	Total wind speed	m s ⁻¹
u	Horizontal (longitudinal) wind velocity component	m s ⁻¹
u^*	Friction velocity	m s ⁻¹
v	Horizontal (lateral) wind velocity component	m s ⁻¹
w	Vertical wind component	m s ⁻¹
WD	Wind direction	°
WS	Wind speed	m s ⁻¹
z	Height above surface	m
z_0	Roughness length	m
z_s	Surface height	m
z_m	Measurements height	m
C_{L1}	Empirically derived constant	1.066
C_{T1}	Empirically derived constant	95,000 J mol ⁻¹
C_{T2}	Empirically derived constant	230,000 J mol ⁻¹
T_M	Empirically derived constant	314 K
R	Gas constant	8.314 J K ⁻¹ mol ⁻¹
L	Monin Obukov Length	m
P	Ambient air pressure	mbar
P_{std}	Pressure at standard conditions	1013 mbar
V	Volume	m ³
l_{ws}	Integral timescale of turbulent fluctuations	s
RH_i	PTR-MS ion counts	cps
RH_{zero}	PTR-MS background ion counts	cps
$M21$	Primary ion count	cps
$M37$	First water cluster ion count	cps
T_d	Drift tube temperature	°C
P_d	Drift tube pressure	mbar
k	Reaction rate constant	2 × 10 ⁻⁹ cm ³ s ⁻¹
t	Reaction time	1.05 × 10 ⁻⁴ s
M_r	Molecular mass	daltons

* * *

GREEK SYMBOLS

θ	Potential temperature	°C, K
θ_v	Virtual potential temperature	°C, K
ρ_a	Density of air	1.01 g m^{-3}
τ	Momentum flux – Wind shear	N m^{-2}
χ	Any atmospheric compound	-
χ_{voc}	VOC concentration	ppbv
α	Empirically derived constant	$0.0027 \text{ m}^2 \text{ s } \mu\text{mol}^{-1}$
β	Empirically derived constant	0.09°C^{-1}
γ	Light and temperature dependent activity factor	-
γ_T	Temperature dependent activity factor	-
σ_w	Standard deviation of the vertical wind velocity	m s^{-1}
η	Volume of air in canister	ml

* * *

ABBREVIATIONS

amu	Atomic Mass Units
A/O	Analogue Output
AT	Flux attenuation
AVOC	Anthropogenic Volatile Organic Compound
BEIS	Biogenic Emissions Inventory System
BEMA	Biogenic Emissions in the Mediterranean Area
b/t	Ratio of Benzene to Toluene
BLH	Boundary Layer Height
BVOC	Biogenic Volatile Organic Compounds
CC	Cross-Correlation function
CEH	Centre for Ecology and Hydrology (Edinburgh)
DDE	Dynamic Data Exchange
DEC	Disjunct Eddy Covariance
DFS	Disjunct Flux Sampler
DSI	Disjunct Sampling Interval
DSI&AT	Error due to disjunct sampling interval and flux attenuation
EA	Eddy Accumulation
EBL	Equilibrium Boundary Layer
EC	Eddy Covariance
FLX	Flux mode
GC-MS	Gas Chromatography – Mass Spectrometry
GMT	Greenwich Mean Time
G95	Guenther BVOC emission algorithm (1995)
HS	High Sensitivity PTR-MS instrument
ICPs	Ion Counts Per Second
IENS	Institute of Environmental and Natural Sciences (Lancaster University)
IPCC	International Protocol for Climate Change
IRGA	Infra Red Gas Analyser
ISR	Intermediate Storage Reservoir
LU	Lancaster University

MEGAN	Model of Emissions of Gases and Aerosols from Nature
mip	PTR-MS measurement file
MS	Mass Scan
<i>m/z</i>	Mass charge ratio
NAEI	National Atmospheric Emission Inventory
NERC	Natural Environment Research Council
NETCEN	National Environmental Technology Centre
NI	National Instruments
PTR-MS	Proton Transfer Reaction – Mass Spectrometer
PAR	Photosynthetically Active Radiation
PBL	Planetary Boundary Layer
REA	Relaxed Eddy Accumulation
REPARTEE	REgents PARk and Tower Environmental Experiment
SL	Surface Layer
SOA	Secondary Organic Aerosol
sonic	Ultrasonic anemometer
Std	Standard PTR-MS instrument
UN ECE	United Nations Economic Commission for Europe
UTC	Universal Time Coordinated
vDEC	Virtual Disjunct Eddy Covariance
VOC	Volatile organic compound
ZA	Zero air

Chapter I

1. Introduction

1.1 Biosphere - Atmosphere Interactions

The exchange of trace gases between the biosphere and atmosphere directly influences the chemical composition of our atmosphere and also plays an important role in climate, ecology and human health (Dabberdt *et al.*, 1993). All biosphere-atmosphere interactions take place within the planetary boundary layer (PBL), which is the section of the atmosphere most closely coupled to the Earth's surface. Here, surface forcings, including land heating and wind shear, generate atmospheric turbulence which is a highly efficient mechanism for the transport of trace gases (Stull, 1988). Consequently, compounds emitted from the surface become rapidly mixed throughout the PBL over a time period of typically less than 1 hour, although this time scale is ultimately dependent on the depth of the PBL, which can vary from a few tens of meters when the atmosphere is stably stratified, to a few kilometres when convectively unstable (Lenschow, 1995). The relative ease with which trace gases are transported demonstrates the sensitivity of the atmosphere to changes occurring at the Earth's surface, and underlines its ability to respond quickly to trace gas emissions.

Biosphere-atmosphere interactions are driven by both natural and anthropogenic processes and can impact upon air quality across a wide range of spatial scales, from the local to the global. Currently, there is widespread concern over the global effects of anthropogenic emissions on the state of our atmosphere. The global increase in carbon dioxide is perhaps the most well documented example, and since the industrial revolution, concentrations have risen from 280 ppm to > 370 ppm (Heath *et al.*, 2005). Although direct emission of carbon dioxide from the combustion

of fossil fuels is thought to be the primary cause, some of this increase can be attributed to changes in land use and deforestation. There is now a growing body of evidence to suggest that these emissions are impacting on the global climate system (IPCC, 2007), and hence surface exchanges of CO₂ are of particular interest to scientists and policy makers alike.

This is just one example of the role that surface exchanges play in the major geochemical cycles but there are many other examples of how biosphere-atmosphere interactions can affect air quality at both the local and regional scales. For instance, one group of compounds, volatile organics (VOCs), are known to have a profound impact on our atmosphere. Figure. 1.1 shows the important role their emissions play in generating a negative feedback loop for the global climate system (Seufert *et al.*, 1997). In addition to this key function, VOCs also control the formation of photochemical pollutants such as tropospheric ozone and peroxyacetyl nitrate (PAN) (Sillman, 1999). After emission to the atmosphere VOCs react with oxides of nitrogen to form secondary oxidants such as ozone. At elevated concentrations, ozone is a major environmental problem as it can impact upon human health (Lippman, 1993), crops and forest ecosystems (Sillman, 1999) and is also a precursor for the formation of secondary organic aerosol (SOA). Although the ozone precursors tend to be emitted from localised urban environments, the resultant photochemically reactive air masses can be advected over the regional scale (Derwent & Jenkin, 1990). In the 1970s it was first observed that U.K. emissions of VOCs were contributing to ozone episodes across North West Europe (Cox *et al.*, 1970). Since then, member states of the European Union have agreed to legislation laid out by the United Nations Economic Commission for Europe (UN ECE) which proposed to reduce the emission of ozone

precursors such as oxides of nitrogen (UN ECE, 1988) and VOCs (UN ECE, 1991) (Derwent *et al*, 2003).

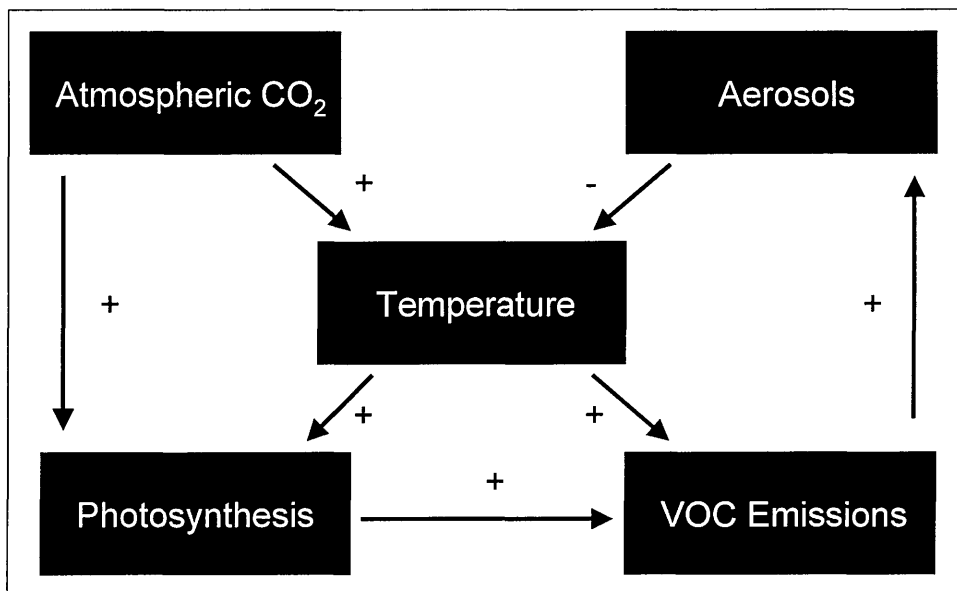


Figure 1.1 Diagram re-drawn from Kulmala *et al* (2004) showing the simple feedback loop between global climate and biosphere-atmosphere interactions involving CO₂ assimilation and VOC emissions.

These are further examples of how the fluxes of trace gases can directly impact upon air quality at both the regional and global scales, and force governments into introducing counteractive measures. From this it is clear that if we are to better understand the chemistry of our atmosphere, and control photochemical pollutants such as ozone, or suppress the global increase of CO₂, we must first quantify the fluxes of trace gases between the biosphere and atmosphere. In order to do this we can adopt one of two approaches. The first is the “bottom up” approach, where computer models and algorithms are used to scale up small scale observations to give regional or global emission estimates. The second is the “top down” approach, where regional scale or global scale emissions are measured directly using micrometeorological or remote sensing techniques.

1.2 Bottom up approach to quantifying trace gas emissions

Computer modelling techniques have become increasingly popular and have been readily adopted by the policy-making community. Not only do they help us understand the current state of our atmosphere, but more importantly they enable us to predict how the atmosphere will respond to future perturbations brought about by anthropogenic activities. This makes them important tools in assessing the effectiveness of potential control strategies such as the UN ECE directive (1991) to cut VOC emissions. In order for these models to return accurate predictions, they must first be supplied with accurate input variables such as information on surface exchange processes as well as some basic meteorological information. Currently much of this information is supplied by emission inventories (many of which are themselves model based), which are compiled by most national governments, although the method of compilation and the pollutants included varies from country to country.

In the U.K, the National Atmospheric Emission Inventory (NAEI) is assembled by the National Environmental Technology Centre (NETCEN, AEAT), and provides gridded emission estimates for 25 atmospheric pollutants with a spatial resolution of 1 km². Data for the inventory is compiled using a “bottom up” approach, where a combination of reported and estimated emission rates are scaled to give an overall emission estimate across a number of source sectors. Source sectors include categories such as road transport, industrial combustion processes and waste disposal, which are all further sub-divided to help produce an accurate and detailed estimate of emissions from across the whole of the U.K (King *et al.*, 2003). Large industrial processes such as power stations are required to report emissions to the Environment Agency who are the regulators of industrial processes in the U.K., as a commitment under the EU IPPC (Integrated Pollution Protection and Control) Directive

(96/61/EC). In contrast, for area sources, estimated emissions are calculated by applying an emission factor, such as an emission rate to a given activity statistic, such as a transport statistic. For example, the emission of benzene from the road transport sector may be expressed as the amount of benzene contained in car exhaust (emission factor), multiplied by the number of kilometres driven on U.K roads per year (activity statistic) (King *et al.*, 2003). Obviously the accuracy of the estimated emissions is governed by the accuracy of the statistical information used to generate activity statistics. Therefore reported or point source emissions are considered more robust than estimated emissions as they tend to be based on large quantities of reliable data. Consequently, the overall accuracy of the emission inventory is likely to be influenced by the ratio of reported emissions to estimated emissions.

Emission inventories also exist for biogenic compounds, which also play a hugely important role in governing the state of the atmosphere. Isoprene is perhaps the most influential of these biogenic compounds, accounting for approximately 45% (600 Tg C yr⁻¹) of the total biogenic volatile organic compounds (BVOC) emitted into the atmosphere (Guenther *et al.*, 2006). It is a highly reactive compound and through its reactions with the hydroxyl radical (OH) has the potential to reduce the oxidative (self cleaning) capacity of the atmosphere. In addition, there is growing evidence that isoprene may be a precursor for biogenic secondary organic aerosol (BSOA). Although the aerosol yield appears to be comparably small, because of the high emissions of isoprene, its contribution to organic aerosol may nevertheless be significant (Zhang *et al.*, 2007). For these reasons, much attention has been devoted to developing biogenic emission inventories specifically for this compound as well as others.

Typically, biogenic VOC emission estimates are made at the regional scale by taking the product of three parameters: (i) the quantity of leaf biomass within the region; (ii) a species specific emission factor to represent the rate of emission at standard conditions per unit biomass; and (iii) a basic meteorological factor to adjust emission estimates from standard to ambient conditions (Steiner *et al.*, 2002). The most comprehensive application of this basic algorithm is the Biogenic Emissions Inventory System (BEIS), which is a model designed to estimate biogenic emissions from the Eastern United States. Since its development in the mid 1980s it has been replaced by both second (BEIS2; Pierce *et al.*, 1991; Geron *et al.*, 1994) and third (BEIS3) generation versions, each more sophisticated than the last. More recently, a new algorithm, Model of Emissions of Gases and Aerosols from Nature (MEGAN) has been developed, in which net terrestrial biosphere emissions can be modelled at both regional and global scales with a 1 km² spatial resolution (Guenther *et al.*, 2006). Although MEGAN is similar to BEIS in some areas, i.e. using leaf scale emission factors, where possible it incorporates “top down” ecosystem level measurements (e.g direct micrometeorological flux measurements). However its canopy level emission estimates are still primarily based on leaf and branch scale emission measurements.

Like the NAEI, both the BEIS and MEGAN models call for detailed and accurate information to supply the basic model input parameters, such as leaf area index and species specific emission factors. The precision and accuracy of these input variables is vital for the overall performance of the model, and is ultimately responsible for the accuracy of the emission inventory.

Emission inventories are thought to be the key uncertainty in the modelling of tropospheric ozone concentrations which are frequently simulated to support policy development: poor predictions in ozone concentration are frequently attributed to

discrepancies in the emission inventory (Placet *et al.*, 2000). For example, when using anthropogenic VOC emission estimates it has become common practice to adjust the emissions by a factor of between 1 and 4 in order to obtain matches between the observed and simulated ozone concentrations (Velasco *et al.*, 2005). This indicates that the “bottom up” approach to estimating the surface exchange is prone to large degrees of uncertainty; therefore, perhaps potential alternative methods should be explored. An obvious choice would be to adopt a “top down” approach, whereby emissions would be measured directly from large area sources at the local or ecosystem level using direct micrometeorological measurements, or even at the global scale, e.g. using remote sensing or inverse modelling.

1.3 Top down approach to quantifying trace gas emissions

In 1996, FLUXNET, a global network of long term mass and energy (CO₂, H₂O and sensible heat) flux density measurement stations, was established (Falge *et al.*, 2001). The goal of this programme and its component projects, such as CarboEurope IP, is to increase our understanding of the terrestrial biosphere, in particular the way in which it responds to a changing atmosphere and the impact this has on global climate. Specifically, the FLUXNET programme measures CO₂ (and H₂O) fluxes to and from the Earth’s surface using automated micrometeorological techniques located on towers. The programme currently operates at 512 sites world wide, covering a diverse set of landscapes, including agricultural, forest and grassland. Data gathered from these sites is used to develop surface parameterisation and aggregation schemes, which, when scaled up, give regional and ultimately global scale flux estimates of carbon dioxide, which can be used to elucidate processes within the

global carbon cycle, quantify C sequestration in forests and study the role of land use change.

The FLUXNET network is perhaps the best and only example of how a measurement approach has been applied at a scale large enough to provide trace gas flux estimates on a global scale. In order for direct measurements such as these to accurately quantify the surface exchange of trace gases such as CO₂, measurement techniques must be based on a sound understanding of the major transport processes that control the surface exchange within the PBL. In the subsequent sections the major atmospheric transport processes will be described and a basic introduction to micrometeorology and some of the fundamental flux measurement techniques will be given.

1.4 Atmospheric transport processes

The major transport mechanism within the PBL is turbulence. Atmospheric eddies are generated by wind shear. These eddies vary in size, from very high frequency eddies, with a time period of less than 0.1 s, to low frequency eddies, where the time period can often exceed 1 hour. The random motion of these eddies controls the transport of heat momentum and mass within the PBL and are ultimately responsible for carrying the flux of any given compound.

Where the surface topography is uniform or level, the volume of air transported upwards by turbulent eddies should equal that being displaced towards the surface. Therefore over a given time period the mean vertical wind velocity w should equal zero (where up-draughts are taken as positive values and down-draughts negative), as should the net movement of an atmospheric scalar. It is only when there

is spatial variability of a scalar such as a concentration gradient that net transportation can take place through the instantaneous fluctuations of w about the mean. For instance, in Fig. 1.2 emissions of compound (χ) from the tree canopy cause significant concentrations of χ above the canopy. However at the top of the surface layer the concentrations of χ are much lower. As the air depleted in χ in the upper surface layer approaches and interacts with the surface it becomes infused with compound χ before being transported upwards in its newly enriched state. Thus there is a net movement of compound χ away from the surface. Similarly, if χ is prevalent in the upper boundary layer, but depleted near the surface, an inverse gradient is realised and the air transported by down draughts moves compound χ towards the surface, thus a net deposition is observed (Plantaz, 1998).

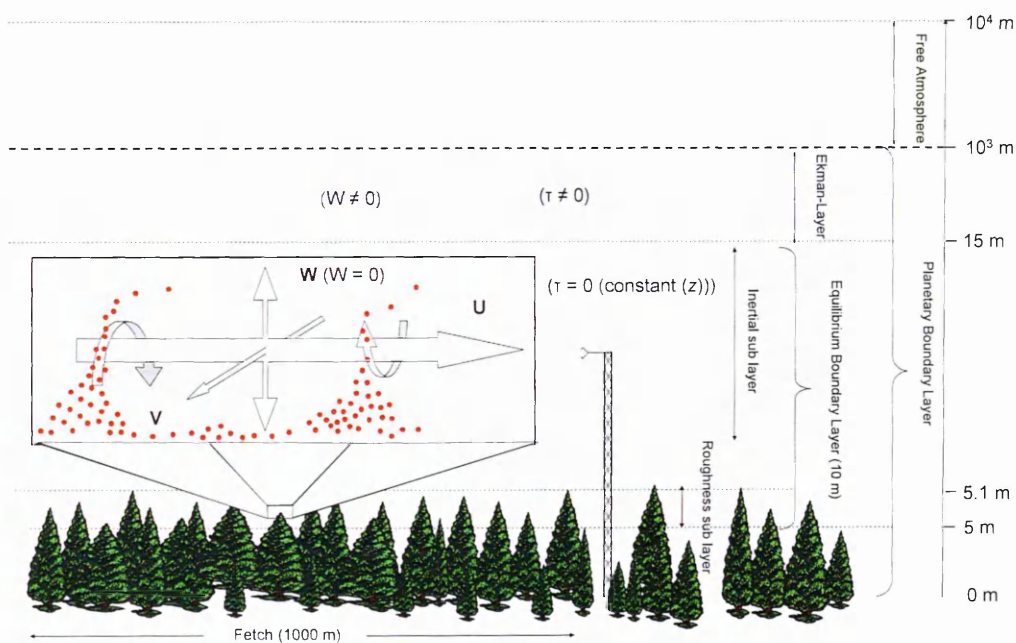


Figure 1.2 Diagram illustrating the mechanism of turbulent transport which is the dominant transport process within the planetary boundary layer.

1.5 The conservation equation

The turbulent exchange process described above is perhaps the most apparent means of transport in the PBL, but there are further chemical and atmospheric

processes occurring within this layer which cannot be neglected. Turbulent exchange is a one dimensional process, occurring in the vertical, as a product of up and down-draughts. However, lateral transport can also occur in the form of advection, a process that occurs when the scalar varies in concentration laterally rather than vertically. Micrometeorological flux measurement techniques, that derive canopy-level fluxes, derive the surface exchange from measurements made at a reference height well above the surface. There are several factors that can lead to flux divergence between the surface and this measurement height. The theoretical framework for each of these is provided by the conservation equation which parameterises the four major transport processes: turbulent exchange, horizontal advection, chemical reaction (source & sink terms) and molecular diffusion (D) and forms the basis for a range of aerodynamic and non-aerodynamic measurement techniques. It can be expressed as:

$$\overline{\partial \chi / \partial t} = \underbrace{-\overline{u} \frac{\partial \chi}{\partial x} - \overline{v} \frac{\partial \chi}{\partial y} - \overline{w} \frac{\partial \chi}{\partial z}}_{\text{Advection terms}} - \underbrace{\overline{\partial u' \chi' / \partial x} - \overline{\partial v' \chi' / \partial y} - \overline{\partial w' \chi' / \partial z}}_{\text{Divergence terms}} + \underbrace{D + S}_{\text{Source sink terms}} \quad (1.1)$$

Here the concentration of the scalar is given as χ and the values of u , v and w represent the velocity of the horizontal (aligned with mean wind flow), lateral and vertical wind components, respectively, and the values of x , y , z , relate to their Cartesian coordinates. The first three terms on the right hand side of the equation refer to the advection of a scalar in the horizontal, lateral and vertical directions due to gradients in concentration. This commonly occurs when air of a differing composition is driven by a pressure gradient and/or diverted by some topographic obstruction and mixed over the area of exchange.

The next three terms refer to the convergence or divergence of the flux, again in the horizontal, lateral and vertical (turbulent exchange) directions. These terms relate to chemical processes which affect the transport of a compound and may represent a significant source of error when measuring exchange processes. In most land-atmosphere exchanges it is assumed that the formation or removal of a compound occurs only at the surface, a premise that does not consider chemical reaction within the air column itself. Sesquiterpenes ($C_{15}H_{24}$) for example, are a highly reactive group of biogenic volatile organic compounds (BVOC). Upon emission from a tree canopy, they can undergo reaction with tropospheric ozone and can be removed from the atmosphere in a matter of minutes, never reaching the point of measurement (Bonn *et al.* 2006). In such situations, the measured flux only represents a local flux at the point of measurement, and not of what is occurring at the surface, therefore the emission flux is underestimated due to divergence. Analogously, the flux may be overestimated due to convergence, where chemical reactions cause “in air” production of a compound. It should be recognised that the chemical formation or removal of a compound only becomes significant if the rate of reaction is shorter or of a similar magnitude as the transport time-scale.

The atmospheric transport processes described above form the basic principles of any direct measurement. The subsequent sections illustrate how these concepts are used within a range of flux measurement techniques.

1.6 Enclosure techniques (non-aerodynamic)

The enclosure approach is a non-aerodynamic flux measurement technique, which has become a popular method for the measurement of VOC emissions from vegetation, under both laboratory and field conditions (Cao & Hewitt, 1999).

Enclosures usually take the form of a leaf, branch or plant cuvette, and can either be static or dynamic in their operation. With static cuvettes, emission rates are derived from the rate of change in species concentration within the cuvette headspace, whereas, with dynamic cuvettes, air is continuously pumped through and a concentration difference is realised between the incoming and outgoing air (Rinne, 2001). Obviously, the measured emission or assimilation is only representative of that section of leaf tissue / branch within the cuvette; therefore up-scaling is required to give flux estimates on larger length scales.

The relative simplicity, low cost and physical robustness of enclosures make them very appealing, and given their capacity for slow responding chemical sensors, they seem an appropriate choice for the measurement of VOCs. While enclosures have intrinsic worth, some obvious shortcomings arise through their use. By erecting physical boundaries around the domain of interest, the natural biological function of the vegetation within is perturbed, often yielding unrepresentative results. Changes in temperature, radiation balance, pressure and turbulence (wind speed and vertical profile) are often apparent when compared to conditions prior to the placement of the enclosure (Fowler, 2001). In addition the use of enclosures places a limit on the number of leaves or branches that can be encompassed within a wider spatial context such as a forest canopy. Thus, given that inter-leaf variability exists within the tree canopy, due in part to strong vertical gradients in photosynthetic capacity, sampling with any statistical confidence becomes difficult (Baldocchi, 2003). Similarly, enclosure techniques are unsuitable for very 'sticky' compounds that interact with the cuvette walls. Nevertheless, the concentration differences that need to be quantified by the chemical sensors in the enclosure technique are significantly larger than those in

the micrometeorological approaches, making the enclosure technique the method of choice when fluxes are small and low flux detection limits are required.

1.7 Micrometeorological techniques (aerodynamic)

Another option is to adopt a micrometeorological approach using the conservation equation (Equation 1.1) and the concept of a control volume mass balance. As we have seen, this volume can be defined implicitly through the use of a physical enclosure, but instead, here, a Cartesian coordinate frame is used to define a rectangular prism in the open air (Finnigan *et al.*, 2002). Within this coordinate system the streamwise wind components u , v , and w correspond to the Cartesian coordinates x , y and z respectively, and define the boundaries of the prism over the exchange area. Accurately measuring fluctuations across each plane of the control volume to separate the true turbulent exchange in the vertical, from the effects of advection in the horizontal, would require a number of multidimensional (x , y , z) measurements at differing locations. Where the control volume has been defined physically through the use of a cuvette or branch enclosure this task is simplified, as the air entering and leaving the enclosure headspace can be measured directly, but when a single, tower mounted, aerodynamic technique is deployed the complexity of the task remains.

Fortunately, under certain “ideal” conditions, where the upwind area (fetch) of the measurement point is spatially uniform or level, an equilibrium boundary layer (EBL) may develop, in which the horizontal variability of fluxes (advection) is negligible (Fowler, 2001). Hence, where chemically inert compounds are to be measured and storage terms are equal to zero, the conservation equation may be reduced to include only the effect of turbulent exchange, allowing a greatly simplified, one dimensional (vertical) flux measurement to be made (Equation 2) (Denmead, 1993).

$$F\chi = \overline{w'\chi'} \quad (1.2)$$

Within this thin surface layer the profiles of gas concentration are at equilibrium with the local rate of exchange occurring at the surface (Denmead, 1993), so effectively a layer of constant flux (Prandtl-Layer) is formed in which micrometeorological measurements can be made at any height, yet still be representative of the exchange occurring at the surface below. Elevating the point of measurement allows these techniques to operate on much larger length scales ($100 \text{ m}^2 - 10^6 \text{ m}^2$) compared to the enclosure method ($0.1 \text{ m}^2 - 10 \text{ m}^2$), but stringent height restrictions demand that sensor height does not exceed the depth of the EBL. Outside of this region, the influence of horizontal advection can no longer be neglected, and fluxes may vary by more than 10% compared to the true exchange occurring at the Earth's surface.

A new EBL forms over each new surface the wind moves across, characterised by differences in roughness height, heat flux and emissions. The depth of the EBL over a given surface is dependent upon the length of fetch in the upwind direction (i.e. the distance to the next surface heterogeneity upwind) as well as the atmospheric conditions at that time (Fig 1.3). A general rule of thumb is that the ratio of fetch to EBL depth is roughly 100:1 (McMillen, 1988), but when the atmosphere is stably stratified, the requirement for fetch may increase due to memory effects of distant upwind obstructions (Businger, 1986). More exact predictions of the fetch requirement have been made using theoretical footprint models in a number of studies (Leclerc & Thurtell, 1990 ; Scheupp *et al.*, 1990 ; Horst & Weil, 1992) (Dabberdt *et al.*, 1993). Therefore under neutral or unstable atmospheric conditions, an upwind fetch of 200 m, the height of instrumentation should not exceed 2 m. When measuring over aerodynamically rough surfaces such as tree canopies or cities, wake turbulence is generated as the air flow interacts with the tree crowns or building tops, causing a

disruption to the constant flux layer and making measurements close to the tree tops unreliable (Baldocchi, 1988). Wind tunnel experiments have suggested this roughness layer to be approximately $h + 1.5 L_t$ for tree canopy measurements, where h is the average height of the tree canopy and L_t the approximate width of the tree crown. Therefore the workable measurement height must be above $h + 1.5 L_t$ (Raupach,

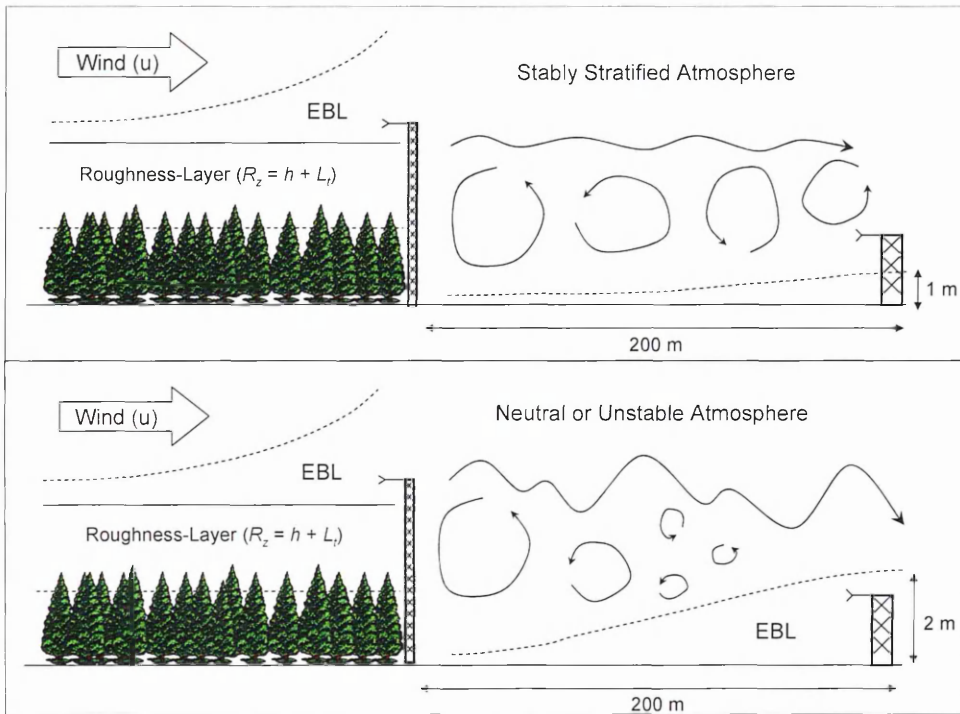


Figure 1.3 Diagrams illustrating the effect of atmospheric stability on the formation of an equilibrium boundary layer.

1980). Over cities, the situation is more complicated as the surface is highly irregular and often roads, buildings, urban parkland and construction sites are found in close proximity. Nemitz *et al.* (2002) and Dorsey *et al.* (2002) were able to demonstrate fluxes could still be reliably measured over an urban environment provided the measurement height exceeded at least 3 times the average building height. In these studies, where CO_2 and aerosol fluxes were measured above the city of Edinburgh, the chosen measurement site was Nelson monument, a 32 m tall stone tower located on Calton Hill (45 m tall), which gave them an effective elevation of 67 m above

street level. At this height it was shown that the wake turbulence, generated by the roughness elements below, blended into a homogenous net flux, therefore allowing them to make direct city scale flux measurements.

Although the previous sections have given a basic introduction to micrometeorology, briefly touching on some of the fundamental concepts of turbulent transport and some of the theoretical requirements, it is apparent that micrometeorological techniques offer two distinct advantages over enclosure techniques. Firstly, they can integrate the measured flux over a much wider source area than enclosure techniques (Guenther, 2002), making them ideal for regional scale surface exchange measurements occurring above fields, tree canopies or cities, and secondly, as the instrumentation is tower mounted, downwind of the source area, they are non-intrusive, do not alter the local environment and leave the exchange processes free from bias. We have seen how these techniques can be applied over a wide range of environments, including both homogenous, and non-homogenous landscapes, and the theoretical concepts that allow us to do so have been outlined. The subsequent sections will now focus on some of the more common micrometeorological methods used for the measurement of surface layer fluxes.

1.8 Eddy Covariance (EC)

At present the eddy covariance technique (EC) is the most direct approach available for the measurement of turbulent exchange, and where field sites have sufficient fetch and are free from upwind obstructions it may be applied in its simplest form. As discussed above, the advective and source-sink terms of the conservation equation can be neglected when measuring non reactive species within the EBL, through careful field site selection. Thus in EC, only the fluctuations of the vertical

wind component (w) and scalar concentration (χ) are recorded over a time period (t). Measurements are direct and rapid, using fast responding analytical sensors to resolve high frequency flux contributions, which are responsible for the transport of a substantial share of surface-layer fluxes (Rinne, 2001). Eddies by nature are irregular and random, therefore, micrometeorological techniques tend to quantify their behaviour through the use of statistical averages, hence in the case of EC, time t , is an averaging period of typically 30 minutes. Using a time series of this length not only ensures the calculated averages of w and χ are statistically well behaved (e.g. $\overline{w} = 0$) (Lenschow, 1995), but also ensures the flux contributions from larger eddies are resolved within the flux calculation.

The flux of a compound, F_χ , is given as the time averaged covariance between w and χ .

$$F_\chi = \overline{w\chi} + \overline{w'\chi'} \quad (1.3)$$

The first term of equation (3) refers to the mean vertical transport of air during the averaging period (denoted by over bars), which should equal zero provided fetch requirements have been fulfilled ($\overline{w} = 0$). Therefore the equation can be reduced to:

$$F_\chi = \overline{w'\chi'} \quad (1.4)$$

Here the flux is calculated from the transport resulting from instantaneous fluctuations of both wind and scalar values about their respective means ($w' = w - \overline{w}$) (Plantaz, 1998). In the convention adopted here, the flux (F_χ) and vertical wind component (w)

are taken as positive where there is net movement away from the surface, and negative, when movement is towards the surface (Nemitz, 1998).

1.8.1 Theoretical requirements - Stationarity

As mentioned above, flux measurements tend to be calculated as statistical averages and are therefore integrated over long time periods. Extending the averaging period can be desirable as it increases the statistical robustness of the measurement but this can conflict with the requirement for stationarity. A measurement may be considered stationary when its statistical properties represent those of the process being measured and not those of the averaging period, i.e. the measured process is independent of time (Dabberdt *et al.*, 1993). At the local scale meteorological conditions often change rapidly, therefore averaging periods are usually limited to less than 1 hour. Eliminating periods of non-stationarity is difficult but a number of tests have been developed which allow these periods to be filtered and removed from data sets. These tests will be outlined in more detail in the methods section.

1.8.2 Coordinate rotation

It is readily assumed that within the constant flux layer vertical wind velocity is equal to zero over time, but under field conditions a non-zero value is often observed, not due to degradation of the constant flux layer, but due to misalignment or tilt of instrumentation. Tilting of the anemometer and consequently the coordinate frame causes the w wind component to become non zero due to contamination from the u and v components (Fig. 1.4).

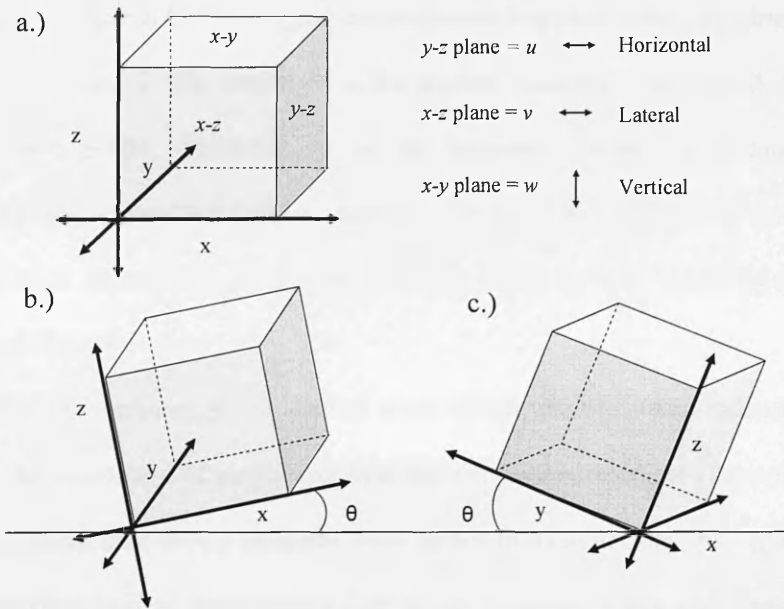


Figure 1.4 Diagram (a) shows the Cartesian coordinate system used in micrometeorology. Small tilt errors in the mounting of the sonic anemometer along either the y or x axis as seen in (b) and (c) respectively can result in the contamination of the w wind vector. Applying two coordinate rotations, the first to align u into the x direction and the second to align w into the z direction, effectively setting $w = 0$ and $v = 0$.

To correct for these tilt errors it has now become conventional to rotate the coordinate frame, first around the (z) axis to align the (x) axis with the mean horizontal wind direction U , thus setting ($\bar{v} = 0$) (Stull, 1988), and secondly rotating around the (x) axis to align w with the (z) axis, thus setting ($\bar{w} = 0$) (Baldochi, 1993).

1.8.3 Sensor requirements

Successful application of the EC technique is dependent upon the response times of the analytical instrumentation employed. Sensors for vertical wind speed and concentration must respond concurrently, at a rate sufficient to resolve the turbulence scales contributing to the flux (McMillen, 1988) and since the mean wind speed (and thus eddy size) varies with the logarithm of height, response times must increase as the measurement height is closer to the ground (Kanemasu, 1979). Field experiments

conducted by Deacon (1959) suggest the frequency response times of instrumentation should be at least $2 U/z$, where U is the highest expected wind speed, and z the measurement height. Therefore, a 10 Hz frequency would be required when measuring over a grassland field at a height of 2 m ($U = 10 \text{ m s}^{-1}$), whereas measuring above a 10 m tree canopy, at a height of 15 m, response times could be relaxed to around 1.3 Hz.

For the measurement of vertical wind speeds, the ultrasonic anemometer has become the instrument of choice amongst the micrometeorological community. This well established field sensor measures wind speeds in three vectors, the vertical w , the horizontal (longitudinal mean surface flow) u and the lateral v , at a high frequency and with good sensitivity. Sonic signals are transmitted along the fixed orthogonal directions, and the wind speed is calculated by a microprocessor, as well as virtual temperature, which is calculated from a measurement of the speed of sound. The sonic anemometer has a typical measurement resolution of between 10 and 20 Hz, which makes it ideally suited to the monitoring of small scale fluctuations in both wind speed and temperature. This makes it an ideal instrument for the measurement of sensible heat fluxes, but if the eddy covariance technique is to be applied to the fluxes of mass, analytical sensors with similar response times are required. As described earlier in the FLUXNET programme, these criteria can be met for some compounds such as CO_2 , heat and H_2O , but for many others, they cannot, and hence the eddy covariance technique is unsuitable, and will remain so until future technological advances improve sensor response times.

Although it is encouraging to have a network of monitoring stations measuring exchanges of important greenhouse gases such as CO_2 and H_2O , there are many other trace gas exchanges which we currently cannot measure directly, or for which

chemical sensors are too costly and labour intensive to run to make a large-scale flux monitoring network a viable option. Of particular concern are reactive trace gases such as VOCs, which as mentioned earlier can have a profound influence on our atmosphere. Quantifying their emission could help to elucidate factors controlling photochemical pollution episodes and aid policy makers in developing suitable amelioration strategies. Unfortunately, at present, with the exception of the relatively new analytical technique proton transfer reaction mass spectrometry (PTR-MS) (Chapter 2), there are few VOC sensors available with fast enough response times for the EC technique to be applied. Consequently much attention has been devoted to developing alternative flux methodologies where the sampling rate can be reduced and hence the measurement response time of the sensor no longer becomes the limiting factor of the flux measurement. In the following section some of the more notable VOC flux measurement techniques are described and a short discussion of their respective merits and drawbacks is given.

1.9 Eddy Accumulation (EA)

Sampling fluxes at reduced rates was first suggested by Desjardins (1972). The conditional sampling method he proposed, now termed Eddy Accumulation (EA), involved the partitioning of air samples into either an up-draught or down-draught storage reservoir depending upon the sign of the vertical wind velocity. Air samples were directed into the appropriate reservoir at a flow rate proportional to the vertical wind velocity at the moment of sampling using a complex set of valves and mass flow controllers. As with the EC method, measurements are integrated over a long time period t (5-30 mins), resulting in a concentration differences between the up sampled eddies and the down, hence the flux of a compound (F_x) is simply given as the

concentration difference between the up and down reservoirs over time t , multiplied by a pumping coefficient which describes the relationship between w and sample flow rate. This method is numerically identical to standard eddy covariance, but avoids the need for fast-response analysers as only the integrated reservoirs need to be analysed after each averaging period. The directness of this approach makes it appealing, particularly for those compounds where poor sensor response times restrict the use of EC. However, there are a number of drawbacks to be considered. Storage reservoirs, in the majority of cases need to be analysed offline, which can be a hindrance for long-term studies. Furthermore, the use of the reservoir itself may lead to losses of the compound(s) of interest to reservoir walls, or in the case of highly reactive chemical species, to the reaction with other compounds present in the reservoir, resulting in an underestimation of the flux. The method of sample capture is very demanding, and hence there is an overt need for technical precision and accuracy as even small discrepancies between the magnitude of w and the magnitude at which air is actually sampled can have a large erroneous effect on the total flux estimation (Hicks, 1984).

1.10 Relaxed Eddy Accumulation (REA)

In 1990 the operation of the eddy accumulation system was greatly simplified, when it was suggested by Businger & Oncley (1990) that the speed at which air was sampled could be made constant by introducing an empirical proportionality coefficient β . This greatly relaxed the technical demands associated with this method and hence the revised technique became known as Relaxed Eddy Accumulation (REA). The flux (F_χ) of a compound (χ) is now calculated as:

$$F_\chi = \beta \sigma_w (C_{up} - C_{down}) \quad (1.5)$$

where β is the empirical proportionality constant and σ_w is the standard deviation of the vertical wind velocity. The value of β can be verified by deriving it from independent flux calculations of other scalars who are subject to atmospheric transport by the same mechanism as mass, i.e. heat (Oloffsen *et al.*, 2003). These measurements are usually made using the eddy covariance technique, since most commercially available sonic anemometers measure wind speed and temperature concurrently.

Although the original REA theory suggested that air be sampled into the appropriate reservoirs when w is either $w > 0$ or $w < 0$, it has become common practice to introduce a “dead band” to further increase the concentration gradient between the up and down reservoirs and to avoid ambiguity when $|w|$ is small. For example, Olofsson *et al.* (2003) found it suitable to establish a dead band between $+0.5\sigma_w$ and $-0.5\sigma_w$ in their study of VOC fluxes from a Swedish golf course. They demonstrated that by increasing the concentration gradient between the up and down sampled reservoirs, the demand on the detection limit of their system could be lowered. The REA technique has been used in many other studies for the measurement of VOC fluxes and a lot of these have focused on measuring fluxes at ecosystem level above tree canopies (e.g. Greenberg *et al.*, 2003; Valentini *et al.*, 1997; Ciccioli *et al.*, 2003). Other notable work has included validation studies (e.g. Komori *et al.*, 2004; Gallagher *et al.*, 2000) where REA fluxes have been compared with those measured by EC and a good agreement between data sets has been found. Studies such as these suggest the REA technique to be a good alternative to the EC technique, however there are some draw backs which need to be mentioned. Firstly, some problems associated with EA, such as offline analysis of samples, and possible compound losses to chamber walls still remain. Secondly, by sampling the air at a

constant rate and introducing a proportionality constant, the method can no longer be considered a direct measure of the flux, but it relies on the parameter β . Finally, as air samples are taken online, in accordance with the “live” wind velocity measurements, there is no scope for the post processing of data, therefore procedures such as the coordinate rotation need to be implemented during sampling and cannot be improved afterwards.

1.11 *Disjunct Eddy Covariance (DEC)*

Although the eddy covariance technique is the most direct technique available for the measurement of surface layer fluxes, it has two significant drawbacks. The first is the need for fast measurement response times which has already been touched upon in Section 1.8.3, and therefore will not be discussed further here. The second, which involves the volume of data generated, arises as a direct consequence of the response time. The typical response time for EC measurements is often of several Hertz and consequently large volumes of data are generated over short periods of time. During the 1970s, both the EC technique and computers were in their infancy. Serious problems ensued due to the large quantities of data which needed to be stored for post processing. Consequently a new method for calculating fluxes, disjunct eddy covariance, was proposed by Haugen (1978) as a way of reducing the amount of data needed to calculate the flux. Rather than sampling at fast rates to generate a quasi-continuous data set, it was proposed that the flux could be calculated using a subset of the continuous time series, i.e. the time series could be made discontinuous, while each data point remains a fast-response measurement. This concept is demonstrated in Figure 1.4. Since its initial concept, it has been demonstrated that, provided samples

are acquired at a rate fast enough to resolve the flux contributions from high frequency eddies, the flux can be adequately resolved using a temporally discontinuous data set (Lenschow *et al.*, 1994). This makes the disjunct technique an ideal tool for reducing the volume of existing EC data sets. However, over the last 30 years computer technology has advanced rapidly, and consequently data storage is no longer the problem it once was, therefore the concept of DEC was never readily adopted by the scientific community.

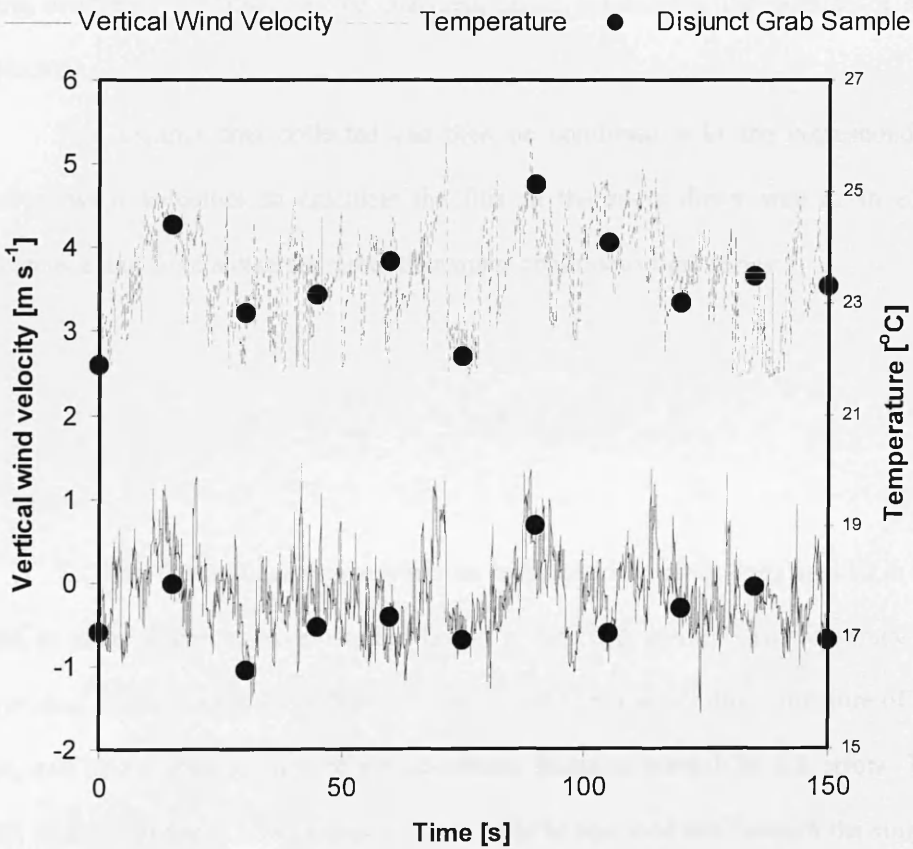


Figure 1.4 Plot of vertical wind velocity (w) and temperature (T). Closed circles represent the disjunct sampling protocol.

This technique still has relevance today as it can be adapted for the measurement of compounds such as VOCs where the lack of fast responding sensors restricts the use of EC. Although it is still crucial for samples to be acquired at fast

rates, they do not necessarily need to be measured directly by the sensor as is the case with EC. Instead a sampling system where a grab sample of air is rapidly aspirated into a canister can be used to allow slower sensors to draw upon air from the canister over a time period of a few seconds. When analysis has been completed, the chamber can be evacuated, and a new sample taken. The more samples acquired over the averaging period the more statistically robust the flux measurement becomes, therefore, two storage reservoirs may be used in parallel, thus, when one reservoir is being evacuated the other can be analysed, hence maximising the volume of data collected.

The disjunct data collected can then be combined with the corresponding vertical wind velocities to calculate the flux in the same direct way as in eddy covariance, but from a discrete rather than quasi continuous time series:

$$F_{\chi} = \frac{1}{n} \sum_{i=1}^n (w_i - \bar{w}) \cdot (\chi_i - \bar{\chi}). \quad (1.6)$$

To date, the disjunct eddy covariance technique has rarely been applied in the field, as many scientists have opted in favour of the REA method. This is somewhat surprising considering the fact that unlike REA, DEC remains a direct measure of the flux, and also allows rotation of the coordinate frame to correct for tilt errors. The REA method produces fewer samples that need to be analysed and remains the single-height technique of choice where samples need to be processed manually. By contrast, DEC is becoming the method of choice for compounds for which analysers of intermediate response time 3 – 30 s are available. One emergent family of analysers that fulfil this requirement are quadrupole based mass spectrometers, which are fast, but usually need to cycle through a range of m/z . Of the few field applications that

have taken place, the results have been encouraging. The first studies focused on VOC from Alfalfa fields, coupling the disjunct sampling system with the proton transfer reaction mass spectrometer (PTR-MS). The objective of these studies was to establish the effect of cutting on the emission of leaf injury compounds such as C₆ aldehydes, alcohols and ester derivatives (Rinne & Guenther, 2001; Warneke *et al.*, 2002). More recently, Grabmer *et al.* (2005) deployed the technique at canopy level, measuring the flux of various VOCs from a Norway Spruce forest. The results they obtained compared well with data collected by an REA system and enclosure techniques and clearly demonstrate the potential of the DEC technique.

1.12 Aims and objectives

In view of the important roles played by both anthropogenic and biogenic volatile organic compounds in regional and global scale atmospheric chemistry, a better understanding of the processes controlling their emission is of paramount importance. Bottom-up style emission models such as MEGAN for biogenic emissions and the NAEI for anthropogenic emissions represent the most effective means of generating emission estimates at the desired length scales, but their accuracy is highly dependent on inputted variables such as basal emission rates or activity factors. In contrast direct measurement approaches such as eddy covariance flux measurements can integrate emissions over a significant source area thus removing the need to characterise emission sources and strengths. To this end, the work presented in this thesis is focused on developing new “top down” techniques for the measurement of volatile organic compound fluxes which will have the potential to work with and alongside the existing “bottom-up” modelling approaches. The specific aims of the work are threefold:

- (i) To develop and validate a DEC system for the measurement of volatile organic compound fluxes.
- (ii) To deploy the system over a range of canopy types, including both urban and rural locations.
- (iii) To compare the “top-down” flux measurements with “bottom-up” modelling approaches.

Chapter II

2. Methodology

In this chapter a description of the main methods used throughout this thesis will be given. The first section will describe in detail the proton transfer reaction mass spectrometer (PTR-MS) which is the analytical instrumentation used throughout this study for the measurement of volatile organic compound mixing ratios. The next section will elaborate on the disjunct eddy covariance technique, focusing on its design and testing as well as reporting on results from both theoretical and practical validation tests. After this, the virtual disjunct eddy covariance technique will be introduced, and its implementation outlined. Finally, the methods of data analysis and quality checks will be described.

2.1 The proton transfer reaction – mass spectrometer

During this work, VOC measurements were made using a proton transfer reaction mass spectrometer (Ionicon GmbH, Innsbruck, Austria). This instrument was chosen as it is the only commercially available VOC sensor that allows for the online measurement of a wide range of compounds with both a high sensitivity and fast response times. These characteristics set the PTR-MS apart from other techniques such as gas chromatography mass spectrometry (GC-MS) and make the instrument ideally suited for micrometeorological flux measurements. Unlike most conventional mass spectrometers, the PTR-MS does not directly ionise the compound(s) of interest using electrons or radiation; instead it uses a softer ionisation of the VOC, based on the low energy proton transfer reactions (Ammann *et al.*, 2004). The protonated VOC are then separated according to their mass charge ratio (m/z) and are subsequently

detected downstream (Hewitt *et al.*, 2002). A detailed description of the PTR-MS can be found elsewhere (Lindinger *et al.*, 1996; Hansel *et al.*, 1995; de Gouw & Warneke, 2006), therefore only a brief description will be given here.

The PTR-MS instrument is comprised of four key elements which are shown in Figure 2.1; a primary ion source, a drift tube, a quadrupole mass spectrometer and a mass detection system (Hewitt *et al.*, 2002). The ion source consists of a high voltage hollow cathode which is continually flushed with pure water vapour to provide a stable source of primary (H_3O^+) reagent ions. The number of reagent ions produced is typically in the range of $(2.5 - 10) \times 10^6$ ICPs (ion counts per second), but this number can be varied by altering the flow of water vapour to the cathode and also by varying the voltages of the two elements that make up the ion source. An increased primary ion count is desirable as the sensitivity of the instrument may be increased but this may come at the cost of producing a higher fraction of NO^+ and O_2^+ impurity ions. These impurities are unwanted as they can undergo charge-transfer reactions with most VOC which competes with the proton transfer reaction and are harsher forms of ionisation than the desired proton transfer reactions and may thus lead to increased fragmentation of analytes (de Gouw & Warneke, 2006).

Once the primary ion count has been optimised, the H_3O^+ ions are passed through a Venturi type inlet and accelerated into the low pressure region (~ 2 mbar) of the drift tube (reaction chamber). The drift tube is comprised of a number of stainless steel rings which are separated by a series of insulating Teflon rings. A series of voltages is applied across the rings to create a homogenous electric field E ($E \sim 62.5$ V cm^{-1} under normal operating conditions). The electric field is used to dissociate the $\text{H}_3\text{O}^+(\text{H}_2\text{O})_n$ cluster ions which form when H_3O^+ ions become hydrated. The abundance of cluster ions within the reaction chamber is dependent on the humidity of

the sample air and typically cluster ions make up < 5% of the total reagent ion count and are dominated by the first cluster ($n = 1$; $m/z = 37$). Suppressing the reagent clusters is important as they can react with VOC which can complicate the interpretation of the instrument spectrum (Hewitt *et al.*, 2002).

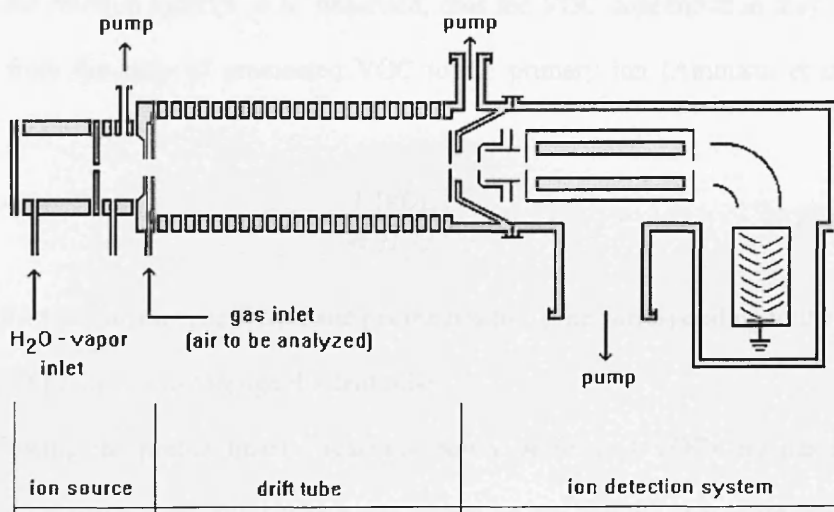
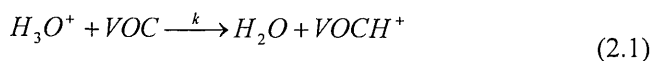


Figure 2.1 Schematic of the PTR-MS instrument showing the three major component parts, ion source, drift tube and detection chamber.

Once the H_3O^+ ions are in the drift tube, they react with any constituent of air with a higher proton affinity than that of water. Given that the major components of air such as N_2 , O_2 , CO_2 and CO all have proton affinities less than that of water and will therefore only undergo non reactive collisions with the primary ions, air for analysis by PTR-MS can be flushed directly into the drift tube without the need for prior conditioning or pre-concentration. At typical ambient concentrations the number of primary ions should be in great excess of that of the VOC thus in the case of most analytes the following proton transfer reaction will occur:



Provided the VOC remain at a typical, stable, ambient concentration (< 1 ppm), the concentration of H_3O^+ ions will not be diminished significantly by Reaction (1), unless the initial supply from the hollow cathode is reduced. Such a scenario allows for the reaction kinetics to be linearised, thus the VOC concentration may be calculated from the ratio of protonated VOC to the primary ion (Ammann *et al.*, 2004).

$$VOC \approx \frac{1}{kt} \frac{[VOC]}{[H_3O^+]} \quad (2.2)$$

where k is the reaction rate coefficient and t is the reaction time corresponding to the transit time of primary ions through the drift tube.

Following the proton transfer reaction, newly protonated VOCs are passed through a quadrupole mass filter which can either be set to scan the entire mass spectrum or run in a selective ion mode, where the mass filter steps between a suite of pre-determined m/z . The primary and selected product ions are subsequently detected as ion counts per second or “hits” by a secondary electron multiplier (SEM) (Tani *et al.*, 2002).

2.1.1 Mass Detection System

The low energy chemical ionisation used in PTR-MS means that many of the reactions in the drift tube are non-dissociative, that is to say that the protonated ions do not fragment. For example, the C_6 compound Benzene has a molecular mass of 78.1 therefore once protonated it can be detected at m/z 79. However, this may not always be the case as higher energy reactions occurring with cluster ions can often lead to the fragmentation of VOC, which means the parent VOC may be detected at a

number of different masses. Examples of this are the monoterpenes which are known to dissociate in the PTR-MS and can be detected as fragment ions at m/z 81 and m/z 137.

As the quadrupole mass spectrometer has a unity resolution, i.e. compounds with a similar molecular weight are detected at the same integer amu, it can be difficult to attribute ion counts to specific VOC without the aid of ancillary measurements. Examples of this include isoprene and furan which have protonated molecular weights of 69.117 and 69.074 respectively. Measurement of either one of these compounds by PTR-MS alone may result in the over estimation of the VOC present.

2.1.2 Instrument Background

The PTR-MS can be subject to high background counts of VOC; therefore it is important to monitor these counts and subtract them from measured concentration. In order to accurately quantify contributions from the instrument background it is necessary to sample from a zero air source which is free from all VOC. Previous studies have shown that the instrument background is not always constant and is likely to fluctuate with changes in sample air humidity as the VOC have a tendency to desorb from tube walls when the air is hydrated. This means that wherever possible the instrument background should be monitored at regular intervals.

In order to generate a zero air source for the PTR-MS instrument, a number of scrubbing agents were compared in order to find the most effective VOC scrubber. Filters containing each scrubbing agent were fitted in front of the PTR-MS inlet which continually sampled laboratory air. A monitoring sequence was programmed to control a small 1/8" 3-way Teflon headed solenoid valve which switched continually

between ambient air and the scrubber every 25 measurement cycles. The scrubbing agents tested included, activated charcoal, silica gel, molecular sieve, and drierite. The results for these filters are shown in Figures 2.2, 2.3, 2.4 and 2.5 respectively.

Of the four filters tested, the molecular sieve was the most effective in actively removing methanol, acetaldehyde and acetone from the sample air to give background concentrations of 1.7 ppb, 0.5 ppb and 0.3 ppb. Although the drierite filter also actively removed these compounds, the recorded backgrounds were higher than that of the molecular sieve. The fact that the isoprene concentration (m/z 69) remained unaltered with all tested filters suggests that either these filters cannot remove this compound or that the concentrations present within the laboratory were less than that of the instrument background.

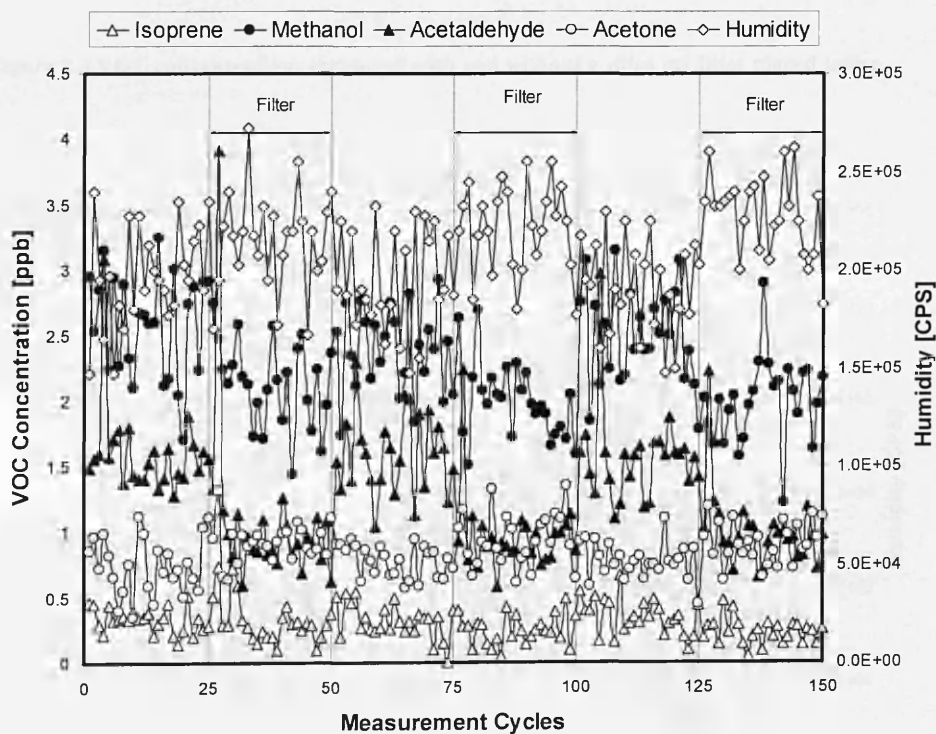


Figure 2.2 VOC concentrations measured with and without a charcoal filter placed inline.

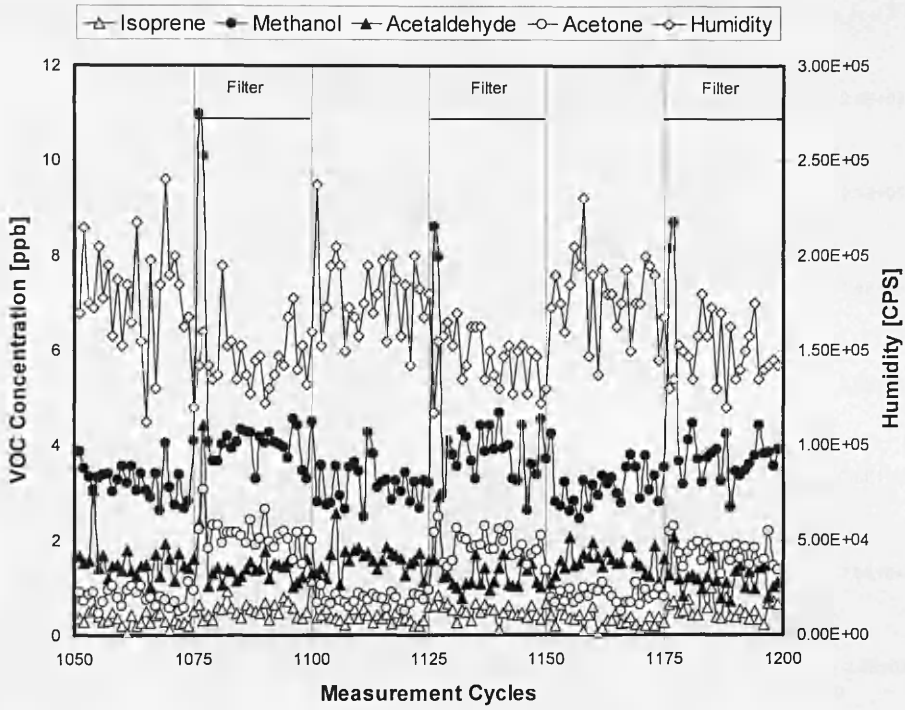


Figure 2.3 VOC concentrations measured with and without a silica gel filter placed inline.

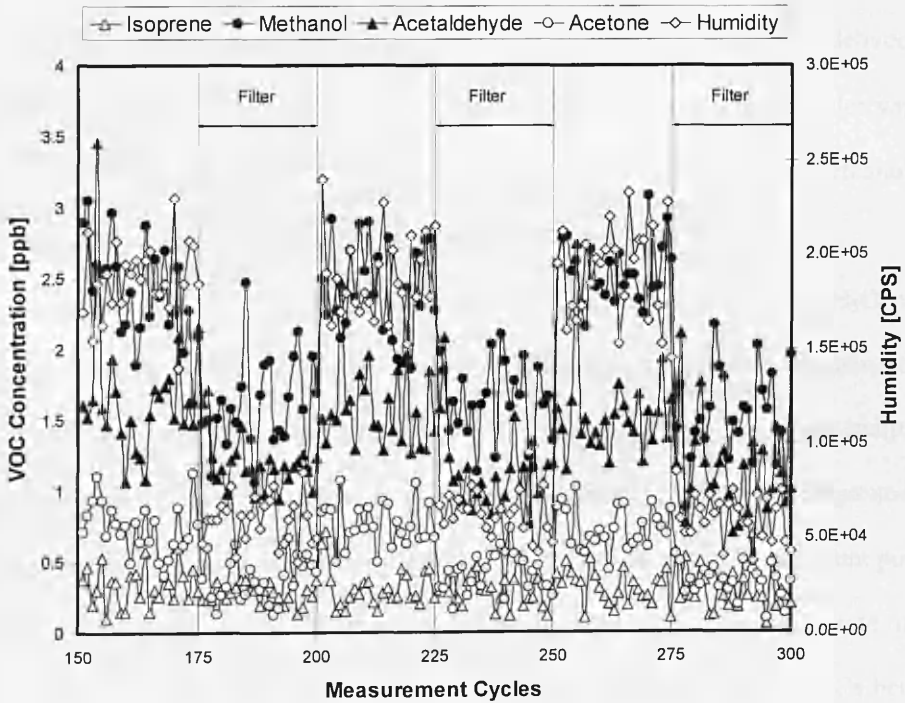


Figure 2.4 VOC concentrations measured with and without a drierite filter placed inline

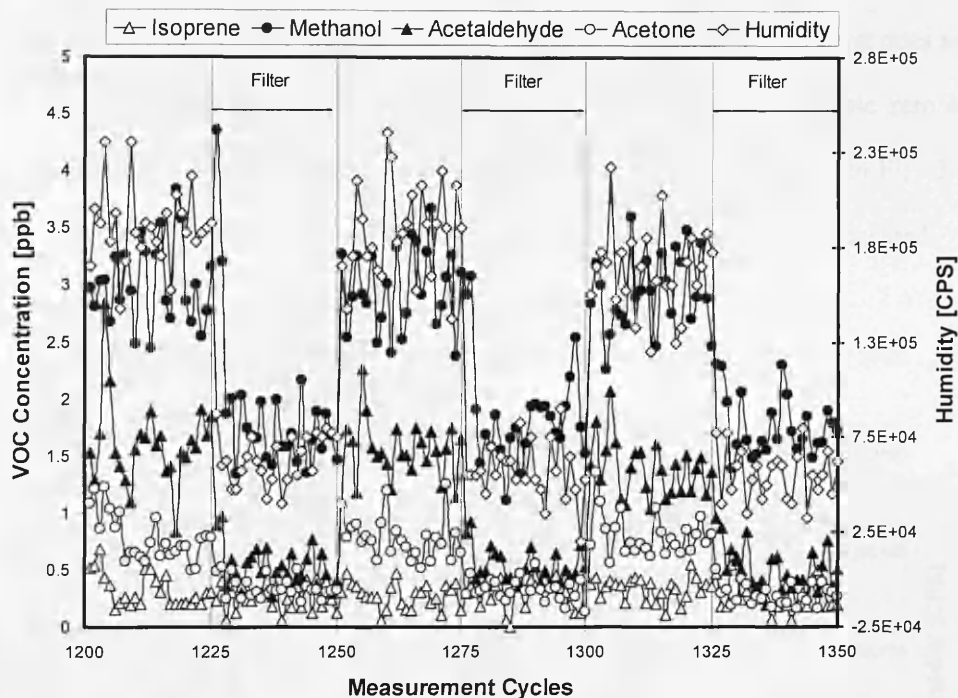


Figure 2.5 VOC concentrations measured with and without a molecular sieve filter placed inline

The charcoal filter performed less well and only removed acetaldehyde and methanol and worryingly increased the concentrations of acetone and water vapour. The silica gel also showed signs of contamination as concentrations of methanol and acetone measured through the filter exceeded that of the laboratory air.

Each of the filters tested affected the concentration of m/z 39, the H_3O^+ water cluster, by either stripping the water vapour or in the case of the charcoal filter, adding humidity. It is important that the humidity of the zero air be the same as the sample air as large variations can lead to an erroneous measure of the instrument background. On this basis an alternative method was tested. A glass tube packed with platinum powder catalyst was heated to 200°C and sample air was pushed through at a flow rate of 600 ml min^{-1} by a small pump. As the catalyst reaches the set temperature VOCs become oxidised by the powder and are removed from the air stream. Air for analysis by the

PTR-MS was cooled using a peltier system and then sub-sampled from the outflow at a flow rate of 300 ml min^{-1} . Unlike the previous filters, the platinum catalyst does not affect the humidity of the sample air; therefore it was chosen as a suitable zero air source in this work. The performance of the platinum catalyst is shown in Fig. 2.6, where acetone, methanol and water vapour (m/z 37) concentrations were measured.

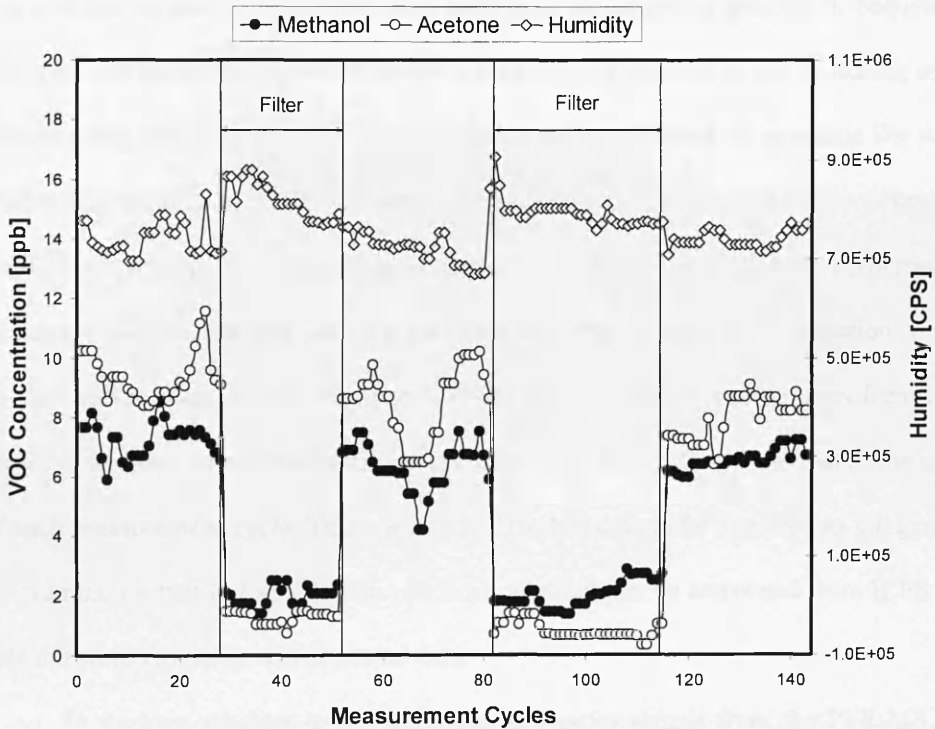


Figure 2.6 VOC concentrations measured with and without a platinum catalyst placed inline.

2.1.3 The PTR-MS control software

The Quadstar control software (Balzers GmbH) that shipped with the PTR-MS used during this study allows the user to operate the instrument in a number of different modes. VOC can either be measured in a selective ion mode, where a measurement file (mip) can be created to measure a predetermined suite of masses, or in a mass scan mode, where the entire mass range will be measured sequentially. In each mode data is outputted in an ASCII format and VOC are recorded as ion counts

per second (CPS). In order to convert the data into meaningful concentrations, data must be further manipulated outside the Quadstar software in what can be a time consuming process. In order to avoid this and also to allow the simultaneous data acquisition of both the PTR-MS data and wind speed data to a single file, an alternative approach was developed. Within the Quadstar software exists a function that enables the user to write text based command sequences (Appendix I). Sequence files can contain instructions such as the activation of a mip file or the switching of a sample valve and allow the PTR-MS to become fully automated. A sequence file was written that enabled the PTR-MS data to be exported to the data acquisition software LabVIEW using the “dynamic data exchange” (DDE) protocol. DDE is a Microsoft Windows based technology which allows data to be passed between applications on a client – server basis, where the client (LabVIEW) continually requests data from the server (Quadstar) who subsequently sends or “pokes” new data to the client at the end of each measurement cycle. This allows the PTR-MS data to be exported to a logging programme written in LabVIEW in real time, where it can be converted from ICPS to ppb and stored together with the wind data.

In the past attempts have been made to transfer signals from the PTR-MS to the operating system using either optical interface cables (very costly), by wiring the output into the A/O of the sonic anemometer (technically demanding and introducing additional uncertainty due to digital-analogue conversions), or where PTR-MS and wind data were recorded on different PCs with different clocks. The DDE approach utilises existing software, so its application comes at no added cost, and no external hardware or wiring is required, making it simple to setup and use and an ideal choice for this study.

2.1.4 *Maintaining optimum secondary electron multiplier operating voltage*

Protonated VOCs and their fragment ions are detected as ion counts by a secondary electron multiplier. During the measurement process the surface of the SEM gradually degrades and thus the sensitivity of the instrument is reduced. To compensate for this drop in sensitivity, the voltage supplied to the secondary electron multiplier (SEM) may be periodically increased to maintain optimum instrument sensitivity. Should the voltage supplied to the SEM be set too low then the ratio of $\text{VOC:H}_3\text{O}^+$ will change and result in a large underestimation of the true ion count. Conversely, if the operating voltage is set too high both the signal to noise ratio and the operating life of the SEM will be reduced (Wilkinson, 2006). Therefore it is necessary to ascertain and maintain the correct operating voltage throughout any measurement campaign.

The operating voltage of the SEM was tested routinely during each measurement campaign using a programme developed in LabVIEW and Quadstar. Firstly a sequence file written in Quadstar was used to activate a 3-way solenoid valve which flicked between the VOC sampling line and a 5 litre Tedlar bag filled with breath isoprene. Next, the sequence set the SEM voltage to 2000 V before measuring the primary ion (m/z 21) and isoprene (m/z 69) counts for a period of 10 cycles. Upon completion of the cycles, the sequence file increased the SEM voltage by 50 V and the measurement process was repeated. The SEM voltage continued to be ramped up in 50 V increments until the maximum operating voltage of 3500 V had been reached (NB – the 2000-3500 V range was applied for the Pfeiffer SEM and a 1400 – 2500 V range was applied for the Mascom SEM). Measured ion counts were transferred to a LabVIEW logging programme using the DDE application described above. Here, m/z 69 counts were converted to mixing ratio of isoprene in ppb and the average ratio of

the signals at m/z 69 and m/z 21 over the 10 cycles measured at each operating voltage was calculated. The results were then plotted on screen in “real time” which allowed the user to quickly ascertain the optimum operating voltage with a minimal disruption to the flux measurement process as shown in Fig. 2.7.

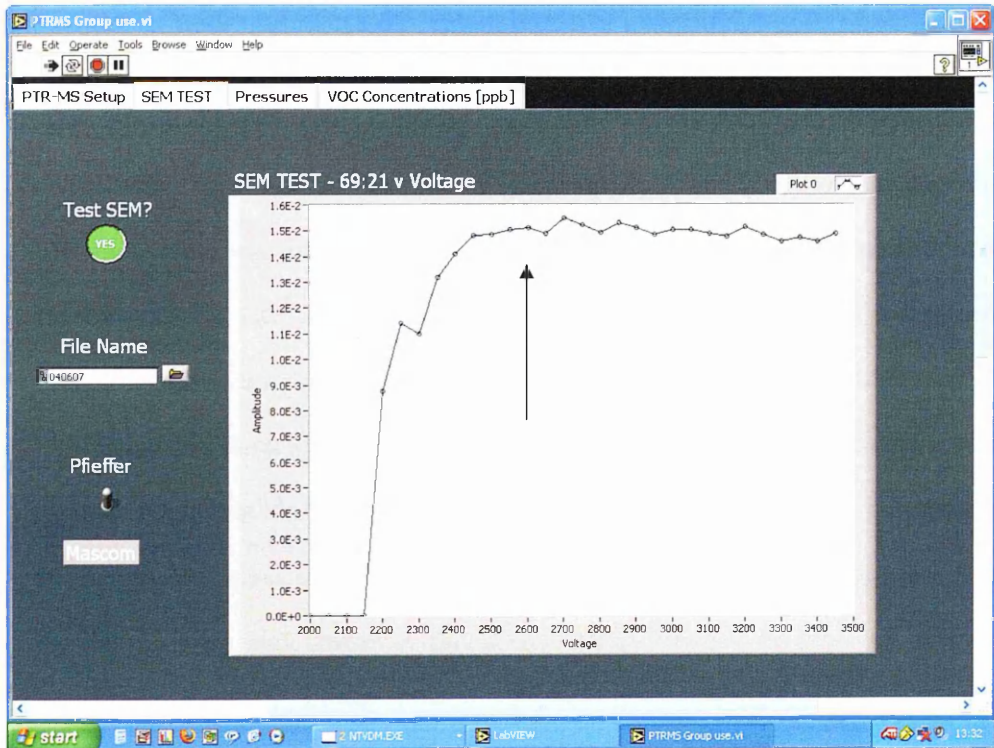


Figure 2.7 Screen-shot from the LabVIEW logging software showing the result from an SEM test of a relatively new SEM. The point at which the ratio of m/z 69 to m/z 21 begins to plateau is considered to be the optimum operating voltage. Therefore in this case the SEM voltage was adjusted to 2500 V.

2.2 Disjunct eddy covariance – concept and design

The flux of VOC between the land surface and atmosphere is carried by the motion of turbulent eddies. These eddies span a wide frequency spectrum, with both large and small fluctuations contributing to the transport, thus the total flux is spread across this spectrum. In order to accurately quantify the VOC flux it is therefore necessary to resolve the entire spectrum of frequencies that contribute to the vertical flux within the flux calculation. In practice this may not be possible for two reasons:

firstly even the fastest responding analytical sensors are restricted to measurement speeds of several Hertz and, secondly, contributions from lower frequency eddies may be of the order of hours, which can result in the inclusion of non-stationarities. Therefore all flux measurement systems are in effect bandwidth limited and thus for accurate flux estimates to be made it must be ensured that the section of the turbulence spectrum being measured is responsible for carrying the majority of the flux. This “flux carrying” bandwidth is not fixed and tends to vary as a function of measurement height, wind speed and atmospheric stability with high frequency flux contributions becoming more important as the measurement height approaches the surface, wind speed increases and during increasingly stable conditions. Currently the eddy covariance method is the technique that offers the widest flux bandwidth due to the high frequency sampling rates used. However, the disjunct eddy covariance method can match this provided a good approximation of the frequency spectrum is obtained. In order to do this sample air must be acquired at the same rate as in eddy covariance, thereby resolving high frequency flux contributions. This can be achieved in one of two ways, either by measuring it directly at a fast rate (i.e. EC) or by rapidly capturing a grab sample of air which can be analysed offline. Repeating this process at regular intervals throughout the averaging period results in a statistically robust approximation of the frequency spectrum from which a flux may be calculated.

2.2.1 Theoretical testing of the DEC concept

The disjunct eddy covariance technique can be tested theoretically using a subset of a quasi-continuous eddy covariance time series. Extracting data points at regular intervals from the EC data file can simulate a disjunct time series and by increasing or decreasing the number of data points used in the flux calculation it is

possible to assess the statistical error introduced through the use of a discrete time series.

A programme was written in LabVIEW to read in 30 minute quasi-continuous EC data files and calculate the flux of sensible heat. The programme then recalculated the flux extracting single data points every 1 s (20 data points at 20 Hz or 10 data points at 10 Hz), 3 s, 5 s, 10 s, ... 55 s and 60 s. The results are summarised in Fig. 2.8 as a scatter plot and detailed in full in Table 2.1. It becomes apparent that as the disjunct sampling intervals are increased and the number of data points used in the flux calculation becomes fewer, the uncertainty in the individual measurement is increased. However, despite the wider spread of the data, the mean remains unchanged as errors either side of the mean cancel, hence comparison of the sum of the fluxes measured by EC with those measured by DEC results in a bias of typically less than 2%, even at intervals as long as 60 s.

Table 2.1 Analysis of the effect of using the disjunct eddy covariance sampling protocol. Here it is shown that although the correlation coefficient becomes reduced as the disjunct sampling intervals (DSI) are extended, no systematic bias is introduced to the flux, as shown by the gradient of the line (*m*) which was obtained from scatter plots of EC and DEC flux measurements and compared to the assumed 1:1 relationship.

<i>DSI</i> [s]	1	5	10	15	20	25	30	35	40	45	50	55	60
R²	1.00	0.97	0.93	0.90	0.85	0.81	0.79	0.80	0.71	0.71	0.69	0.63	0.63
m	1.00	0.99	1.00	1.04	0.98	1.05	1.00	1.02	0.96	1.09	1.11	1.00	1.01

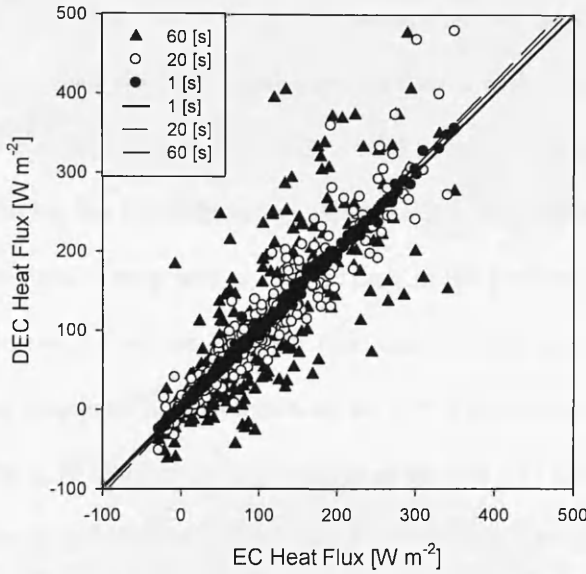


Figure 2.8 The relationship between a set of eddy covariance sensible heat fluxes and disjunct eddy covariance sensible heat fluxes with differing disjunct sampling intervals.

Figure 2.9 illustrates the linearity of the relationship between the statistical uncertainty of the flux measurement, in this case shown as standard deviation, and increasing disjunct sampling intervals. This relationship has been tested at a number of different measurement heights and the results always yield a linear regression line.

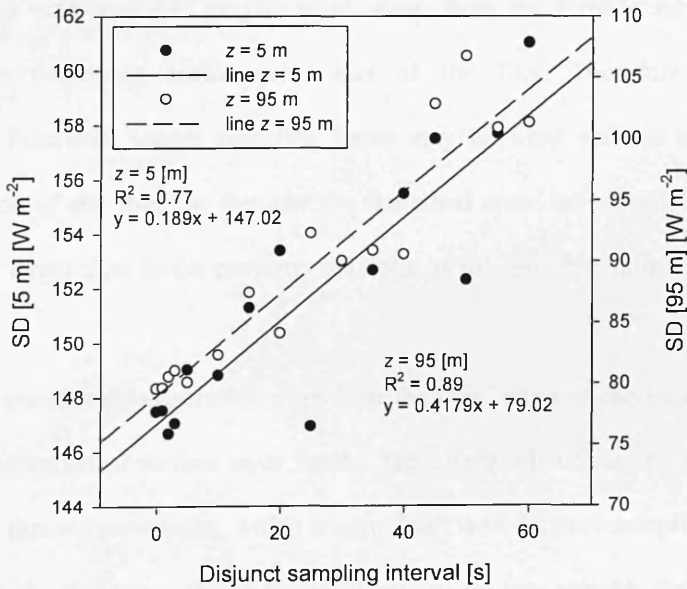


Figure 2.9 Evaluation of disjunct sampling intervals shows an increase in standard deviation (SD) of the calculated heat fluxes [W m⁻²] measured at heights of 5 and 95 m as the disjunct sampling interval is increased. A linear relationship holds for a range of measurement heights (z).

Further theoretical tests were applied to each data set to investigate the effect of decreasing the speed at which a grab sample of air is collected (i.e. decreasing the grab sample time from 0.05 s, to 0.1 s, 0.2 s or 0.5 s etc). In practice this is simulated by simply averaging the EC temperature data over 2, 4 or 10 data points, rather than picking out individual data points as was the case in the previous example. In theory the flux will be reduced as the effective flux measurement bandwidth is shortened, therefore higher frequency flux contributions are lost. This process can be clearly seen occurring in Fig. 2.10 which plots the gradient of the line (m) applied to scatter plots between EC fluxes and simulated DEC fluxes measured at a height of 5 m. Here, m , which should be equal to one if there is no flux loss, is systematically reduced as the grab sample time increases and at longer integration times the error becomes larger than the random statistical error introduced by the DEC sampling protocol.

Applying this procedure to a second set of EC data recorded at a height of 95 m (Fig. 2.11) demonstrates how the bias scales inversely with height. This is because the mean eddy size increases as you move away from the Earth's surface, which means higher frequency eddies carry less of the flux. Therefore, at higher measurement locations, longer sampling times may be used without a significant underestimation of the flux. At this site the statistical error introduced by the DEC approach was larger than in the previous example, as the absolute value of the fluxes was smaller.

These numerical experiments show how the DEC concept can be used to give a good approximation of surface layer fluxes. The increased statistical uncertainty in the individual flux measurements, which is associated with disjunct sampling intervals of a few seconds or more, suggest the technique to be less suitable for measuring accurate individual 30-minute fluxes than EC. However, in situations where an

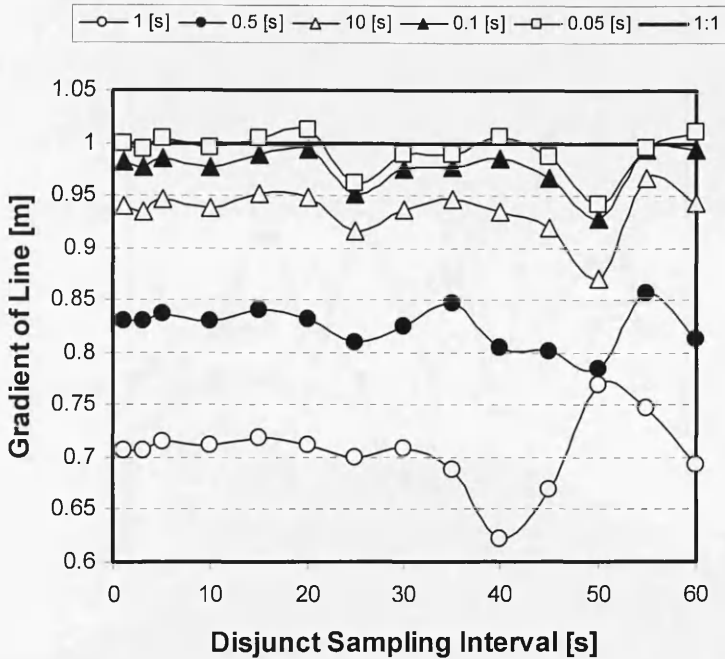


Figure 2.10 The relationship between eddy covariance and disjunct eddy covariance fluxes measured at a height of 5 m (Castelporziano, Italy). DEC fluxes were calculated using different grab sampling times (0.05, 0.1, 0.2, 0.5 and 1 s). DEC fluxes are systematically biased towards lower values at longer sampling times as higher frequency flux contributions are attenuated and lost.

estimate of the net exchange occurring over a day, week, month etc. is required (i.e. an inventory approach) the uncertainty associated with individual measurements is averaged out, and an approximation of the flux can be given to within a few percent of the “true” (EC) value. It should be noted, however, that typical difference between fluxes measured with two collocated EC systems already tends to differ by typically 15-25%, due to statistical horizontal variability of turbulence (Wilson & Myers, 2001).

The study has also demonstrated that the effective response time (i.e. grab sample time) of the sampling system is likely to be a larger source of bias than the use of a discrete time series for the flux calculation at lower measurement heights.

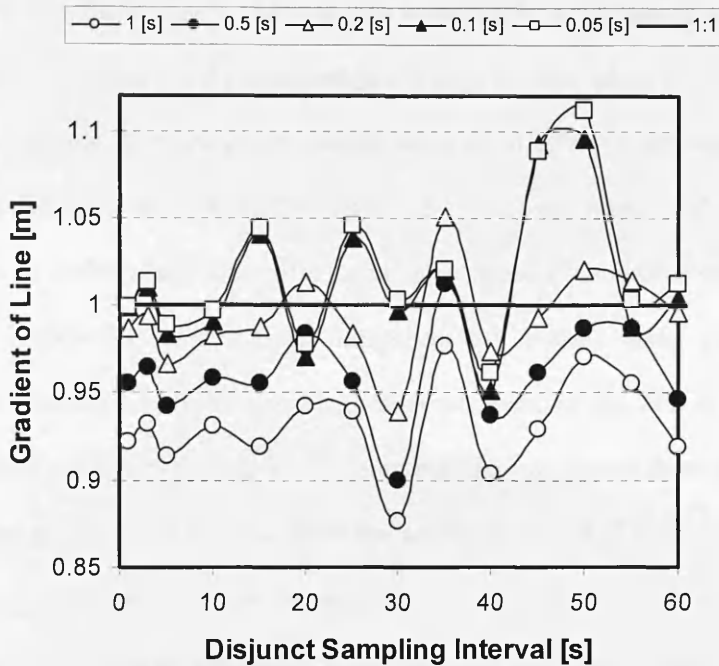


Figure 2.11 The relationship between the sum of eddy covariance and disjunct eddy covariance fluxes measured at a height of 95 m. DEC fluxes were calculated using different grab sampling times (0.05, 0.1, 0.2, 0.5 and 1 s). DEC fluxes are systematically biased towards lower values at longer sampling times as higher frequency flux contributions are attenuated and lost.

Therefore, steps should be taken to minimise the time taken to acquire a grab sample of air and thus maximise the flux bandwidth of the technique.

2.3 The disjunct flux sampler

In order to measure VOC fluxes using the PTR-MS, a disjunct flux sampling system (DFS) was constructed following the design outlined by Rinne *et al* (2001). The DFS comprised two stainless steel canisters which acted as intermediate storage reservoirs (ISR) for sampled air. The canisters were cylindrical in shape in order to reduce surface area and limit losses of VOC to chamber walls. Furthermore heater cable was applied to each canister to maintain a temperature of 40 °C which prevented condensation forming within the sampling system. In order to rapidly capture grab samples of air, ISRs were first evacuated to a low pressure (150 – 300 mbar). The

solenoid valve fitted to each ISR was then activated for a fraction of second to allow the canister to pressurise. As illustrated previously, the time taken for the ISR to reach ambient pressure is an important consideration as in effect it determines the lower limit of the flux bandwidth. Therefore fast switching high conductance valves (Lucifer, E121K45, Parker-Hannifin Corporation) were fitted to each canister, as their 11 mm orifice decreased sample times from 0.8 s when using standard valves (Lucifer, Hycontrol Ltd) to 0.5 s. The design schematic of the DFS is shown in Fig. 2.12. The DFS has two independent sampling channels to optimise the number of samples that can be taken throughout the averaging period. Thus as one channel is being evacuated the other can be analysed by the PTR-MS and vice versa. This approach helps to reduce the statistical uncertainty in the measurement.

Before the system was deployed in the field it was first optimised in a series of laboratory tests.

2.4 Laboratory Testing

The disjunct eddy sampler (DFS) is a passive air sampler designed to take almost instantaneous (0.1 - 0.5 s) grab samples of air at regular intervals. As mentioned previously, sample air is taken on two separate channels in order to maximise the number of samples taken during a set averaging period. While one channel is sampling the other is being evacuated and vice versa. This multiple channel setup, although beneficial to the statistical robustness of recorded data, has the potential to introduce mixing and dilution errors between samples in those areas where valves and pipe work interconnect the two channels. Such mixing effects are already present within the system due to the ~10% carryover between samples which occurs due to the incomplete evacuation of the intermediate storage reservoirs (ISRs). This

memory effect between samples has been shown to result in a $\sim 4\%$ underestimation of the flux (Rinne *et al*, 2001). Mixing, or the dilution of samples between the two channels, should not occur in an air tight system, with this in mind a simple experiment was designed to test the independence of the two channels and the validity of the system as a whole.

The DFS was setup under “normal” operating conditions; intake valve switching set for 0.5 s opening (the minimum time required for an evacuated ISR to be pressurised to ambient level), and sample analysis time (disjunct interval) set to 12-15 s. The latter parameter being variable depending upon the number of masses under analysis and the dwell (analytical time) set for each mass.

A Tedlar® bag filled with breath isoprene was attached to the intake valve of one channel, the other left open to ambient air. A short length of $\frac{1}{4}$ ” PTFE tubing connected the bag to a manually operated 2-way solenoid valve (Swagelok, Manchester Fluid Systems), with a further inlet line connected directly to the DFS and the other line to the PTR-MS instrument. Such a setup allows the PTR-MS to freely switch between analysing the air within the Tedlar® bag and the air from the DFS.

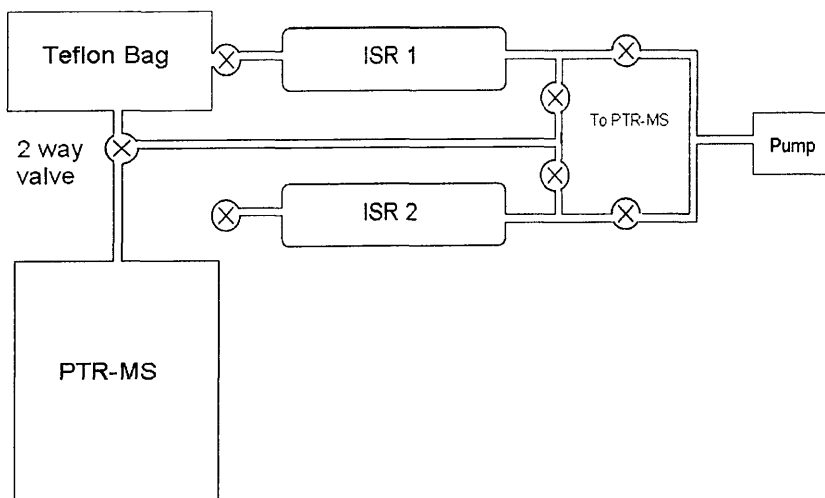


Figure 2.12 Schematic of the disjunct eddy sampler and experimental setup. Crossed circles represent computer automated switching valves and red circles areas of the system where the two independent channels converge.

The results of the experiment are shown in full in Appendix III and are briefly summarised here. Figure 2.13 shows the testing of the disjunct flux sampler (channel 2) after optimisation. Mixing ratios of isoprene measured from the bag and DFS are similar, indicating the system to be well sealed. Surprisingly, isoprene concentrations measured from the DFS are slightly elevated over concentrations measured directly from the bag. This is thought to relate to changes in drift tube pressure and is discussed further in section 2.4.1.

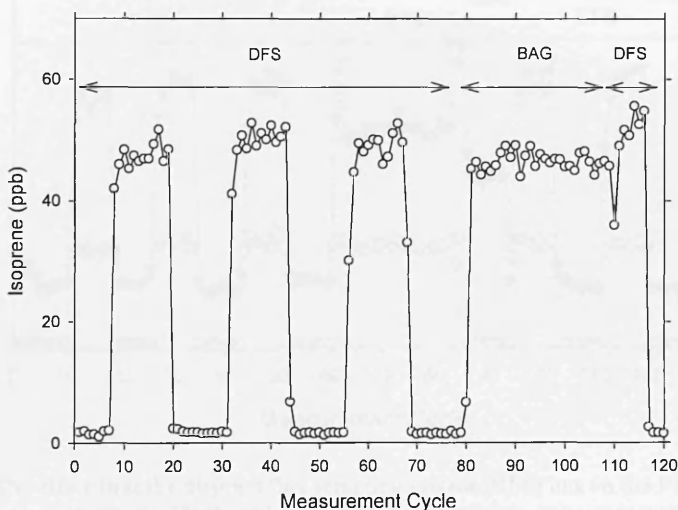


Figure 2.13. Results from a leak test carried out on Channel 2 after the reorientation of valves 3 and 6. Concentrations now being representative of that of the bag indicate an air tight system.

2.4.1 Effects of changing drift tube pressure

Under normal operating conditions the PTR-MS is set to a specific Townsend ($T_d = \text{Townsend}$; $1 \text{ Td} = 10^{-17} \text{ V cm}^2 \text{ mol}^{-1}$). The Townsend is a measure of E/N (where E is a measure of the electric field strength and N the number density of the buffer gas) within the drift tube (Tani *et al.*, 2003). The Townsend is controlled by a number of parameters such as drift tube temperature, drift tube electric field and drift tube pressure, thus any changes in these parameters will result in a changing E/N ratio. The E/N ratio of the PTR-MS has been shown to be an important factor in the fragmentation of monoterpenes such as α - and β -pinene under certain humidity

conditions and water vapour pressures and controls the dissociation of the water clusters (Tani, *et al.*, 2003). It therefore becomes an important consideration to monitor the E/N ratio when such monoterpenes are under investigation.

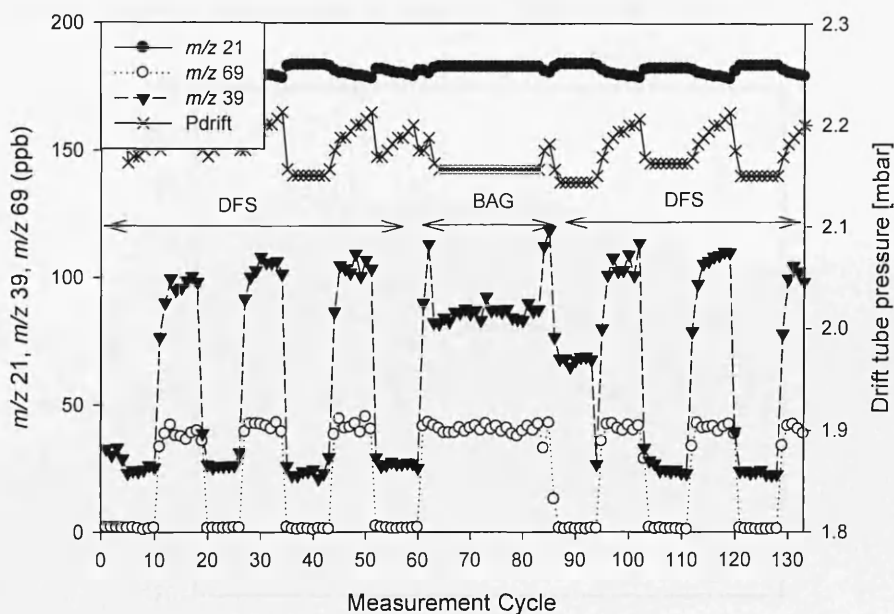


Figure 2.14 The effect that the disjunct flux sampling system (DFS) has on the PTR-MS drift tube pressure (crosses) is clearly illustrated, which in turn impacts upon measurements of m/z 21 (closed circles), m/z 39 (closed triangles) and m/z 69 (open circles).

During sampling with the DFS system, a slight back pressure is created as the PTR-MS draws air from the intermediate storage reservoir for analysis, as shown in Fig. 2.14. The volume of air taken from the canister during the analysis period is small but sufficient to see fluctuations in drift tube pressure which coincide with the channel valve switching, which in turn cause fluctuations in the E/N ratio to as much as 4-5 Td as shown in Fig. 2.15. It is clear that as the drift tube pressure increases, the E/N ratio decreases, which reduces cluster dissociation in the drift tube and explains the increased concentrations of m/z 39 ($\text{H}_3\text{O}^+(\text{H}_2\text{O})_n$) measured by the DFS relative to that observed in the bag. In order to curtail this problem, two steps were adopted during

field operation to minimise the volume of air that needed to be taken from the ISRs during analysis. Firstly the length of tubing linking the PTR-MS to DFS was kept as short as possible and the diameter of the tube reduced to 1/8". Secondly the flow rate of the PTR-MS was reduced from 300 ml min⁻¹ to 150 ml min⁻¹ which effectively reduced the observed backpressure by 50%.

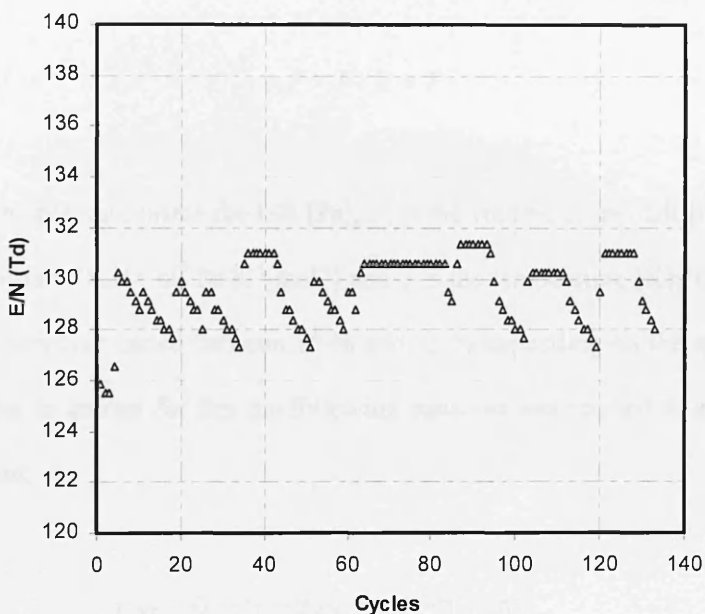


Figure 2.15. Fluctuations of the E/N ratio as a result of changing drift tube pressure due to the operation of the DFS system. Initial operating conditions were set at 125 Td but rose to an average of 129 Td.

2.4.2 Correction for sample carry-over

The carryover of sample air between one ISR grab sample and the next is a potential source of error within the DEC measurements and therefore a correction factor is necessary. The volume of residual air in each ISR is dependent on both the strength of the pump used to evacuate the ISR and the time available for evacuation and is typically in the region of 150 – 300 mbar. The effective carryover is also influenced by the volume of air in the ISR when full, which under certain conditions may not always equate to the 1000 mbar ISR volume. Such scenarios present themselves when an inadequate sampling time is used (< 0.5 s) or when it is not

possible to mount the DFS on a mast, therefore valves are teed directly into a sample line which may be subject to a large pressure drop (~200 mbar). In order to express the carryover between one ISR sample and the next in terms of a percentage, it is first necessary to calculate the amount of air contained within the ISR when both full and empty. In order to do this the ideal gas law was rearranged to give:

$$\eta = P \times V / R \times T \quad (2.3)$$

where P is the pressure inside the ISR [Pa], V , is the volume of the ISR [m^3], R is the ideal gas constant [$8.314 \text{ m}^3 \text{ Pa K}^{-1} \text{ mol}^{-1}$] and T is the temperature [K]. Typically the percentage carryover varied between 15 % and 35 % depending on the system setup used. In order to correct for this the following equation was applied to all measured concentrations.

$$\chi_{corr} = (\chi \times \eta_1 - \chi_{old} \times \eta_2) / (\eta_1 - \eta_2) \quad (2.4)$$

where χ is the concentration within the ISR, χ_{old} is the previous concentration of the same ISR, η_1 is the amount of air within the ISR when full and η_2 is the amount of air within the ISR when evacuated.

2.5 Field testing – evaluation against EC

In order to evaluate the performance of the newly developed disjunct flux sampling system, it was tested under field conditions against an existing eddy covariance setup. Although the DFS is a system designed to measure the fluxes of VOC, for a direct comparison to be made with the EC technique, test compounds

which are measurable by both techniques must be used. For this reason the DFS was setup to measure the fluxes of both carbon dioxide and water vapour, and the results were compared with those measured from an eddy covariance system which operated close by.

2.5.1 Field experiment and setup

During October 2005, CO₂, H₂O and sensible heat fluxes were measured from the Easter Bush field site near Penicuik, Edinburgh (3° 12' W, 55 ° 52' N). The site is situated on the boundary line (running NW to SE) between two intensively-managed grasslands and has a fetch of approximately 200 m in the main SW and NE wind directions (Fig. 2.16). Both fields are grassland and are predominately composed of Ryegrass (*Lolium perenne*) which accounts for over 90% of the species present. Due to the nature of the surrounding topography, with the Pentland Hills to the northwest, the wind is predominantly channelled in either a south westerly (27.1 %) or north easterly (69.4 %) direction, allowing micrometeorological flux measurements to be made in one field or the other for 96.5 % of the time, as the boundary line separating the two fields is orientated in a NE-SW direction. The history and management of both fields is very similar. More details have been provided by Marco *et al.* (2004).

An ultrasonic anemometer (Solent Research R3, Gill Instruments Ltd, Lymington, Hants, U.K.) and the disjunct flux sampler were mounted at a height of 2.1 m above ground level (Tower [A]), 3 m from an existing eddy covariance system which operated at a similar height (Tower [B]). Concentrations of CO₂ and H₂O were measured by a closed path infrared gas analyser (IRGA, Model 7000, Li-Cor). The

IRGA has a response time of >10 Hz making it suitable for both the eddy correlation and the disjunct eddy correlation method, allowing a direct comparison to be made.

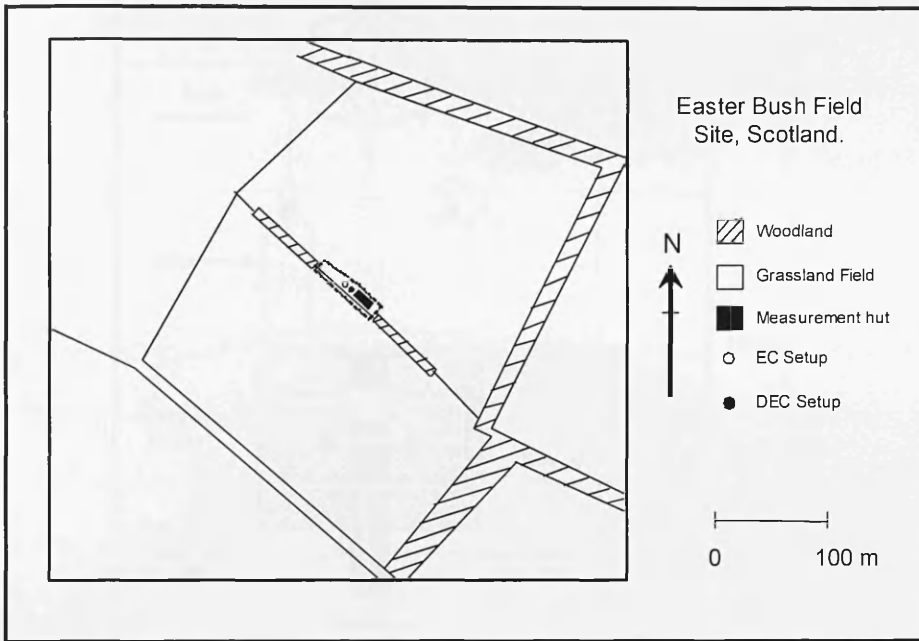


Figure 2.16 Diagram of the Easter Bush field site adapted from Marco *et al* (2004). A fetch of 200 m exists in the north east and south westerly directions which are also the predominant wind sectors.

2.5.2 Disjunct Flux Sampler - setup

The sampler was mounted vertically below the ultrasonic anemometer at a measurement height of 180 cm, with a 30 cm separation between inlet valves and anemometer. This location was chosen as vertical displacement of the chemical sensor or air intake to the bottom leads to the smallest flux loss (Kristensen *et al.*, 1997). Solenoid valves and pipe work were mounted on a perforated metal sheet minimising the disruption of airflow around the sampler. Two rain shields protected the inlets from precipitation, while a fine wire mesh stopped foreign bodies entering the valves.

As one ISR was evacuated the other was analysed by the IRGA. As air is drawn from the ISR, a pressure drop is created which can affect the sensitivity of the IRGA despite the built-in pressure correction. With this in mind the IRGA was placed

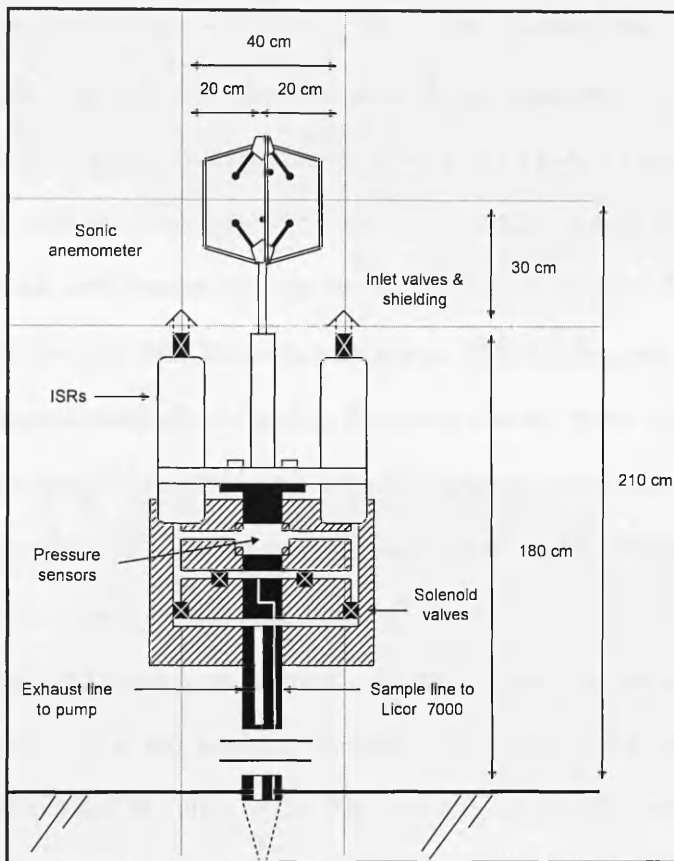


Figure 2.17. Schematic of the disjunct flux sampler setup at the Easter Bush field site in Scotland.

directly below the DFS and connected using a short length of 1/8" PTFE tubing, minimising the volume. Furthermore, the internal pump of the IRGA was run at a relatively low flow rate and plumbed to be upstream of the measurement cell, which therefore was kept at ambient pressure, thus reducing the effect of the canister vacuum. The DFS was set-up in such a way that the sample line to the IRGA alternately sampled from the two ISRs. To ensure the independence of each grab sample, an average of only the last 50 data points (the last 5 s) was used. This way the effect of inter-channel mixing within the sample line was minimised.

The solenoid valves used to initiate the sampling and analysis phases of the disjunct sampler were controlled by a programme written in LabVIEW™ (version 6.1,

National Instruments). Although the inlet valves had a response time of 10 ms, the sampling time was limited by the time taken for the canister to fully pressurise, therefore the sampling and analysis times were set to 0.5 s and 15 s respectively. Two small silicon pressure sensors (OMEGA®, PX137-015DV) were fitted in-line, one behind each ISR, and ensured canisters were consistently evacuated to a minimum of 0.15 bar. The raw data from the sonic anemometer, IRGA and pressure sensors were logged for post-processing and filtering. Preliminary online fluxes of sensible heat, CO₂ and H₂O were calculated for the purposes of quality control, allowing potential system errors to be spotted during the initial stages of the study. Other meteorological data such as wind speed and direction were also recorded.

As the inlet valves were activated, and the grab sample taken, the values of wind vectors u , v , w and potential temperature (T) were recorded for the flux calculation (Eq. 1.6) The filling of the ISRs was considered to be instantaneous and concentrations were combined with the wind data at the time the valves were activated, resulting in a zero time lag.

2.5.3 Eddy covariance - setup

Eddy-covariance measurements were performed on a second, independent tower and combined measurements with a sonic anemometer (USA-1, Metek GmbH) and a second IRGA (also LiCor 7000). Flux calculations were performed according to the CarboEurope IP methodology (Aubinet *et al.*, 2000). The measurements have been described in more detail by Campbell *et al.* (2006).

2.5.4 Results and Discussion

2.5.5 Concentrations

Figure 2.18 shows the concentrations of CO₂ and H₂O, measured by the two infrared gas analysers. During the experiment technical difficulties with both the EC IRGA and the DFS, meant the overlap of the two data sets was restricted to just 3 days. During this time there appeared to be no significant or prolonged drift in the CO₂ analysers and concentrations were in good agreement, with an R² value of 0.72. On the 15th, between 13.00 hrs and 14.30 hrs CO₂ concentrations measured by the DFS IRGA were significantly higher than those measured by the EC IRGA which can explain the reduced R² value. The cause of this deviation is unclear, one possible explanation might be the fluctuation of air pressure in the IRGA sampling line which is caused due to the incomplete pressurisation of ISRs, this is however unlikely, as the H₂O concentration remained unaffected. During the 3 days CO₂ concentrations were typically around 380 ppm, but dropped to a minimum of 369 ppm during the day time when photosynthetic activity removed CO₂ near the surface and a maximum of 402 ppm at night, when night-time respiration accumulates in the shallow nocturnal boundary layer.

The EC IRGA had not been recently calibrated for H₂O. The lack of calibration meant there was a systematic offset in H₂O concentrations, however, the range of the data was very similar to that measured by the calibrated DEC IRGA, therefore after mean removal for the flux calculation, the two data sets compared very well, with an R² value of 0.92, indicating that the difference in the calibration was due to different zero calibrations and that the span calibration agreed well. Clear diurnal trends were apparent in both data sets with a typical midday maximum of around 1.2 kPa, an average concentration of 0.9 kPa and a night time low of 0.5 kPa.

2.5.6 Comparison of EC sensible heat fluxes

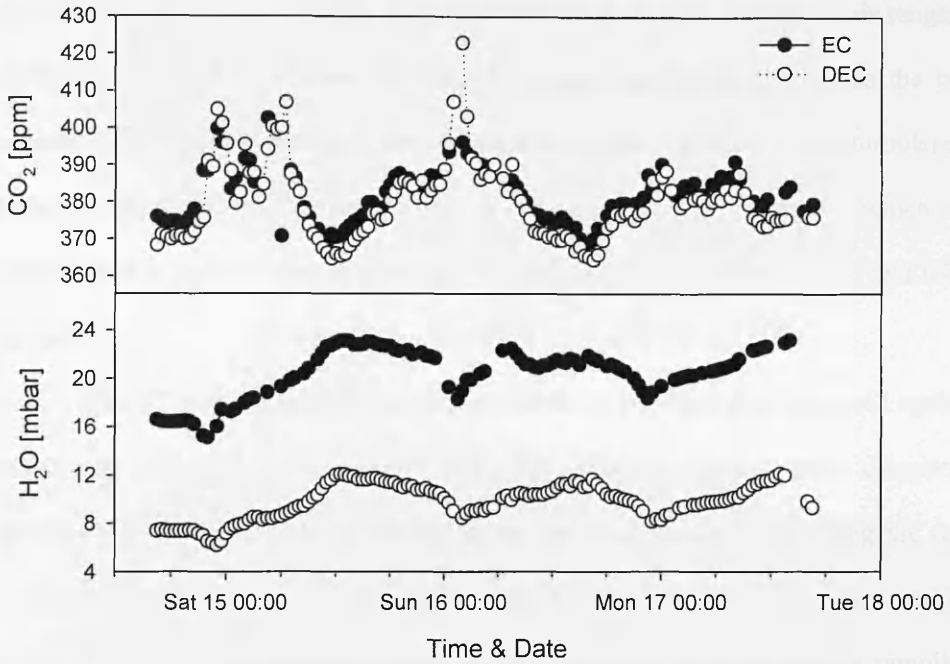


Figure 2.18 CO_2 and H_2O concentrations measured using an IRGA for both the eddy covariance and disjunct eddy covariance flux measurement techniques at the Easter Bush field site.

In a well adjusted surface layer, over a horizontal patch of surface, an equilibrium boundary layer may form in which the flux above the surface remains constant with height (Fowler *et al.*, 2001). However, due to the spatial variation of turbulence, the flux may vary considerably in the horizontal (Wilson & Meyers., 2001). Therefore it is important to assess how spatial variability may impact on the comparison of the two systems. In order to do this sensible heat fluxes, which were measured using the direct EC technique at both tower [A] and [B], were compared. During the experiment, the trend of measured fluxes were in reasonable agreement, and had an R^2 value of 0.65, however the average of fluxes measured at tower [A] underestimated those measured at tower [B] by approximately 32%. Some of this underestimation may be attributed to the different measurement resolutions of the two systems. The sonic anemometer mounted on tower [B] operated at 20 Hz, twice the rate of the sonic anemometer at tower [A], allowing flux contributions from very high frequency eddies to be resolved which may have been missed by the slower resolution

anemometer. However, the percentage contribution of the flux carried in this range is unlikely to exceed more than 5%. Thus the remaining difference between the two systems is most likely related to the statistical horizontal variation of the turbulence. Importantly, this simple comparison provides an estimate of the uncertainty which can be expected in comparisons of fluxes of CO₂ and H₂O measured by the EC and DEC systems.

The EC sensible heat fluxes measured at tower [A] were also compared against simulated DEC fluxes of sensible heat. The simulated fluxes were calculated according to the methodology outlined in the previous section. Comparing the flux calculated from the original time series with the new disjunct time series can be useful, as it gives an indication of the systematic error introduced by the sampling intervals. It cannot however, offer any information on the systematic and random errors introduced by the sampler itself, such as losses of compounds to walls, or carryover effects from one grab sample to the next.

Data points for the simulated DEC heat flux were picked out from the EC time series to correspond exactly with the moment grab samples of air were taken, approximately every 15 s. This was made possible due to the LabVIEW logging programme which placed a flag next to the data the moment inlet valves were activated. A linear regression of the two data sets showed a good agreement, with an R² value of 0.78, yet the cumulative flux measured by the DEC underestimated those measured by EC by about 11%. In Section 2.2.1 it was shown that the use of a discontinuous data set can cause considerable uncertainty in the flux measurement, however, over a sufficient length of time this error cancels and the cumulative flux gives a very good approximation of the “true” flux. Given the discrepancy between the DEC and EC data sets, it is apparent that the 3 days of measurements presented

here may not have been sufficient to get a good approximation of the cumulative flux. On this basis, DEC fluxes of CO₂ and H₂O could be expected to differ from those measured by EC by a similar magnitude.

2.5.7 Comparison of CO₂ & H₂O fluxes

Figure 2.19 shows the average diurnal fluxes of CO₂ and H₂O measured by both the eddy covariance and disjunct eddy covariance techniques. During the early hours of the morning, fluxes of both CO₂ and H₂O measured by the disjunct method follow closely with those measured by EC. For CO₂, the disjunct method appears to significantly underestimate the flux between the hours of 08:00 and 13:00 hrs. In contrast, fluxes of H₂O remain closely correlated with those measured by EC throughout the day with only minor deviations occurring in the late afternoon between 16:00 and 18:00 hrs.

A correlation between the EC and DEC techniques yielded R² values of 0.72 for 0.69 for H₂O and CO₂ respectively. As expected, the correlation between these two spatially separated data sets is reduced when compared with the co-located theoretical comparison of DEC to EC heat fluxes which yielded an R² of 0.78. Comparing the sum of the fluxes measured by the EC technique with those measured by the DEC technique and expressing the error as a percentage, shows the DEC to underestimate the flux by less than 1% for measurements of H₂O, but by 29% in measurements of CO₂. These values are both within the 32% uncertainty calculated from the sensible heat flux comparison of EC systems which suggest there to be no major systematic or random errors linked to the disjunct sampling device.

The largest source of error associated with the DFS measurements would most likely have been linked to the method of sample collection. The time taken to “grab” a

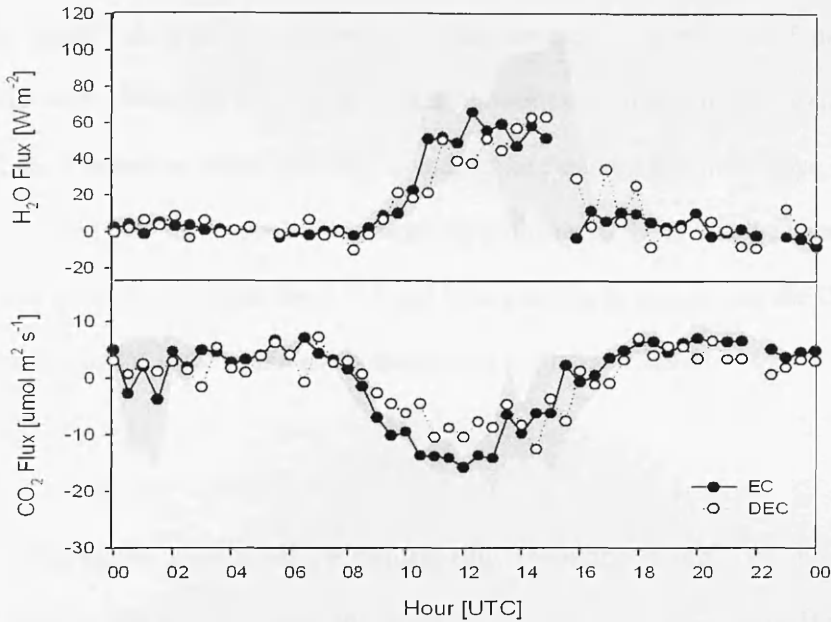


Figure 2.19. Average diurnal profiles of CO₂ and H₂O fluxes measured by the eddy covariance (closed circles) and disjunct eddy covariance (open circles) flux techniques at the Easter Bush field site. Greyed area represents $\pm 1 \sigma$ of the eddy covariance flux measurements.

sample of air was effectively controlled by (i) the pressure of the evacuated ISR and (ii) the diameter of the inlet orifice. During this experiment this time was limited to 0.5 s, giving an effective measurement frequency of 2 Hz, approximately 10 times slower than that of the EC system. This meant the EC system was able to resolve the portion of the flux carried in the range between 10 Hz and 1 Hz, which would have been missed by the DFS. These errors however, are small in comparison with those that arise due to the spatial separation of the two independent flux systems.

2.5.8 Potential experimental improvements

While this experiment persuasively demonstrates that the error between the EC and DEC setup lay within the uncertainty typically found between two independent EC systems, the experiment could have been improved in a number of ways. Firstly,

the duration of the experiment, as demonstrated by the theoretical comparison of heat fluxes, could not establish the long term performance or durability of the DFS. Unfortunately, failure of both the analytical instrumentation and the DFS combined with time restrictions meant this study could not be extended beyond 3 days, leaving only a limited data set from which to make the comparison. Secondly, the comparison would have been even more direct if it had been possible to mount both the DFS and EC systems on the same tower, using data from a single sonic anemometer.

2.5.9 Conclusions

During this experiment the disjunct eddy covariance technique has shown a great deal of promise. Although the fluxes of CO₂ and to some extent H₂O were underestimated, they remained within the calculated uncertainty. The general trends between the two data sets were very encouraging, and may have been improved further had it been possible to implement the changes stated in Section 2.5.8. Although these initial results are very encouraging, much has also been learnt about the practical problems of operating this system in the field. The weight and awkward shape of the DFS make it difficult to mount on a mast. Over a grassland field, at a height of 2 m, such difficulties can be overcome, but for future studies where large masts (20 – 30 m) are to be used further problems present themselves. Firstly, the inlet valves of the DFS require 240 V of mains electricity, which means long lengths of expensive, and more importantly heavy, armoured cable would be required. Secondly, with a large distance between the DFS and gas analyser, sample air must be drawn along a long sample line, which would mean a large volume of air would be drawn from the ISR creating a substantial back pressure which would affect the sensitivity of the gas analyser. Finally, should a technical fault occur with the system, at heights of

20 – 30 m, there would be no opportunity to provide a quick fix, which would mean taking the mast down and subsequently a disruption to ancillary measurements.

2.6 Virtual Disjunct Eddy Covariance (vDEC)

Although field testing of the DFS system proved partially successful, the experiment also highlighted some of the practical difficulties of implementing the technique. Whilst these could be overcome at this low measurement height, it was felt that for future campaigns deployment of the DFS may be problematic. Therefore a second technique, virtual disjunct eddy covariance was investigated as a more practical alternative.

The PTR-MS is capable of returning concentration information on individual VOCs at fast rates, in theory making it ideally suited to the eddy covariance flux measurement approach. In reality, the quadrupole can only filter one m/z at a time; therefore the temporal resolution of the data is governed by the total number of compounds measured. Consequently, rather than outputting a quasi-continuous high frequency data set, an array of measurements is returned as each measurement cycle is completed, in effect creating a disjunct time series of fast (~ 0.2 s) measurements, which are made every few seconds. This process was first adopted by Karl *et al* (2002) who termed it virtual disjunct eddy covariance (vDEC). During their study of VOC emissions from a sub-alpine forest, Karl and co-workers demonstrated that a flux could be calculated using this reduced data-set, provided that the averaging time of each individual measurement was kept sufficiently short (typically 0.2 s). Subsequently this technique has been successfully applied above a range of vegetation types, including grassland fields and forest canopies (Spirig *et al.*, 2005; Lee *et al.*,

2005; Brunner *et al.*, 2007), but it has very rarely been applied to the urban environment.

The setup and operation of the vDEC technique is very simple and consequently vDEC is not logistically limited in the same way as in DEC. Typically sample air is pumped at a high turbulent flow rate (60 l min^{-1}) through a 3/8" OD Teflon line which is mounted directly below the sonic anemometer. Air for analysis by PTR-MS is then sub-sampled from the Teflon line via a 3/8" to 1/8" reducing union tee at a flow rate of approximately 300 ml min^{-1} . The length of 1/8" OD tubing into the PTR-MS is kept to a minimum to reduce the dead volume of air. Operating the system in such a configuration helps to ensure the air in the sampling tube is kept turbulent, which is an important consideration as laminar flow can dampen the VOC signal which will result in the underestimation of the flux. The power consumption of this system ranges between 0.9 and 1.3 kW and is largely determined by the draw from the PTR-MS (0.75 kW) and the type of pump used for the main inlet line which can vary from between 0.19 and 0.56 kW.

During the application of this technique it is not uncommon for there to be a large distance separating the sonic anemometer and the PTR-MS and therefore a significant lag time may exist between the measurements of the vertical wind speed and the acquisition of the corresponding VOC concentrations. In order to correct for this temporal shift, a cross correlation function was developed in LabVIEW which looked for the maximum correlation (R^2 value or product of the covariance) between the vertical wind velocity and the PTR-MS measurements, as in theory a maximum should exist at the moment of zero time lag. This concept is demonstrated in Fig. 2.20 where the results of a cross-correlation function applied to data collected at the Telecom Tower by a PTR-MS and IRGA gas analyser are shown.

In this example, both gas analysers sub-sampled from the same 45 m long inlet line. The disjunct PTR-MS data is noisier than the IRGA data due to fewer data points and lower atmospheric concentrations, but the lag is still clearly identifiable. The

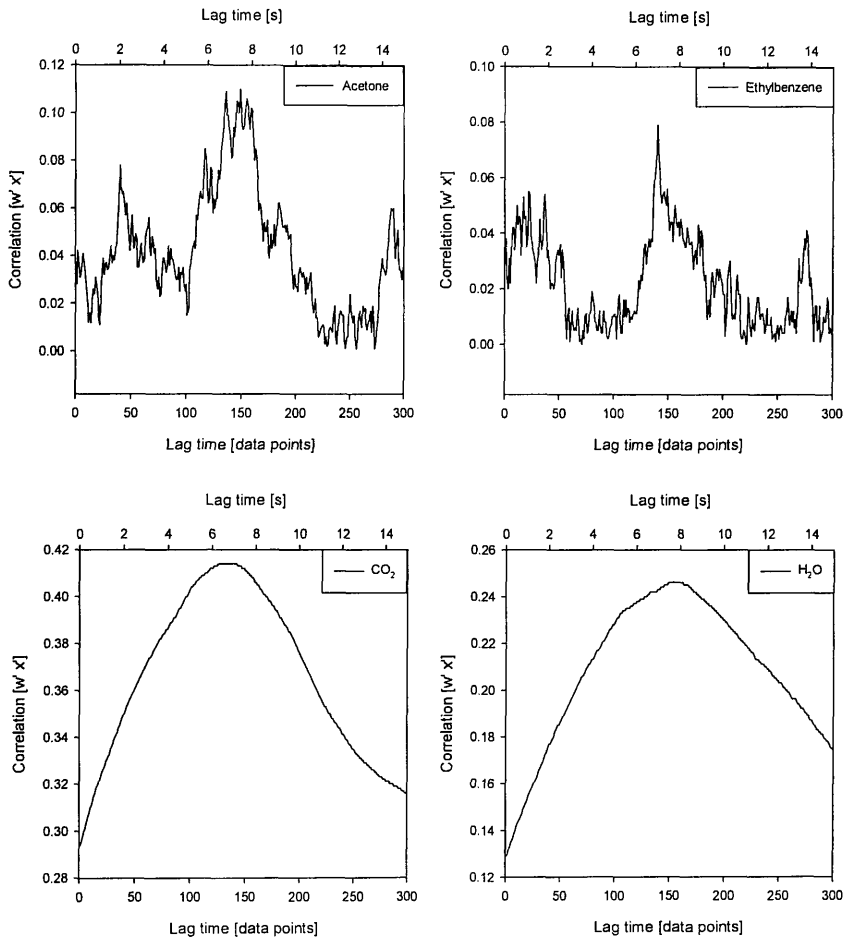


Figure 2.20 Cross correlation analysis applied to data collected at the Telecom Tower by a PTR-MS and IRGA. The disjunct PTR-MS data is noisier than the IRGA data due to fewer data points and lower atmospheric concentrations, but the lag is still clearly identifiable. The IRGA sub-sampled directly after the PTR-MS therefore the lag times agreed very closely.

peak in the covariance function occurs at around seven seconds for both VOCs and CO₂, but for H₂O the peak is broader with a maximum occurring at eight seconds. This delay is typical in water vapour measurements and occurs due to the “stickiness” of the water molecules which adsorb onto the walls of the sample line. Similar behaviour should be expected for some of the more “sticky” VOCs such as methanol

and therefore the vDEC technique may be prone to underestimate the flux for certain compounds.

2.7 Post processing of data

All measured fluxes in this thesis were calculated and filtered to meet stringent quality controls using a programme written in LabVIEW. In brief, this programme, which developed further between each measurement campaign, read in flux data files, applying the standard rotations (Baldocchi, 1993) to the coordinate frame using the following procedure:

$$U_{hor} = \sqrt{V^2 + U^2} \quad (2.5)$$

$$U_{tot} = \sqrt{W^2 + U_{hor}^2} \quad (2.6)$$

$$\text{Cos } \eta = U / U_{hor} \quad (2.7)$$

$$\text{Sin } \eta = V / U_{hor} \quad (2.8)$$

$$\text{Cos } \theta = U_{hor} / U_{tot} \quad (2.9)$$

$$\text{Sin } \theta = W / U_{tot} \quad (2.10)$$

$$U_{corr} = -u \times \text{Sin } \eta + v \times \text{Cos } \eta \quad (2.11)$$

$$V_{corr} = u \times \text{Cos } \theta \times \text{Cos } \eta + v \times \text{Cos } \theta \times \text{Sin } \eta + w \times \text{Sin } \theta \quad (2.12)$$

$$W_{corr} = -u \times \text{Sin } \theta \times \text{Cos } \eta - v \times \text{Sin } \theta \times \text{Sin } \eta + w \times \text{Cos } \theta \quad (2.13)$$

where, U , V and W represent the average 3D wind components averaged over a given flux averaging period (typically 30 minutes) and u , v , w are their instantaneous values. This sets the averages of the vertical and cross-wind components (v and w) to equal zero and therefore ensured errors introduced by tilting of the sonic anemometer were

corrected. Once rotated, data from the sonic anemometer was used to calculate fluxes of sensible heat:

$$H = \overline{w'T'}\rho C_p \quad (2.14)$$

momentum:

$$\tau = \overline{w'u'} \quad (2.15)$$

and frictional velocity:

$$u_* = \sqrt{-\left(\frac{\tau}{C_p}\right)} \quad (2.16)$$

as well as the Monin-Obukov length which is a measure of the height at which mechanical turbulence (wind shear) gives way to buoyant production of turbulence (Stull, 1988). Here K is the von Karman's constant (0.41) and g is the acceleration due to gravity (9.8 m s^{-2})

$$L = \frac{-\rho C_p u_*^3 T}{K g H} \quad (2.17)$$

The average wind speed (WS) was calculated using Eq. (2.18) and averaging periods where the mean wind speed dropped below 1 m s^{-1} were rejected and not included in the final data analysis.

$$WS = \sqrt{U^2 + V^2 + W^2} \quad (2.18)$$

Concentration measurements of VOC in ion counts per second (ICPS) were converted to volume mixing ratios using the following equation (Wilkinson, 2006):

$$VOC_{PPB} = \frac{(RH_i \times 1 \times 10^9 \times p_{std} \times 22400 \times (T_{std} + T_d) \times Trans)}{(k \times t \times M21 \times M37 \times p_d \times 6.022 \times 10^{23} \times T_{std} \times TransRH_i)} \quad (2.19)$$

where RH_i and $TransRH_i$, were the ion count and transmission of the target VOC, T_{std} and P_{std} standard temperature (273.15 K) and pressure (1013 mbar), T_d and P_d , the drift tube temperature and pressure, $M21$ and $Trans$, the primary ion count and transmission number, $M37$, the ion count of the reagent water cluster and k and t , the reaction rate constant and reaction time which had values of $2 \times 10^{-9} \text{ cm}^3 \text{ s}^{-1}$ and $1.05 \times 10^{-4} \text{ s}$ respectively.

PPB values were then converted into $\mu\text{g VOC m}^{-3}$ using the relationship:

$$\chi_{VOC} [\mu\text{g m}^{-3}] = \frac{\chi_{VOC} [\text{ppb}] \times 1E^{-6} \times 1E^6 \times Mr}{\left(\frac{1013 \times 22.4 \times (273 + T_{sonic})}{273 \times p} \right)} \quad (2.20)$$

where M_r was the molecular weight of the target VOC, P was the ambient pressure in mbar and T_{sonic} was the temperature of sampled air as measured by the sonic anemometer. These values were then paired with the associated vertical wind velocity and the flux was calculated using Eq. (1.6). The resultant flux was then multiplied by 3600 s h^{-1} to give a measurement of the VOC flux in units of $\mu\text{g m}^{-2} \text{ h}^{-1}$.

Finally calculated fluxes were subjected to a data quality test whereby each averaging period was tested for non-stationarities. The stationarity test followed the theory outlined by Foken & Whichura (1996), which states that a time series χ is stationary, when the flux (F_χ) is equal to the mean average flux of its components ($F_{\chi1}$, $F_{\chi2}$, $F_{\chi3}$...). Here we took F_χ to be the flux over the averaging periods, and the components $F_{\chi1}$ to $F_{\chi6}$ to be the flux calculated from individual 5 minute blocks of the original time series. Following criteria specified by Velasco *et al* (2005), if the mean

of $F_{\chi l} - F_{\chi 6}$ differed by more than 60% of the value of F_{χ} the time series was considered non stationary and the data were discarded. Time series where the fluxes differed between 30% and 60% were considered stationary, but to be of a lower quality. High quality stationary data was taken to be any time series where the fluxes differed by less than 30%.

Chapter III

3. Mixing ratios and eddy covariance flux measurements of volatile organic compounds from an urban canopy (Manchester, U.K.)

This chapter details the deployment of the disjunct eddy covariance sampling system, developed in chapter 2, for the measurement of VOC above the city of Manchester. The sampler was located on the roof of Portland Tower, an 80 m office block located in the city centre, and sampled for a period of three weeks between the 5th and 21st of June 2006. In addition to the disjunct eddy covariance flux measurements, a secondary sampling technique, virtual disjunct eddy covariance was also deployed, tested and compared to results from the DEC system. As each system relied on the PTR-MS for VOC concentration measurements, the two systems operated in alternate half hours allowing an indirect comparison of the two techniques to be made.

The following work was submitted to the journal of Atmospheric Chemistry and Physics on the 4th of December 2007 and accepted for publication in ACPD on January the 8th, 2008. The manuscript is currently under review. The authors and their contributions are listed below.

Ben Langford (Lancaster University & CEH): Developed the disjunct eddy covariance system and software, developed the virtual disjunct eddy covariance software, operated the instruments during the field campaign, post processed the raw data and wrote the manuscript.

Brian Davison (Lancaster University): Helped compile the hardware for the disjunct eddy sampler, helped with the installation of the systems and with the compilation of the manuscript.

Eiko Nemitz: (CEH) Co-wrote the software for the virtual disjunct eddy covariance system, helped with the installation of the systems and the compilation of the manuscript.

Nick Hewitt (Lancaster University): Helped with interpretation of results and the compiling of the manuscript.

Mixing ratios and eddy covariance flux measurements of volatile organic compounds from an urban canopy (Manchester, U.K.)

B. Langford¹, B. Davison¹, E. Nemitz² and C. N. Hewitt¹.

[1] Lancaster Environment Centre, Lancaster University, Lancaster, LA1 4YQ

[2] Centre for Ecology & Hydrology (CEH) Edinburgh, Bush Estate, Penicuik, EH26 0QB, U.K.

Correspondence to: C.N. Hewitt (n.hewitt@lancaster.ac.uk)

Abstract

Concentrations and fluxes of six volatile organic compounds (VOC) were measured above the city of Manchester (U.K.) during the summer of 2006. A proton transfer reaction-mass spectrometer was used for the measurement of concentrations, and fluxes were calculated using both the disjunct and the virtual disjunct eddy covariance techniques. The two flux systems, which operated in alternate half hours, showed reasonable agreement, with R^2 values ranging between 0.2 and 0.8 for the individual analytes. On average, fluxes measured in the disjunct mode were lower than those measured in the virtual mode by approximately 19%, of which at least 8% can be attributed to the differing measurement frequencies of the two systems and the subsequent attenuation of high frequency flux contributions. Observed fluxes are thought to be largely controlled by anthropogenic sources, with vehicle emissions the major contributor. However both evaporative and biogenic emissions may account for

a fraction of the isoprene present. Fluxes of the oxygenated compounds were highest on average, ranging between $60 - 89 \mu\text{g m}^{-2} \text{h}^{-1}$, whereas the fluxes of aromatic compounds were lower, between $19 - 42 \mu\text{g m}^{-2} \text{h}^{-1}$. The observed fluxes of benzene were up-scaled to give a city wide emission estimate which was found to be significantly lower than that of the National Atmospheric Emissions Inventory (NAEI).

3.1 Introduction

The compilation of spatially and temporally detailed inventories for the emission of anthropogenic volatile organic compounds (VOCs) from urban areas is a necessary requirement for air quality regulatory purposes, effects assessment and research. Current emission estimates are associated with large degrees of uncertainty (Friedrich & Obermeier, 1999) which may limit their usefulness. Much of this uncertainty can be attributed to the large variety of different source categories which contribute to urban VOC emissions, which can be difficult to characterise and validate. Rather than taking a “bottom-up” inventory approach, an alternative is to make direct micrometeorologically based measurements which can integrate observations of wind speed and scalar concentrations to give a city-wide flux estimate of pollutant emissions (Nemitz *et al.*, 2002; Dorsey *et al.*, 2002; Velasco *et al.*, 2005). Currently, the eddy covariance (EC) technique is considered the most direct micrometeorological method available for estimating surface / atmosphere exchange fluxes, as it measures the turbulent flux directly, without reliance on any empirical parameterisations. This approach requires high frequency measurements (typically in the order of 5 - 20 Hz) of both vertical wind speed and concentration to resolve all

eddies that contribute to vertical transport (Lenschow, 1995). Although this technique is now well established for the measurement of some trace gases, such as CO₂ and H₂O (Aubinet *et al.*, 2001), its application to VOC fluxes has been restricted because of the slow response times of most VOC sensors.

A number of alternative micrometeorological approaches have been developed which relax the demands placed upon instrument response times. The technique most commonly applied to VOCs is the relaxed eddy accumulation method (REA), a conditional sampling technique where samples of air are directed into an up or down draught reservoir according to the sign of the vertical wind velocity at the time of sampling (Businger & Oncley, 1990). Air from each reservoir is subsequently analysed off-line and a flux is calculated from the difference in concentration generated between the two reservoirs. Unlike the eddy covariance method, REA is not a direct measure of the flux as it relies on empirical parameterisation. Furthermore, there is no scope for retrospective corrections to the coordinate frame (Bowling *et al.*, 1998). Despite these drawbacks, the REA method has been successfully applied to a range of vegetation types including grass land (Olofsson *et al.*, 2003) and forests (Greenberg *et al.*, 2003; Ciccioli *et al.*, 2003; Friedrichs *et al.*, 1999).

More recently a second technique, disjunct eddy covariance (DEC), has been developed for “relaxed” flux measurement. Rather than measuring at high frequencies as in EC, in DEC the flux is calculated using a sub-set of a quasi-continuous time series. In order to retain the flux contributions carried by small scale eddies, DEC utilises near instantaneous grab samples of air which are aspirated into a storage reservoir at regular intervals. The “dead” time between the sampling periods is then used to analyse the air at a rate suitable for the gas analyser. Provided the interval between samples is kept to less than the integral time scale, then the discontinuous

dataset can be used to give high precision flux information, which is numerically similar to the EC approach, but with reduced statistics (Grabmer *et al.*, 2006). The DEC approach is particularly useful for sensors with a response time of 1 to 20 s.

With the advent of quadrupole mass spectrometers (QMS) for the use of atmospheric composition measurements, a range of analysers is now becoming available that can provide fast measurements (as determined by the dwell time on a given m/z), which is nevertheless discontinuous (as the QMS scans through a range of m/z 's). One such instrument is the proton transfer reaction-mass spectrometer (PTR-MS) which allows for the measurement of most VOCs with good sensitivity (10 ppt) and fast response times (10 Hz).

The quadrupole mass spectrometer in the PTR-MS can be programmed to scan over a small suite of masses in what is termed a duty cycle. Although in theory the instrument has a sufficient response time to be compatible with the eddy covariance method, in reality the quadrupole can only scan one mass at a time; therefore the data set returned on completion of each duty cycle is in effect disjunct.

To optimise flux measurement approaches for these kind of data, the DEC concept has been developed further to calculate fluxes from the discontinuous time-series at each m/z by pairing up each concentration measurement with the associated wind measurement in software, a process known as virtual disjunct eddy covariance (vDEC) (Karl *et al.*, 2001; Karl *et al.*, 2002; Spirig *et al.*, 2005; Lee *et al.*, 2006; Ammann *et al.*, 2006; Brunner *et al.*, 2007). The advantage of this technique is that air can be sampled directly into the instrument, as individual masses are measured at a sufficiently fast rate, therefore no additional sampling system is required. Furthermore, analysis times are shorter than in DEC, allowing more data to be

collected during each averaging period; consequently the resultant flux estimates are statistically more robust.

The vDEC method has been successfully applied to give VOC flux estimates over vegetation canopies, including grassland (Karl *et al.*, 2001; Ammann *et al.*, 2006; Brunner *et al.*, 2007), forests (Karl *et al.*, 2002; Spirig *et al.*, 2005; Lee *et al.*, 2006), and over an urban environment (Velasco *et al.*, 2005).

In the current study we deployed both the DEC and vDEC techniques for the measurement of a range of VOCs above the city of Manchester (U.K). The recorded data were then used to calculate a city-wide emission flux, and in the case of benzene this was compared to the UK National Atmospheric Emission Inventory (NAEI) for Manchester (http://www.naei.org.uk/datachunk.php?f_datachunk_id=174).

The NAEI is compiled using a bottom-up approach, where combinations of reported and estimated emissions across numerous source sectors are used to provide a spatially disaggregated (1×1 km) emission inventory. The uncertainty associated with these estimates is dependant on the ratio of reported to estimated (modelled) data and hence for compounds such as VOCs, where reported emissions are limited and uncertainty levels are high, micrometeorological methods offer a useful alternative.

3.2 Methods

3.2.1 Measurement site and general setup

The work presented here formed part of the UK CityFlux project, which aimed to (i) directly measure pollutant emissions from urban areas, (ii) investigate controls of these emissions, (iii) derive emission factors relative to CO₂ and CO and (iv) study pollutant transformation by comparing fluxes at the plume, street canyon and urban canopy scale. During the summer of 2006, micrometeorological measurements of

VOC emissions were made over the city of Manchester, together with measurements of fluxes and concentrations of VOCs, aerosols, O₃, CO₂ and H₂O, as well as mobile measurements with a mobile laboratory, measurements in a street canyon, tracer releases and aircraft-borne measurements. The VOC flux measurements were taken from the roof of Portland Tower (53°28'41''N; 2°14'18''W), an 80 m tall office block, which is located in central Manchester. The building is situated on Portland Street, which is approximately 600 m distance from the Arndale centre, (the city's principal shopping district) 475 m from Piccadilly railway station, (the north-west's busiest station), and 100 m from China Town (a concentrated area of restaurants). The building is surrounded by trafficked streets on three sides and a multi-storey car park on the other.

The roof of Portland Tower is not uniformly flat but has three levels. On the lowest level a small shed was erected which housed the PTR-MS. The second level, 2 m above, contained a utility substation which was used to house the sonic anemometer signal box. The roof of the substation was used as the foundation for a 15 m mast which was fitted with a sonic anemometer (Solent Research R3, Gill Instruments Ltd, Lymington, Hants, U.K.) and Teflon gas inlet line (1/2'' OD). The mast was erected to get above the wake effects generated from both the edges of the building and the inhomogeneous roof surface and increased the effective measurement height to 95 m above street level.

Fluxes were measured between the 5th and 20th of June 2006. During the first few days of measurements (5th-10th) a high pressure system was centred over Northern Ireland which dominated the weather during this period, with mostly dry conditions, clear skies and temperatures between 16 - 30 °C. Between the 13th - 16th a cold front

slowly moved across southern England and during this time temperatures at the measurement tower dropped to a maximum of 24 °C and a minimum of 14 °C on the 16th. For the later part of the campaign, temperatures slowly increased as a high pressure ridge moved in behind the cold front, increasing the average temperature to 21 °C. Throughout the campaign the wind direction shifted between SW and NNE, but also came from the SEE at certain times. The wind speed ranged between 0.4 and 11.2 m s⁻¹, with an average of 3.3 m s⁻¹

3.2.2 The proton transfer reaction mass spectrometer (PTR-MS)

A standard PTR-MS instrument (Ionicon Analytik, Austria) was used for the measurement of VOC concentrations as it offered the desired sensitivity and response times required for both flux systems. Detailed descriptions of this instrument can be found elsewhere (Lindinger *et al.*, 1998; Hayward *et al.*, 2003; de Gouw & Warneke., 2007), therefore only a brief account of the instrument setup will be given here.

The PTR-MS was optimised to an E/N ratio of 125 Td and programmed to sequentially scan a suite of six protonated target compounds: methanol (m/z 33), acetaldehyde (m/z 45), acetone (m/z 59), isoprene/furan (m/z 69), benzene (m/z 79) and toluene (m/z 93). In addition to these compounds, the H_3O^+ primary ion count and two reagent cluster ions were also recorded at m/z 21, m/z 39 and m/z 55 respectively. A further mass, m/z 25, was used at the start of each measurement cycle as a spacer to ensure the monitored air did not contain residues from the previous sample.

The mass detection system of the PTR-MS can only record VOC (ion counts per second) in atomic mass units (amu); therefore it is difficult to attribute ion counts to individual VOC species. Interference from other ions at amu 33, 45, 79 and 93 has been shown to be insignificant in previous studies (de Gouw *et al.*, 2007), but both

acetone and propanal have been detected at amu 59. Although this can generate some uncertainty in the measurement of acetone, the signal of acetone is always dominant in ambient air (Kato *et al.*, 2004), therefore ion counts recorded at m/z 59 were ascribed solely to acetone in the present study. Similarly m/z 69 may be isoprene and/or furan, although the latter is normally present at very low concentrations in ambient air (Christian *et al.*, 2004). Mass m/z 69 was therefore solely attributed to isoprene.

The VOC concentrations were calculated using reaction rate constants (k) from Zaho and Zhang (2004) and transmission numbers (the time taken for each mass to traverse the drift tube) calculated using $t = L/v_d$, where L is the length of the drift tube and v_d is the drift velocity (Lindinger *et al.*, 1998).

3.2.3 Flux measurements

During the campaign, two flux measurement techniques (DEC and vDEC) were employed to measure surface layer fluxes of VOCs from the urban canopy. As both techniques utilised a single PTR-MS instrument to give VOC concentrations, it was not possible to operate the systems simultaneously, and therefore fluxes were measured by the two methods in alternate half hours. A Teflon 3-way solenoid valve (001-0017-900, Parker Hannifin) sat in line and enabled the PTR-MS to switch freely between the two systems. Flux measurements in each mode were averaged over a 25 minute period and the remaining 5 minutes of each half hour were used to scan the entire mass spectrum (m/z 21 – 146) to give basic ambient concentration information on a wide range of VOCs. Figure 3.1 shows a typical PTR-MS operating sequence during 1 hour of measurements and includes the PTR-MS duty cycles for each flux mode.

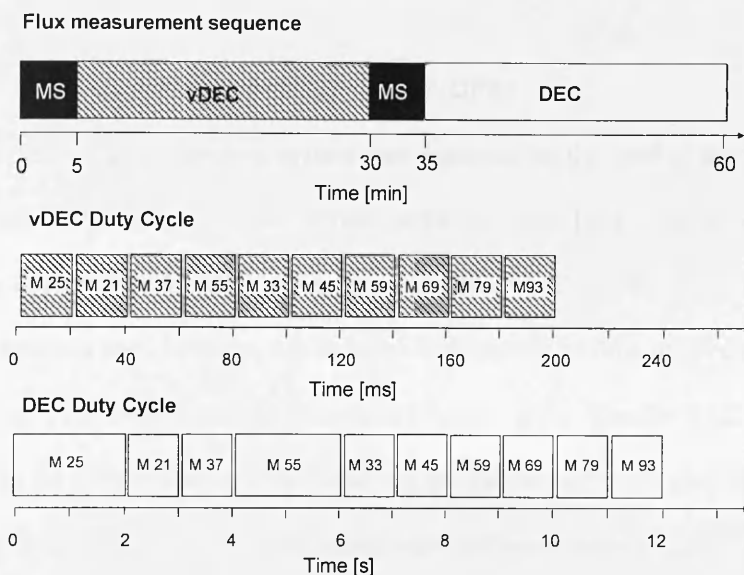


Figure 3.1. Representation of the PTR-MS measurement sequence used at Portland Tower. When operating in vDEC mode the duty cycle lasted for a total of 200 ms, whereas in DEC mode dwell times were increased and a 12 s duty cycle was used.

3.2.3.1 Virtual disjunct eddy covariance sampling system (vDEC)

During the first period of each hour, the 3-way solenoid valve was triggered to enable the PTR-MS to sub-sample directly from the main sample line in a virtual disjunct eddy covariance mode. The quadrupole was set to scan each mass at a rate of 20 ms, allowing sample air to be purged directly into the instrument without the use of an additional sampling system. The inlet for the sample line was mounted a short distance below the sonic anemometer, as vertical displacement has been shown to result in the smallest flux losses (Kristensen *et al.*, 1997). In order to maintain a turbulent flow through the sample line, and thus avoid dampening of the VOC signal, a flow rate of 60 l min^{-1} was used. Upon the completion of each PTR-MS duty cycle, data were exported to a LabVIEW logging programme using the Microsoft Windows “dynamic data exchange” (DDE) protocol, which stored the data alongside those from the sonic anemometer.

3.2.3.2 Disjunct flux sampling system (DFS)

A disjunct flux sampling system was deployed on the roof of the building to monitor the VOC fluxes for the second period of each hour. The schematic and operating sequence of the DFS are depicted in Fig. 3.2. The sampler comprised two one litre stainless steel canisters, which act as intermediate storage reservoirs (ISR) for sampled air. Fast switching high flow conductance valves (Lucifer E121K45) were mounted to the inlet of each canister, enabling the ISR to take a fast grab sample once activated. Each ISR was coiled with heater cable and insulated with aluminium foil to maintain an internal temperature of 40 °C. This, combined with the cylindrical shape of the canisters which reduced surface area, helped to minimise losses of VOC to walls, and minimised condensation and the formation of liquid water, which can remove soluble compounds such as methanol.

Before grab samples of air were taken, each ISR was first evacuated to a pressure of 250 mbar. The time taken to evacuate the canister, 12 s, was the limiting factor in determining the length of time between sampling. By contrast, the time taken to fully pressurise the ISRs, 0.5 s, proved to be the limiting factor in determining sampling times. Therefore the overall effective response time of the DFS setup is about 0.5 s, which is sufficient to resolve turbulent fluctuations of up to 2 Hz.

Grab samples of air acquired by the DFS were analysed for VOCs using the PTR-MS, which was connected to the DFS via a 4 m length of 1/8" PFA tubing. The rate at which the PTR-MS draws air from the ISR is important as a vacuum is gradually generated as air is sampled. This back-pressure can affect the pressure in the drift tube, which can lead to small changes in the E/N ratio of the instrument. In order

to prevent this problem, the flow rate of the PTR-MS was reduced from 300 ml min^{-1} to 150 ml min^{-1} .

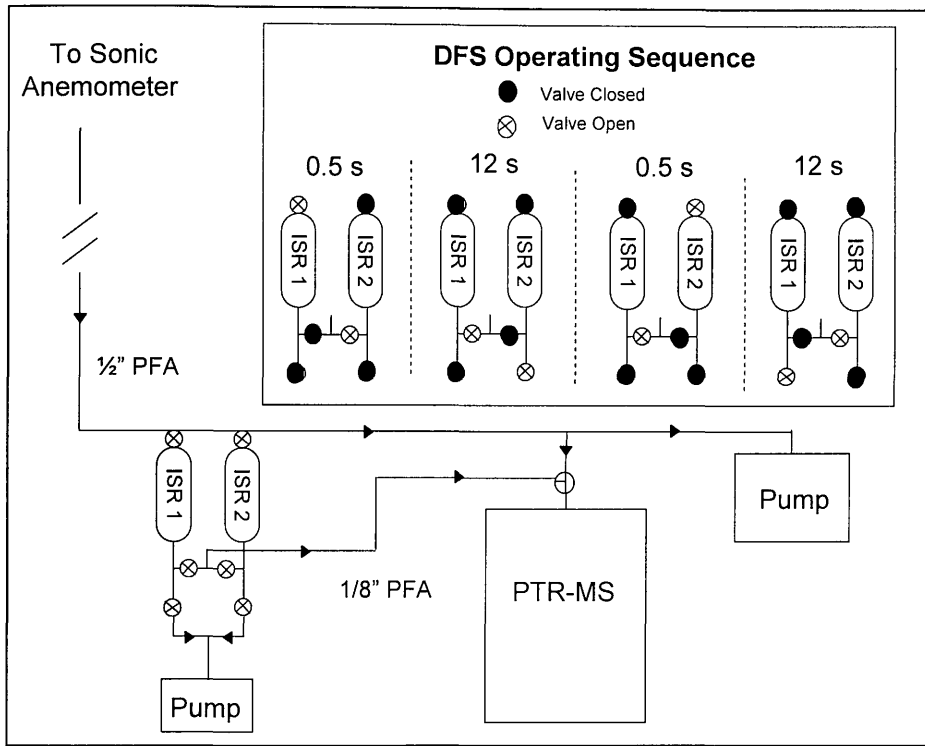


Figure 3.2. Schematic of the experimental setup used at Portland tower. The inset diagram shows the operating sequence of solenoid valves which controlled the sample and analysis phase of the disjunct flux sampler (DFS). ISR = Intermediate storage reservoir.

The PTR-MS was housed some distance from the sonic anemometer. Thus the sampling line between ISRs and PTR-MS would have been too long for the DFS to be mounted on the anemometer mast. Instead it was located at the base of the tower, with each sample valve connected via a ‘T-piece’ into the $\frac{1}{2}$ ” OD sampling line. As a drawback of this setup, the sample line is subject to a pressure drop of approximately 200 mbar, caused by the high flow rates used. Consequently, upon activation of sample valves each ISR could only pressurise to 800 mbar, increasing their effective carryover between samples from 25% under normal operating conditions (at 1000 mbar) to $\sim 31\%$. The carryover was corrected using the following equation:

$$\chi_{cor} = (\chi \times \eta_1 - \chi_{old} \times \eta_2) / (\eta_1 - \eta_2) \quad (3.1)$$

where χ is the VOC concentration within the ISR, χ_{old} is the previous concentration of the same ISR, P_1 is the ISR pressure when full and P_2 is the ISR pressure after evacuation.

The sequence of valve switching used to control both the sample and analysis phases of the DFS, which combined with valve switching, pressure recording, sonic anemometer and PTR-MS data recording, were all coordinated using LabVIEW software (National Instruments – v 6.1). The valves were controlled through a multifunction IO card (6071E, National Instruments), which also recorded the analogue signals from the pressure sensors of the ISR (OMEGA, Stamford, Connecticut, PX137-015DV).

3.2.3.3 Flux calculations

In the eddy covariance technique, the flux of an atmospheric scalar is calculated using the covariance between continuous time series of vertical wind speed and scalar concentration at a fixed point in space over a statistically representative time period. Since the data generated by the disjunct flux systems are simply a sub-set of the continuous time series, the flux may be calculated in the same way; thus observations of vertical wind velocity (w) were paired with the corresponding PTR-MS data (χ) to give a flux as follows:

$$F\chi_{log} = \overline{w'\chi'} \quad (3.2)$$

where primes indicate instantaneous fluctuations about the mean and over-bars denote time averaging (i.e. $w' = w - \bar{w}$). The only difference between this and direct eddy covariance measurements is the reduced number of data points used for the flux calculation, which results in an increase in the statistical uncertainty of the measurement.

Before the flux can be calculated it is first necessary to correct for the time lag that exists between the two data sets, which occurs because of the ~ 25 m separation between the sonic anemometer and the PTR-MS. This time lag was calculated from the maximum value in a cross correlation function between w and χ within a 5 second time window. This value was then used to realign the time series of w' and χ' and calculate the flux. Typically the peak in the cross correlation was noted between 3 and 5 s, which compared closely with the theoretically calculated lag time of ~ 3 seconds.

Standard rotations of the coordinate frame were applied to correct for tilting of the sonic anemometer. The vertical rotation angle showed a clear relationship with wind direction, with maximum values of up to 15° . This is similar to other flux measurements in the urban environment (e.g. Nemitz *et al.*, 2002) and suggests that, although the mean airflow at the anemometer is affected by the building, the influence can be compensated by standard rotational corrections.

Calculated fluxes were subject to a post-processing algorithm which filtered and removed data that failed to meet specified quality controls. These included removal of large spikes in vertical wind speed or VOC concentration and the omission of data where the average wind speed dropped below 1 m s^{-1} . This latter QA procedure resulted in the loss of 7% of the flux data.

In addition, during post-processing of the data, it was found that the inlet pump was occasionally shut down by its thermal trip. The affected time periods were filtered

and the spikes removed, affected averaging periods were not included in the final flux analysis. This meant approximately 31% of measured flux data was deemed unusable and are not shown here.

3.3 Results & Discussion

3.3.1 VOC concentrations

Concentrations of VOCs are summarised in Table 1 and the 25 minute average values are plotted alongside temperature and wind direction in Fig. 3.3. The oxygenated compounds, methanol, acetone and acetaldehyde, were the most abundant (methanol 1.3 - 8 ppbv; acetone 0.3 – 4.4 ppbv; acetaldehyde 0.44 – 3.2 ppbv). The larger concentrations of methanol compared with the other analytes are typical for urban VOC measurements and can be attributed to its relatively low photochemical reactivity (Atkinson, 2000) and the numerous anthropogenic/biogenic sources which contribute to its emissions both in and outside of the city (de Gouw *et al.*, 2003). Comparisons of methanol concentrations with previous studies shows the values observed here to be within the lower range of concentrations measured in Barcelona (Filella and Penuelas, 2006) and within the range of values recorded in Innsbruck (Holzinger *et al.*, 2001). The concentrations of the other two oxygenated compounds, acetone and acetaldehyde, both lie within the range of data reported from other major conurbations such as Rome (Possanzini *et al.*, 1996), Los Angeles (Grosjean *et al.*, 1996) and Rio de Janeiro (Grosjean *et al.*, 2002).

Concentrations of isoprene ranged between 0.07 - 0.75 ppbv, which is consistent with values obtained from the national air quality monitoring network (http://www.airquality.co.uk/archive/reports/cat13/0602011042_q3_2005_rat_rep_issue1_v5.pdf) for other U.K. cities, including Bristol and London. The aromatic compounds, benzene and toluene, were the least abundant of the VOCs measured, ranging between 0.02 – 0.2 and 0.03 – 0.73 ppbv respectively. These values also compared well with data obtained from the National network (www.airquality.co.uk)

Table 3.1. Summary of VOC concentration and flux measurements between the 5th and 20th of June 2006, in Manchester (U.K)

<i>Concentrations</i> [ppb]	<i>Methanol</i> (m/z 33)	<i>Acetaldehyde</i> (m/z 45)	<i>Acetone</i> (m/z 59)	<i>Isoprene</i> (m/z 69)	<i>Benzene</i> (m/z 79)	<i>Toluene</i> (m/z 93)
Mean	3.10	1.20	1.10	0.30	0.10	0.20
Median	2.92	1.14	1.00	0.29	0.08	0.14
Range						
- 5 th	1.77	0.63	0.52	0.13	0.03	0.06
- 95 th	5.25	1.83	1.94	0.50	0.14	0.35
SD	1.15	0.41	0.48	0.12	0.04	0.10
Geo SD	1.40	1.40	1.50	1.60	-	1.70
N	354	354	354	353	353	354
<i>Fluxes</i> [$\mu\text{g m}^{-2} \text{h}^{-1}$]						
Mean	78.8	59.6	87.8	-	18.9	42.4
Median	80.3	49.5	63.1	-	16.3	39.2
Range				-		
- 5 th	-143.6	-85.1	-111.7		-47.0	-67.3
- 95 th	327.8	241.3	356.5		89.3	160.6
SD	159.8	105.6	152.1	-	42.8	67.8
N	200	200	195	-	186	200

automatic monitoring station on Marylebone Road, London, although, on average, concentrations from the London site were higher, presumably due to the kerbside location of the sampler, compared with a sampling height of 95 m for the concentrations reported here.

Strong linear relationships were observed between the concentrations of each of the measured VOCs, with R^2 values ranging between 0.24 and 0.85, suggesting some commonality between the sources of emission for each of the compounds.

Clear day-night trends in mixing-ratios were not apparent, with maxima occasionally observed at night time (Thurs 8th, Sat 11th), whereas on other days (Sat 17th – Tue

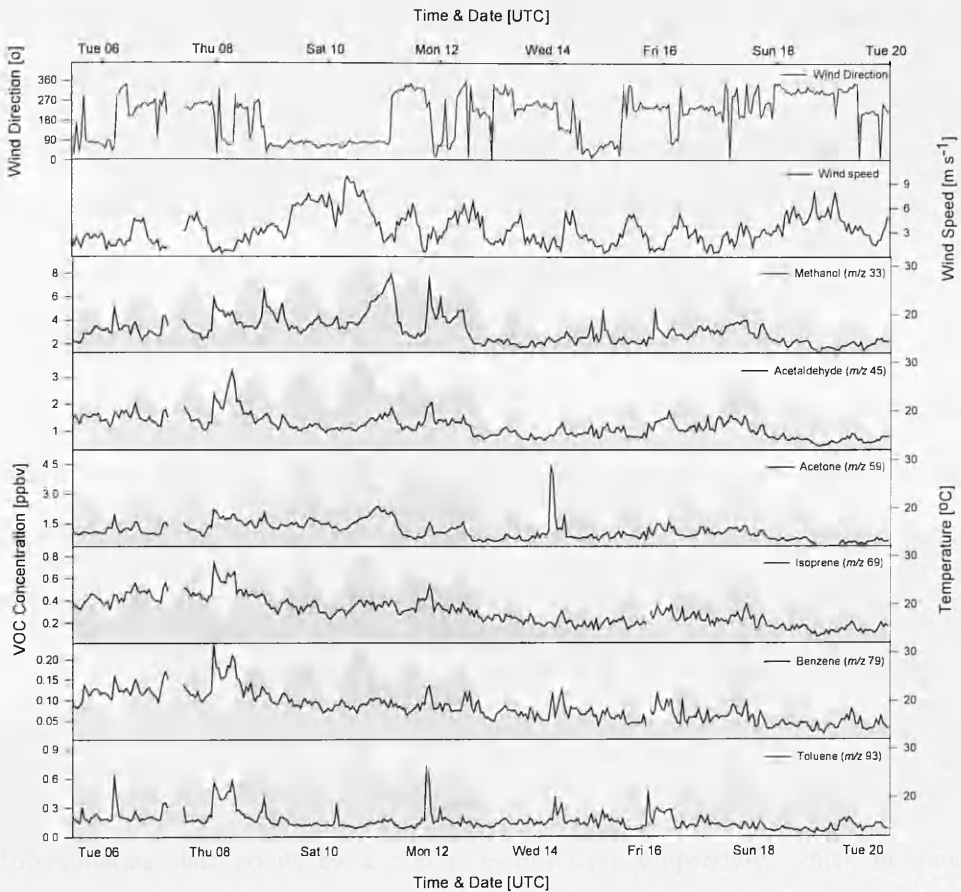


Figure 3.3. Plot showing 30 minute average wind direction and the 25 minute average concentrations of VOCs measured by the PTR-MS between the 5th and 20th of June 2006. Shaded areas represent the 30 minute average temperature as recorded by the sonic anemometer.

20th) they tended to peak during the late afternoon. Spikes were frequently observed in the concentration of methanol during the early morning. This often corresponded to low temperatures and low wind speed in the early morning and is consistent with previous urban VOC studies which have attributed this increase to condensation processes (Fiella & Penuelas, 2006). The nocturnal increase in concentrations for the other compounds is unclear, but is likely a combination of small night-time emissions accumulating in the shallow nocturnal boundary layer, the dynamics of which differed between the different nights. These emissions may include combustion and fugitive

emissions from industrial activity outside the flux footprint, on the outskirts of the city.

Additional spikes in VOC concentrations can be observed in Fig. 3.3. While some of these can be ascribed to changes in wind direction, such as those observed in acetone on the 14th, others, as seen in toluene on the 16th cannot.

Figure 3.4 shows scatter plots of VOC mixing ratios measured during the vDEC mode between the 5th and 20th of June. These plots are useful for the interpretation and source apportionment of data. For example, strong linear relationships, as seen in panel (I), may suggest a similar source contributing to the emission of the two compounds, whereas in panel (K), where a bimodal distribution is evident, it is possible that there are two separate sources contributing to the observed VOC concentrations. Further information can be obtained from these plots by differentiating data points by a *z* axis, in this case temperature, which in some instances (panel (E)) can reveal what appears to be a temperature dependency in the measured concentration of the VOC. To help with the further interpretation of the data shown in Fig. 3.4, Table 3.2 lists some of the known anthropogenic, biogenic and chemical sources of the measured compounds and also includes atmospheric lifetimes with respect to OH, NO₃, O₃ and photolysis.

Figure 3.4, panel (A), shows the correlation between isoprene (*m/z* 69) and benzene (*m/z* 79). Both these compounds are known constituents of petrol fuel (Borbon *et al.*, 2001), and consequently they are emitted to the atmosphere by the same two anthropogenic sources: direct emissions from vehicle exhausts and evaporative emissions from petroleum products, hence the strong linear relationship ($R^2 = 0.87$ ($p < 0.0001$)) observed between the two compounds during this study.

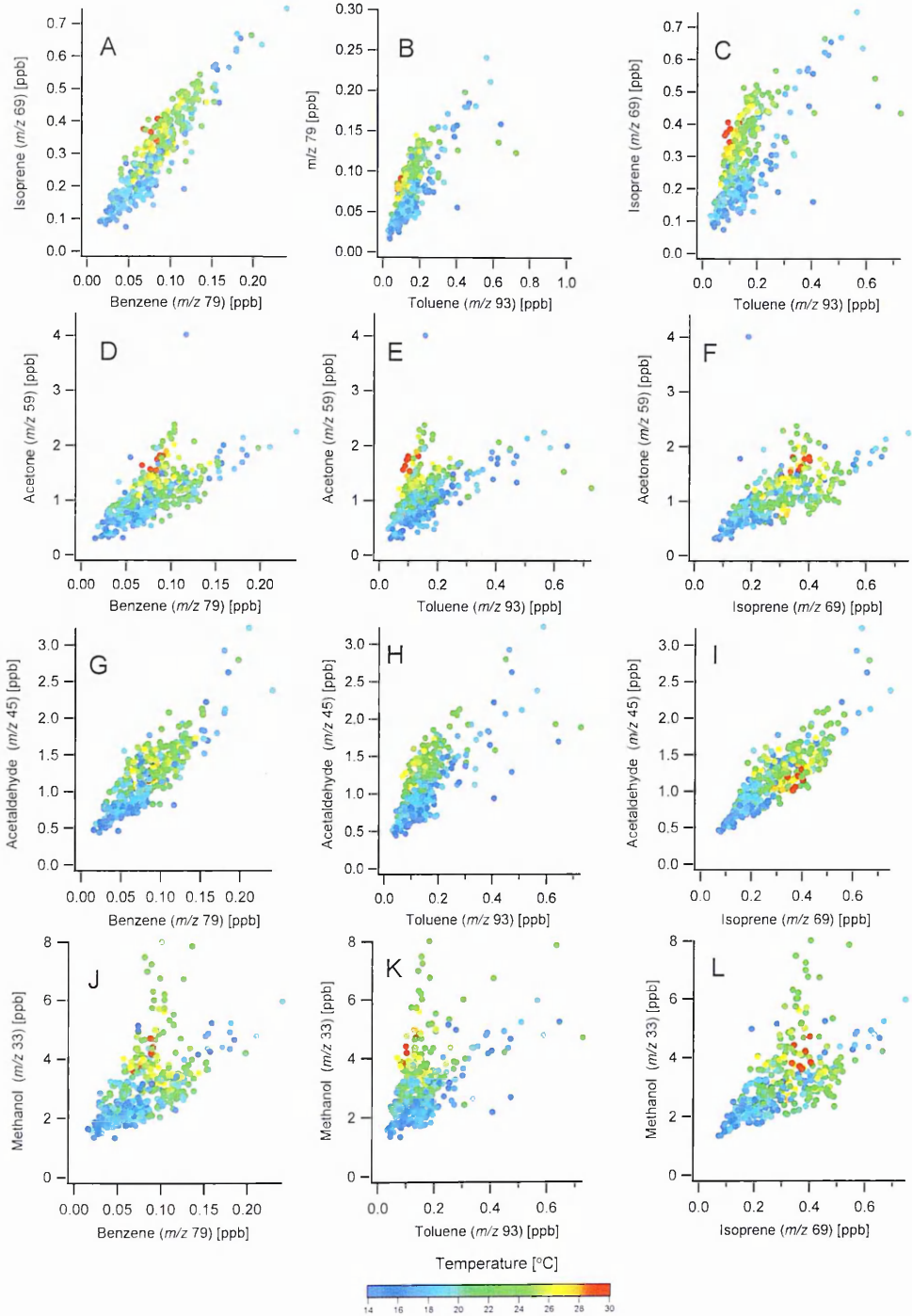


Figure 3.4. Scatter plots of VOC concentrations measured at Portland Tower, Manchester. Colour bar corresponds to ambient air temperature at the time of sampling.

Table 3.2. List of biogenic, anthropogenic VOC sources, including atmospheric lifetimes with respect to OH, NO₃, O₃ and photolysis. The temperature

Sources	Methanol [m/z 33]	TD	Acetaldehyde [m/z 45]	TD	Acetone [m/z 59]	TD	Isoprene [m/z 69]	TD?	Benzene [m/z 79]	TD	Toluene [m/z 93]	TD?	TD?	
Biogenic	Direct emissions from plants -Plant defence (Guenther et al., 2006)	?	Biomass burning (Lipari et al., 1984; Husk et al., 1994). Direct emissions from plants: (Körner et al., 1999) - Leaf decomposition (Fah, 2003; Wannke et al., 1999) - Leaf wounding (de Gouw et al., 2008) - Light-dark transition emission (Holzinger et al., 2000; Kari et al., 2002) -Plant defence - Cut and drying of vegetation (Guenther et al., 2006)	?	Wetting of dried leaf litter which has been subjected to high daytime temperatures (Wannke et al., 1999) -Plant defence - Cut and drying of vegetation (Guenther et al., 2000)	?	Emission from plants	No known sources	?	No known sources	?	TD?	
Anthropogenic	Primarily used as an industrial solvent, dyes, paint and varnish remover. Ingredient of gasoline where it is used as an antifreeze and it is likely to become an important source in the future. Antifreeze	Fossil fuel combustion (Andersen et al., 1996) Tail pipe emissions - 0.5 % of carbon is emitted as Acetaldehyde (Sigsby et al., 1987) Exhaust emission in urban areas 1.4 mg km ⁻¹ (petrol) and 4.4 mg km ⁻¹ (Diesel) (Cupham et al., 2006) Evaporative emissions	Produced in industry, for use as a solvent. Tail pipe emissions (Sigsby et al., 1987) estimated total emission - 1 % of total pipe total exhaust. Evaporative Emissions	Tail pipe emissions (Barbon et al., 2001) 1.6 - 15.3 mg km ⁻¹ (Chang et al., 2007)
Atmospheric Chemistry			Oxidation of Hydrocarbons (Grogan et al., 2003) >C1 alkanes (e.g. ethane, propane, n-butane) and >C2 alkenes (e.g. 1-butene, 1-pentene) can form acetaldehyde as an intermediate oxidation product	Oxidation of propane (which has an atmospheric lifetime with respect to OH of 10 days), isobutene and isopentane (Singh et al., 1994) [Propane 0.2 - 2.4 mg km ⁻¹ (Hwa, 2002; Chang et al., 2007), isobutene (5.6 mg km ⁻¹ (Hwa, 2002) and isopentane (40.1 mg km ⁻¹ (Chang et al., 2007)) have all been shown to be emitted in vehicle exhaust.								
Atmospheric lifetime with respect to OH[†]	12 day	8.8 h			55 days		1.4 h		9.4 day		1.9 day			
NO₃[†]	1 yr	17 day			> 11 yr		50 min		> 4 years		1.9 yr			
O₃[†]	-	> 4.5 yr			-		1.3 day		> 4.5 years		> 4.5 yr			
Photolysis[†]														
Vapour Pressures at 25 [C]	16.9 [kPa]	98.7 [kPa]			53 [kPa] (15°C)		39 [kPa]		12.6 [kPa]		3.73 [kPa]			

dependency (TD) of each source is listed, where 5 stars represent a very high dependency and 1 star a very low dependency.
[†] Atmospheric lifetimes of VOCs are taken from Atkinson (2000).

Despite the apparent clarity of this relationship, more detailed analysis of the data with respect to temperature, as shown in Fig. 3.5, indicates the observed isoprene concentrations to be partially influenced by the ambient air temperature, with higher concentrations relative to those of benzene observed during warmer conditions. It is reasonable to presume that the composition of vehicle exhaust is unlikely to vary significantly with changes in the observed ambient air temperature (16–30°C), therefore it must be assumed that this increase occurs either due to increased evaporative emissions, as isoprene is more volatile than benzene, or that there are emissions of isoprene from a third source, independent of that of benzene. Biogenic emissions of isoprene are an obvious candidate, as isoprene emission rates from plants have been shown to be both temperature and light dependent (Guenther *et al.*, 1995).

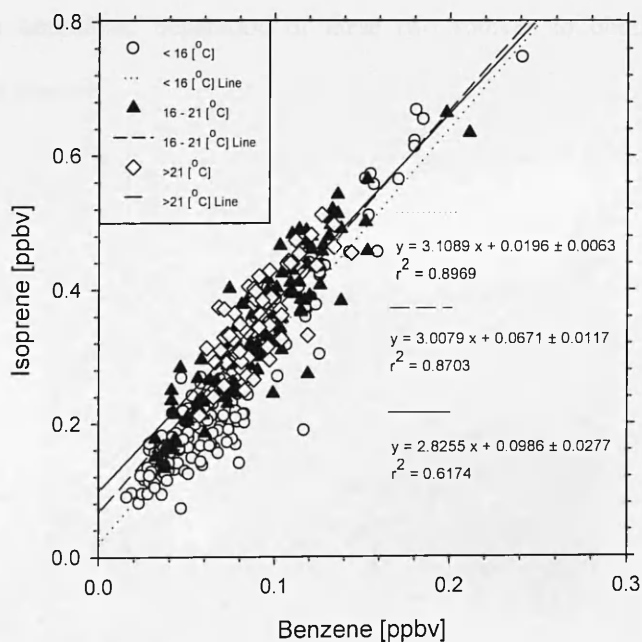


Figure 3.5. Isoprene concentrations (m/z 69) against benzene (m/z 79) measured at Portland Tower, Manchester during June 2006. Open diamonds correspond to data points above 21 °C, closed triangles correspond to data in the range of 16 – 21 °C and open circles represent data below 16 °C.

Yet, analysis of an isoprene inventory for Great Britain (Stewart *et al.*, 2003) shows few biogenic sources of isoprene within the city centre. Analysis of the meteorology during the period, when the ambient air temperature was at its highest, shows the average wind speed to be approximately 8 m s^{-1} . Although isoprene has a short atmospheric lifetime in the daytime, typically on the order of 1 hour (Atkinson, 2000), due to reactions with the OH radical, at such wind speeds, air masses containing isoprene emitted from rural areas, outside of the city could have reached the tower before removal by OH. Consequently it is assumed that the temperature-dependent fraction of isoprene observed during this study was a combination of both evaporative and biogenic emissions. The percentage contribution of temperature-dependent isoprene is shown in Fig. 3.6. This plot suggests that at $30 \text{ }^\circ\text{C}$ as much as 32% of the observed isoprene within the city centre could be due to a combination of evaporative and biogenic emissions. Separation of these two sources to obtain the biogenic fraction is not possible.

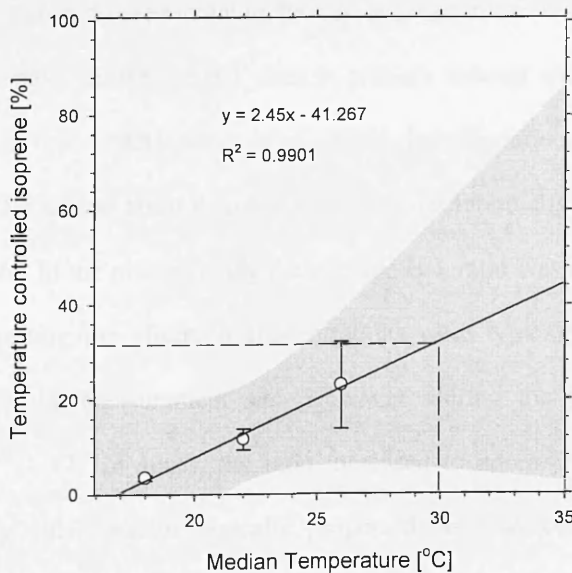


Figure 3.6. The percentage contribution of temperature controlled isoprene at 18, 22 and 26 °C. Dashed line indicates the percentage of temperature controlled isoprene that might be expected at 30 °C. Error bars represent 1 standard deviation at the 95% confidence interval and the greyed area represents the 95% confidence band of the fit.

Toluene was the least volatile of the compounds measured during this study and the ratios of its concentration against those of benzene, isoprene, acetone, acetaldehyde and methanol did not vary with temperature (Fig. 3.4: panels (B), (C), (E), (H) and (K) respectively). However, in each of these plots, bimodal distributions were observed and each of the aforementioned compounds appeared to demonstrate some degree of temperature dependency with respect to toluene, although this varied between compounds. Acetone appearing to be highly temperature dependent, whereas benzene showed only a slight variation with temperature. In the case of benzene, the observed temperature dependence may be coincidental and due to the prevailing wind direction and increased wind speeds which accompanied the elevated temperatures. This point can be highlighted by investigation of the ratio of benzene to toluene concentrations in Fig. 3.7. As both of these compounds are known to be present in primary vehicle exhaust emissions (Jobson *et al.*, 2005), and have differing atmospheric lifetimes with respect to the OH radical, analysis of the benzene to toluene ratio (B/T) can be used to gauge the age of an air mass (Warneke *et al.*, 2001). Previous studies have shown the B/T ratio in primary exhaust emissions to typically lie in the range of 0.41 – 0.83 (Heeb *et al.*, 2000), but this ratio increases as toluene reacts with the OH radical faster than benzene and is preferentially removed over time in the atmosphere. In the present study the average B/T ratio was approximately 0.55 (Fig. 3.7), suggesting the observed concentrations were typically originating from sources close to the measurement site. However, during the period of elevated temperatures (9th - 12th of June), the ratio increased to approximately 0.67, which suggests slightly older, photochemically processed, air was being advected from outside of the city. In the days before this period (6th - 9th June), the wind direction was from the SW. As the temperatures increased between the 9th and 12th, the wind

direction rotated 180° and the air that had left the city in the days previously was transported back across Manchester. The atmospheric lifetime of toluene with respect to OH is approximately 2 days (Atkinson, 2000), which corresponds to an advection distance of ~ 1300 km under the prevailing average wind speed. Taking this into account, the returning air mass would be depleted in toluene and therefore the ratio of benzene to toluene in the air mass would increase, which can be seen occurring in Fig. 3.7.

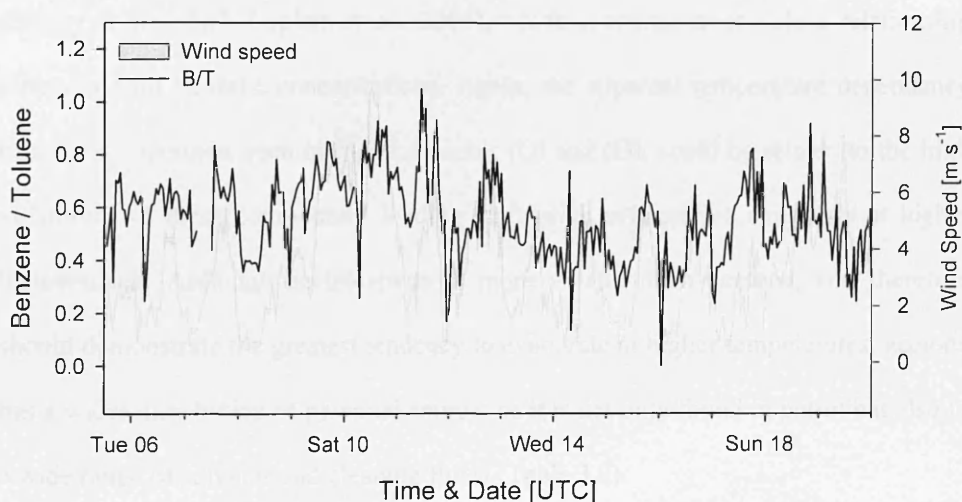


Figure 3.7. Graph of the ratio of benzene to toluene (solid line) and average wind speed (greyed area).

In addition, the removal rate of toluene may have been increased due to higher concentrations of the OH radical corresponding to the increase in temperature. Therefore it can be concluded that, although some temperature dependency may be observed due to increased evaporative emissions and OH concentrations, the bimodal distributions observed in Fig. 3.4 panels (B), (C), (E), (H) and (K) are, in part, a result of an older air mass being advected back across the city, in which the toluene has been removed through reaction with the OH radical. Fig. 3.7 also demonstrates the diurnal cycle in the B/T ratio due to changes of OH concentrations over the day.

Acetone (m/z 59) appeared to show the greatest degree of temperature dependence out of all the measured VOCs. Like acetaldehyde, acetone can be formed in the atmosphere as a product of the photooxidation of hydrocarbons, including propane, isobutene and isopentane (Singh *et al.*, 1992). These are primary vehicle exhaust pollutants (Hwa, 2002; Chiang *et al.*, 2007); however, the atmospheric lifetime of each is typically on the order of tens of days, therefore temperature-dependant photooxidation is unlikely to be a major source of acetone within the city. Both acetone and acetaldehyde are themselves found in vehicle exhaust emissions (Sigsby *et al.*, 1987; Caplain *et al.*, 2006), which accounts for the close relationship observed with benzene concentrations. Again, the apparent temperature dependency of these compounds, seen in Fig. 3.4 panels (D) and (G), could be related to the high volatilities of these compounds, leading to fugitive evaporative emissions at higher temperatures. Although acetaldehyde is more volatile than acetone, and therefore should demonstrate the greatest tendency to evaporate at higher temperatures, acetone has a wider distribution of potential sources as it is not only found in petrol but also in a wide range of solvents and cleaning fluids (Table 3.2).

3.3.2 VOC fluxes

Averaged diurnal fluxes for the period 5-20th June 2006, as measured by both the DEC and vDEC techniques, are shown in Fig. 3.8. Despite some variability between the two systems, both techniques show VOC fluxes to have a clear diurnal trend, with fluxes at their largest in the mid to late afternoon and lowest in the early

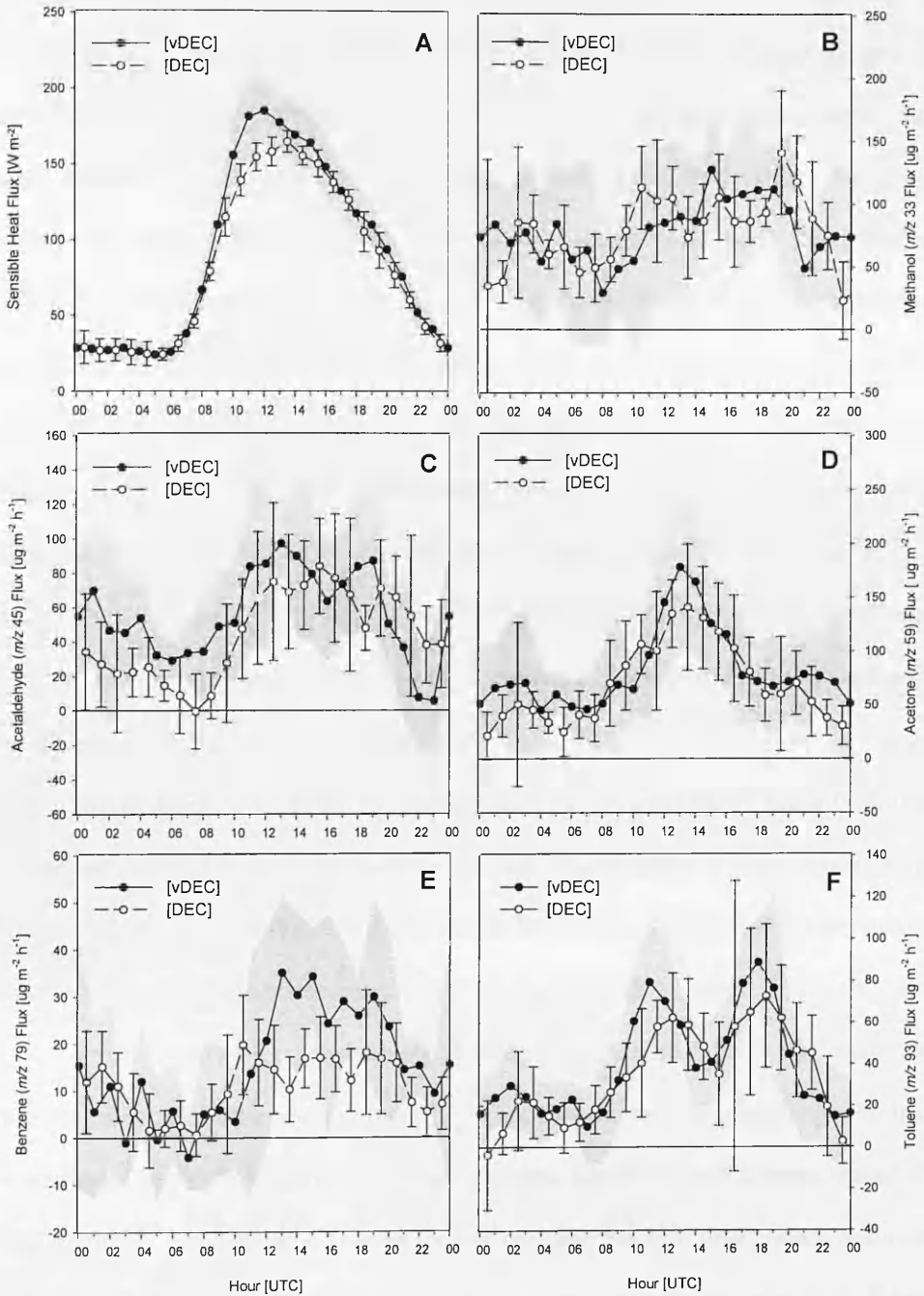


Figure 3.8. Panel A shows the effect of the reduced measurement resolution on simulated disjunct eddy covariance sensible heat fluxes. Panels B – F show the averaged daily fluxes of methanol, acetaldehyde, acetone, benzene and toluene respectively between the 5th and 20th of June 2006. Black circles represent measurements from the vDEC system, white circles show DEC measurements, greyed areas represent 1 standard error for the EC fluxes and error bars denoted 1 standard error for DEC fluxes.

hours of the morning. On average, fluxes were positive for most of the day, indicating the city to be acting as a net source of VOC to the atmosphere, although deposition was observed for short periods in the night. Typically, emissions rose sharply just after sunrise between 06.00 and 10.00 hrs, peaking at around midday for most compounds. This morning rise coincided with the peak in traffic counts which were taken on Oxford Road, a busy street adjacent to Portland Street, which provides a good proxy of the relative change of the diurnal traffic pattern in the area.

On average, fluxes of acetone were the largest ($88 \mu\text{g m}^{-2} \text{h}^{-1}$) followed by methanol, ($79 \mu\text{g m}^{-2} \text{h}^{-1}$) and acetaldehyde, ($60 \mu\text{g m}^{-2} \text{h}^{-1}$), whereas fluxes of the aromatic compounds benzene and toluene were lower ($19 \mu\text{g m}^{-2} \text{h}^{-1}$ and $42 \mu\text{g m}^{-2} \text{h}^{-1}$ respectively). Isoprene fluxes were omitted from the final analysis, as significant differences were observed between the two techniques, indicating a possible source of contamination in one or other of the systems.

Panel B, Fig. 3.9, shows the average daily flux of methanol. Typically, fluxes of methanol started to increase at around 08.00, rising steadily until an early evening maximum between 17.00 and 19.00 hrs. At this time fluxes dropped off sharply before levelling and reaching a minimum during the early morning.

Panel C shows the flux of acetaldehyde, which tended to have two afternoon maxima, the first and largest at around 13.00 hrs, and the second coinciding with that of methanol at 19.00 hrs. Similarly, both benzene (panel E) and toluene (panel F) demonstrated a two peak trend. In the case of benzene, the first peak, which occurred typically around 13.00 hrs was higher than the second, which occurred at 19.00 hrs. For toluene the reverse was true, with the second peak, again occurring at 19.00 hrs, being larger than the first at 11.00 hrs. Acetone (panel D) did not follow the same pattern of emission; instead, it demonstrated a clear single peak (13.00 hrs) which was

not dissimilar to that of the sensible heat flux shown in panel A. Unlike the other compounds, acetone had no peak at around 19:00 hrs, which may suggest a shift in emission sources at this time.

These diurnal trends suggest that toluene, benzene and acetaldehyde are primarily derived from direct traffic emissions as they follow the traffic pattern most closely. Acetone shows a different pattern which may be due to emission from other anthropogenic activities such as solvent use. Methanol emissions are broader over the day, consistent with a large contribution from fugitive sources that are coupled to a combination of temperature and anthropogenic activity.

Despite the indirect nature of this comparison, the two flux measurement systems showed reasonable agreement, with measured fluxes falling within the range of the calculated uncertainty (standard error of hourly fluxes). The highest observed correlations between the DEC and vDEC techniques were observed in the fluxes of toluene and acetone, which had R^2 values of 0.79 ($p < 0.0001$; $N = 48$) and 0.72 ($p < 0.0001$) respectively. Methanol ($R^2 = 0.2$ $p < 0.0288$) and acetaldehyde ($R^2 = 0.45$ $p < 0.0003$) compared less well, as did benzene ($R^2 = 0.36$ $p < 0.0001$), which, during the mid to late afternoon showed discrepancies between the two techniques. During this time the DEC system underestimated fluxes measured by the vDEC technique in a trend that was noticeable in all measured fluxes with the exception of methanol.

On average fluxes recorded by the vDEC system were 19% (absolute error) larger than those measured by the DEC system, although this value varied significantly between the individual masses, with no observed underestimation for methanol and approximately 40% underestimation for benzene. The most likely cause of this discrepancy is the difference in the effective response times of the two systems, as the vDEC system was able to resolve turbulent fluctuations of up to 10 Hz as

opposed to 1 Hz for the DEC system. The slower sampling resolution of the DEC system meant high frequency flux contributions may have been attenuated and lost and therefore the total flux was underestimated.

The portion of the flux attenuated by the slower measurement resolution can be estimated theoretically using wind and temperature data [20 Hz] to calculate the sensible heat flux. Extracting data points to correspond with the activation of DEC sampling valves generates a disjunct time series which can be compared to the original EC sensible heat flux. Reducing the effective sampling times of the data from 0.05 s to 0.5 s is achieved by simply extracting ten temperature measurements instead of one and using the average value for the flux calculation. When this technique was applied to the sensible heat data (Figure 3.9, panel A), the simulated DEC fluxes typically underestimated the EC fluxes by approximately 8 %. This suggests that some of the underestimation observed between the two systems is caused by the slower resolution of the DEC system but not all; therefore there are other sources of error which have yet to be quantified. One possible explanation is that the sampling response of the DFS is < 2 Hz, possibly because of adsorption / desorption effects in the ISRs for more “sticky” compounds. In addition, the differences between the two techniques seemed to be inversely proportional to VOC concentrations, hence benzene, which was the least abundant compound measured, demonstrated the largest deviation between the two data sets. This suggests the measurements of benzene were close to the detection limit of the instrument. In future this could be improved by increasing the integration time of the vDEC measurement from a dwell time of 20 ms to 0.1 or 0.2 s

3.3.3 Comparison of measured benzene fluxes with NAEI estimates

Measured fluxes of benzene were up-scaled and compared against the most recent (2005) emission estimate for Manchester taken from the National Atmospheric Emission Inventory (http://www.naei.org.uk/datachunk.php?f_datachunk_id=174). The flux estimates from the vDEC system were used for the comparison as they did not suffer from the attenuation of high frequency flux contributions. In order to compare the up-scaled fluxes with the inventory it was first necessary to calculate the flux foot print (surface area contributing to the flux) so that the appropriate NAEI grid(s) could be selected for comparison.

Footprints were calculated using a simple parameterisation model developed by Kljun *et al* (2004) which was run using typical urban meteorology to give footprints under stable, neutral and convectively unstable atmospheric conditions. This model is designed for dynamically homogenous terrain, therefore its application to the urban environment is not ideal; however there are few if any operational footprint models designed for this type of environment. Therefore the flux footprints obtained are treated as a first-order estimate only. The following parameters were used in the model: standard deviation of vertical wind velocities measured at Portland tower $\sigma_w = 0.3 \text{ m s}^{-1}$; friction velocity $u^* = 0.3 \text{ m s}^{-1}$ (average for measurement period); measurement height $z_m = 95 \text{ m}$; roughness length $z_0 = 1.5 \text{ m}$ (estimated as $1/10^{\text{th}}$ of the average building height (15 m)); and boundary layer height $h = 2000 \text{ m}$. The results are shown in Fig. 3.9 and list the distance at which the maximum contribution to the flux can be expected (X_{max}) and the distance at which 80% of the flux is contained (X_r). The results show the footprint size to scale with increasing turbulence, ranging from 1 km at low u^* values (0.2 m s^{-1}) to over 3.3 km at higher values (0.75 m s^{-1}) with an average size of approximately 1.5 km.

In order to calculate an emission estimate for the city using these data, it was assumed that the observed average fluxes were representative of the benzene emission rates occurring throughout the year (although the emission rates of benzene are likely

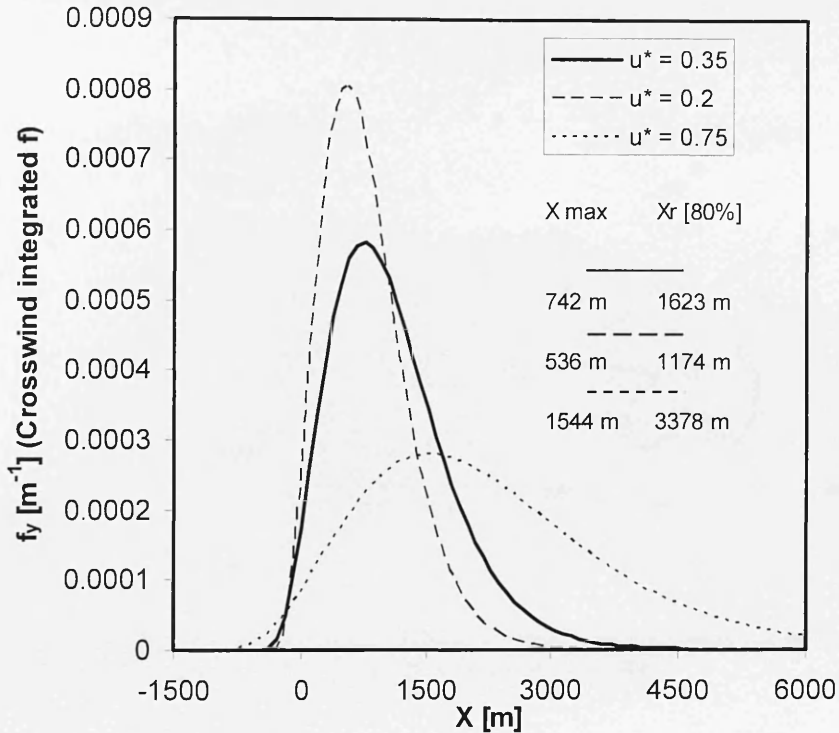


Figure 3.9. Predicted one-dimensional flux footprint from Portland Tower, Manchester, where the solid, dashed and dotted lines represent the predicted footprint for u_* values of 0.2 (minimum observed), 0.35 (average for campaign) and 0.75 m s^{-1} (maximum observed).

to show some seasonal variation, with increased vehicle use during the winter months causing higher direct emissions, this may be balanced by the increased fugitive emissions in the summer months). In addition, it was assumed that benzene fluxes were relatively consistent throughout the flux footprint. Figure 3.10 shows an analysis of the wind sector dependence of benzene concentrations and fluxes measured between the 5th and 20th of June. Benzene concentrations are skewed, with higher concentrations observed during south westerly wind directions and lower concentrations during south easterlies. In contrast, benzene fluxes are fairly well

distributed across each wind sector. The difference between the concentrations and fluxes occurs because concentration measurements are influenced by both local and distant point/diffuse sources, whereas fluxes are only controlled by emissions from sources within the footprint.

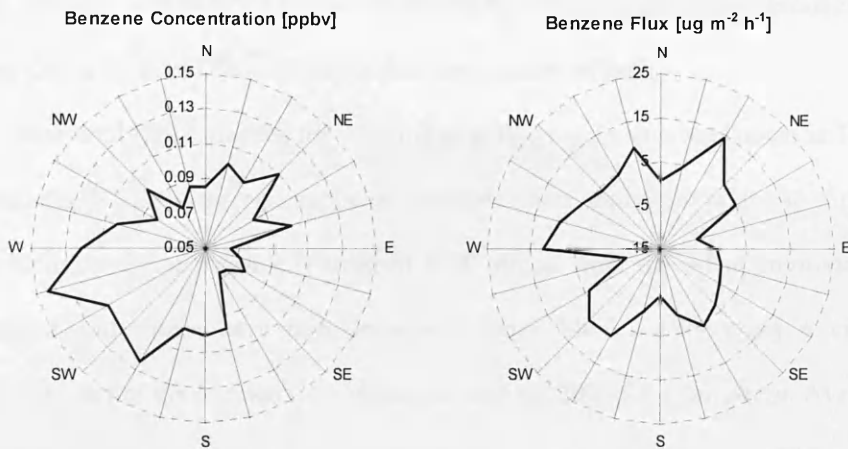


Figure 3.10 Analysis of the wind sector dependence of benzene concentrations and flux measurements made from Portland Tower, Manchester, in June 2006.

Therefore the measured average total daily flux of benzene ($454 \mu\text{g m}^{-2} \text{d}^{-1}$) was extrapolated to give an annual emission estimate of $0.17 (\pm 0.12) \text{ t km}^{-2} \text{ yr}^{-1}$. This value was six times lower than that predicted (average of NAEI grid squares contained within the predicted flux footprint) by the NAEI ($0.98 \text{ t km}^{-2} \text{ yr}^{-1}$) for Manchester city centre in 2005.

Since the implementation of both the Geneva VOC (UN ECE, 1991) and the Gothenburg multi-pollutant Protocols (UN ECE, 1999) annual average mean benzene concentrations have declined in the U.K at a rate of approximately -20% per year (Dollard *et al.*, 2007). This decrease has been brought about largely through the implementation of three way catalysts to control vehicle emissions and the use of

canisters to control the evaporative emissions. Taking this decline into consideration and readjusting the 2005 NAEI emission estimate accordingly, a revised emission estimate of $0.78 \text{ t km}^{-2} \text{ yr}^{-1}$ for 2006 is realised. However this figure is still significantly higher than the measured fluxes. Reasons for this large discrepancy are uncertain, but are likely to involve either poorly characterised VOC sources and/or activity statistics within the NAEI, or, a statistically unrepresentative measurement of benzene fluxes by the vDEC technique, or a combination of both.

Measured flux estimates for the remaining five compounds are shown in Table 3.3, but the NAEI does not explicitly estimate their emission rates, so further comparisons were not possible. Published VOC fluxes from the urban environment are limited, but fluxes have been measured above Mexico City using a vDEC approach as part of the Mexico City Metropolitan Area 2003 field campaign. Average fluxes of methanol ($1044 \mu\text{g m}^{-2} \text{ h}^{-1}$), toluene ($828 \mu\text{g m}^{-2} \text{ h}^{-1}$) and acetone ($396 \mu\text{g m}^{-2} \text{ h}^{-1}$) were found between four and nineteen times higher than those observed in

Table 3.3. VOC emission estimates for Manchester city centre based on micrometeorological flux measurements from Portland Tower.

	<i>Methanol</i>	<i>Acetaldehyde</i>	<i>Acetone</i>	<i>Benzene</i>	<i>Toluene</i>
Emission Estimate [$\text{t km}^{-2} \text{ yr}^{-1}$]	0.69 (± 0.44)	0.52 (± 0.29)	0.77 (± 0.41)	0.17 (± 0.12)	0.37 (± 0.18)
NAEI Emission Estimate (2005) [$\text{t km}^{-2} \text{ yr}^{-1}$]	-	-	-	0.98 (± 0.02)	-

Manchester. This is unsurprising given the much older vehicle fleet, less dominance of catalytic converters and poorer fuel quality in Mexico City, where vehicle emissions are not regulated by the aforementioned protocols.

3.4 Conclusions

In the past the virtual and disjunct eddy covariance techniques have been successfully applied to give flux information from a range of vegetation canopies. In the present study we have shown that these techniques can be extended to the urban environment provided a measurement site with suitable elevation above street level can be found. We have also demonstrated the effectiveness and limitations of each approach. The vDEC technique is thought to be more suited for urban flux work due to its relative simplicity and fast response time. However, the DEC technique has also been shown to be effective and, with improvements to the system design, such as increased measurement frequency and tower mounting capabilities, could become an important tool in increasing our understanding of both anthropogenic and biogenic VOC emissions.

Emission estimates derived using flux data from the vDEC technique demonstrate the potential of using VOC flux measurements in determining emission estimates on a city wide scale. Although emission estimates obtained in this study are based on a “snap shot” of the total yearly emission, they demonstrate the potential of the technique, which, if deployed on a longer time scale such as a year could give very detailed information on urban-scale emissions, including both spatial and, more importantly, temporal trends, which are currently not accounted for in the NAEI emission estimates.

Finally, we have demonstrated that ambient air temperature plays an important role in the relative concentrations of VOCs in urban air. While some compounds are solely governed by their volatility and increased evaporation rates at higher temperatures, others such as isoprene, can also be influenced by increased biogenic emissions occurring both in, and outside of the city.

Acknowledgements

We thank Bruntwood Estates Ltd for allowing access to Portland Tower and for the cooperation and support of their staff. The work was funded by the UK Natural Environmental Research Council through the “CityFlux” grant and an NCAS studentship and by the ESF VOCBAS programme. We thank Ian Longley (Manchester University) who was responsible for the organisation and logistics of the campaign, Gavin Phillips (CEH Edinburgh) for his help transporting the instrumentation and Malcolm Possell (Lancaster University) for helpful discussion.

Chapter IV

4. Eddy covariance flux measurements and ambient concentrations of volatile organic compounds in central London

In this chapter measurements of volatile organic compound fluxes from central London are presented. Measurements were made using the virtual disjunct eddy covariance technique, which, during the Manchester campaign, was found to be more easily installed and operated than the DFS. The system was deployed on the Telecom tower, a 200 m communications mast located in the borough of Westminster. Ancillary measurements of CO concentrations and fluxes were made and compared to measured VOCs. In addition, the measured VOC fluxes were related to local traffic density and up-scaled to give an annual emission estimate which was compared to data taken from the national atmospheric emission inventory.

This research will be submitted to the journal of Atmospheric Chemistry and Physics. The authors and their contributions are listed below.

Ben Langford (Lancaster University & CEH): Developed the vDEC system and software, operated the instruments during the field campaign, post processed the raw data and wrote the manuscript.

Eiko Nemitz (CEH): Co-wrote the software for the vDEC system, helped with the installation of the systems, processed the CO fluxes and helped with the compilation of the manuscript.

Emily House (Edinburgh University & CEH): Helped with the installation and set-up of the PTR-MS at the tower.

Gavin Phillips (CEH): Co-operated the CO analyser.

Daniela Famulari (CEH): Co-operated the CO analyser.

Brian Davison (Lancaster University): Helped with interpretation of results and the compiling of the manuscript

Jim Hopkins (University of York): Co-operated the GC-MS sampling system.

Ally Lewis (University of York): Co-operated the GC-MS sampling system

Nick Hewitt (Lancaster University): Helped with interpretation of results and the compiling of the manuscript

Eddy covariance flux measurements and ambient concentrations of volatile organic compounds in central London

B. Langford^{1,2}, E. Nemitz², E. House^{2,3}, G. J. Phillips², D. Famulari², B. Davison¹, J. Hopkins⁴, A. Lewis⁴ and C. N. Hewitt¹

[1] Lancaster Environment Centre, Lancaster University, LA1 4YQ, UK.

[2] Atmospheric Sciences, Centre for Ecology and Hydrology, Bush Estate, EH26 0QB, Edinburgh, UK.

[3] School of Chemistry, Edinburgh University, West Mains Road, EH9 3JJ, Edinburgh, UK.

[4] Department of Chemistry, University of York, York, YO10 5DD, UK

Abstract

Concentrations and fluxes of eight volatile organic compounds (VOC) were measured above central London during October 2006. Daily averaged VOC concentrations were within the range of 1 – 13 ppb for the oxygenated compounds methanol, acetaldehyde and acetone, 0.2 – 1.3 ppb for the aromatics, benzene, toluene and ethylbenzene and typical VOC fluxes were in the range of 70 – 130 $\mu\text{g m}^{-2} \text{h}^{-1}$. Concentrations were comparable with long term measurements at a nearby monitoring station. Detailed analysis of data from the station showed biogenic sources of isoprene to account for a significant fraction of the total measured isoprene within the city during warmer periods. The relationship between traffic density and VOC fluxes was demonstrated and the resultant parameterisation applied to a year long set of traffic

data to derive annual emission estimates for each VOC. Comparison of the measured benzene fluxes with the U.K national atmospheric emission inventory showed measured values to be of a similar magnitude as inventory estimates.

4.1 Introduction

Volatile organic compounds (VOCs) in ambient air influence local and regional air quality and can also impact upon human health through both primary and secondary pathways. For example, long-term exposure to compounds such as benzene and 1-3 butadiene has been linked with both acute and chronic forms of leukaemia (Johnson *et al.*, 2007). In addition, tropospheric ozone, a photochemical air pollutant formed as a consequence of VOC precursor emissions, has been associated with a number of respiratory conditions (Burnett *et al.*, 1997). At elevated concentrations, tropospheric ozone can also cause damage to crops, forest ecosystems and buildings. Similarly, certain VOCs are iteratively oxidised in the atmosphere and thus act as precursors for the generation of secondary organic aerosol (SOA), which contributes to particulate matter with implication on human health and the climate system.

VOCs are the subject of much scientific interest, and efforts have been made to curtail and better regulate the emission of anthropogenic VOCs (AVOCs). In Europe much of this has been achieved through the implementation of both the Geneva VOC (UN ECE, 1991) and Gothenburg multi-pollutant protocols (UN ECE, 1999), which promote the introduction of 3-way catalysts to all newly manufactured road vehicles and forced steps to be taken to reduce evaporative emissions from petroleum products.

In order to quantify the effectiveness of such emission control measures accurately it is necessary to compile spatially disaggregated emission inventories. In

the U.K. this is done using a “bottom-up” approach to produce a yearly emission estimate for 25 separate air pollutants as part of the UK National Atmospheric Emission Inventory (NAEI) activity. Only two VOCs, benzene and 1-3 butadiene, are explicitly included in this, leaving other important VOCs, such as those with high ozone forming potentials, including toluene, largely unaccounted for. Furthermore, the compilation of an annual estimate means short term temporal trends in VOC emission rates, which may be important in helping elucidate the processes involved in local photochemical pollution episodes, are not quantified.

In contrast to the NAEI, micrometeorological flux measurement techniques such as eddy covariance and virtual/disjunct eddy covariance (vDEC) offer a “top down” approach to emission estimates, giving insight into both spatial and temporal changes in VOC emission. To date most VOC flux measurements made with these methods have focussed on emissions of biogenic volatile organic compounds (BVOC) from vegetation canopies such as grassland (Karl *et al.*, 2001; Rinne *et al.*, 2001; Warneke *et al.*, 2002; Ammann *et al.*, 2006; Brunner *et al.*, 2007) and forests (Karl *et al.*, 2002; Grabmer *et al.*, 2005; Spirig *et al.*, 2005; Lee *et al.*, 2006), avoiding the urban environment due to the difficulties associated with its high variability in surface cover and roughness elements (Velasco *et al.*, 2005). However, recent studies have demonstrated that these techniques can also be extended to the urban canopy provided a measurement site with a suitable elevation above street level can be found (Nemitz *et al.*, 2002; Dorsey *et al.*, 2002; Velasco *et al.*, 2005; Langford *et al.*, 2008).

Direct micrometeorologically-based observations such as these offer several advantages over modelled emission inventories such as the NAEI. Firstly they integrate direct observations of vertical wind speed and scalar concentration over a wide spatial area, which ensures the numerous sources of VOC emissions at street

level are resolved within the flux measurement. This is highly advantageous as it does not require the characterisation of individual sources as in the NAEI, nor does it rely on the accuracy of activity statistics such as traffic counts, fleet composition, driving patterns or fuel consumption. Secondly, changes in emission rates can be resolved temporally, revealing changes in emission rates on time scales of minutes and longer, something which is not currently possible using an emission inventory. Finally, the use of the proton transfer reaction – mass spectrometer (PTR-MS), an online VOC monitoring instrument, enables the simultaneous measurement of a number of VOCs, providing scope for the development of speciated emission estimates.

Although there are uncertainties associated with any flux measurement technique, urban emission estimates derived using the vDEC technique have compared closely to modelled emission estimates in the past (Velasco *et al.*, 2005). In the current study we demonstrate the use of the vDEC technique to derive emission estimates for eight volatile organic compounds above central London and, where possible, we compare the results to emission estimates within the most recent (2005) NAEI data base for London. We also compare VOC data with ancillary measurements of CO concentrations and fluxes.

4.2 Experimental

4.2.1 Measurement site

During the autumn of 2006 (30/09/06 – 30/10/06), micrometeorological measurements of VOC concentrations and fluxes were made over central London. The measurements were conducted as part of the REgents PARK and Tower Environmental Experiment (REPARTEE) in the framework of the UK CityFlux project, which encompassed a wide range of scientific activities, including measurements of fluxes of

H₂O, CO₂, CO, O₃ and aerosols. In addition to these tower based activities, ancillary ground-level measurements were made in Regent's Park.

Greater London is made up of 32 district Borough Councils, covering approximately 1600 km², with over 7.5 million inhabitants. The site selected for the study was the Telecom Tower (51°31'17.4'' N; -0 °8'20.04''W), a telecommunications tower, which is located in the Borough of Westminster in central London. The tower is situated 8 km east of the cities central business district and is surrounded by a mixture of commercial and residential buildings giving the location an urban classification of 2 (Intensely developed high density urban with 2 – 5 storey, attached or very close-set buildings often of brick or stone, e.g. old city core) according to the criteria described by Oke (2004). A short distance from the tower in the SW and NW directions are two large amenity areas, Hyde Park and Regents Park. To the NE are three major railway stations and directly to the south is Oxford Street, one of the principal shopping streets in central London.

The structural design of the Telecom Tower makes it an ideal platform from which to make micrometeorological measurements. It stands at a height of 191 m and has a typical diameter of 16 m. The cylindrical shape minimises the distortion of air flow around the building, while the 185 m elevation above the average surrounding building height is sufficient to escape the effects of roughness elements below, offering a homogenous fetch in all directions. A 12 m tall lattice structure is erected on the Tower's flat roof, upon which was mounted a 3 m mast supporting an ultrasonic anemometer (Model R3-50, Gill Instruments, U.K.) and gas inlet. Air was pumped down a 45 m long Teflon tube (3/8" OD) at a flow rate of 60 l m⁻¹ to the instruments which were housed in the Tower.

4.2.2 VOC sampling

VOC mixing ratios were measured using a proton transfer reaction mass spectrometer. Unlike some conventional mass spectrometers, the PTR-MS uses the transfer of a proton to “softly” ionise the compound(s) of interest. A detailed description of this instrument can be found elsewhere (Lindinger *et al.*, 1998; de Gouw *et al.*, 2007; Hayward *et al.*, 2004). Briefly, H_3O^+ primary ions are produced in a high voltage hollow cathode by the introduction of pure water vapour. From here the primary ions are accelerated into a drift tube region which is continually purged with sample air. Subsequently a proton is donated by the H_3O^+ ions to any atmospheric constituent with a proton affinity greater than that of water. The protonated ions are then mass (atomic mass unit; amu) selected as they pass through a quadrupole mass spectrometer, before being detected by a secondary electron multiplier (SEM). The design of this instrument allows VOC mixing ratios to be measured with both fast response times (< 200 ms) and good sensitivity (10 -100 ppt) (Hayward *et al.*, 2004; Hewitt *et al.*, 2003).

In the current study an Ionicon (GmbH, Innsbruck, Austria) high sensitivity PTR-MS (fitted with 3 Varian turbo pumps and a silico steel heated inlet) was used for the measurement of VOC concentrations and operated in two modes, SCAN and FLUX. During the first five minutes of every hour the total mass range (m/z 21 – 146) was scanned to give basic concentration information on a wide range of hydrocarbons. The PTR-MS was then operated in FLUX mode for two 25 minute averaging periods per hour, with the quadrupole scanning through 11 pre-determined masses (0.1 s per m/z) in duty cycles lasting just over 1 s per cycle. The targeted protonated masses included: methanol (m/z 33), acetonitrile (m/z 42), acetaldehyde (m/z 45), acetone/propanal (m/z 59), isoprene/furan (m/z 69), benzene (m/z 79), toluene (m/z 93)

and ethylbenzene (m/z 107). The remaining 5 minutes of each hour were used to measure the instrument background by sampling air which first passed through a platinum catalyst.

During the period of measurements the PTR-MS was optimised to an E/N ratio of 125 Td with the drift tube pressure set to 2 mbar and a flow rate of 300 ml min^{-1} . The H_3O^+ primary ion count ranged between $8 - 10 \times 10^6$ ion counts per second (CPS) with less than 2 % O_2 and target ions ranged between $1 \times 10^1 - 1 \times 10^3$ CPS after background subtraction.

One of the major issues regarding PTR-MS measurements arises as a result of the mass detection system. As the quadrupole filters ions for detection, it separates them into integer m/z classes (m/z 21, m/z 22...etc), making it difficult to attribute an individual VOC to a particular m/z , since more than one VOC may be detectable at that mass number (Ammann *et al.*, 2004). For example, when measuring at m/z 59, one might expect to see acetone; however, propanal can also be detected at this amu. Complimentary techniques such as GC-MS are often required to ensure correct compound identification. For the eight m/z 's presented in this study there are thought to be only very minor contributions from unknown or unexpected VOC, therefore we assume each m/z to correspond to the VOC mentioned previously.

4.2.3 Data acquisition

The sonic anemometer recorded temperature and 3-D wind speeds at a rate of 20 Hz. The signal from the sonic was split six ways, allowing each analytical instrument to record both wind speed and concentration data simultaneously on their respective logging systems. The raw data were logged and archived for post-processing by a programme written in LabVIEW (National Instruments, Version 7.1).

This programme also recorded ion counts directly from the PTR-MS using the Microsoft Windows “dynamic data exchange” protocol (DDE) and converted these signals to volume mixing ratios and performed preliminary online flux calculations.

4.2.4 Calculation of fluxes

The PTR-MS is capable of returning concentration information on individual VOCs at fast rates, in theory making it ideally suited to the eddy covariance flux measurement approach. In reality, the quadrupole can only filter one m/z at a time; therefore the temporal resolution of the data is governed by the total number of compounds measured. Consequently, rather than outputting a continuous high frequency data set, an array of measurements is returned as each measurement cycle is completed, in effect creating a disjunct time series of fast (0.1 s) measurements, which are made every 1.2 s or so. A flux may still be calculated using this reduced dataset, provided the averaging time of each individual measurement was sufficiently short (here 0.1 s). In some flux measurement setups this is achieved using a disjunct eddy covariance approach (DEC), where a grab sample of air is rapidly aspirated into a chamber and the contents analysed offline with slower sensors (Grabmer *et al.*, 2005). Here, however, the need for grab samples becomes redundant, as the PTR-MS can still scan each individual mass at the desired sampling rate, just not simultaneously. Therefore the flux is calculated in the same direct way as the eddy covariance approach, the only difference being a reduced data set. Hence concentration data (χ) were combined with the corresponding vertical wind velocity (w), and the flux (F_χ) was derived from the time averaged covariance between the instantaneous deviations of w' and χ' from their respective means:

$$F_{\chi} = \frac{1}{n} \sum_{i=1}^n (w_i - \bar{w}) \cdot (\chi_i - \bar{\chi}) \quad (1)$$

As the air sample for PTR-MS analysis had to be pumped ~ 45 m down from the inlet to the instrument, a significant time lag was introduced between the two datasets. To correct for this temporal shift, concentration data were shifted back in time until a maximum in a cross-correlation function between w' and χ' could be found within a user-defined time window. The maximum correlation typically occurred at around 6 s (or 120 data points at 20 Hz). This agreed closely with the same cross-correlation function applied to CO₂ data recorded by a fast response instrument (Infrared gas analyzer LI-COR 7000) which sub-sampled directly after the PTR-MS. The precision of each flux measurement was determined following the criteria specified by Spirig *et al* (2005), where the noise of the covariance function is characterised by the standard deviation of the function at distances far from the peak value. Working under the assumption of a normal distribution, multiplying the standard deviation by 3 gives the measurement precision at the 99.7% confidence interval, this value also acts as a proxy for the flux detection limit and provides an additional quality check for the data.

In addition to VOC measurements, CO fluxes were measured with a fast-response VUV CO analyser (AeroLaser AL5002).

4.2.5 Quality assessment of fluxes

A post-processing algorithm was written in LabVIEW which not only re-processed fluxes but also filtered out data files which did not meet specific quality criteria. The algorithm involved the following steps: (i) rotation of the coordinate system to correct for sonic anemometer tilt relative to the terrain surface, where u was

aligned with the mean wind direction, therefore setting $\overline{w} = 0$, (ii) removal of hard spikes caused by electrical interference and buffering, (iii) conversion of raw PTR-MS ion counts to ppb mixing ratios, (iv) calculation and setting of lag times using a cross-correlation function, (v) calculation of fluxes, including sensible heat, momentum, frictional velocity (u^*) and VOCs, (vi) calculation of flux precision, rejecting files where the peak in the CC function was below three times the measurement precision (vii) testing of mean wind speed (U), rejecting data files where $U < 1 \text{ m s}^{-1}$ or $u^* < 0.15 \text{ m s}^{-1}$ and (viii) testing of fluxes for stationarity, rejecting failed data files.

The stationarity test applied followed the theory outlined by Foken & Whichura (1996), which states that a time series χ is stationary when the flux (F_χ) is equal to the mean average flux of its components ($F_{\chi 1}, F_{\chi 2}, F_{\chi 3} \dots$). Here we took F_χ to be the flux over the 25 minute averaging periods, and the components $F_{\chi 1}$ to $F_{\chi 5}$ to be the flux calculated from individual five minute blocks of the original time series. Following criteria specified by Velasco *et al.*, (2005), if the mean of $F_{\chi 1}$ to $F_{\chi 5}$ differed by more than 60% of the value of F_χ the time series was considered non-stationary and the data were discarded. Time series where the fluxes differed between 30% and 60% were considered stationary, but to be of a low quality. High quality stationary data were taken to be any time series where the fluxes differed by less than 30%.

During the current study an average 13% of the data were rejected due to lack of stationarity, 22% were removed because of insufficient turbulence ($u^* < 0.15 \text{ m s}^{-1}$) and a further 25% were rejected as fluxes were below the limit of detection. Of the 40% of the data that passed the quality assessment, 68% were ranked as high quality and 32% low quality.

4.2.6 NAEI Emission Estimates

The emission estimates used in this study were taken from the 2005 National Atmospheric Emission Inventory (NAEI). The NAEI provides disaggregated, 1 km × 1 km gridded emission estimates for 25 atmospheric pollutants. A detailed description of the NAEI mapping methodology is described elsewhere (King *et al.*, 2003). Briefly, the NAEI generates emission estimates from 11 source sectors. Each estimate is a combination of reported and estimated emissions, the latter calculated theoretically by multiplying an emission factor by a given activity statistic.

For example, the emission of benzene from road transport may be expressed as the amount of benzene contained in car exhaust (emission factor), multiplied by the number of kilometres driven per year (activity statistic). Intuitively, the accuracy of estimated emissions is governed by the quality of the statistical information used. Therefore emissions reported by the operator of the process (e.g. from large plant point sources) are often considered more robust than those estimated for area sources, as the former tend to be based on more reliable data. From this it follows that the accuracy of an emission inventory is related to the ratio between reported and estimated emissions. For benzene, this ratio is very low, with just 10% of emission estimates coming from reported data, whereas for CO₂, for example, the ratio is much higher, with 46% of data originating from known point sources.

Measured fluxes of both VOCs and CO were compared with the NAEI. The NAEI emission estimates are broken down into 1 × 1 km grid squares. Therefore, in order to generate an emission estimate for comparison, it was first necessary to calculate the footprint of flux measurements and then integrate the encompassed grids to give a single annual emission estimate. The selected grids and flux footprint are shown in Fig. 4.1.

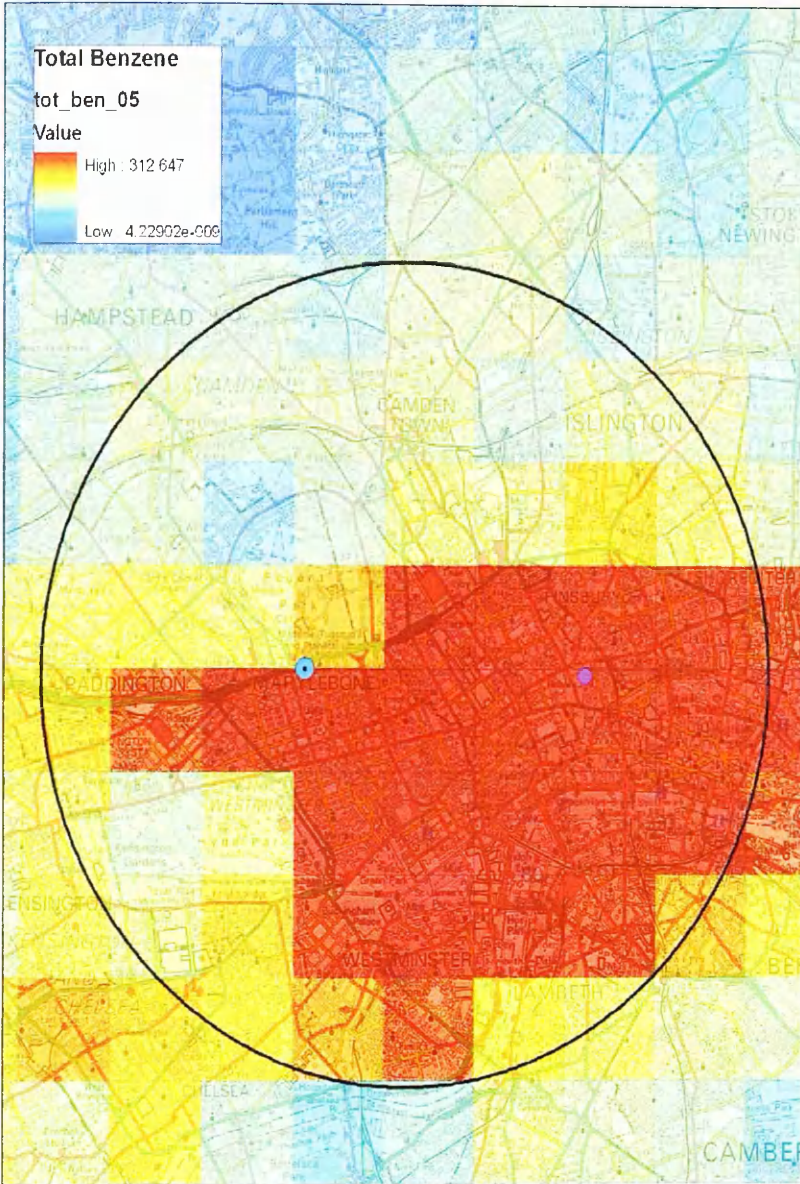


Figure 4.1. National atmospheric emission inventory map of benzene in central London (in tonnes $\text{km}^{-2} \text{yr}^{-1}$). The black circle represents the approximate area of the flux footprint (area containing 80% of the measured flux). The red circle in the centre marks the location of the Telecom Tower and the turquoise and purple circles represent the Marylebone automating monitoring station and the London Weather Centre, respectively.

4.2.7 Calculation of the Flux Footprint

The typical daytime flux footprint for micrometeorological measurements conducted at the Telecom Tower was calculated using a simple parameterisation

model developed by Klujan *et al.*, (2004). Although originally developed for dynamically homogenous terrain, this model has been extended to the urban environment with some success, hence its application here. Typical values of urban meteorology were used to determine footprint estimates under stable, neutral and convectively unstable atmospheric conditions, as well as for the average conditions experienced during the measurement campaign. The following parameters were used in the model: standard deviation of vertical wind velocity $\sigma_w = 0.3 \text{ m s}^{-1}$; friction velocity $u_* = 0.3 \text{ m s}^{-1}$; measurement height $z_m = 200 \text{ m}$; roughness length $z_0 = 0.4 \text{ m}$; and boundary layer height $h = 250 \text{ m}$ (stable), 1000 m (neutral) and 2000 m (unstable).

4.3 Results and discussion

4.3.1 Concentration measurements

4.3.1.1 Trends in VOC concentration

Averaged diurnal concentration plots for each of the eight compounds are shown in Fig 4.2. During the study period, clear day-night trends were observed in the measurements of VOCs, with the highest concentrations recorded during the daytime and the lowest at night. Temporal trends on a weekly time scale were also evident, with VOC concentrations typically 15% higher during weekdays when compared with weekends. Furthermore, at weekends, concentrations of some compounds began to rise much later in the day, frequently beginning to rise at 06.30 hrs [UTC], three or four hours later than was typical during the week. Throughout the measurement period

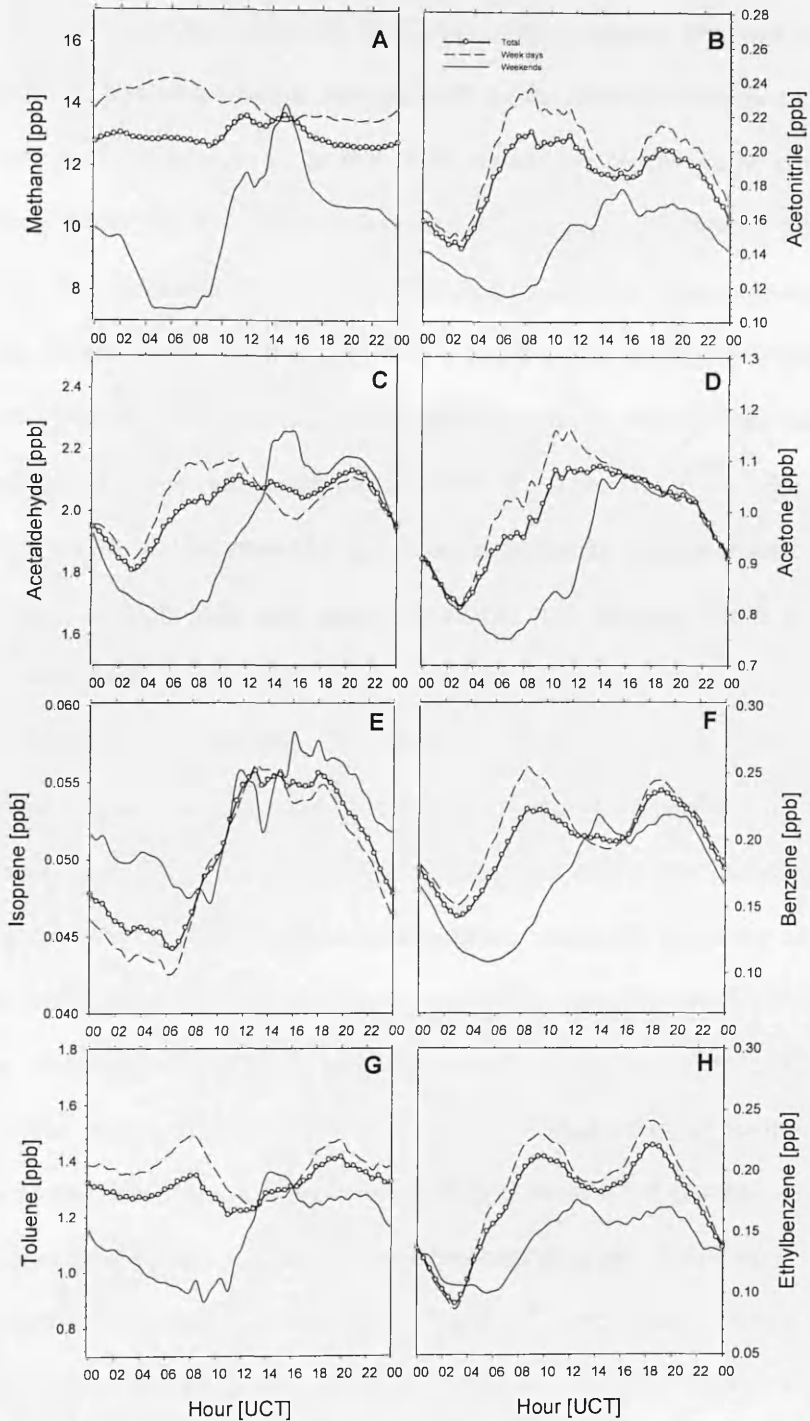


Figure 4.2. Average diurnal concentration plots for eight of the measured volatile organic compounds measured between the 30th of September and the 30th of October 2006. White circles represent the total average concentration, solid line represents the average weekend concentration and the dashed line represents average week day values.

concentrations of the oxygenated compounds were highest, followed by those of the aromatics and isoprene. On a day to day basis, each analyte typically followed one of two patterns. The first, characterised most typically by the aromatic compounds, had two day time peaks, one occurring around 10.00 hrs and the second, larger peak at approximately 19.00 hrs. A third, much less well defined peak, occurring at around 14.00 hrs was also evident on certain days, although this tended to be more prominent at weekends. In addition to the aromatics, both acetonitrile and acetaldehyde loosely followed this 2-peak trend, whereas acetone and isoprene did not. Instead, only a single midday maximum was observed, followed by a decline in concentration throughout the mid to late afternoon and evening. Methanol concentrations were highly variable on both daily and weekly timescales and therefore could not be likened to either trend.

Figure 4.2A shows the plot for methanol. During the campaign, methanol concentrations ranged between 5 and 54 ppb, with an average of 13 ppb, making it the most prevalent of the VOCs measured. This was consistent with a previous study by Langford *et al.*, (2008), where methanol concentrations measured above the city of Manchester were found to be significantly higher than all other measured VOCs. In the present campaign, methanol concentrations varied significantly on both weekly and daily time scales. During the first week of measurements, concentrations increased steadily from 7 ppb, to a maximum of 54 ppb on the 8th of October. A slow decline in concentration was recorded in the subsequent days and, following a short disruption to the measurements between the 15th and 19th, concentrations returned to the level (7-10 ppb) observed at the start of the campaign. Unlike the other measured VOCs, strong diurnal trends were not apparent. During the working week, concentrations tended to be highest during the night time and lowest during the day,

whereas at weekends the reverse was true, with a maximum peak typically occurring in the mid to late afternoon. This may suggest that, at weekends, the dominating influence on the concentrations are the dynamics of the boundary layer (leading to higher concentrations at night), while during weekdays the change in anthropogenic sources such as emissions from industrial activities dominates diurnal variations.

For acetonitrile (Fig. 4.1B) diurnal trends were apparent throughout the week. Mixing ratios typically ranged between 0.09 and 1.1 ppb, with an average of 0.2 ppb. Concentrations began to rise from 03.00 hrs, before reaching a broad peak between 08.00–11.30 hrs. During the mid afternoon, concentrations dipped before reaching a second, reduced, peak at around 19.00 hrs. At weekends a different, single peak was apparent, with concentrations rising much later in the morning at approximately 07.00 hrs and peaking around 15.30 hrs.

Figure 4.1C shows the average diurnal trend in measurements of acetaldehyde, which was the second most abundant compound observed, ranging between 0.3 and 6.3 ppb, with an average of 2 ppb. The trend in acetaldehyde concentrations closely mirrored that of acetonitrile, which is unsurprising as both of these compounds are largely derived from fossil fuel combustion and biomass combustion. Differences between the two compounds only became apparent at weekends, when acetaldehyde concentrations were marginally higher.

Measurements of acetone (Fig. 4.2D) showed a very broad, single peak, with typical values ranging between 0.3 and 2.8 ppb and an average of 1 ppb, making it the fourth most prevalent VOC measured during the study. The mixing ratios of acetone rose from 03.00 hrs during the week, levelling slightly at 07.00 hrs, before reaching a maximum between 10.00 and 14.00 hrs. A slow decline in concentration throughout the remainder of the day was typical during both weekdays and weekends, although

during the latter, the morning rise and afternoon peak did not occur until 07.00 hrs and 14.00 hrs respectively.

Isoprene (Fig. 4.2E) was present in the atmosphere at much lower concentrations than acetone, between 0.01 and 0.1 ppb, with an average of 0.05 ppb, but demonstrated a similar trend. Morning increases in isoprene concentrations did not occur until approximately 07.00 hrs on both weekdays and weekends, which was significantly later than that observed for the other measured compounds. Subsequently the morning rise was rapid, with a broad peak forming between 13.00 and 18.00 hrs. Concentrations decreased abruptly during the evening, which was in contrast to the observed behaviour of acetone. In addition to this dissimilarity, isoprene concentrations, unlike any of the other VOCs measured, were marginally higher (6%) at the weekends, especially during the night. The ambient air temperature was also found to be higher at the weekends (2%), with the largest difference in temperature occurring at night time.

Measurements of benzene and ethylbenzene are shown in Figs. 2F and 2H, respectively. These two compounds showed remarkable similarities, with almost identical trends observed on both weekdays and weekends. Ethylbenzene was the more prevalent of the two compounds, ranging between 0.03 and 1.3 ppb, with an average of 0.2 ppb, compared with 0.05 - 1 ppb for benzene with an average concentration of 0.2 ppb. Typically concentrations of both compounds began to rise at 03.00 hrs, before reaching the first of two peaks at 10.00 hrs. From 10.00 hrs onward concentrations decreased and levelled before reaching a second, marginally larger peak at approximately 19.00 hrs. Concentrations then decreased during the evening and through the night.

Toluene (Fig. 4.1G) was more abundant than both benzene and ethylbenzene, ranging between 0.2 - 0.9 ppb, with an average of 1.3 ppb. Despite the higher concentrations, toluene demonstrated the same 2-peak trend, although some differences were apparent. Firstly, the morning and evening peaks were much better defined, in part due to a significant drop in concentration between 10.00 and 17.00 hrs. Secondly, at weekends, the reverse was true, with much higher concentrations in the afternoon and lower values recorded in the evening and morning respectively, resulting in a single-peak trend.

4.3.1.2 Comparison with GC-MS and national monitoring network data

In addition to the high resolution PTR-MS measurements, secondary VOC concentrations were recorded for validation and comparison purposes at a much slower time resolution using a gas chromatography – mass spectrometer (GC-MS). This system took canister samples of air over 30 minute time periods, with a 4 hour gap between each sample. Canisters were later analysed offline using a split column GC-MS. The results obtained, tended to be slightly higher than PTR-MS measurements for compounds in the low C₂ to C₃ range, while the heavier hydrocarbons, shown here in Fig. 4.3, such as benzene, toluene and ethylbenzene all showed excellent agreement.

During the study period VOC concentrations including, benzene, toluene and ethylbenzene, were also recorded by the U.K. government's automatic urban and rural monitoring network (AURN) at their Marylebone road kerb site. This site is 900 m from the base of the Telecom Tower in a westerly direction. Comparisons of the trends in concentrations between the two sites were in good agreement for benzene and ethylbenzene with R² values of 0.5 and 0.6 respectively, whereas for toluene, the

trend observed at the PTR tower differed significantly from that seen at street level. Typically, at street level, concentrations of toluene were highest during the day with a broad peak between 07.00 hrs and 17.00 hrs and at their lowest during the night. On

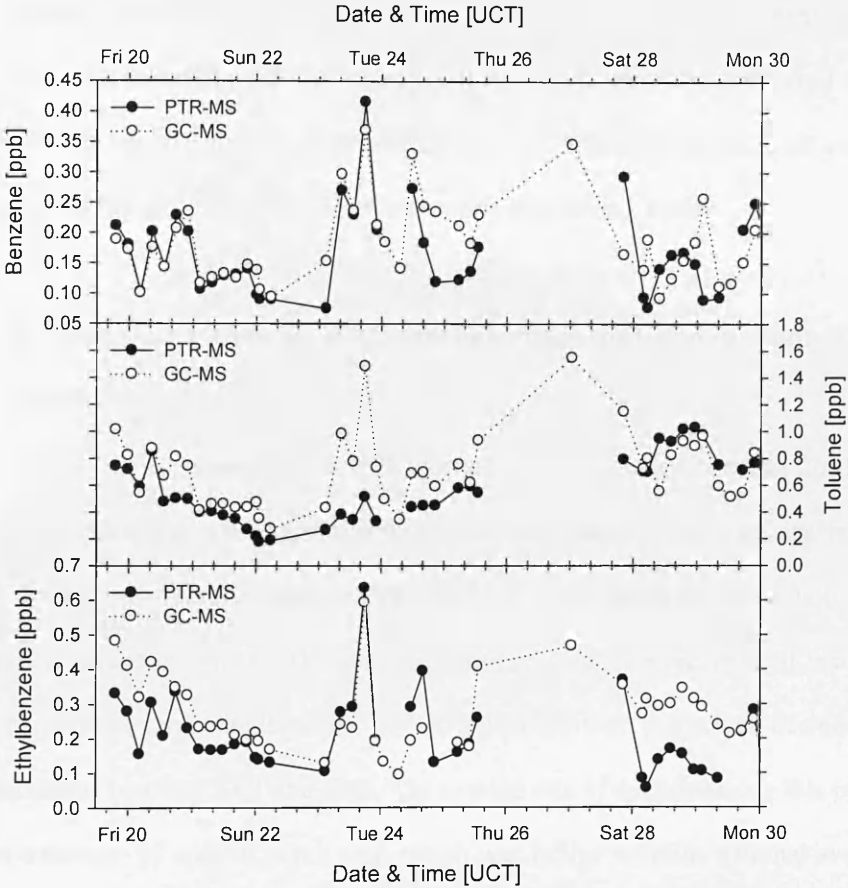


Figure 4.3 Comparison of PTR-MS data with GC-MS data which both sampled VOC concentrations from the Telecom Tower during the CityFlux campaign.

the tower the reverse was true, with concentrations tending to be depleted during midday and peaked during the night. Similar night time maxima in toluene concentrations (but not in other VOCs) were observed during a study by Kato *et al.* (2001) where VOCs were measured by PTR-MS outside of Tokyo. This trend in toluene concentration was attributed to the presence of a nocturnal surface inversion layer, which may also be the case in the current study. In addition to this,

measurements at the tower are likely to be strongly influenced by air masses originating from outside of the city, whereas at street level, where the sampling location is in close proximity of the primary emission sources, the influence of advected air masses is likely to be negligible. Despite good agreement in the concentration trends (with the exception of toluene), concentrations measured at the kerbside were significantly higher than those observed at the Tower, with, on average a 2 times dilution of concentrations between street canyon and Tower.

4.3.1.3 Temporal trends in VOC concentrations in London from 2001 - 2006

Historical measurements of VOC concentrations recorded between 2001 and 2006 by the AURN monitoring station located on Marylebone Road were analysed to look for long term trends or seasonal variations in VOC concentration to help place the current results in context. The analysed data included measurements of benzene, isoprene, toluene and ethylbenzene, all of which showed a gradual decrease in concentrations between 2001 and 2006. The average rate of decline during this period ranged between -16 and -21% per year, which was in line with the national average during the same time period (Dollard *et al.*, 2007).

Benzene concentrations were typically 18% higher during the winter months (October – April) when compared to the summer (May – September), with the highest concentrations typically observed in November and the lowest values found between April and July. Values recorded in October were 13% higher than the yearly average, suggesting that the measurements in the current study are likely to be slightly greater than the annual benzene concentration.

Similar winter - summer variation was observed in measurements of ethylbenzene and toluene, although the difference between the two seasons was less, with average differences of 9 and 5% respectively. The highest concentrations were observed in November for toluene and October for ethylbenzene, which were 15 and 18% higher respectively than the annual average.

The increase in aromatic VOC concentrations during the winter months could be linked to changes in the primary sources within the city, with a shift from traffic activity, which showed no variation with season, to combustion related emissions linked to both domestic and commercial heating, and/or industrial processes. It should be noted however, that although traffic density did not vary with season, vehicle emissions may show some variation, with increased emissions possible during colder temperatures due to the more frequent occurrence of cold engine starts. Higher concentrations of the OH radical, which is the major oxidant of most VOC and is photochemically produced, may also actively lower VOC concentrations during the summer months.

The ratio of benzene to toluene concentrations (b/t ratio) measured between 2001 and 2006 is shown in Fig. 4.4. An increase in the b/t ratio is often associated with an elevated photochemical age of the airmass, i.e. a longer time between emission and sampling or higher photochemical activity (e.g. Warneke *et al.*, 2001), but may also reflect changes in the emission ratio. A strong seasonal trend in the ratio is evident, with more benzene relative to toluene during the winter and more toluene relative to benzene during the summer. Similar seasonal trends were observed in ratios of benzene to isoprene, although the summer increase in isoprene was markedly higher, and on average summer values were over 50% higher than in winter. Benzene, toluene and isoprene are all constituents of petrol fuel (Borbon *et al.*, 2001) and

therefore within the urban environment they share the same two major anthropogenic sources: direct emissions from vehicles and evaporative emissions from petroleum products. For isoprene, a third possible source is biogenic emission from plants, where emission rates are both temperature and light dependent (Loreto & Sharkey, 1990). An attempt was made to separate the biogenic fraction of isoprene within the city using regression plots of isoprene (y axis) and benzene (x axis) concentrations over a range of ambient air temperatures ($-5-0, 0-5...30-35$ °C) (surface temperature measurements obtained from the London Weather Centre – 3.1 km east of Marylebone Road). The intercept of the regression line was used to indicate the background concentration of isoprene which was not attributable to direct emissions from cars, and the temperature-dependent fraction [%] was calculated using this value as a percentage of the total isoprene present (5th – 95th percentile range).

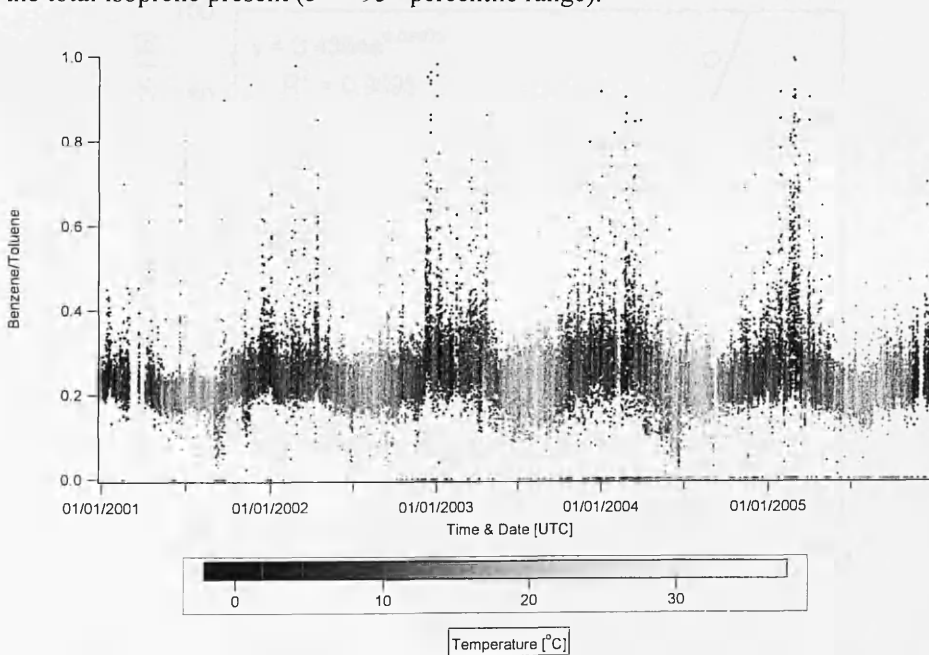


Figure 4.4. Ratios of benzene/toluene concentrations measured at the Marylebone automatic monitoring station between 2001 and 2006 relative to ambient air temperature measurements taken from the London Weather Centre.

In order to isolate the biogenic fraction from the evaporative fraction a similar procedure was applied to concentrations of iso-pentane, a compound that shares the same two major sources as benzene and has a similar volatility to isoprene, but importantly has no biogenic component. The results of both experiments are plotted in Fig. 4.5. and show only slight increases in iso-pentane relative to benzene at higher temperatures due to increased evaporative emissions. In contrast, the temperature-dependent fraction of isoprene was significant and therefore biogenic isoprene is thought to account for a significant fraction of the total observed isoprene within the city. The percentage contribution of biogenic isoprene is thought to be in excess of ~65% at temperatures of 30°C.

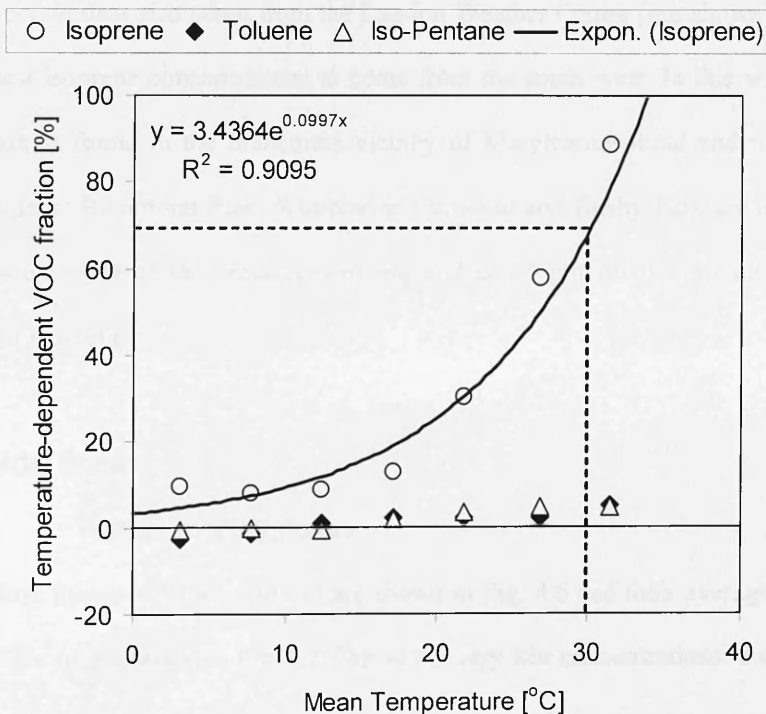


Figure 4.5. Plot showing the temperature dependency of isoprene (circles), toluene (diamonds) and iso-pentane (triangles), calculated using 5 years of hydrocarbon data collected at the Marylebone Road automatic monitoring station and temperature data from the London weather centre. Temperature bands -5 - 0, N = 114; 0-5, N = 3405; 5-10, N = 9539; 10-15, N = 12176; 15-20, N = 9340; 20-25, N = 3171; 25-30, N = 673, 30-35, N = 73.

In a study of VOC concentrations and fluxes above Manchester in June 2006 similar conclusions were reached, where temperature-dependent isoprene was found to contribute over 30% of the total observed concentrations at temperatures above 30°C (Langford *et al.*, 2008). The higher percentage contribution in London is likely to stem from the large areas of urban parkland that are located close to the measurement site, combined with the use of a much larger dataset (5 years, compared with 20 days) which gives a much more statistically robust estimate and importantly in this context there were generally higher temperatures in London than in Manchester.

Windroses of isoprene concentration between 2001 – 2005, calculated using wind direction data also taken from the London Weather Centre (not shown), indicate the highest isoprene concentrations to come from the south west. In this wind sector Hyde Park is found in the immediate vicinity of Marylebone Road and Syon Park, Kew Gardens, Richmond Park, Wimbledon Common and Bushy Park are all located further south west of the measurement site and could potentially provide biogenic sources of isoprene.

4.3.2 VOC fluxes

4.3.2.1 Trends in VOC fluxes

Raw fluxes of VOCs and CO are shown in Fig. 4.6 and their averaged diurnal flux profiles are presented in Fig. 4.7. Due to the very low concentrations, the majority of isoprene fluxes were below the limit of detection and are therefore not presented here. For the remaining compounds the diurnal pattern of the fluxes shows that, for the duration of the measurement campaign, the city was acting as a net source of VOC to

the atmosphere. However, during the weekends, when traffic activity within the city

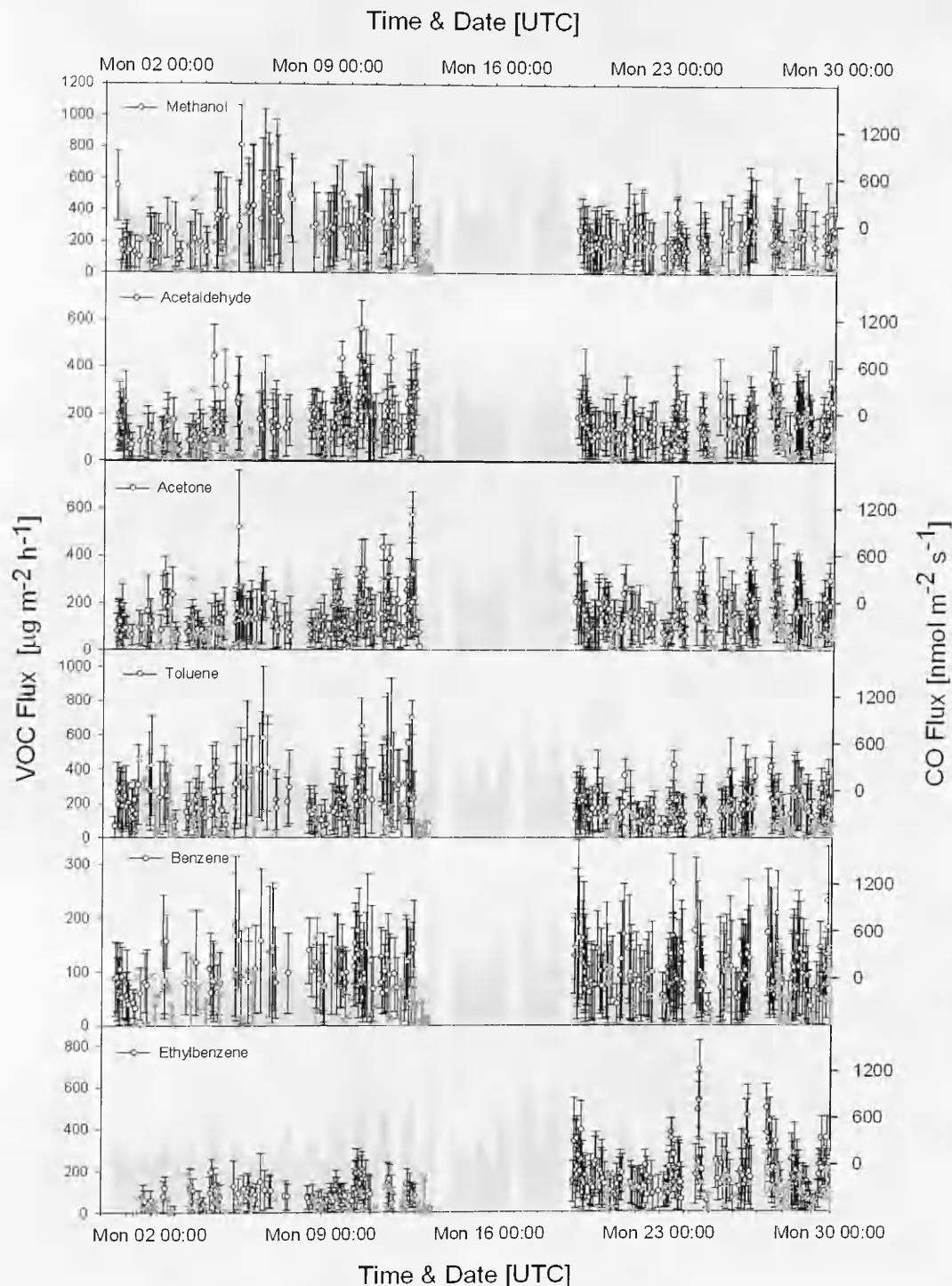


Figure 4.6. Time series of volatile organic compounds (VOCs) compared with carbon monoxide (CO) fluxes measured during the month of October, 2006, from the Telecom Tower, London (U.K). Solid line represents VOC fluxes and greyed areas show CO fluxes.

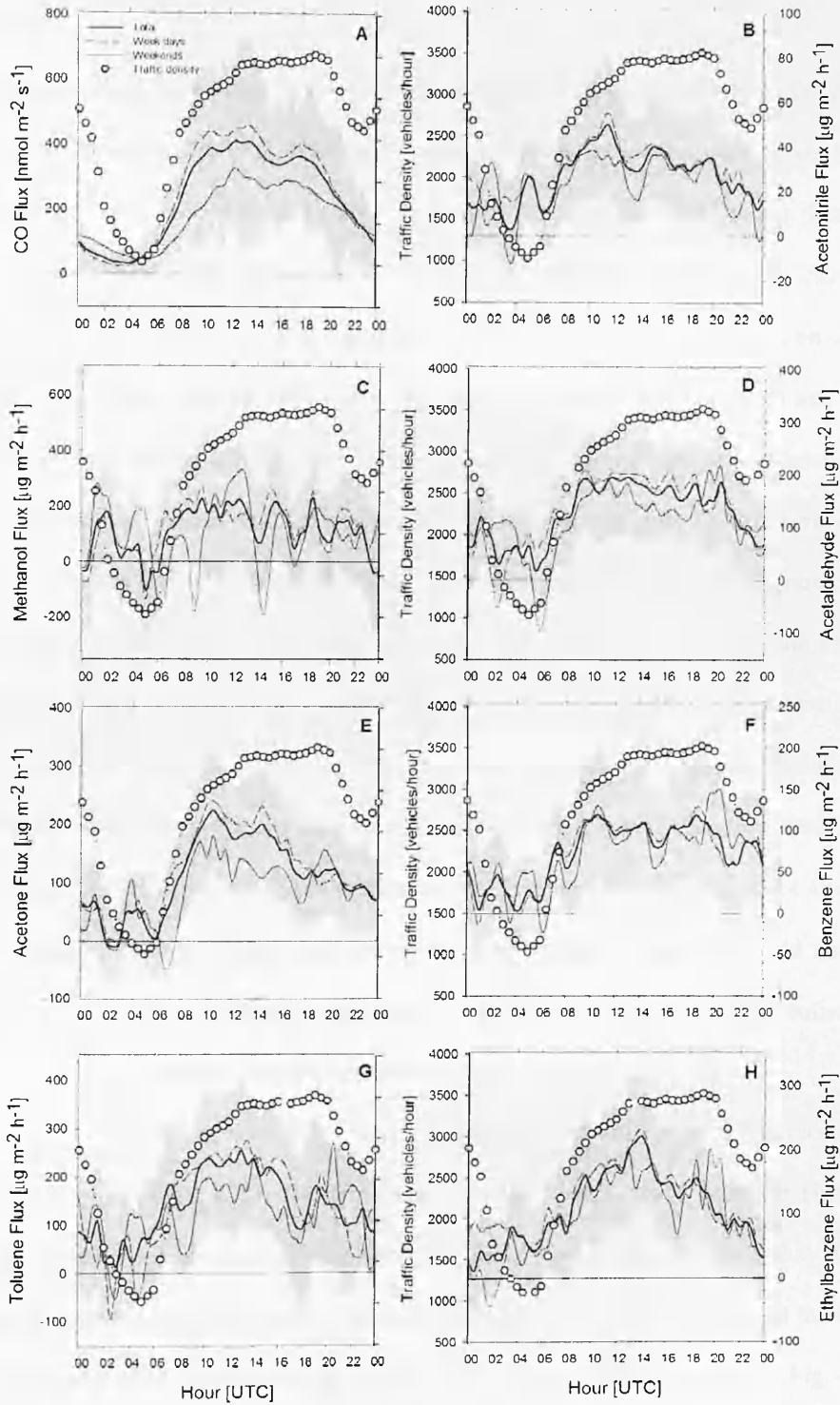


Figure 4.7. Average diurnal flux profiles of volatile organic compound fluxes measured during the month of October, 2006, from the Telecom Tower, London (U.K). Solid bold line represents the month of October, 2006, from the Telecom Tower, London (U.K), solid line denotes the average weekend flux, dashed line represents the

average weekday flux and open circles show the traffic density. Greyed areas represent the measurement precision – see text.

decreased, fluxes of some compounds became negative for short periods in the early morning, indicating deposition. Figure 4.7 also illustrates the tendency for fluxes to be reduced at weekends, and on average they were found to be ~11% lower than on weekdays. The morning increase in VOC fluxes typically coincided with the increase in traffic, which occurred at approximately 06.00 hrs (5 am local time). Yet, on some days, VOC fluxes were not seen until much later, between 07.00 and 08.30 hrs. It is probable, that during the night, due to the elevation of the measurement location, the site became de-coupled from the street-canyon activity and that fluxes were only observed as the nocturnal boundary layer broke up in the morning. This phenomenon was most noticeable on the morning of the 12th and is shown here in relation to the measured traffic activity in Fig. 4.8. The “saw-tooth” shaped curve is symptomatic of the venting of nocturnal/early morning emissions and demonstrates the storage of pollutants within the street canyon at certain times. Thus, the local flux measured with the DEC approach at the comparably tall measurement height of 200 m is not always representative for the surface emission at that time because the storage could not be quantified during this campaign. However, it is expected that the integrated emission over the day nevertheless provides a robust estimate.

Although measurements of boundary layer height (BLH) were not recorded during this campaign, estimates of mixed layer depth were taken from the Hysplit model (<http://www.arl.noaa.gov/ready/hysplit4.html>) and compared with flux data. These show the nocturnal boundary layer to break up at around 07.00 hrs and the flux to rise shortly after. Spikes seen on the 10th, 11th, 12th and 23rd of October in Fig. 4.6, are thought to relate to the storage and venting of VOCs from the boundary layer in

the process described above. Although the mixed layer depth estimates suggest a nocturnal boundary layer height of 250 m, some 50 m above the measurement location

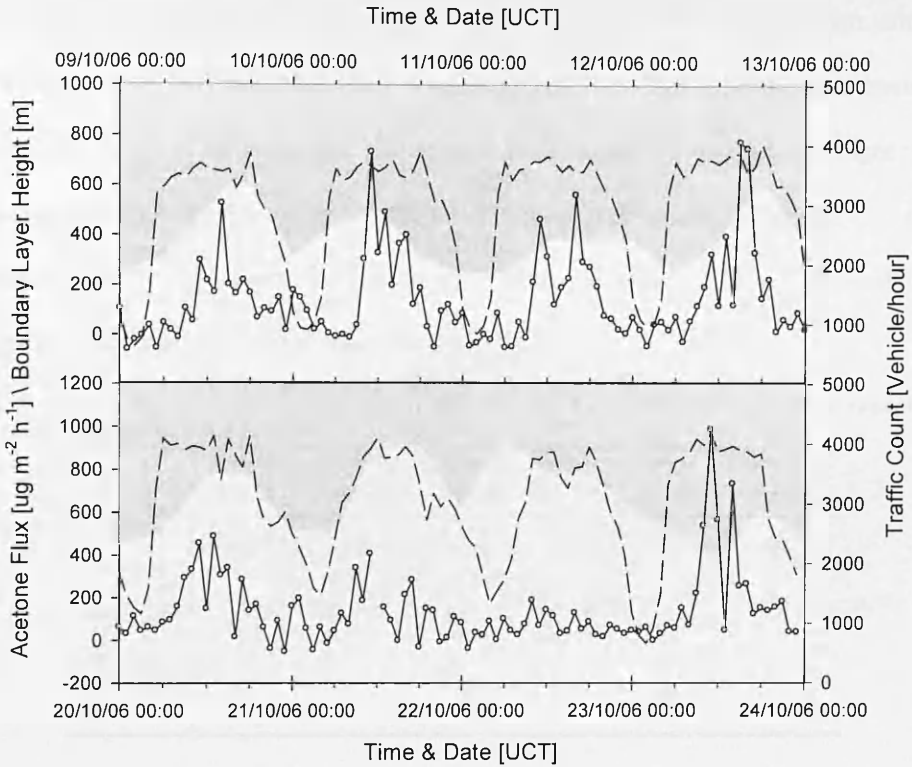


Figure 4.8. Graph of acetone fluxes (running mean) measured during the 2nd (top panel) and 4th (bottom panel) week of the campaign relative to typical vehicle counts (2004). The top panel shows acetone fluxes (open circles) rising after vehicle counts (dashed line) due to the suspected formation of a nocturnal boundary layer (greyed area indicates boundary layer height) and subsequent de-coupling of the measurement from the street canyon activity below.

(200 m), the Hysplit model uses this value as a lower limit and the actual BLH might be much lower. Hence the measurement location may be located above the nocturnal boundary layer at night.

Throughout the campaign, the largest observed fluxes were of toluene (average daily flux $140 \mu\text{g m}^{-2} \text{h}^{-1}$), followed by acetaldehyde ($127 \mu\text{g m}^{-2} \text{h}^{-1}$) and acetone ($110 \mu\text{g m}^{-2} \text{h}^{-1}$). The magnitudes of the fluxes were variable from day to day with much larger fluxes observed on certain days: for example, on Wednesday 11th October an emission fluxes in excess of $500 \mu\text{g m}^{-2} \text{h}^{-1}$ was recorded for toluene and

acetaldehyde. The remaining average daily fluxes are shown in Table 4.1, which compares findings from VOC flux studies above Mexico City and Manchester. Fluxes of acetone and methanol were approximately 1.3 times larger in London when compared with summer time flux measurements over the city of Manchester. Similarly, fluxes of both benzene and toluene were between 3 and 4 times higher in London, which can presumably be attributed to the larger volumes of traffic. This is consistent with the observation of larger organic aerosol emission fluxes above London compared with Manchester (Thomas, 2007).

Table 4.1 Average daily VOC fluxes [$\mu\text{g m}^{-2} \text{h}^{-1}$] measured over a number of urban canopies, including Manchester and Mexico.

	<i>Methanol</i> [m/z 33]	<i>Acetaldehyde</i> [m/z 45]	<i>Acetone</i> [m/z 59]	<i>Benzene</i> [m/z 79]	<i>Toluene</i> [m/z 93]	<i>Ethylbenzene</i> [m/z 107]
London (Autumn)	110	127	110	73	140	106
Manchester (Summer)	78.8	59.6	87.8	18.9	42.4	-
Mexico City	1044	-	396	-	828	468

Despite the differences in their relative magnitudes, the diurnal flux profiles are roughly similar for each compound and approximately follow the pattern of traffic activity in the city. The absence of a clear two-peak rush hour pattern is consistent with earlier CO₂ flux measurements made above the city of Edinburgh (Nemitz *et al.*, 2002). Rush hour behaviour tends to be more pronounced on commuter roads, thus affecting concentration measurements, which are influenced by air masses advected from outside of the city centre. By contrast, in the central areas (the flux footprint of the tower), traffic density increases steadily throughout the day.

Despite the fluxes of VOCs following a similar pattern, there are also differences. For example, acetone emissions peak in the morning whereas emissions of ethylbenzene peak in the afternoon. Some fluxes remain relatively large into the

late evening hours (benzene, toluene and acetaldehyde), while others decreases more rapidly (acetone and ethylbenzene). This may be due to a change in the sources in the evening (e.g larger contribution of residential heating sources, shift of the traffic composition away from HGV, larger fraction of taxi journeys) or a different relative contribution of combustion vs. evaporative sources which respond differently to changes in the meteorological drivers (such as temperature for biological and fugitive sources).

4.3.3 Comparisons of VOC and CO concentrations

Figure 4.9 shows the time series of VOC (25 min averages) and CO concentrations (30 minute averages) measured between the 20th and 30th of October. Each of the measured VOC appears to roughly follow the trend in CO concentration, although this was more apparent for some compounds compared with others. For example, both benzene and ethylbenzene follow the trend in CO very closely, matching the day-to-day variations while maintaining a relatively constant ratio. The good agreement between these compounds and CO (benzene: $R^2 = 0.47$ $p < 0.0001$; ethylbenzene: $R^2 = 0.40$, $p < 0.0001$) is not unexpected as vehicle emissions are thought to be the primary source of both the aromatic VOC and CO. In contrast, concentrations of the other aromatic compound, toluene, which also follows the trend very closely in places, show a more dynamic range than that of CO, with concentrations elevated relative to those of CO between the 20th and 22nd and between the 24th and 30th. This could indicate there to be an additional source of toluene which has no association with CO. Analysis of Fig. 4.5, where VOC flux measurements are plotted alongside CO fluxes during the same time period, shows the toluene flux to mirror the CO flux for the duration of the time series more closely. This suggests that

the secondary source of toluene is originating from outside of the flux footprint (the increased toluene concentrations appear to have no bearing on the flux, indicating horizontal advection of toluene past the measurement site rather than the vertical transport of emissions from the ground below). The source of secondary toluene is unknown, but due to its independence of CO, it is likely to be unrelated to combustion.

Similar behaviour was observed with the concentrations of isoprene. Again, as expected, isoprene, a known constituent of petrol fuel, followed the trend in CO concentrations, but only between the 23rd and 30th ($R^2 = 0.31$ ($p = <0.0001$)). Before this period (19th – 23rd) no correlation between the two compounds was apparent ($R^2 = 0.04$ ($p = <0.0027$)), suggesting either an additional source of isoprene to be present or interference from other masses such as furan.

Whilst both toluene and isoprene provide examples of VOC sources which are independent of traffic, more subtle examples can be observed within the CO time series. For example, on the morning of the 29th, as VOC concentrations are generally at their lowest, concentrations of CO have already reached a morning peak. This might suggest a source of CO that is independent of VOC emissions which may be linked to a change in primary sources. Such changes are likely to involve a shift from traffic related emissions, which are at their lowest during the early hours of the morning, to sources normally secondary in nature, such as central heating in homes and businesses.

Concentrations of acetonitrile, acetone, m/z 41 (a number of fragment ions, including, acetone, propanal and methacrolein can be detected at this m/z) and m/z 43 (multiple species detected at this m/z , including, propylene and fragments of acetone, acetic acid and PAN (de Gouw and Warneke, 2006)) also showed some agreement

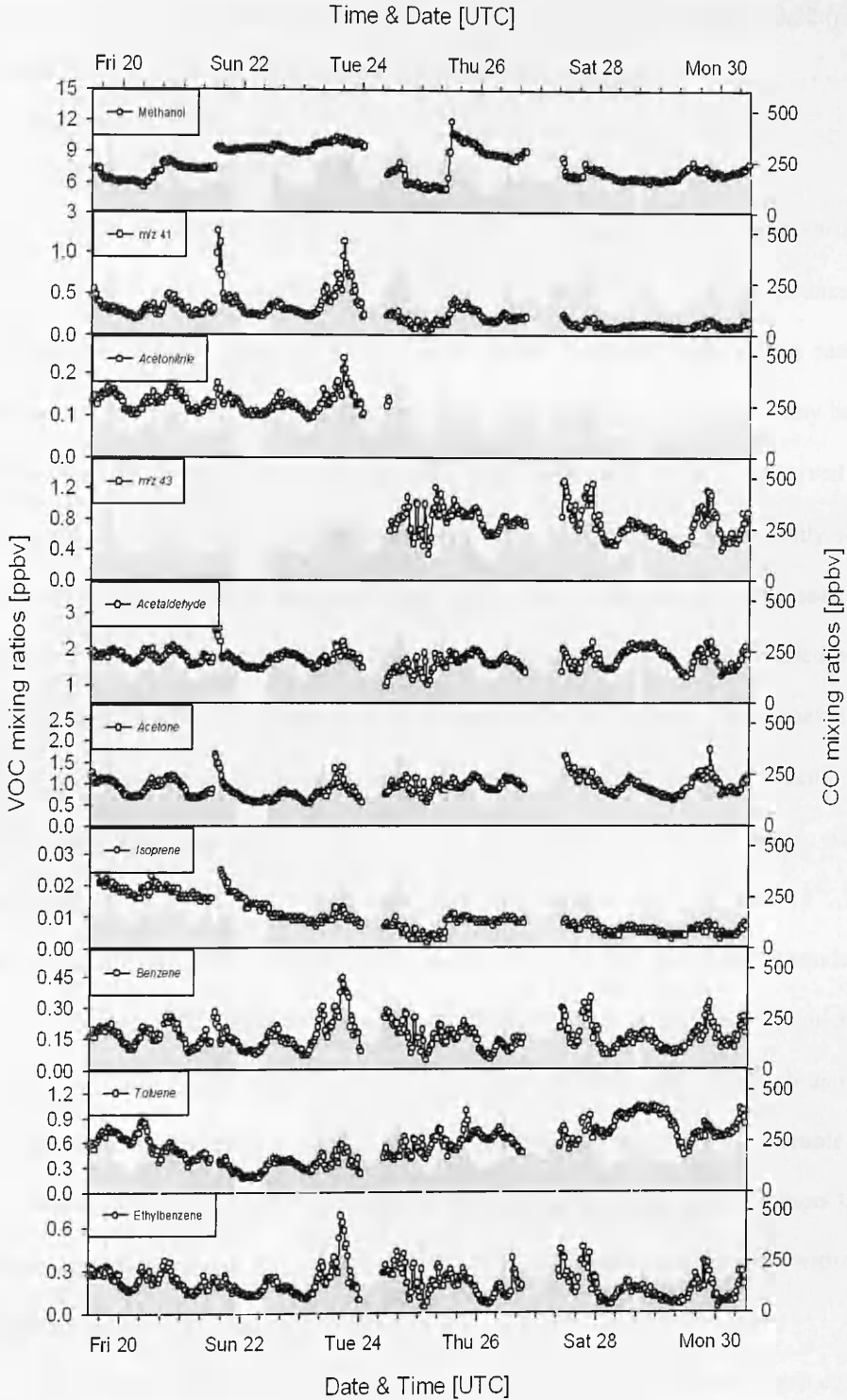


Figure 4.9. Time series of concentrations of volatile organic compounds between the 19th and 30th of October, 2006, measured using a proton transfer reaction-mass spectrometer from the roof of the Telecom Tower in central London, compared with CO concentrations (grey shaded area).

with the observed CO concentrations, with R^2 values of 0.39 ($p = <0.0001$), 0.22 ($p = <0.0001$) 0.37 ($p = <0.0001$) and 0.35 ($p = <0.0001$), respectively.

4.3.4 Comparison of VOC and CO fluxes

Figure 4.6 shows a time series of VOC fluxes alongside CO fluxes measured between the 30th of September and 30th of October. Despite the noisy appearance of the data, it is clear that fluxes of VOCs and CO follow a similar trend. Fluxes can be seen to vary on both daily and weekly time scales. For example, on a day to day basis the shape of the flux was not constant, with a saw tooth shaped curve observed on some days, thought to relate to the break up of nocturnal inversions (commonly seen during the second week of measurements), and a more symmetrical curve seen on others when no inversion was present. The magnitudes of the fluxes also varied both diurnally and weekly. For example, a clear increase in VOC fluxes from week 1 to week 2 can be seen in the measurements of acetone, acetaldehyde, and toluene and this change was also mirrored by the CO fluxes. During the 5th week when measurements resumed after instrument downtime between the 13th and 18th, the fluxes were still relatively large, but decrease steadily to a low on the 22nd (Sunday). On the 23rd (Monday) a large flux is observed for most VOCs as well as CO, which is much higher than on previous week days. Variations in flux magnitude such as this can sometimes be related to the meteorological conditions at the time. For example, in this instance, the larger fluxes may relate to the venting of urban concentrations that accumulated during a day time inversion (Fig. 4.8), which may be associated with the relatively low average wind speeds of 5.8 m s^{-1} .

Day-to-day variation in the magnitude of the aromatic compound fluxes could be brought about by changes in wind direction, with shifts from heavily trafficked areas to wind sector where urban parkland is the dominant feature (North – Reagent's

Park, South west – Hyde Park) and traffic density is low. For other compounds such as acetone, acetaldehyde and methanol, all of which may or may not be under some biological control, the ambient air temperature could play an important role in determining emission rates.

4.3.5 Ratios of VOC to CO – Concentrations and fluxes

Analysis of the ratios of both concentrations and fluxes of VOCs to CO can be useful in the determination and identification of sources. The ratios of concentrations and fluxes may agree or disagree depending on whether or not the major sources are contained within the flux footprint. Ratios may change throughout the day due to shifts in the major emission sources, or through removal processes such as reaction with the OH radical or scavenging by rain. Here, average VOC/CO ratios for the campaign are presented in Table 4.2 and the typical diurnal pattern of the ratio is shown in Fig. 4.10 for each of the measured compounds.

Ratios of benzene and ethylbenzene with CO concentrations remain relatively constant throughout the day indicating both sets of compounds to share a similar source. For the remaining compounds, ratios with CO concentrations all follow a similar trend, with a higher ratio during the night time and mid afternoon. The two troughs in the VOC/CO ratio coincide with peak traffic flows on the commuter roads outside of the city centre. Explanations for these troughs may include the following; (i) emissions of CO may be elevated in congested traffic situations relative to VOC emissions, or (ii) during transport the air is photochemically processed before reaching the tower and therefore the VOC are depleted in relation to CO which reacts more slowly. The latter point is consistent with the isoprene/CO ratio showing a more pronounced trough than the other compounds, with isoprene being the most reactive

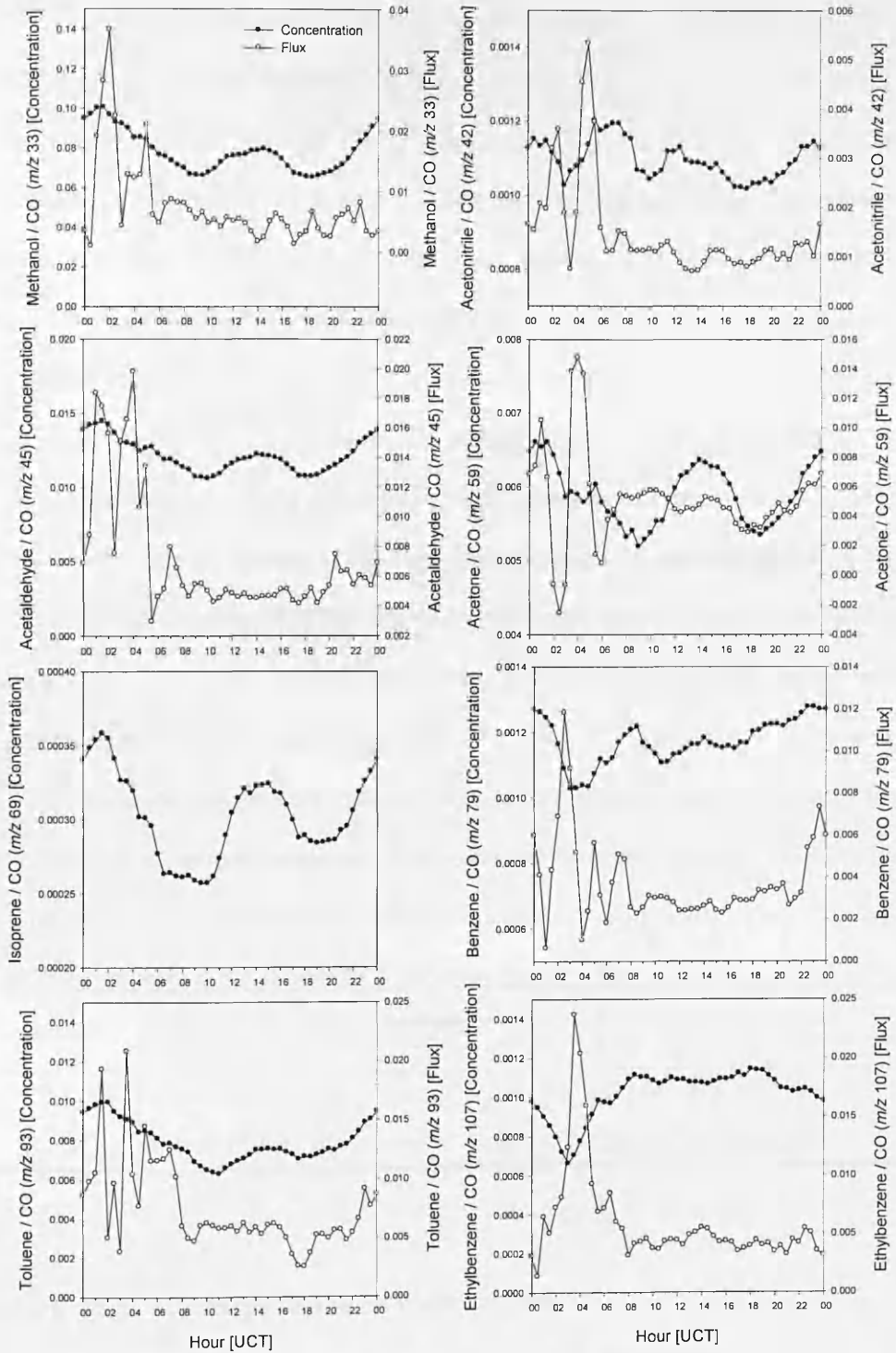


Figure 4.10. Typical daily ratios of CO to VOC measured during the month of October, 2006 from the Telecom Tower, London (U.K). Black circles represent concentration measurements and white circles show flux measurements.

of the compounds measured. The main explanation, however, is that some of the VOC have additional sources that are not related to combustion.

The ratios of VOC/CO fluxes differ from concentration ratios, which is an indication that some of the sources contributing to the concentration measurements were located outside the flux footprint. Between the hours of 07:00 and 22:00 the ratio of VOC/CO remains relatively constant suggesting both sets of compounds to originate from a similar source. However during the night time the ratio becomes elevated, with more VOC relative to CO. Although this increase could be linked to a shift in the major sources of CO and VOC, in this instance it is thought more likely to relate to the post-processing of the data. The stricter quality controls applied to the VOC data which removed fluxes below the calculated limit of detection as well as files where u^* was below 0.15 m s^{-1} , may have meant night time fluxes were systematically biased towards higher values.

Flux and concentration ratios of VOC to CO differ for each compound. This indicates VOC sources originating from outside of the flux footprint and helps to substantiate earlier observations of toluene concentrations and fluxes.

Table 4.2 Averaged VOC/CO ratios for both concentrations and fluxes.

<i>VOC/CO</i>	<i>Methanol</i> [<i>m/z</i> 33]	<i>Acetonitrile</i> [<i>m/z</i> 42]	<i>Acetaldehyde</i> [<i>m/z</i> 45]	<i>Acetone</i> [<i>m/z</i> 59]	<i>Isoprene</i> [<i>m/z</i> 69]	<i>Benzene</i> [<i>m/z</i> 79]	<i>Toluene</i> [<i>m/z</i> 93]	<i>Ethylbenzene</i> [<i>m/z</i> 107]
Concentrations [ppb]	7.82×10^{-2}	1.10×10^{-3}	1.21×10^{-2}	5.90×10^{-3}	3.03×10^{-4}	1.17×10^{-3}	7.89×10^{-3}	1.01×10^{-3}
Fluxes [$\mu\text{g m}^{-2} \text{h}^{-1}$]	7.43×10^{-3}	1.48×10^{-3}	7.09×10^{-3}	5.09×10^{-3}	-	3.37×10^{-3}	7.43×10^{-3}	5.85×10^{-3}

4.3.6 VOC flux dependence on traffic activity

The NAEI (2005) suggests road transport to be the second largest source of benzene in the U.K, accounting for approximately 25% of the total emission. In 1990, approximately 73% of benzene was attributable to the road transport sector, but since

the introduction of three-way catalysts in 1991, emissions from industrial, commercial and residential combustion now make up the bulk of the total. However, in inner city locations road transport is the dominant source of benzene, and in 2005 it was thought to contribute 73% of the total benzene emission in Westminster (NAEI, 2005). Traffic also accounts for 91% of the total CO emission in this area.

An attempt was made to characterise the relationship between observed fluxes of VOCs and CO with the pattern of traffic activity within the city. Traffic density data recorded on Marylebone Road (2004) were used as a proxy for traffic activity across the whole flux footprint and compared to the measured VOC fluxes, the results of which are shown in Fig. 4.11. These plots indicate a clear relationship with traffic, with an increase in both VOC and CO emission with increasing volumes of traffic. The non-linear regression was chosen after analysis of the average vehicle speed with respect to vehicle counts, as shown in Fig. 4.12. As the volume of traffic increases, the roads become congested and the average vehicle speed drops from the permissible 50 kph (30 mph) on this road to 34 kph at peak times. Both VOC and CO emissions from vehicles increase with decreasing vehicle speed (Heeb *et al.*, 2000), therefore the slower average vehicle speed combined with increased 'stop – start' driving conditions, explains the exponential rise in emissions.

The plots show good correlation between the measured fluxes and traffic activity, yet in places the fit to the data is close to the limit of uncertainty. This is particularly noticeable at vehicle counts of between 3100 and 3300 and is best illustrated in plot of acetone and toluene. Vehicle counts in this range typically occurred between 08.00 hrs and 11.00 hrs, which coincided with the breakdown of the nocturnal boundary layer and subsequent venting of night time and early morning VOC emissions. Therefore, in reality, these points would most likely have had a much

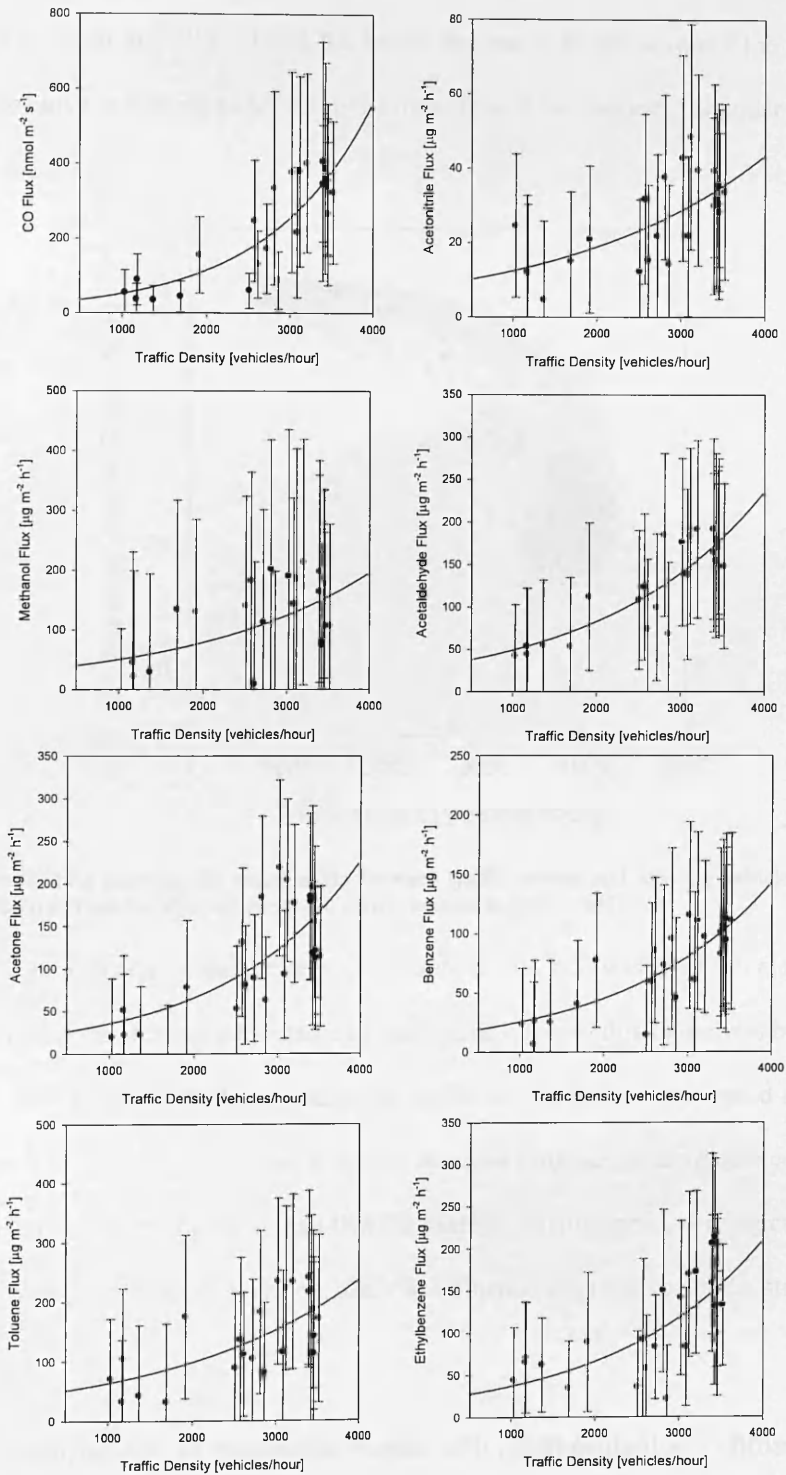


Figure 4.11. Scatter plots showing the correlations between traffic activity in the city centre (counts – Marylebone Road (2005)) and CO and VOC fluxes. Error bars show flux measurement precision.

closer fit to the curve. Conversely, when vehicle counts are at their peak, between 19.00 and 20.00 hrs, VOC fluxes fall below the curve. In this instance the deviation from the curve is thought to be due to the formation of the nocturnal boundary layer.

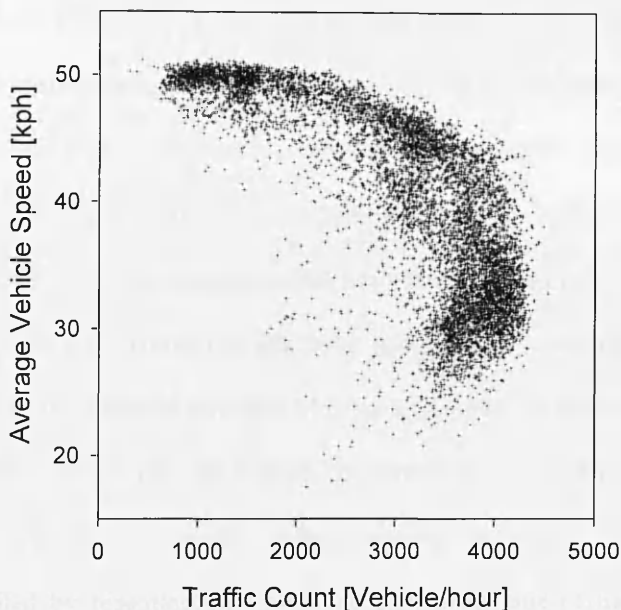


Figure 4.12. Plot showing the relationship between traffic counts and average vehicle speed on data collected from the Marylebone Road traffic monitoring site (2005).

The intercept of the curve with the zero traffic line was used to calculate the proportion of the flux not attributable to road traffic. Overall this figure was between 12 and 20% of the peak fluxes, indicating traffic counts to be a very good surrogate for most VOC fluxes at this site. It should be noted however, that vehicle counts are not the only contributing factor and that the average driving speed, driving conditions and ambient air temperature are all likely to influence the relative source strength of VOCs.

4.3.7 Comparison of measured fluxes with NAEI emission estimates

An attempt was made to calculate an emission estimate using measured VOC fluxes for comparison with the NAEI. Previously this has been done by simply

extrapolating average daily flux measurements to give an annual estimate. Here, we use the equation of the line from Fig. 4.11 (Section 3.6), where VOC fluxes were plotted against traffic density, to produce an emission estimate using a year long set of traffic data from Marylebone Road (2004). As the parameterisation is based on a “snap-shot” of the total yearly fluxes, this method relies heavily on the assumptions that (i) vehicle emissions account for the bulk of the VOC emissions within the city (ii) the observed traffic density is representative of traffic activity occurring throughout the flux footprint and (iii) that there is little or no seasonal variation in the emission of VOCs. This last assumption has been shown to be untrue for some of the measured VOC, but no correction has been applied here, potentially introducing significant bias to the emission estimates of those VOC most temperature dependent.

The traffic density data set was not continuous over the whole year, therefore missing sections, which were usually confined to one or two lanes of traffic (6 lanes in total), were filled by repeating data from the equivalent lane of traffic. Where no equivalent data were available, data were taken from the previous month, taking care to match both time of day and day of week. In total less than 15% of the traffic data set was filled in this way.

Emission estimates for benzene generated using the flux data suggest an average emission of $0.88 \text{ t km}^{-2} \text{ yr}^{-1}$. This value is ~ 1.8 times lower than that suggested by the NAEI ($1.55 \text{ t km}^{-2} \text{ yr}^{-1}$) which calculated the flux by integrating the values of grids contained within the flux footprint (shown in Fig. 4.1). Despite being considerably lower than the value given by the NAEI, the measured estimate was within the calculated uncertainty of ± 1 standard deviation ($0.7 \text{ t km}^{-2} \text{ yr}^{-1}$). Estimates of CO emissions ($329 \text{ t km}^{-2} \text{ yr}^{-1}$) from the city compared more favourably with NAEI estimates ($427 \text{ t km}^{-2} \text{ yr}^{-1}$), with the calculated emission found to be 30% lower than

the NAEI and well within the calculated uncertainty ($SD = \pm 230 \text{ t km}^{-2} \text{ yr}^{-1}$). The closer agreement of CO estimates compared with those of benzene may relate to the higher percentage contribution of vehicle emissions within the NAEI estimate (93% compared with 73%) and suggest non-traffic related sources are being overestimated by the NAEI for benzene.

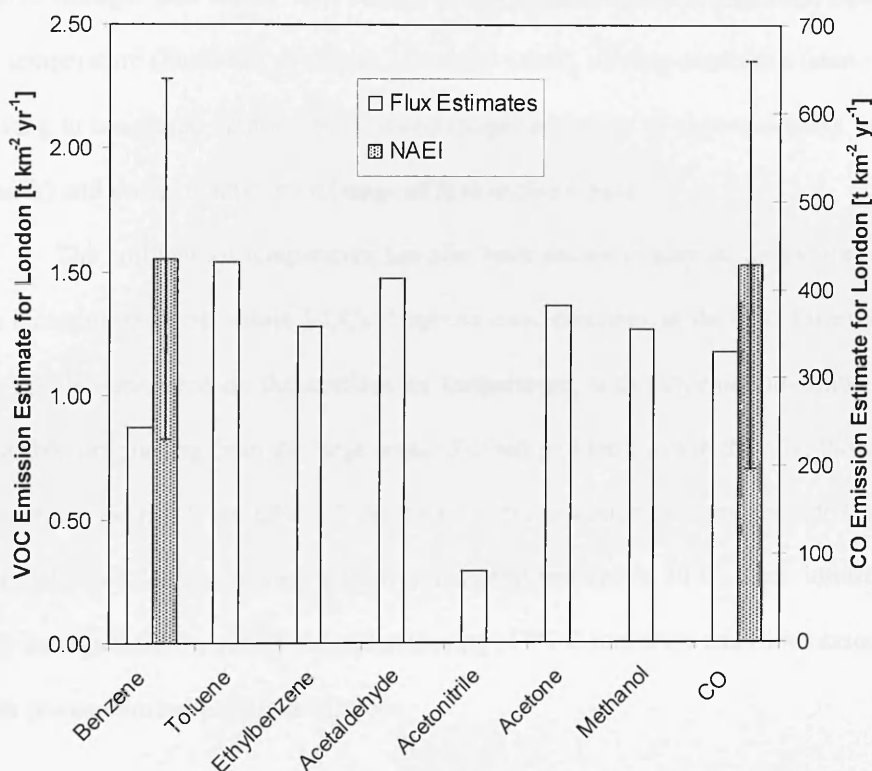


Figure 4.13. Comparison of emission estimates derived using measured fluxes with the National Atmospheric Emission Inventory.

Emission estimates for the seven remaining VOCs are shown in Fig. 4.13, but further comparisons with the NAEI were not possible. Toluene had the largest calculated annual emission rate ($1.54 \text{ t km}^{-2} \text{ yr}^{-1}$). Acetaldehyde ($1.48 \text{ t km}^{-2} \text{ yr}^{-1}$), acetone ($1.37 \text{ t km}^{-2} \text{ yr}^{-1}$) and ethylbenzene ($1.28 \text{ t km}^{-2} \text{ yr}^{-1}$) had the next largest emission estimates, followed by methanol ($1.27 \text{ t km}^{-2} \text{ yr}^{-1}$) and acetonitrile ($0.29 \text{ t km}^{-2} \text{ yr}^{-1}$).

4.5 Conclusions

Traffic density within the city has been shown to be the primary source of VOC fluxes to the atmosphere within central London, but its relative contribution varies from compound to compound and also temporally, with changes occurring from hour to hour and in some cases even season to season. It is thought that the relative source strength also varies, with vehicle counts just one of many variables, including air temperature (increased emissions from cold starts), driving conditions (start – stop driving in congested areas) vehicle speed (larger emissions at slower average vehicle speeds) and traffic composition (range of fuel/engine types).

The ambient air temperature has also been shown to play an important role in the emission rates of certain VOCs. Isoprene concentrations in the city, for example, are highly dependent on the ambient air temperature, with biogenic emissions, most probably originating from the large areas of urban parkland within the city, thought to contribute as much as 68% of the total isoprene concentrations recorded at the Marylebone Road monitoring station at temperatures above 30°C. Such information may be significant in aiding our understanding of VOC precursor emissions associated with photochemical pollution episodes.

Acknowledgements

We thank British Telecom for allowing us access to the Telecom Tower and the riggers, Bob, Gareth and Zach, who installed the sampling equipment on the lattice tower. The work was funded by the U.K. Natural Environmental Research Council through the “CityFlux” grant and an NCAS PhD studentship. The REPARTEE campaign was co-funded by the BOC Foundation and co-ordinated by Prof. Roy

Harrison and his team at the University of Birmingham. We thank Duncan Wyatt (Lancaster University) for his help with GIS and the emission inventory.

Chapter V

5. Mixing ratios and fluxes of volatile organic compounds above Mediterranean macchia vegetation (Castelporziano, Italy)

In this chapter the virtual disjunct eddy covariance technique was applied to a typical Mediterranean ecosystem type in the grounds of the Castelporziano nature reserve near Rome, Italy. Fluxes of five volatile organic compounds, including isoprene and monoterpenes, were measured above macchia vegetation using two independent PTR-MS instruments, one standard model (Std), the other a high sensitivity model (HS). The experiment aimed to both establish the reliability and reproducibility of the vDEC technique as well as to generate a set of direct “top down” emission estimates for isoprene and monoterpenes, which could be compared to a well established “bottom up” model for BVOC emissions. Within this chapter, the interpretation of VOC fluxes and concentrations, with the exception of the inter-comparisons, relates solely to data collected using the Std PTR-MS.

This work was contributed to by the following participants:

Ben Langford (Univ. Lancaster & CEH): Developed the vDEC system, operated the Lancaster Std PTR-MS instrument, Logged data from the EGM, post processed concentration and flux data for the Std PTR-MS, performed calibration of Std PTR-MS, Calculated model emission estimates and wrote the chapter.

Pawel Misztal (Univ. Edinburgh & CEH): Operated the CEH HS PTR-MS instrument, post-processed concentration and flux data from the HS PTR-MS, Performed calibration of HS PTR-MS.

Chapter V

5. Mixing ratios and fluxes of volatile organic compounds above Mediterranean macchia vegetation (Castelporziano, Italy)

5.1 Introduction

In Chapters 3 and 4, the virtual disjunct eddy covariance (vDEC) technique was applied to urban canopies and gave detailed flux information for a number of predominantly anthropogenic volatile organic compounds. However, emissions of biogenic VOCs (BVOCs) also play an important role in atmospheric chemistry, which probably exceeds that of anthropogenic VOCs (AVOCs) (Guenther *et al.*, 2000). In many locations, emissions of BVOCs, in particular isoprene, are much larger than AVOC emissions and are also potentially more reactive, as they are emitted as a function of both light and temperature, which can predispose them to photolysis. When VOCs undergo photolysis in atmospheres rich in NO_x , tropospheric ozone is formed, potentially causing damage to crops, forest ecosystems, buildings and impacts on human health (Silman, 1999).

In areas such as the Mediterranean, where both photolysis and emission rates of BVOCs are high, photochemical air pollutants such as ozone can be a problem. In order to better understand the processes controlling photochemical pollution episodes, much attention has been devoted to developing regional as well as global scale models of BVOC emissions. Within Mediterranean type ecosystems, isoprene and monoterpene emissions form the bulk of the total emitted BVOC, and their emission rates are known to be strongly regulated by specific species distributions and variations in light and temperature (Guenther *et al.*, 1993). These controls have been well characterised in a number of models

(Guenther *et al.*, 1993, Guenther *et al.*, 1995), but the models have been limited by the high level of uncertainty that accompanies input variables such as basal emission rates. Until the mid 1990s, model estimates for biogenic emissions from ecosystems similar to those found in the Mediterranean (Guenther *et al.*, 1995), including regions of Chile, California, South Africa, Australia and Europe, were calculated using basal emission rates taken from Californian Mediterranean type ecosystem species only (Owen *et al.*, 1997). As both isoprene and monoterpene emissions are very much species specific, this generated considerable uncertainty in the model. Since then, efforts have been made to generate emission rates for a number Mediterranean ecosystem types. In Europe, BVOC emissions in Mediterranean areas were extensively studied as part of the Biogenic Emissions in the Mediterranean Area (BEMA) project (Seufert *et al.*, 1997; Street *et al.*, 1997; Owen *et al.*, 1997; Kesselmeier *et al.*, 1997; Bertin *et al.*, 1997; Ciccioli *et al.*, 1997; Valentini *et al.*, 1997; Owen *et al.*, 2001), which focused on emissions of monoterpenes and isoprene from the Castelporziano nature reserve near Rome, Italy. The site comprised a number of vegetation types and allowed the estimation of both species specific and averaged ecosystem (forest, pseudosteppe or macchia) emission rates, which could improve modelled BVOC emission estimates within this region. These earlier measurements were made with enclosure techniques and manual relaxed eddy-accumulation, which were not ideal for sticky oxygenated compounds such as methanol.

In this work, we utilise the recent developments in PTR-MS to measure fluxes of methanol, acetaldehyde, acetone, isoprene and monoterpenes are measured above macchia vegetation in the grounds of the Castelporziano nature reserve, Italy, using both standard and high sensitivity PTR-MS instruments.

Concentration and flux measurements from the two instruments are compared and discussed to establish the reliability and reproducibility of the vDEC technique. In addition, fluxes of isoprene and monoterpenes are compared with modelled emission estimates which are calculated using the algorithm of Guenther *et al.*, (1995) using basal emission rates taken from data collected during the earlier measurements at Castelporziano within the BEMA project.

5.2 Method

5.2.1 Site description

The Castelporziano Presidential estate is located ~ 20 km SSW of central Rome, on the western coast of Italy. The estate covers an area of 6100 ha, comprising a number of typical Mediterranean land types, which have been preserved for centuries thanks to restrictions on public access and the prevention of encroachment from the heavily urbanised surrounding areas. These land types include oak/pine plantation (*Santo Quercio*), cork-oak (*Quercus subur*) forest, pasture, Mediterranean macchia sand dunes and beach.

The oak/pine plantation is made up of a wide variety of plant species, but is dominated by *Quercus ilex* (50%), a known emitter of monoterpenes. To the south of the estate, is the macchia vegetation which comprises high macchia (2 – 2.5 m; *Q. ilex*, *Phillyrea*, *Pistacia*, *Rosmarinus*, *Arbutus*, *Juniperus* and others), low macchia (0.5 – 0.7 m; *Cistus*, *Erica Helichrysum*) and grasses, and is followed by a beach which extends approximately 200 m to the shoreline (Seufert *et al.*, 1997).

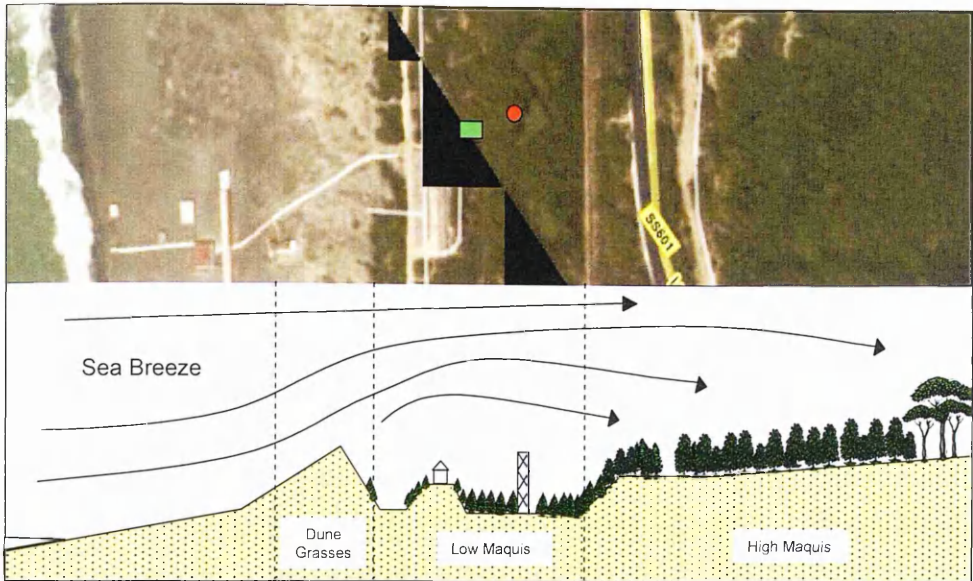


Figure 5.1 Satellite image (Google Earth, 2008) and sketched cross section of the sampling location inside the Castelporziano presidential estate.

There are few roads within the estate and traffic is restricted to estate workers and police, so localised vehicle emissions are very low. However, along the western edge runs a busy public commuter road which links the residential area of Ostia with central Rome, some 3.5 km west of the measurement site. In addition, a smaller public coast road (SS601) transects the southern-most end of the estate, creating a clear boundary between the high and low macchia vegetation, which can be found north and south of the road respectively. It is the low macchia, sandwiched between the beach/grasses and the SS601 coast road that forms the focus of this study.

5.2.2 Climate and meteorology

The climate in the region of the Castelporziano estate can be characterised as typically Mediterranean, with a pronounced aridity during the summer months (May-August) which can lead to drought stress of the vegetation. Temperatures during the summer months reach an average maximum of 25 °C and are typically

very dry with little or no precipitation. In contrast, the winter is cool, with temperatures ranging from 6-12 °C and increased precipitation. The Castelporziano catchment receives an average annual precipitation of 740 mm.

The meteorology in the area is very characteristic of Mediterranean coastal areas. During the summer the sea-land breeze becomes the dominant air mass circulation pattern. During the afternoon and early evening the sea breeze is active until around 19.00 hrs, at which point the circulation reverses and from about 03.00 hrs the land breeze dominates until about 11.00 hrs (Manes *et al.*, 1997). During the winter the meteorology at the site is dominated by synoptic scale circulations, with cold winds from the N-NE direction bringing air masses and pollutants directly from Rome to the site (Mantes *et al.*, 1997).

5.2.3 Instrumentation

An ultrasonic anemometer (Solent R1012, Gill Instruments) was mounted on a mast 5 m above ground level, and fixed to the south-west corner of the central measurement tower. This positioning gave a fetch of approximately 300 m to the north-west, > 500 m to the south-east, but < 60 m in the two major wind directions (south west and north east).

A small shed was positioned 15 m to the SE of the measurement tower which housed the analytical instrumentation. Air for analysis by PTR-MS was pumped at a flow rate of approximately 18 l min⁻¹ through 20 m of 3/8" OD Teflon tube, the inlet of which was mounted 30 cm below the sonic anemometer. A uv-absorption ozone monitor sub-sampled air from the same tube at a rate of 0.1 Hz and ancillary measurements of temperature, humidity, air pressure, and photosynthetically active radiation (*PAR*) were recorded by an EGM which was

located at the measurement hut and logged by a programme written in LabVIEW (National Instruments, v 7.1) with a 20 s time resolution.

5.2.4 VOC sampling

Two PTR-MS instruments, one high sensitivity (HS) model and the other standard (Std), were used for the monitoring of VOC concentrations. Each instrument was optimised to an E/N ratio of 128.2 Td and was operated with <1% O₂ background signal. The two PTR-MS sub-sampled from the same main sample line at a flow rate of 0.25 l min⁻¹ via a teed reducing union (3/8" to 1/8") and two 3-way Teflon solenoid valves (Parker, Hannifin) which were controlled by the A/O channels of the PTR-MS. The first valve allowed the PTR-MS to switch freely between the sample line and an open inlet which could be used to attach either calibration standards or a Tedlar bag filled with breath isoprene which allowed for the periodical measurement of the SEM voltage. The second valve was connected to the outflow a platinum catalyst (flow rate of 0.5 l min⁻¹) which provided a zero air source for the instrument. This valve was activated once every hour for five minutes, allowing the instrument background concentrations, which can change with fluctuations of humidity, to be monitored throughout the experiment. The excess zero air was purged through a length of PFA tubing and vented.

The two PTR-MS were setup to measure in three modes, flux mode (FLX), mass scan mode (MS) and zero air mode (ZA). When in FLX mode, each PTR-MS scanned through a small suite of protonated masses which included the primary ion count (m/z 21), water cluster (m/z 39), methanol (m/z 33), acetaldehyde (m/z 45), acetone (m/z 59), isoprene (m/z 69) and Σ monoterpenes

(which includes compounds such as α -pinene, β -pinene, limonene, sabinene and Δ^3 -carene) which can be measured as the sum of m/z 81 and m/z 137.

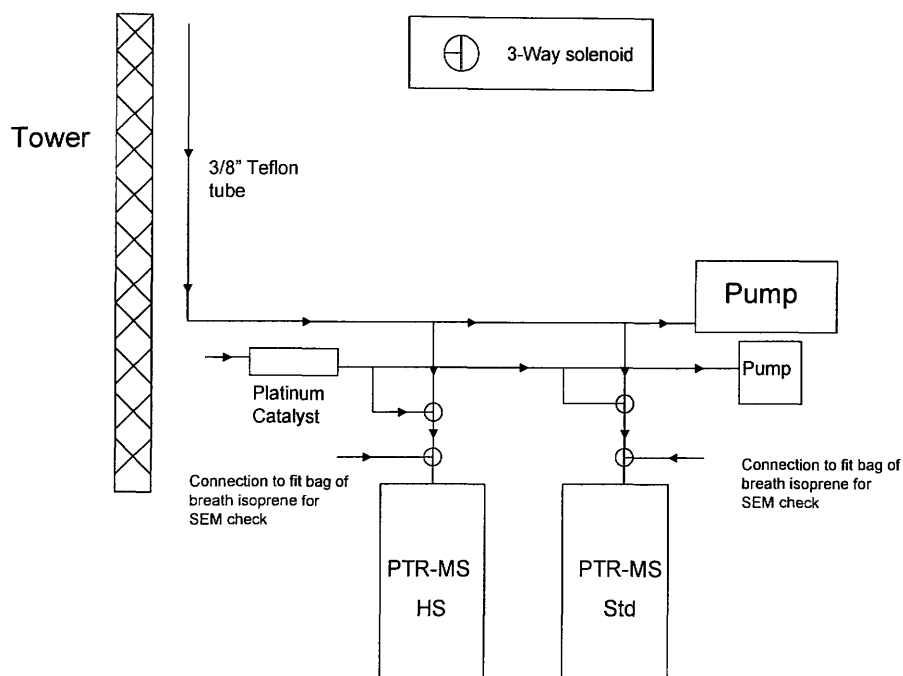


Figure 5.2 Schematic of the system setup used at the Castelporziano field site.

Each m/z was given a dwell time of 0.2 s with the exception of m/z 21 and m/z 39 which were both measured at 0.1 s. This gave a total duty cycle time of 1.4 s, which corresponds to ~ 1070 data points during a 25 minute averaging period.

During the first five minutes of each hour the Std PTR-MS switched valve one and was operated in ZA mode, using the same duty cycle described above. Between 30 and 35 minutes into each cycle, the PTR-MS was operated in MS mode, measuring a number of different BVOCs as well as some anthropogenic VOCs which can be used as markers to identify air masses that have been advected from inland locations. The mass scan sequence included the measurement of the following masses: dimethylsulphide (DMS) (m/z 63),

Methyl-ethyl-ketone (MEK) (m/z 73), peroxyacetyl nitrate (PAN) (m/z 77), benzene (m/z 79), toluene (m/z 93), ethylbenzene (m/z 107) and C₉ aromatics (m/z 121). In this mode, each m/z was monitored with a dwell time of 1 s as this data was solely used to provide concentration information. The same measurement modes were used for the HS PTR-MS, but in reverse, with the MS followed by the ZA.

5.2.5 Calibration

The two PTR-MS systems were calibrated against the same gas standards, which contained methanol, acetaldehyde and acetone at a concentration of 1 ppm (Appendix IV). Calibration standards were prepared using 0.6 l Tedlar bags and a high precision glass syringe, and were diluted using a high purity N₂ gas. In total 5 calibration standards were made in the range of 2 - 750 ppb as well as one blank.

In order to help with the inter-comparison of the two instruments, VOC concentrations were calculated using the approach used by Rinne *et al* (2007) which standardises the PTR-MS operating conditions by normalising the primary ion counts to 1×10^6 and the drift tube pressure to 2 mbar. Concentrations were then calculated using the following equation:

$$\chi_{ppb} = S \left(\frac{\frac{RH_i}{1 \times 10^6}}{M21 + M37} - \frac{\frac{RH_{zero}}{1 \times 10^6}}{M21_{zero} + M37_{zero}} \right) \times \left(\frac{2.0}{pDrift} - \frac{2.0}{pDrift_{zero}} \right) \quad (5.1)$$

where S is the calibration coefficient (see Appendix IV), RH_i is the signal of the mass in ion counts per second, RH_{zero} is the signal of the mass measured from the zero air source, $M21$ and $M37$ are the counts of the primary and reagent cluster ions respectively measured during the flux mode, $M21_{zero}$ and $M37_{zero}$ are the

primary and reagent cluster ions when measuring in ZA mode and p_{Drift} is the pressure of the drift tube in mbar.

For isoprene and monoterpenes, for which no gas standard was available, concentrations were calculated using Eq. (5.1) and calibration coefficients were taken from the transmission curve.

5.2.6 Data logging

Data from the sonic anemometer and PTR-MS were logged to a single laptop computer using a programme written in LabVIEW which separated the data into 30 minute files. Ion counts from the PTR-MS were passed to the LabVIEW programme using the Microsoft protocol “Dynamic Data Exchange” which was operated by a sequence file written in the PTR-MS software (Quadstar) (Appendix IV). A separate LabVIEW programme was written to log data from an ozone sensor (2b Technologies) and Environmental gas analyser (EGM) (PP-Systems), which measured temperature, humidity and PAR , into separate half hourly files.

5.2.7 Flux calculation

In order to calculate VOC fluxes it is first necessary to calculate the lag time that exists between the vertical wind speed data (w) and the PTR-MS data (χ) which arises due to the ~ 20 m separation distance between the two sensors. This was first calculated theoretically using measured flow rates to give a rough estimate, and then calculated experimentally, using a cross correlation function. The latter approach is needed as the performance of the pump may be influenced by changes in temperature and pressure and therefore the lag time may not be constant. Finding the maximum in the cross correlation is sometimes difficult,

especially at night when fluxes are low and turbulence is minimal. In order to ensure the correct lag time was identified, a small humidity sensor was placed inside a ½” tee-piece which was plumbed into the main sample line directly after where the PTR-MS sub-sampled. Data from the humidity sensor was then combined with vertical wind velocities, allowing a cross correlation function to be applied and a clear lag to be identified. The cross correlation applied to VOC data was then refined to a six second time window (3 s before humidity lag and 3 s after). Data points where no clear peak was apparent in the window were not included in the final analysis and are not presented here.

After realignment of the two data sets, vertical wind data was paired up with the corresponding PTR-MS data and the flux was calculated using the following equation which calculates the time averaged covariance:

$$F_x = \frac{1}{n} \sum_{i=1}^n (w_i - \bar{w}) \cdot (\chi_i - \bar{\chi}) \quad (5.2)$$

Where the over bars denote averaging over the 25 minute measurement period.

5.2.8 Post-processing of data

All data files were post-processed using a programme written in LabVIEW. The criterion used to quality assess the data are described in detail in Chapter 2, and included the removal of data where the average wind speed dropped below 1 m s⁻¹ and the rejection of non-stationary averaging periods. In total, an average of 24.7% of the data (low wind speed 19.7% and non-stationary periods 4.0%) was rejected as well as a further 26% for files where no clear lag could be found. These data are not presented here.

5.2.9 Modelling of isoprene and monoterpene fluxes

Measured fluxes of isoprene and monoterpenes were compared against a typical “bottom-up” modelling approach based on the earlier BEMA measurements. In most regional and global scale models the emission flux (F_x , $\mu\text{g m}^{-2} \text{h}^{-1}$) of a given BVOC is calculated using the relationship:

$$F_x = E_N D \gamma \quad (5.3)$$

where E_N is the emission flux normalised to $T_s = 30^\circ\text{C}$ and $L_t = 1000 \mu\text{mol m}^{-2} \text{s}^{-1}$ ($\mu\text{g g}_{\text{dw}}^{-1} \text{h}^{-1}$), D is the biomass density ($\text{g}_{\text{dw}} \text{m}^{-2}$) and γ is a non-dimensional activity factor. For isoprene emission, the light and temperature dependent activity factor (γ_L) is described by the algorithm of Guenther *et al.* (1995) hereafter termed G95, where the isoprene emission rates are described by:

$$\gamma_L = \left[\frac{\alpha C_{LI} L}{\sqrt{1 + \alpha^2 L^2}} \right] \left[\frac{\exp\left(\frac{C_{T1}(T - T_s)}{RT_s T}\right)}{C_{T3} + \exp\left(\frac{C_{T2}(T - T_M)}{RT_s T}\right)} \right] \quad (5.4)$$

where $\alpha = 0.0027 \text{ m}^2 \text{ s } \mu\text{mol}^{-1}$, $C_{LI} = 1.066$ units, $C_{T1} = 95,000 \text{ J mol}^{-1}$, $C_{T2} = 230,000 \text{ J mol}^{-1}$ and $T_M = 314 \text{ K}$ are empirically derived constants, R is the gas constant ($8.314 \text{ J K}^{-1} \text{ mol}^{-1}$), L_t is the flux of PAR ($\mu\text{mol m}^{-2} \text{s}^{-1}$) and T_s is the leaf temperature at standard conditions (303 K used here). Leaf temperature measurements were not recorded during the campaign, therefore ambient air temperature was used as a surrogate. Leaf temperature can fluctuate rapidly which can undoubtedly result in large discrepancies between ambient air and leaf temperature. For example, in a previous study by Singaas *et al.* (1999) leaf and

air temperature were found to vary by as much as 15 °C, however these fluctuations are typically on the order of seconds to minutes, thus averaging of leaf temperature over longer periods as demonstrated by Street, (1995) can provide a more robust estimate and uncertainty can be reduced to as little as ± 1 °C (Owen *et al.*, 2001).

As monoterpene emissions are often assumed to be solely a function of temperature a second G95 algorithm was used.

$$\gamma_T = \exp(\beta[T - T_s]) \quad (5.5)$$

where β is an empirical proportionality constant equal to 0.09°C^{-1} and T and T_s are the leaf temperature and standard leaf temperature (303 K), respectively.

5.3 Results and discussion

5.3.1 Summary of weather and meteorology

Measurements at the Castelporziano site took place between the 7th - 14th of May 2007. In the days before the campaign, heavy rainfall in the region led to flash flooding in and around Rome, relieving the vegetation of any potential drought stress. The unsettled, cloudy weather, which was atypical for the time of year, gradually gave way to clearer skies, and warmer conditions were experienced for the duration of the measurements. The ambient air temperature ranged between 13.3 and 24.1 °C with an average of 19.4 °C and a gradual increase in daily average temperature could be seen between the 7th (18 °C) and 13th (20 °C).

Wind speeds ranged between 0.1 and 4.3 m s⁻¹ with an average of 1.8 m s⁻¹. The highest wind speeds were typically observed around 13:00 hrs (UTC), whereas the low values coincided with the reversal of the sea – land breeze, which occurred between the early evening and midnight.

5.3.2 Measurements of VOC concentrations

Measurements of VOC fluxes measured by the two PTR-MS instruments are presented in Figure 5.3 and are summarised in Table 5.1. Each compound showed a clear diurnal variation with daytime maximums for methanol, acetaldehyde, acetone and isoprene. Monoterpene concentrations differed from the other compounds, with a day time minimum and a night time maximum. This trend was closely related to the wind direction and the oscillating land-sea breeze and will be discussed further in Section 5.3.5.

Concentrations of methanol were highest, ranging between 2 and 8.9 ppb (5th and 95th percentiles). Acetone (0.6 – 4.2 ppb) and acetaldehyde (0.5-2.6 ppb) were the next most abundant compounds, followed by the monoterpenes (0.1 – 1.0 ppb) and isoprene (0.05 – 0.4 ppb). With the exception of the monoterpenes, each of the VOCs followed a very similar trend and regression analysis between the measured compounds showed R² values of between 0.52 (methanol against isoprene) and 0.8 (acetone against acetaldehyde).

Typically concentrations of methanol, acetaldehyde, acetone and isoprene began to increase at around 03:00 hrs (05:00 hrs local time). Methanol and acetaldehyde both peaked in the early morning (06:00 hrs) followed by a gradual decrease throughout the rest of the afternoon and early evening. Measurements of acetone although similar to that of methanol and acetaldehyde, showed some

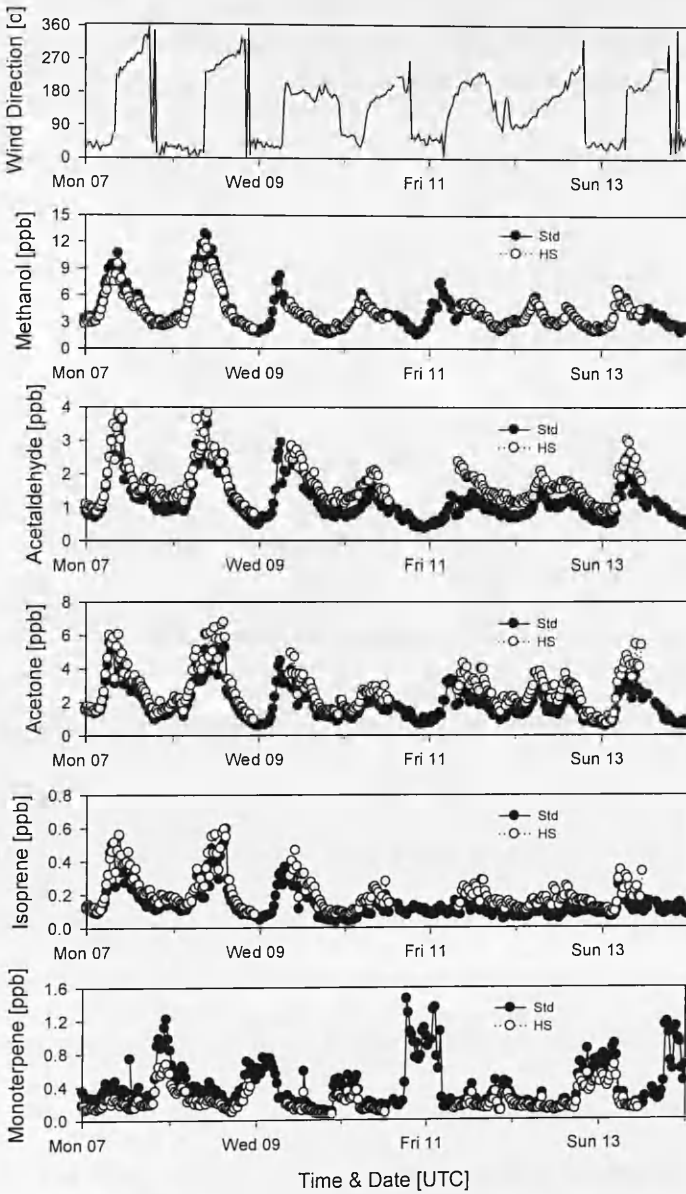


Figure 5.3 Trend in VOC mixing ratios measured between the 7th and 14th of May 2007 using both standard and high sensitivity PTR-MS instruments.

differences, such as a sharp decline in concentration at around 18:00 hrs. Isoprene concentrations increased throughout the afternoon after an initial peak at 06:00 hrs, to reach a maximum at 14:00 hrs, before decreasing sharply in a trend similar to that of acetone.

Table 1 Summary of VOC concentrations and fluxes measured at the Castelporziano nature reserve between the 7th and 13th of May 2007.

	<i>Methanol</i>	<i>Acetaldehyde</i>	<i>Acetone</i>	<i>Isoprene</i>	Σ <i>Monoterpene</i>
Concentrations					
<i>[ppb]</i>					
Mean	4.1	1.2	1.9	0.1	0.4
Median	3.5	0.1	1.6	0.1	0.3
Range 5 th	2.0	0.5	0.6	0.05	0.1
95th	8.9	2.5	4.2	0.4	1.0
SD	2.1	0.6	1.1	0.1	0.3
<i>n</i>	340	340	339	340	339
Fluxes					
<i>[$\mu\text{g m}^{-2} \text{h}^{-1}$]</i>					
Mean	199.1	150.6	134.4	31.5	132.8
Median	239.8	131.2	139.4	31.6	133.8
Range 5th	-193.2	-103.8	-186.3	-44.5	-104.8
95th	575.1	413.5	514.3	129.6	350.1
<i>n</i>	125	141	123	135	132

Results of the comparison study between the standard and high sensitivity PTR-MS instruments are shown in Fig. 5.4. The two instruments showed excellent agreement in concentration trends, with R^2 values ranging between 0.92 and 0.98 (Fig. 5.4), but the absolute values differed significantly for some compounds. The largest deviation was observed in the measurements of monoterpenes, with > 40% difference in absolute concentration between the two systems. This offset is likely to occur due to the use of transmission numbers instead of gas standard calibration. The offset is made worse as the monoterpenes fall near the end of the transmission curve, and thus small errors in the calculation of the curve are magnified. In addition, total monoterpenes are calculated as the sum of m/z 81 and m/z 137, therefore any offset in the transmission curve is effectively doubled.

The calibrated compounds, methanol, acetaldehyde and acetone as well as isoprene all agreed well with less than 20% difference between the two

instruments. As each PTR-MS was operated by a separate computer, there was often a slight drift between the two system clocks, but this is not thought to have a significant impact on the measured concentrations.

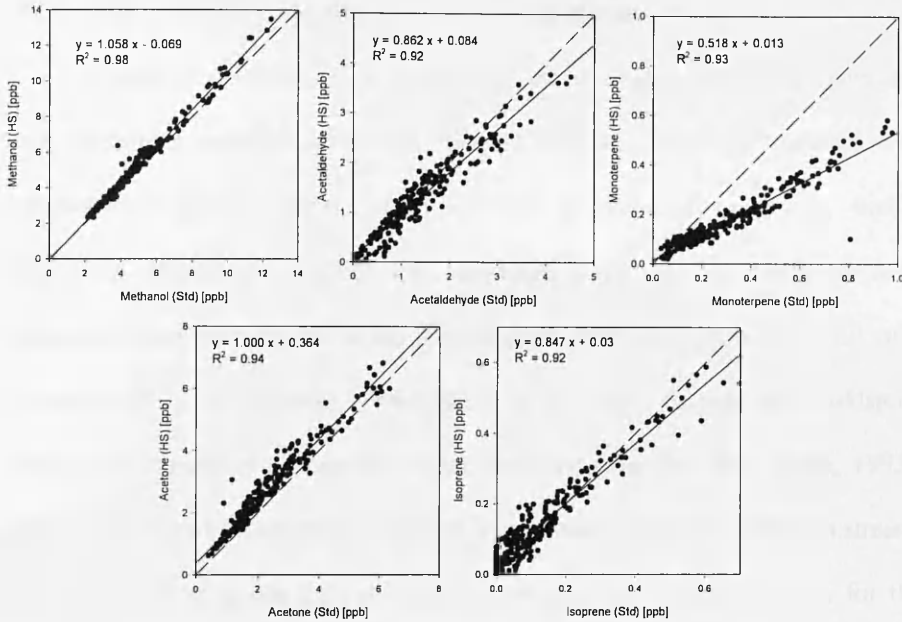


Figure 5.4 Regression plots of VOC concentrations measured by a standard and high sensitivity PTR-MS at the Castelporziano field site between the 7th and 14th of May 2007. Dashed line shows the 1:1 regression line.

5.3.3 Fluxes of VOC from the macchia

Figure 5.5 shows a time series of VOC fluxes measured between the 7th and 13th of May 2007 at the Castelporziano field site and Fig. 5.6 shows the averaged diurnal pattern for each compound. Emission fluxes of all five compounds were observed from the macchia, with emission rates highest during the mid to late afternoon and lowest during the night. In contrast to concentration measurements, fluxes of monoterpenes also showed daytime maxima.

Fluxes of methanol ($199 \mu\text{g m}^{-2} \text{h}^{-1}$) were largest, followed by acetaldehyde ($151 \mu\text{g m}^{-2} \text{h}^{-1}$), acetone ($134 \mu\text{g m}^{-2} \text{h}^{-1}$), monoterpenes ($133 \mu\text{g m}^{-2}$

h^{-1}) and isoprene ($32 \mu\text{g m}^{-2} \text{h}^{-1}$). During the night time, some deposition was observed, although these values should be treated with some caution as night time flux measurements are associated with large degrees of uncertainty due to the often stable atmospheric conditions and low wind speeds.

Fluxes of methanol closely followed the diurnal profile of temperature, with emissions peaking at around midday. This was in slight contrast with concentration measurements, which peaked in the early morning, before decreasing steadily throughout the afternoon. Emissions of methanol from vegetation have been related to the physiological processes within the plant such as growth (Fall and Benson, 1996; Hüebe *et al.*, 2007; Schade and Goldstein, 2006), cell expansion and protein repair reactions (Mudgett and Clarke, 1993). Once inside the plant, methanol emission is controlled via the transpiration stream, which is itself governed by light and leaf temperature (which accounts for the close agreement with temperature), as well as stomatal conductance. Since the synthesis of methanol can occur during the night time when the stomata are closed, methanol builds up in the plant before being released in a burst when the stomata are opened in the morning. This venting process has been demonstrated by Cojocarui and Hewitt (2008) but is not thought to be the reason for the morning maxima in VOC concentrations as similar peaks are not seen in the flux. Instead, it is assumed that the concentration increase is related to an accumulation of early morning emissions into a still shallow nocturnal boundary layer. Cojocarui and Hewitt (2008) also showed smaller nocturnal bursts of methanol in emissions from tobacco plants, which were attributed to the periodical opening of stomata during the night, however this process was not observed over the vegetation in the current study.

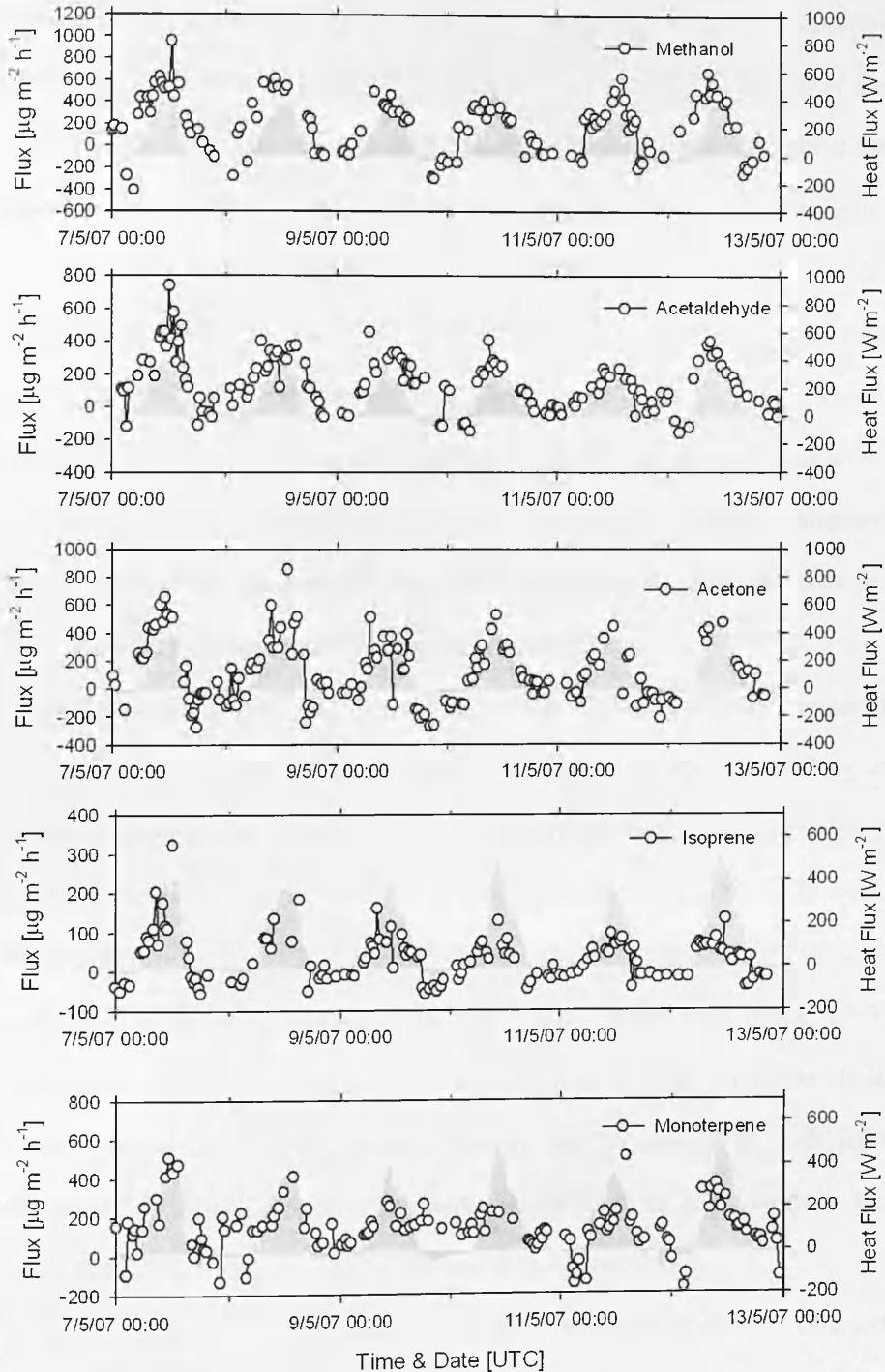


Figure 5.5 Time series of VOC fluxes (open circles) and sensible heat fluxes (greyed area) measured at the Castelporziano nature reserve.

Emissions of methanol are known to be influenced by a number of stress factors, including elevated ozone, frost, drought, flooding and mechanical leaf wounding (Beauchamp *et al.*, 2005; Fukui and Doskey, 1998; Holzinger *et al.*, 2000; Karl *et al.*, 2005). Although flash flooding was widespread throughout the region in the days prior to the campaign, the macchia were situated on a sandy, well drained soil and therefore were unlikely to be affected. Mechanical leaf wounding caused due to the trampling of local vegetation during the set-up in the days prior to the measurements may have contributed to the increased concentrations and fluxes between the 7th and 8th of May. In addition, high levels of ozone (50-60 ppb) on these days may also have caused stress related emissions, however comparison of methanol and ozone concentrations measured over the duration of the campaign showed no significant correlation.

Fluxes of acetone and isoprene follow the diurnal pattern of measured PAR very closely, with emissions starting at sunrise (04:30 hrs), peaking at midday and stopping at sunset (17:00 hrs). The light and temperature dependency of both compounds have been well documented (Shao & Wildt, 2002; Shao *et al.*, 2001; Guenther *et al.*, 1993, 1995). For isoprene, the biosynthetic pathways of its production are well understood (Fall 1999; Kesselmeier and Staudt 1999; Lichtenthaler, 1999), but for acetone our knowledge is still incomplete. It is however known that unlike isoprene, acetone can be emitted as both light dependent or light independent responses in the leaf as well as from the mechanical wounding of plant tissue (Steiner & Goldstein, 2007).

In contrast to isoprene and acetone, emissions of acetaldehyde remained positive until much later in the evening (20:00 hrs). Previous studies have noted

that emissions of acetaldehyde are often triggered during the transition from light to dark (Holzinger *et al* 2000; Karl *et al* 2002). It has been suggested that levels

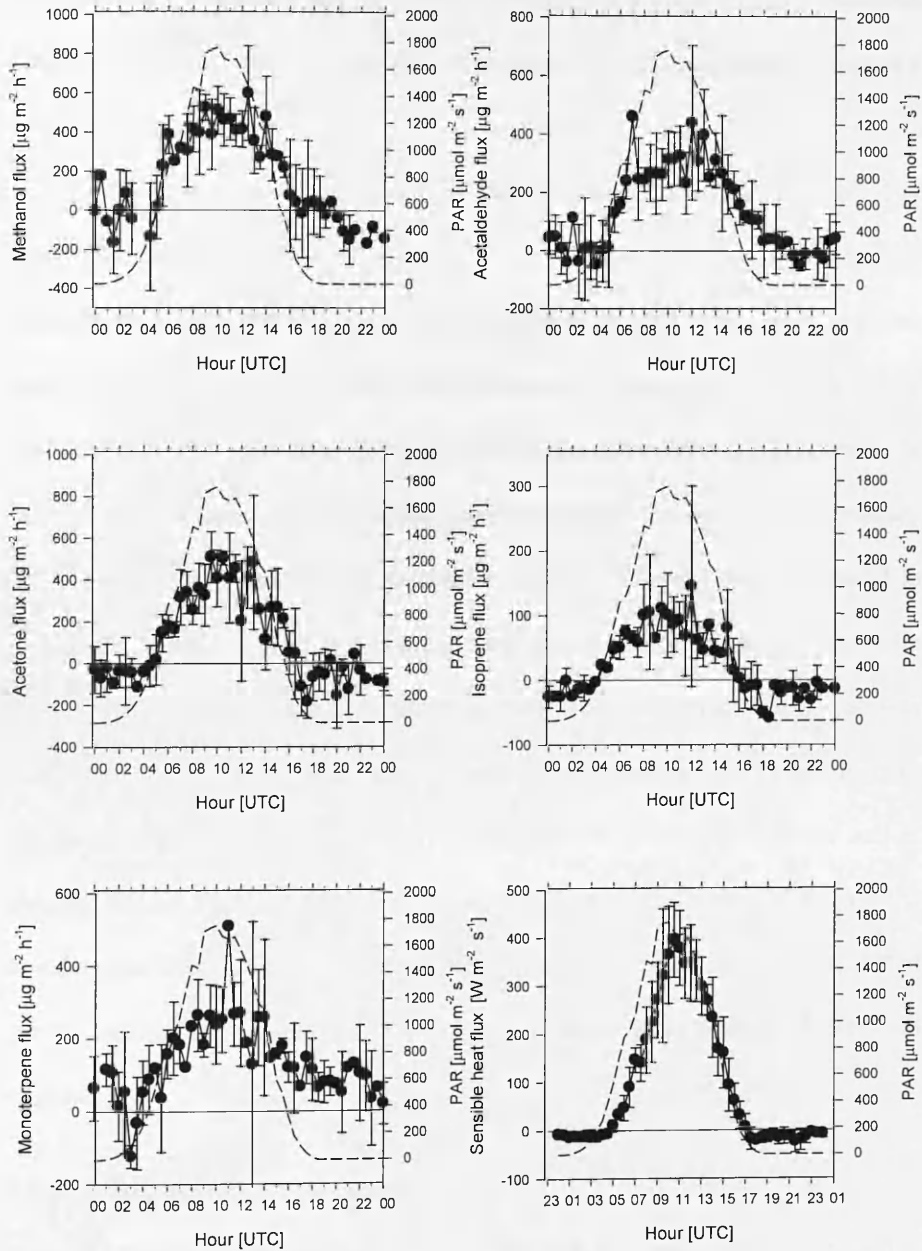


Figure 5.6 Average diurnal profiles of VOCs fluxes (closed circles) and PAR (dashed line) measured between the 7th and 13th of May 2007 at the Castelporziano nature reserve. Error bars show standard deviation of measured fluxes.

of pyruvic acid in the leaf increase as the light fades, causing excess pyruvate to be catalysed by a safety valve to form acetaldehyde, which is subsequently leached from the intercellular space (Steiner and Goldstein 2007). It is possible that the evening emissions of acetaldehyde observed in the current study were as a result of this process.

The monoterpene fluxes also remained positive throughout the night, only becoming negative for short periods in the early morning. Emissions of monoterpenes from vegetation are predominantly controlled either by temperature only or by a combination of light and temperature (Kesselmeier & Staudt, 1999; Loreto *et al* 2001). In temperature dependent terpenoid emitters, the production of monoterpenes is believed to be a defence mechanism for the plant for two reasons. Firstly, after synthesis in the leucoplasts or cytosol, monoterpenes are stored in specialised structures such as glandular trichomes and resin ducts, and secondly specific monoterpenes have been shown to both repel and attract insects (Steiner & Goldstein, 2007). In plant species where monoterpenes synthesis is both temperature and light dependent, production occurs in the chloroplasts and is closely linked to the photosynthetic cycle (Loreto *et al.*, 2001). As the monoterpene fluxes remained positive during night time hours it must be assumed that the macchia was composed of both light and temperature dependent terpenoid emitters.

5.3.4 Comparison of VOC fluxes

Due to the collaborative nature of the PTR-MS inter-comparison, at the time of writing only isoprene and methanol fluxes were available for the HS PTR-MS data set, therefore the comparison presented here was limited to just two compounds. Isoprene fluxes measured by both the HS and Std PTR-MS

instruments are presented in Fig. 5.7. The trend of the two data sets were in good agreement ($R^2 = 0.67$, $p < 0.0001$, $n = 141$), yet, the fluxes measured by the HS PTR-MS appeared to have a more dynamic range. The higher sensitivity of the HS instrument may have had some bearing on the greater amplitude of the fluxes, but it is thought more likely to relate to uncertainties in the identification of sample lag times which can cause a systematic overestimation of the absolute magnitude of the flux. Selecting the correct lag time to use can be difficult and is further complicated at lower measurement heights as the mean eddy size is shorter, which results in more noisy cross-correlation functions. For data collected using the Std vDEC system, which concurrently logged data from the in-line humidity sensor, stricter quality controls could be imposed for the selection of lag times, resulting in fewer, but ultimately more accurate lag estimates.

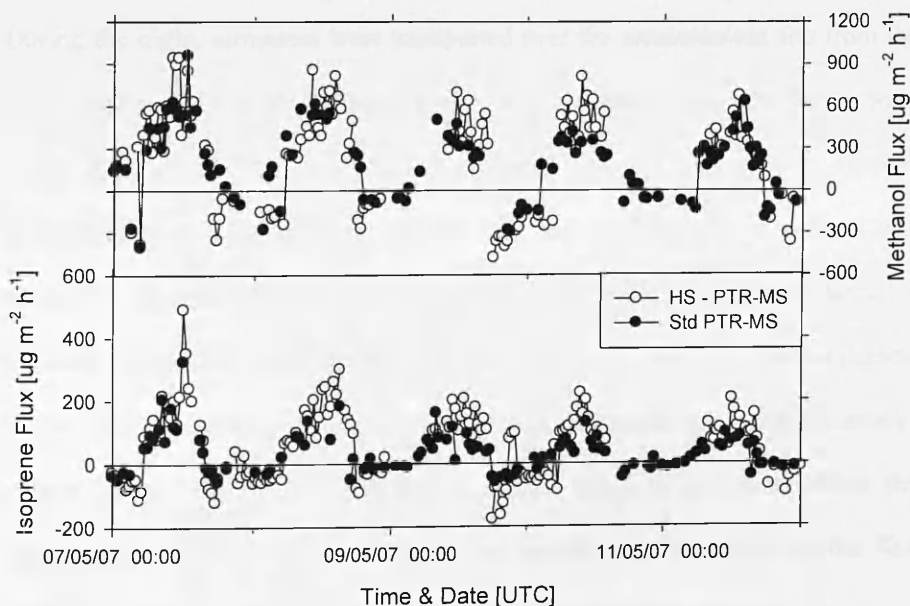


Figure 5.7 Comparison of isoprene and methanol fluxes measured using a standard (Std) and high sensitivity (HS) PTR-MS during the Castelporziano field campaign.

The largest discrepancies between the two systems tended to occur at night, when concentrations (excluding monoterpenes) and wind speeds were at

their lowest. It is perhaps necessary to impose stricter quality controls on data collected at night such as removal of periods where u^* is below 0.15 m s^{-1} , or to simply reject these data completely.

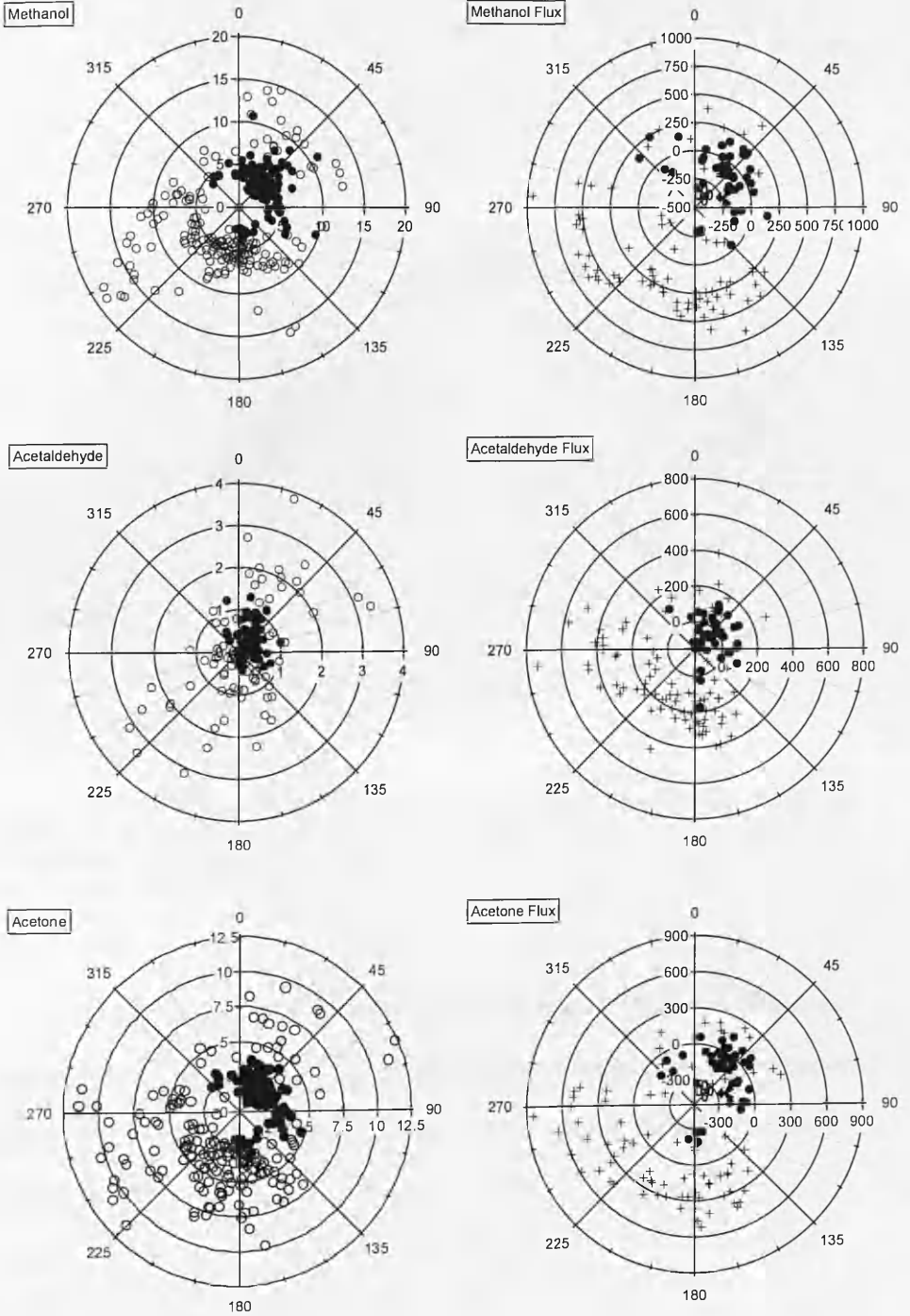
Fluxes of methanol also compared very favourably, with an R^2 value of 0.66 ($p < 0.0001$, $n = 76$). As was the case for isoprene, fluxes measured using the HS instrument had a more dynamic range than those measured by the Std PTR-MS. A comparison of the absolute relative error ($\text{abs}((\text{HS-Std})/\text{Hs} \times 100\%)$) showed that on average the two techniques differed by less than 30%.

5.3.4 Wind sector dependence

Wind roses of VOC concentrations and fluxes are shown in Fig. 5.8. Data were separated into two categories, day (04:30 - 17:30 hrs) and night (18:00 - 04:00 hrs), which roughly corresponded with the rotation of the land-sea breeze. During the night, airmasses were transported over the measurement site from the north-west and for most compounds both VOC concentrations and fluxes were lower than during the day. While this was true for monoterpene fluxes, measurements of concentrations showed nocturnal maxima. This maximum was caused by the advection of monoterpene emissions from the oak/pine plantation (situated North West of the sampling location) where the dominant species present is *Quercus ilex*, a strong light and temperature dependent monoterpene emitter (Bertin *et al.*, 1997). The fact that a similar trend is not seen within the monoterpene fluxes confirms the source of emission to be outside of the flux footprint, which would be consistent with oak/pine plantation emissions.

During the night measurements of benzene made during the MS mode also showed a maximum as anthropogenic emissions from the surrounding urbanised areas were advected over the measurement site as seen in Fig 5.9. Small nocturnal

increases in temperature were also recorded at night, which are thought to relate to heat storage in the surrounding urban areas.



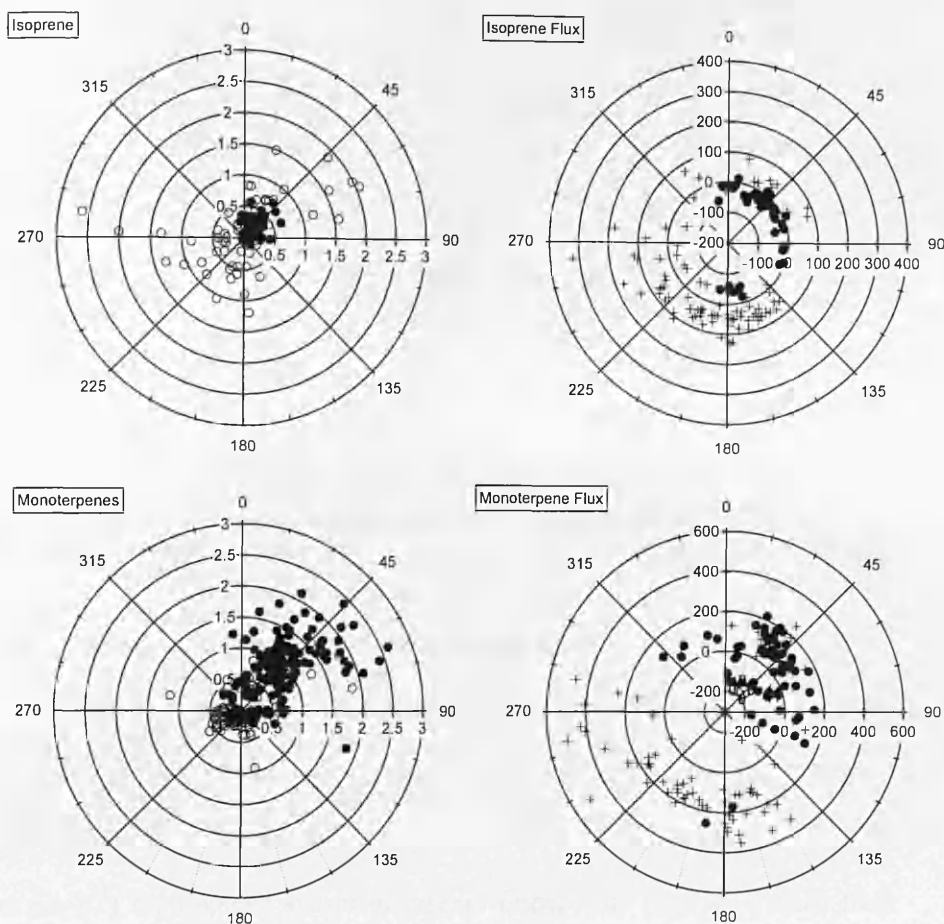


Figure 5.8 Wind roses of VOC concentrations (ppb) and fluxes ($\mu\text{g m}^{-2} \text{h}^{-1}$) measured between the 7th and 13th of May 2007 at the Castelporziano nature reserve. Closed circles represent night time measurements made between 18:00 - 5:30 hrs and open circles / crosses show daytime measurements between 05:30-18:00 hrs.

During the daytime the wind predominantly came from the south-west and was associated with higher VOC concentrations for methanol, acetaldehyde, acetone and isoprene. The highest concentrations and fluxes were observed during westerly winds, which tended to correspond to higher afternoon temperatures.

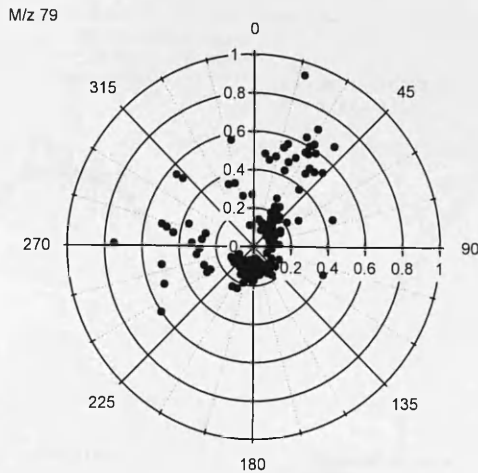


Figure 5.9 Wind rose of benzene concentrations measured during the mass scan mode which operated for five minutes of each hour.

5.3.5 Comparison of measured and modelled fluxes

Estimates of isoprene and Monoterpene emissions were calculated using the G95 algorithms and were compared with the measured fluxes. Typical summertime basal emission rates of 2.5 ± 1.4 ($n = 6$, \pm sd) and 2.6 ± 5.6 ($n = 83$, \pm sd) ($\mu\text{g g}_{\text{dw}} \text{h}^{-1}$) for isoprene and monoterpenes respectively (E_N) were taken from Owen (1998) who performed a detailed screening of the macchia during the BEMA project. A biomass density of 175 g m^{-2} for the measurement site was taken from Seufert *et al.* (1997) who also participated in the BEMA campaign. Light and temperature values were averaged between the 7th and 13th of May to give a typical diurnal flux profile which is shown in relation to the measured fluxes in Fig. 5.10.

Isoprene fluxes measured using the vDEC technique showed excellent agreement with modelled values, with less than 10% difference between the averaged daily emissions of 0.8 and $0.73 \text{ mg m}^{-2} \text{ d}^{-1}$ for measured and modelled, respectively. Measured and modelled fluxes of isoprene both started to rise at 04:00 hrs, but the measured values appear to decrease and approach zero

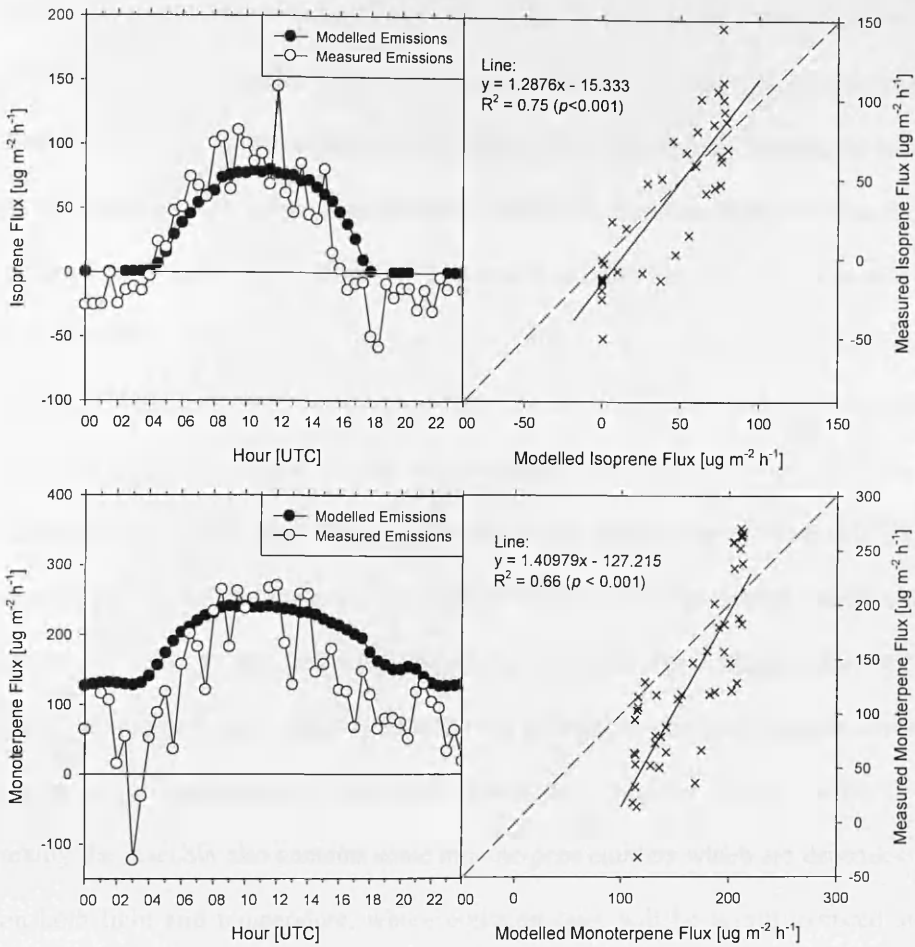


Figure 5.10 Comparison of modelled and measured emission fluxes of isoprene and monoterpenes from the Castelporziano field site between the 7th and 13th of May 2007. Modelled fluxes were calculated using the G95 algorithms and measured fluxes were obtained using the virtual disjunct eddy covariance technique. Dashed line shows 1:1.

approximately 1 hour before the modelled values. The reason for this offset is not clear, but may relate to either a lag between air and leaf surface temperature or the early evening reversal of the land-sea breeze, which is (i) associated with low wind speeds and consequently little or no turbulence for tracer transport or (ii) the 180° shift in the flux footprint, which could influence emission rates in a heterogeneous canopy.

Monoterpene fluxes compared slightly less favourably than isoprene with measured values typically 27% lower than modelled emissions (3 and 4.2 mg m^{-2}

d^{-1} for measured and modelled, respectively). In the morning and late afternoon, modelled fluxes showed a slower increase and decline compared with measured fluxes. This may relate to the use of ambient air temperatures instead of leaf temperature, as leaf temperature responds quickly to direct sunlight, whereas the atmosphere responds more slowly as it is heated indirectly by the Earth's surface. The modelled monoterpene fluxes are also, on average, higher than measured values during the night time, but, importantly, monoterpene emissions also remain positive during the night, which is in contrast with the isoprene emissions. Comparison of night time fluxes should be treated with a degree of caution for reasons stated earlier, however, it is thought that the lower measured values are likely to relate to the heterogeneity of the macchia. For instance, the G95 algorithm applied here was done so under the assumption that the vegetation was comprised of temperature dependent monoterpene emitters only, whereas in reality the macchia also contains some monoterpene emitters which are dependent on both light and temperature, whose emission rates will be greatly reduced at night. During the BEMA campaign, the percentage contribution of light dependent monoterpene emitters was estimated to be approximately 17% (Owen, 1998).

It is clear that changes in light and temperature control emission rates of both isoprene and monoterpenes from vegetation which are well described by the G95 algorithm, but biogenic emissions of methanol, acetaldehyde and acetone have also been shown to have a strong dependency on temperature (Cojocariu *et al.*, 2004; Grabmer *et al.*, 2006; Filella *et al.*, 2007). As the G95 algorithm is specifically tailored to emissions of isoprene and monoterpenes, further modelling of VOC emissions was not possible, but measured fluxes were plotted against temperature as shown in Fig 5.12 and results showed excellent agreement. The

non-linear increase in emissions with temperature appears typical of most BVOC emissions (Filella *et al.*, 2007). However, it is unclear as to whether this relationship is regulated by the physiology of the plant or simply a consequence of vapour pressure and thermodynamics.

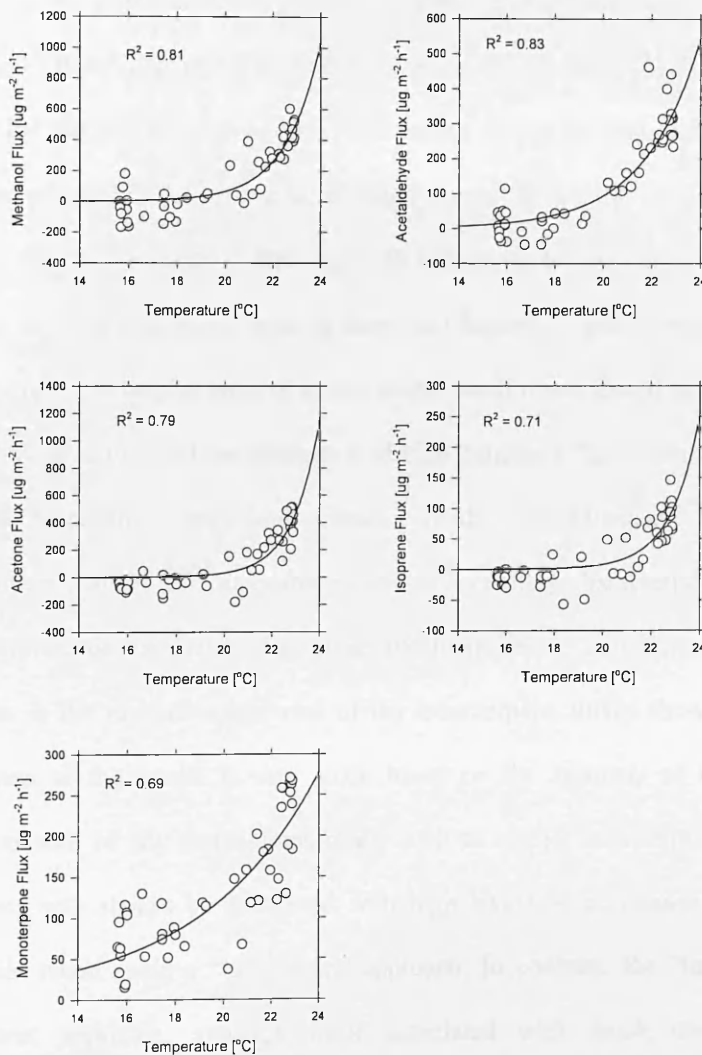


Figure 5.12 Graphs showing the temperature dependence of VOC fluxes measured during the Castelporziano field campaign.

5.4 Conclusions

The vDEC technique has been shown to be a reliable tool for the measurement of volatile organic compound fluxes, with excellent agreement

between two flux measurement systems (though based on the same sonic anemometer). Importantly, the reproducibility of the technique has been demonstrated, although areas for improvement have been highlighted, such as establishing better criteria for the identification of lag times. Simple changes such as increasing m/z dwell times from 0.2 s to 0.5 s would increase the signal to noise ratio of the PTR-MS data and reduce noise in the cross-correlation function, which could aid the identification of lag times and further reduce the uncertainty in the flux measurement. On the downside, it would reduce the number of data points going into the flux calculation. This approach is likely to be most effective when measuring at higher locations such as those in Chapters 3 and 4, whereas, for lower measurement heights such as in this study, dwell times should be extended with caution, so as to avoid the attenuation of high frequency flux contributions.

The favourable comparisons between trends in modelled and measured fluxes confirm that the G95 algorithm is able to accurately characterise the light and temperature dependencies of isoprene and monoterpene emissions. Yet, the differences in the relative magnitudes of the monoterpene fluxes show that the effectiveness of the model is very much based on the accuracy of the input variables as well as any assumptions made, such as species composition. These assumptions will always be associated with high levels of uncertainty and are unavoidable when using a “bottom up” approach. In contrast, the “top down” measurement approach, although itself associated with much uncertainty, integrates the flux over the entire area and therefore negates assumptions on species composition or source strengths, creating a compelling argument for the inclusion of more local scale flux measurements in both regional and global scale models as opposed to typical ecosystem base emission rates.

Chapter VI

6. Analysis of uncertainties and errors

6.1 Systematic and random errors

Flux measurements are often associated with significant uncertainty. It is therefore important to highlight and where possible, quantify potential errors, which may be systematic or random in nature. Systematic errors cause a bias to a dataset, shifting all data so their mean value is displaced, reducing measurement accuracy. The classic example of a systematic error is the stretching of a tape measure, which causes each subsequent measurement to be offset by the same amount. In micrometeorology, an obvious example of a systematic error is flux loss due to the separation distance between the sonic anemometer and the gas inlet. This source of uncertainty was investigated by Kristiansen *et al* (1996), who suggested the effect could be minimised by displacing sensors vertically, positioning the sample line below the sonic anemometer. In each of the field applications of the DEC and vDEC systems described here this advice was followed and therefore errors due to sensor separation are thought to be minimal, especially because measurement heights were mainly high which results in larger and slower eddies.

Other systematic errors can come about due to the configuration of the flux system, such as the dampening of the wind components due to the distortion of air flow around the sonic anemometer and or sampling system. Wind tunnel experiments have suggested flow distortion around the anemometer to cause damping of the wind components by as much as 20% (Foken *et al.*, 1995). In the real atmosphere, this figure may be less, as the effect of flow distortion depends on the ratio of the obstacle length and the turbulence integral scale (Wyngaard, 1981), which can change rapidly

in the atmosphere: therefore a quantitative correction is not easily applied (Foken & Wichura, 1996). Of the work presented in this thesis, damping of the vertical wind component was most likely to have affected the CO₂ validation experiment, where the DFS was mounted directly below the sonic anemometer, although steps were taken to keep this to a minimum. Other systematic errors typical of micrometeorological flux measurement systems can include damping of signals due to long sampling tubing, which are particularly bad under laminar flow conditions, calibration errors, inadequate sensor response times or insufficient elevation above the terrain surface (Moncrieff *et al.*, 1996).

In contrast to systematic errors, random errors cause fluctuations from one measurement to the next, yielding a measurement distributed about some mean value, at a reduced precision. Random errors are typically associated with a lack of sensitivity in a sensor, or extraneous disturbances such as white noise, which can be a particular problem when measuring fluxes of trace gases. In addition, random errors can also be attributed to the varying size of the flux footprint, surface homogeneity and non-stationarities (Moncrieff *et al.*, 1996).

6.2 Potential systematic errors in the DEC systems

6.2.1 Transmission numbers and calibration

The calibration of the PTR-MS has the potential to introduce a considerable systematic error to both the DEC and vDEC systems. For the measurements presented in Chapters 3 and 4, no gas standards were available for the calibration of the PTR-MS and therefore concentrations were calculated using the transmission curve of the instrument and tabulated reaction rate coefficients, which is standard practice in the application of PTRMS (Ammann *et al.*, 2004). The transmission curve describes the

efficiency with which each protonated mass traverses the drift tube and is therefore required to establish the ratio of primary ions to protonated target ions, which is then used in Eq. (2.19) to calculate the VOC mixing ratio. The transmission numbers for the PTR-MS instrument used in Chapters 3 and 4 were both calculated experimentally in the laboratory following the guidelines issued by the manufacturer. Nevertheless, previous studies have shown that determining concentrations in such a way can result in uncertainties as large as a factor of two (de Gouw & Warneke, 2007). This, however, is very much a worst case scenario and confidence in the measurements was gained thanks to the good agreement between concentration measurements from the PTR-MS and GC-MS instrument calibrated with a gas standard (Apel-Riemer Environmental Inc., Denver, CO) which were shown in Chapter 4. For the study presented in Chapter 5, isoprene and monoterpene concentrations were also calculated using transmission curves. For isoprene, deviation between the two instruments was very small (<15%), whereas for monoterpenes the two instruments differed by > 40%, showing a large systematic error which was discussed in Chapter 5. For measurements of acetone, acetaldehyde and methanol, concentrations were verified using gas standards which had an uncertainty of approximately $\pm 5\%$. Comparison between the two PTR-MS instruments for these three compounds showed a difference of between <1 and 13%.

As the concentration is used in the flux calculations, uncertainties in the calibration feed through to uncertainties in the flux. However, since the flux calculation is based on the deviation from the mean, only errors in the span calibration affect the flux, whereas errors in the zero (or instrument background) would not affect the flux.

6.2.2 Disjunct sampling intervals and flux attenuation

The use of disjunct sampling intervals (DSI) means a systematic error is introduced to the flux measurement for each averaging period (Lenschow *et al.*, 1994). The variability of the fluxes is dependent upon the comparable magnitudes of the length of sampling interval and the integral timescale of the turbulent fluctuations (l_{ws}). When the interval is kept short and is below l_{ws} , the variability of the fluxes should be small, but as the interval is increased and approaches l_{ws} the variability becomes large. In order to assess the systematic error incurred due to the choice of sampling intervals during each campaign, sensible heat data were used to simulate the disjunct sampling process following the procedures laid out in Section 2.5. Results are presented in Table 6.1 and show the average error ($\text{abs}((\text{EC}-\text{DEC})/\text{EC} \times 100\%)$) per 30 minute file and the cumulative error, where the sum of fluxes measured during the campaign are compared to the sum of those measured by DEC. The average error in the 30-minute measurements is typically much higher than the relative error in the averages. This is because the cumulative error sums the average error, which is either positive or negative, therefore over a sufficiently long time period the errors cancel and the overall uncertainty is reduced as was demonstrated in Chapter 2, Fig 2.8. It should be noted that relative errors in EC measurements tends to increase as the absolute value decreases. Thus, this numerical analysis will give larger relative errors in conditions where the heat fluxes were lower.

Systematic errors are also incurred due to the loss of high frequency flux contributions, which are attenuated as the sample time (as dictated by the grab sample time in the DEC and dwell time in vDEC) increases. In order to quantify the overall effect of flux attenuation (AT), sensible heat data was again used to simulate disjunct sample intervals and the measurement resolution of the EC data was reduced to the

Table 6.1 Uncertainty in the flux measurements caused due to systematic errors associated with disjunct sampling intervals (DSI) and the attenuation of the flux (AT) from measurement resolution.

<i>Campaign</i>	<i>DSI uncertainty</i>		<i>DSI & AT uncertainty</i>	
	<i>Cumulative Error</i>	<i>Average Error of 30-minute values</i>	<i>Cumulative Error</i>	<i>Average Error of 30-minute values</i>
Edinburgh 15 s, 0.5 s z = 2 m L _d = 3 days	32 %	44 %	11%	48%
Manchester DEC 12 s, 0.5 s z = 95 m L _d = 3 weeks	1 %	25%	8%	25%
Manchester EC 0.6 s, 0.02 s z = 95 m L _d = 3 weeks	0.05%	3%	n/a	n/a
London 1.2 s, 0.1 s z = 200 m L _d = 4 weeks	2%	14%	2%	14%
Italy 1.4 s, 0.2 s z = 5 m L _d = 1 week	0.07%	6%	5%	7%

z = measurement height; *L_d* = duration of campaign

desired amount by simply averaging the required number of temperature data points, as shown in Chapter 2. This process was based on the assumption of identical frequency behaviour between scalars. Separating the uncertainty due to DSI and AT was not possible due to the propagation of the errors, therefore the total uncertainty due to both sampling intervals and flux attenuation are presented alongside DSI errors in Table 6.1.

Comparison of the average errors for the DSI and DSI & AT data sets shows the reduced time resolution to have little effect on the average uncertainty in the flux. In contrast, the cumulative error is consistently much larger in DSI & AT data sets compared to DSI only data sets. This is because the slower sampling times result in the attenuation of the flux, which is subsequently systematically underestimated. Although this causes little difference to the average error in the flux measurement,

when flux values are summed over the entire campaign, the error due to flux attenuation is consistently negative and does not cancel out, therefore a net underestimation of the flux is observed. The magnitude of the underestimation due to flux attenuation is loosely correlated with the measurement height, as the portion of the flux carried by higher frequency eddies scales inversely with height.

Typically errors due to both the choice of disjunct sampling intervals and the attenuation of higher frequency fluxes resulted in an underestimation of the cumulative flux by no more than 10%. The exception to this was the Edinburgh based campaign, where the cumulative uncertainty due to disjunct sampling intervals was much larger (>30%). This large uncertainty may relate to the very short duration of the campaign (3 days), which may not have been sufficient to gain a statistically robust estimate of the average flux.

6.2.3 Attenuation of low frequency flux contributions

As well as being attenuated at the high frequency end of the spectrum, flux measurements can also be attenuated at the low end through the use of insufficiently long averaging periods. Typically, averaging periods of between 10 and 60 minutes are used in eddy covariance, which is, for most situations, thought to be sufficient to fully resolve the contribution from both high and low frequency eddies. Yet, at elevated measurement heights, where the mean eddy size is larger this may not be the case. Of the work presented in this thesis, the most likely to have suffered from low frequency attenuation were the measurements made during the REPARTEE campaign from 200 m tall Telecom Tower. In order to investigate this effect, sensible heat flux data from the campaign were re-analysed by joining individual 30 minute files to create averaging periods of 30, 60, 90, 120 and 150 minutes.

A coordinate rotation was applied to the resulting files which acted as a high pass filter (Finnigan *et al.*, 2003) to the three dimensional wind velocity measurements, ensuring that fluctuations from eddies with a time period greater than that of the averaging period could not contribute to the flux measurement (Moncrieff *et al.*, 2004). The resulting fluxes were then compared back to the average values measured using the standard 30 minute averaging periods which were also rotated to ensure the flux was only made up by turbulent fluctuations of 30 minutes or less. The results are shown in Fig. 6.1, where the y axis shows the fluxes calculated from the extended averaging period and the x axis show the flux calculated from the same period but constructed from the consecutive 30 minute averaging periods. The results show that eddies with a time period of between 30 minutes and one hour increase the flux by 3.4%, similarly eddies with a period of between 1 hour and 1.5 hours increase the flux by 2.5 %. Extending the averaging period further to 2.5 hours shows a total flux increase of 11.5 % but after this little further increase is observed. Similar results were observed in heat fluxes measured at Nelson Monument, Edinburgh (E. Nemitz, personal comm.) and in CO fluxes measured above Boulder, Colorado (Nemitz *et al.*, 2008). These findings show that the flux measurements made at the Telecom Tower were bandwidth limited as low frequency contributions were being missed due to the choice of averaging period. Therefore, VOC fluxes measured at the tower may be underestimating the true flux by some 10 to 15%. However, increasing the averaging period for the PTR-MS measurements to 2.5 hours would have increased the likelihood of non-stationarities affecting the flux measurements. In addition, lower time resolution in the flux measurements contains less information to study the processes affecting the fluxes, which was an important objective of this work. Thus a

30-minute averaging time appears to find the right balance.

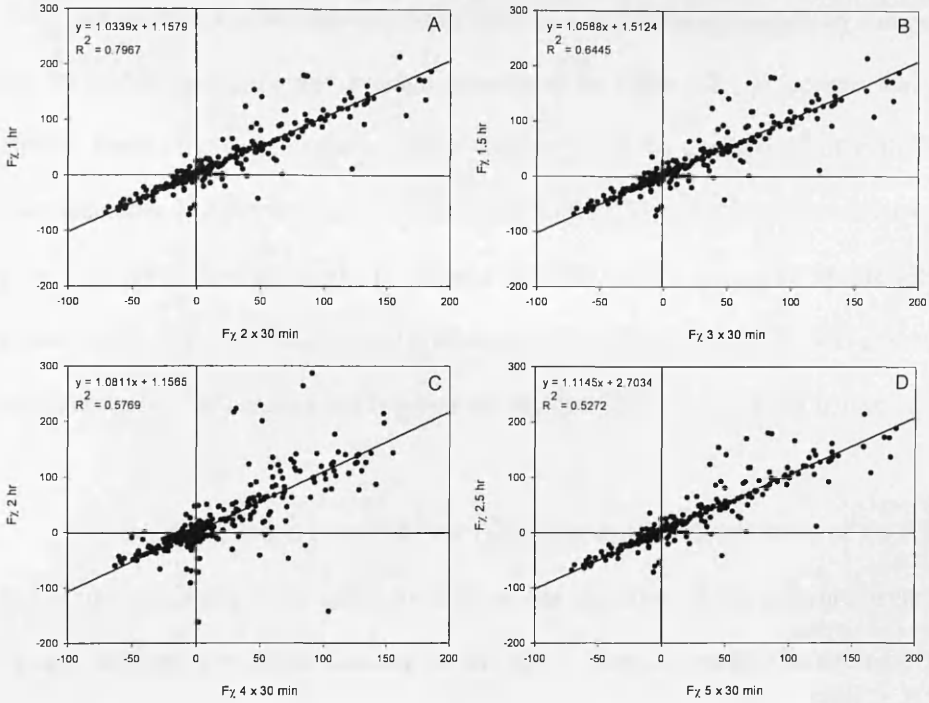


Figure 6.1 Fluxes of sensible heat measured at the Telecom Tower, F_H [$W\ m^{-2}$], calculated using averaging periods of 1, 1.5, 2 and 2.5 hours and compared with fluxes calculated using the more standard 30 minute averaging period.

6.3 Potential random errors in the DEC systems

The use of the proton transfer reaction mass spectrometer for the measurement of VOC concentrations is a potentially large source of random error in both of the DEC systems. As with most mass spectrometers the precision of the instrument is controlled by counting statistics. Lee *et al* (2004) suggest the percent uncertainty in mixing ratios due to the effect of counting statistics can be expressed as:

$$\sqrt{\frac{RH_i}{RH_i \cdot t}} \tag{6.1}$$

where RH_i is the mean count rate (counts per second) and t is the counting time (PTR-MS dwell time). This equation was applied to the data collected during each of the three campaigns. The average count rates for the calculation are displayed alongside the PTR-MS dwell time and average uncertainty in Table 6.2. It is clear that the chosen dwell time is an important factor in controlling the uncertainty of individual measurements. In Manchester, the 1 s dwell of the DEC system meant uncertainty was kept <5% for most compounds. In contrast the 0.02 s dwell time used by the vDEC system resulted in very large uncertainties (3 – 77%), especially for the less abundant compounds such as benzene and isoprene for the raw DEC measurement points.

During the London based REPARTEE campaign, the dwell times of the PTR-MS were lengthened in an effort to increase the precision of the measurements. In theory, at least a 4 times increase in the dwell time is needed to decrease the uncertainty by 50%. To this end, 0.1 s dwell times were chosen which reduced the random error to an average of between <1% and 32%. During the work in Castelporziano, the dwell times were doubled to 0.2 s. Regardless of this action, the uncertainty in measurements of the less abundant compounds was still large and in the case of isoprene, the uncertainty was greater than in measurements made in London. This is initially counter-intuitive given that ambient concentrations of isoprene were higher than they had been in London and dwell times were longer. However, the difference is due to the different sensitivities of the two PTR-MS instruments used in the respective campaigns. In Castelporziano a standard PTR-MS was used, whereas in London a high sensitivity model was used. The addition of a third turbo pump in the HS model

Table 6.2 Uncertainty in individual VOC measurements due to counting statistics for each measurement campaign.

compounds	Manchester [DEC]			Manchester [EC]			London			Italy		
	ICPs	Dwell	Error	ICPs	Dwell	Error	ICPs	Dwell	Error	ICPs	Dwell	Error
Methanol	232	1 s	0.4%	218	0.02 s	3.2%	1555	0.1 s	0.2%	95	0.2 s	2.3%
Acetonitrile	<i>n/a</i>	<i>n/a</i>	<i>n/a</i>	<i>n/a</i>	<i>n/a</i>	<i>n/a</i>	28	0.1 s	11%	<i>n/a</i>	<i>n/a</i>	<i>n/a</i>
Acetaldehyde	181	1 s	0.5%	103	0.02 s	6.8%	217	0.1 s	1.5%	46	0.2 s	4.9%
Acetone	146	1 s	0.7%	114	0.02 s	6.1%	101	0.1 s	3.1%	73	0.2 s	3.1%
Isoprene	25	1 s	4%	11	0.02 s	65%	12	0.1 s	26%	7.5	0.2 s	30%
Benzene	10	1 s	9.6%	9	0.02 s	77%	11	0.1 s	28%	<i>n/a</i>	<i>n/a</i>	<i>n/a</i>
Toluene	26	1 s	3.8%	17	0.02 s	42%	136	0.1 s	2.3%	<i>n/a</i>	<i>n/a</i>	<i>n/a</i>
Ethylbenzene	<i>n/a</i>	<i>n/a</i>	<i>n/a</i>	<i>n/a</i>	<i>n/a</i>	<i>n/a</i>	10	0.1 s	32%	<i>n/a</i>	<i>n/a</i>	<i>n/a</i>
<i>m/z</i> 81	<i>n/a</i>	<i>n/a</i>	<i>n/a</i>	<i>n/a</i>	<i>n/a</i>	<i>n/a</i>	<i>n/a</i>	<i>n/a</i>	<i>n/a</i>	6.4	0.2 s	37%
<i>m/z</i> 137	<i>n/a</i>	<i>n/a</i>	<i>n/a</i>	<i>n/a</i>	<i>n/a</i>	<i>n/a</i>	<i>n/a</i>	<i>n/a</i>	<i>n/a</i>	4.2	0.2 s	53%

means that the inlet to the detection chamber can be widened while still maintaining the desired pressure which in turn increases the measured count rate and instrument sensitivity. This increased sensitivity is demonstrated in Table 6.2, where isoprene counts measured in London can be seen to be double that of those recorded in Italy, despite of their higher absolute concentrations.

The error of limited counting statistics on the flux measurement is inversely proportional to $N^{0.5}$, where N is the total counts during a (30-minute) flux averaging period (Fairall, 1984). N remains similar, independent of whether a concentration is measured frequently with a short dwell time, or less often with a longer dwell time. However, reducing the error associated with individual count rates on the raw DEC data points is important as it can impact upon the cross correlation (CC) function used to calculate the lag time between PTR-MS and vertical wind speed measurements and affect the overall precision of the flux measurements. When the random error is high, the CC function becomes noisy and difficult to interpret, thus reducing the measurement precision. During the Manchester CityFlux campaign, theoretically calculated lags were used (calculated using flow rates and tube lengths) for averaging

periods where no clear peak in the CC function could be identified. This process may have introduced a systematic overestimation of the flux. Comparison of the two techniques in Chapter 3 showed there to be an offset between the two techniques for the less abundant compounds, which could not be fully resolved by the slower measurement resolution of the DEC system. It is thought that the remaining offset is likely to relate to the overestimation of the flux by the vDEC system due to the noisier CC function and incorrect identification of lag times.

Random sensor noise such as that observed in the PTR-MS measurements can strongly affect the variability of flux estimates but will not bias them systematically, provided clear peaks in the CC function can be identified (Wesley & Hart, 1985). Hollinger and Richardson (2005) suggest that when a pair of independent flux measurements, made repeatedly and under identical conditions, is available, the random error ($\sigma(\delta)$) of the flux measurement system can be determined as:

$$\sigma(\delta q) = \frac{1}{\sqrt{2}} \sigma(X_1 - X_2) \quad (6.2)$$

where σ is the standard deviation and X_1 and X_2 are the flux measurements made by the respective systems.

In order to gauge the cumulative effect of the random PTR-MS noise on the flux, this process was applied to the two vDEC flux data sets presented in Chapter 5. Strictly speaking, the two systems were not 100% independent of each other, as they shared a single sonic anemometer, sample line and zero air source. However, this calculation may still give a good indication of the random error associated with the flux measurements. The results showed isoprene and methanol fluxes to have a random uncertainty of $\pm 28\%$ and $\pm 37\%$, respectively. This suggests that despite the

best efforts to reduce the uncertainty in the individual measurements, individual 30-minute flux measurements made by the vDEC may well be accompanied by sizable error bars. However, 30-minute fluxes measured with collocated eddy-covariance setups can also show uncertainties of 20% (Wilson & Meyers., 2001), and it is likely that a fraction of this uncertainty reflects true variability in the air-masses measured by the two systems at the 30-minute time-scale which averages out over time.

6.4 Measurement precision and detection limits

The discussion above has shown that the precision of a flux measurement is largely controlled by the noise of the cross-correlation function. Consequently, in order to calculate the precision of an individual flux measurement it is necessary to characterise this noise. This can be done by calculating the standard deviation of $w' \chi'$ at a distance far away from the true lag time, typically three or four times the integral timescale and multiplying this value by three gives the precision of the measurement at the 99.7% confidence interval (Spirig *et al.*, 2005). In addition to measurement precision, this value also acts as a proxy for the detection limit (LOD) of the measurement and allows an extra quality control to be applied to measured flux data, with the rejection of data files where no clear maximum in the CC function can be identified above the LOD.

These criteria were applied to filter the data collected during the REPARTEE campaign in London presented in Chapter 4. The standard deviation of $w' \chi'$ was measured between -180 to -160 s and 160 to 180 s and three times the average value was used to define both the precision and detection limit of the flux measurements and the results of this process are shown in Fig. 6.2. The peak in the covariance function is

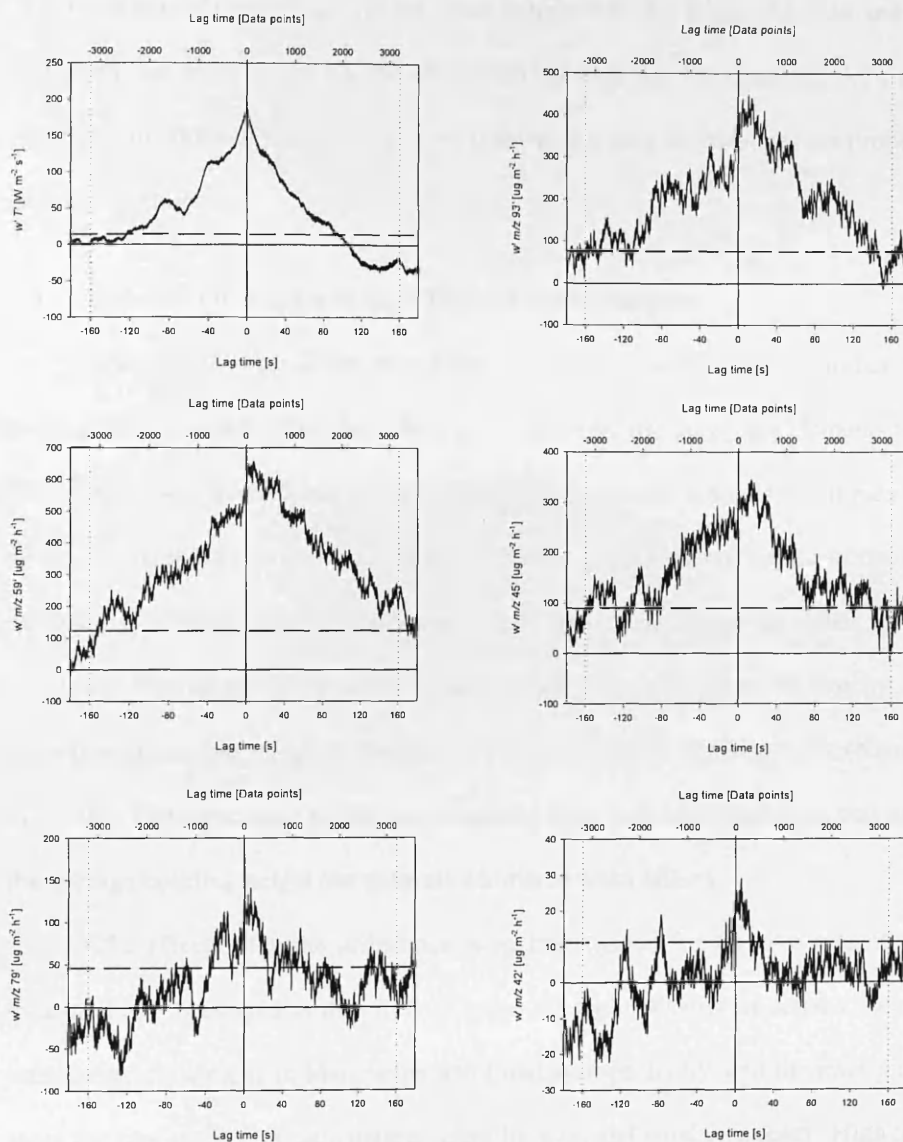


Figure 6.2 Cross-correlation functions for sensible heat and five of the compounds measured during the REPARTEE campaign in London. The limit of detection (Long Dash) of the flux measurement (solid line) is determined by the average of three times the standard deviation of the cross correlation function in the ranges of -180 s - -160 s and 180 s - 160 s (short dash).

offset by between 6 and 10 seconds which accounts for the travel time of sample air through the 40 m inlet line. The cross-correlation function should fluctuate around zero in the 160 s - 180 s zone (marked with short dashed line) where in theory there is no correlation between the two data sets. While this is perhaps true for benzene (m/z

79) and acetonitrile (m/z 42), for the other compounds this is not the case and is an indication that there is still a loose correlation between the two data sets. As a result, the approximations of the detection limit (shown as a long dashed line) are probably a slight overestimation.

6.5 Measurement site and the effect of wake turbulence

When measuring fluxes over a non-homogenous surface errors can occur due to the effects of wake turbulence which is generated by the roughness elements within the measurement fetch. Wake turbulence can be a particular problem when measuring above the urban environment due to the extremely heterogeneous nature of the urban canopy, as surfaces such as buildings, roads, trees and parks are often in close proximity. Provided the measurement location is high enough above the canopy, small scale heterogeneities merge to form one stationary net-flux above the city (Nemitz *et al.*, 2002). However wake turbulence generated from individual buildings that exceed the average building height can generate additional wake effects.

The effects of wake turbulence were investigated for the two sets of urban measurements presented in this thesis. Figures 6.3 and 6.4 show an aerial view of the measurement locations in Manchester and London respectively, and the inset pictures show the roof surface of each measurement location and wind frequency. Highlighted on each figure are the tallest buildings in the surrounding areas, which all exceeded the average building height within the fetch and may have represented a source of additional turbulent mixing. In Manchester (Fig. 6.3), at the time of measurement there were three buildings in the surrounding area which exceeded the height of the measurement location, they were the City Tower (107 m) which was 0.23 km to the North, Arndale House (90 m) located 0.7 km to the north west and Beetham Tower (169 m) which was situated 0.9 km to the south west. In addition, a fourth, shorter

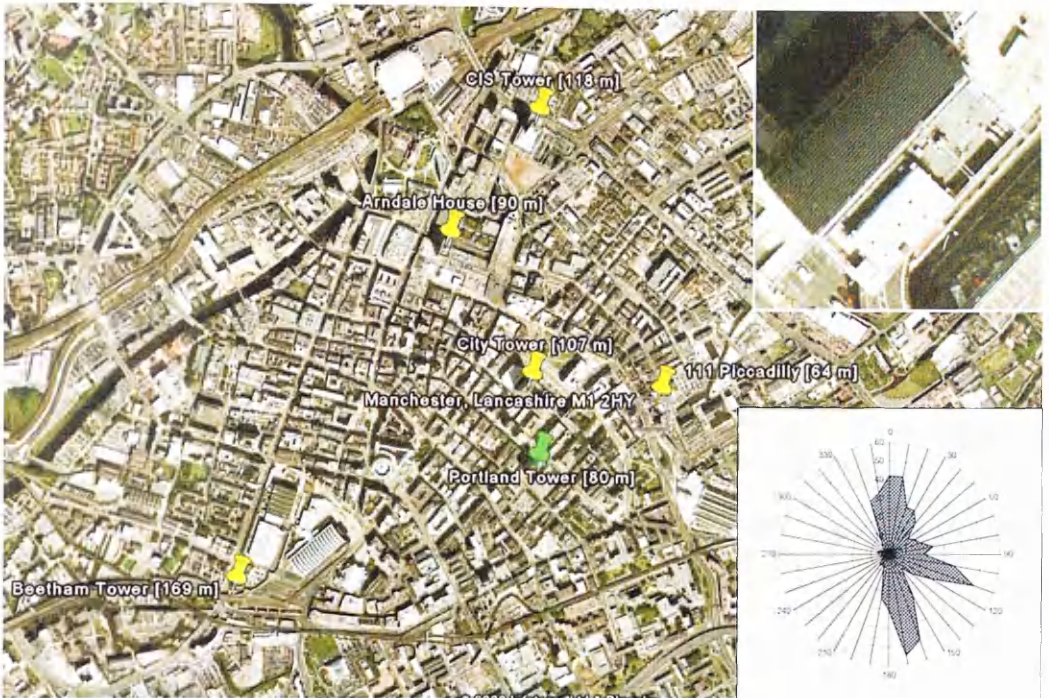


Figure 6.3 Satellite image of Manchester City centre (Google Earth, 2008), highlighting the measurement location Portland Tower (Green) and some of the taller surrounding buildings (Yellow). The inset pictures (top right) show a close up of the roof of Portland tower and a wind rose of wind frequency during the period of measurements (bottom right).

building, 111 Piccadilly (64 m) was located to the north east of Portland tower. During the period of measurements, the prominent wind directions were from the north, east and south, which meant flux measurements made at the Tower may have been influenced by wake turbulence from the City Tower, Arndale House and 111 Piccadilly, as well as from other buildings not listed here.

In London there were very few buildings that exceeded the height of the Telecom Tower and of those that did (One Canada Square (235 m), 8 Canada Square (200 m) and 25 Canada Square (200 m)) they were situated over 8.5 km away. In the immediate vicinity of the Telecom Tower was Euston Tower (124 m) 0.42 km to the north, the Centre Point building (117 m) 0.65 km to the south east and Portland House (101 m) 0.63 km to the south. During the REPARTEE campaign the predominant wind direction was from the south west, a wind sector which was unobstructed by

large buildings, consequently it may be assumed that the effect of wake turbulence generated by surrounding buildings was minimal during the period of measurements.

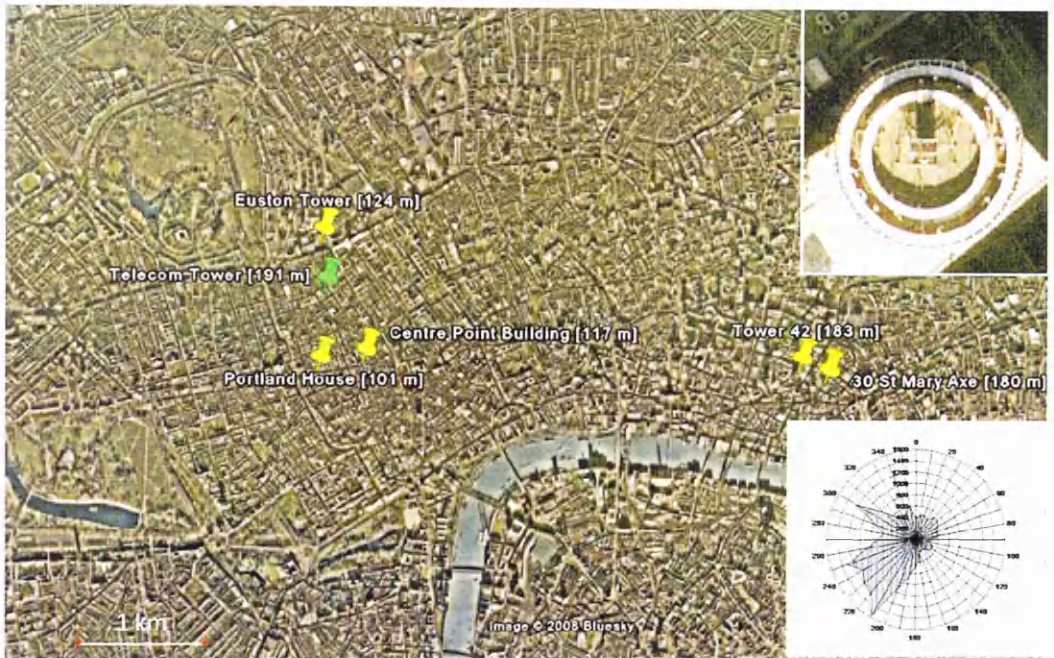


Figure 6.4 Satellite image of central London (Google Earth, 2008), highlighting the measurement location Telecom Tower (Green) and some of the taller surrounding buildings (Yellow). The inset pictures (top right) show a close up of the roof of the Telecom Tower and a wind rose of wind frequency during the period of measurements (bottom right).

Enhanced turbulent mixing can also occur due to the wake effect created by the surfaces of the building from which the measurements are being made. In order to escape the worst of these effects a general rule of thumb suggests that the vertical extension from the rooftop should be at least two times the horizontal extension of the building. At Portland Tower, the rectangular roof surface measured 50×20 m, meaning a mast of between 40 and 100 m would have been required to escape the worst of the buildings wake. At the Telecom Tower the rooftop was circular with a diameter of 16 m, this meant a vertical extension of 32 m would have been required. Unfortunately it was not possible to meet these theoretical requirements at either site

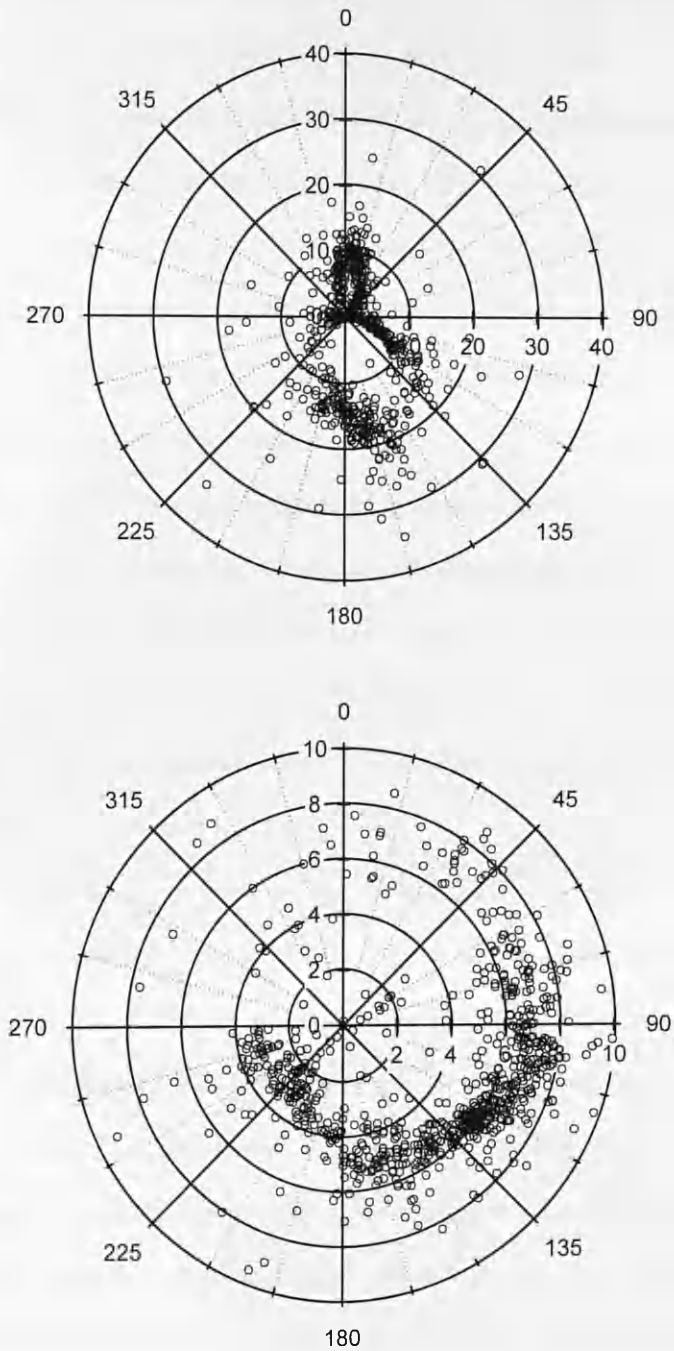


Figure 6.5 Wind rose plots showing the rotation angle θ necessary to set $w = 0$ for the Manchester CityFlux (panel a) and London REPARTEE (Panel b) campaigns.

due to both practical and safety considerations, therefore it cannot be ruled out that the flux measurements presented here were somewhat influenced by the building structure. In order to assess the building's influence on the turbulence measurements, the rotation angle used to realign measurements of u and w , θ , was plotted against wind direction, and the results for each campaign are shown in Fig. 6.5. The rectangular shape of Portland Tower combined with its non-uniform roof surface meant rotations of up to 30° were required to correct for the influence of the building, although rotation angles were mainly $<20^\circ$ for SW and $<12^\circ$ for E and N wind directions. The angular structure of the building caused the angle of rotation to differ significantly with wind direction. In contrast, the cylindrical shape of the Telecom Tower minimised the wake effect and gave relatively consistent rotation angles, consequently rotations of no more than 10° (and typically $<7^\circ$) were required during the entire period of measurements which is well within the permitted angle of attack for the ultrasonic anemometer used ($\pm 25^\circ$).

In order to assess the effect of wake turbulence on flux measurements Foken and Whichura (1996) developed a set of guidelines to classify the overall quality of measurements based on analysis of the integral turbulence statistics of the vertical wind velocity (σ_w/u^* = standard deviation of the vertical wind velocity normalised by the friction velocity) (Anderson & Farrar, 2001). They developed a model to predict σ_w/u^* for a set of ideal conditions which could be used as a standard from which real measurements could be compared. The overall data quality was then rated by the percentage difference between measured and modelled data. In addition to this model, other authors have contributed measured results obtained under ideal conditions (Panofsky & Dutton, 1984; Stull, 1988), including measurements made over urban canopies (Roth, 2000) which can also be used for comparison purposes. In order to

rate the quality of data obtained during the CityFlux and REPARTEE campaigns as well as data collected at the Castelporziano measurement site in Italy, the measurements of σ_w/u^* were compared to the following model (Foken *et al.*, 2004) where z was the measurement height, L was the Monin-Obukhov length and the values of C_1 and C_2 were given by Table 6.3.

$$\frac{\sigma_w}{u^*} = c_1 \left(\frac{z}{L} \right)^{c_2} \quad (6.3)$$

Table 6.3 Table of parameters used for Eq. (6.3) taken from Foken *et al.*, (2004).

Parameter	z/L	C_1	C_2
σ_w/u^*	$0 > z/L > -0.032$	1.3	0
	$-0.032 > z/L$	2.0	1/8

The results of the comparison are shown in Fig. 6.6 which details the 9 quality classes along the x axis and the number of data files per class on the y axis. The classification of data quality for the results was originally developed for the FLUXNET programme and are described by Foken *et al.* (2004) in the following way: classes 1 – 3 (0-50 % difference) Data is of a sufficient quality for fundamental research e.g. development of parameterisations; 4-6 (51-250%) quality sufficient for general use; 7-8 (251-1000%) data quality only sufficient for orientation; class 9 (>1000%) data quality very low and should be rejected completely. Data at class 9 and beyond are rejected as very large differences between measured σ_w/u^* and modelled σ_w/u^* indicate increased turbulent mixing which could point to a lack of similarity in the surface layer, invalidating the fundamental flux Eq. (1.4).

Measurements made at Portland Tower were found to be of the highest quality, followed by Italy and London. This was somewhat surprising given that on average a

larger rotation angle was required at Portland Tower than at the Telecom Tower. The poorer quality of the London data is thought to relate to the very high measurement

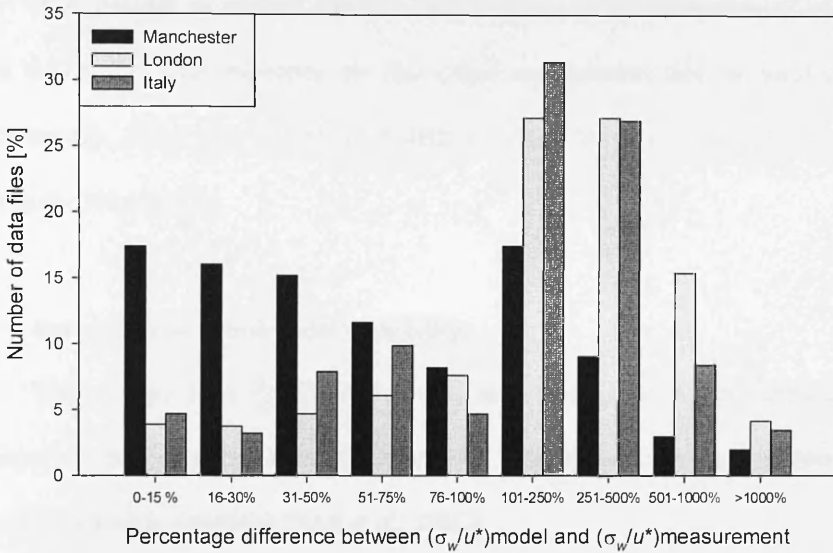


Figure 6.6 Quality assessment of data recorded during the three measurement campaigns (City Flux, REPARTEE and Castelporziano) based on the integral turbulence statistic σ_w/u^* .

location, which resulted in the sampling location moving in and out of the boundary layer. Transition in and out of the boundary layer would invalidate the model used to calculate σ_w/u^* as it designed for surface layer approximations only.

The enhanced mixing observed at the Castelporziano site was also interesting but can be explained by an insufficient fetch in the two major wind directions (NE and SW). To the south west of the site was a sloping sand dune which obstructed air flow from this wind sector and most likely generated a wake effect. When the air flow reversed at night time and returned to the site from the north east, flow was obstructed by the Home Oak forest which probably caused some enhanced turbulence mixing.

Despite the increased turbulent fluctuations caused by individual roughness elements as well as wake effects from the measurement locations themselves, less

than 5% of all the data collected from each of the campaigns failed at level 9 of the quality check.

It is unclear at present whether the reference parameterisation of σ_w/u^* of Table 6.4 is the ideal reference for the urban environment and in particular for measurements above the nocturnal boundary layer. More research is needed to investigate this question.

6.6 Errors due to geophysical variability

Wesley and Hart (1985) have suggested that errors encountered due to geophysical variability may be approximated for both unstable and neutral conditions using the following equations (Karl *et al.*, 2002).

$$\frac{\partial F_x}{F_x} = \sqrt{\frac{12 \times z}{T_{av} \times U}} \quad \text{unstable conditions} \quad (6.4)$$

$$\frac{\partial F_x}{F_x} = \sqrt{\frac{20 \times z}{T_{av} \times U}} \quad \text{neutral conditions} \quad (6.5)$$

where z is the height of the measurement above the surface (m), U is the average wind speed (m s^{-1}) and T_{av} is the averaging period (s).

Using these equations, uncertainties were calculated for each of the four campaigns presented in this thesis and the results are presented in Table 6.4 along with the variables for each campaign. The uncertainty was lower for the Edinburgh and Italy campaigns where measurement heights were close to the terrain surface. In Manchester and London where measurement heights were between 100 and 200 m, the uncertainty was much greater. In order to reduce the variability of flux estimates at these locations, a significant increase in the averaging period would have been required. The averaging length required to give a specific level of accuracy (a) can be estimated by re-arranging Eqs. (6.6) and (6.7) to give:

$$T = 12z(a^2U)^{-1} \text{ unstable conditions} \quad (6.6)$$

and

$$T = 20z(a^2U)^{-1} \text{ neutral conditions} \quad (6.7)$$

Setting a to 20% and using unstable conditions, averaging periods of 3.3 and 2.4 hours respectively would have been required for each campaign. Although the decrease in measurement uncertainty is desirable, using averaging periods of this length may have resulted in further errors associated with non-stationarities as discussed above.

Table 6.4 Uncertainty in flux measurements due to geophysical variability during neutral and unstable atmospheric conditions. Measurement heights (z) show the mast height relative to the ground and the mast height relative to the average canopy height.

	<i>Edinburgh</i>	<i>Manchester</i>	<i>London</i>	<i>Italy</i>
z [m]	2	95, 80	200, 185	5, 4
U [m s^{-1}]	3	3.3	5	1.8
T [s]	1800	1500	1500	1500
Uncertainty [%] [unstable]	7%	47%, 44%	56%, 54%	14%, 13%
Uncertainty [%] [stable]	9%	61%, 56%	73%, 70%	19%, 17%

6.7 The representativeness of flux measurements made over urban canopies

In micrometeorology, when measuring over homogenous canopies, it is generally assumed that an equilibrium boundary layer will form, in which measured fluxes will be representative of the exchange processes occurring at the surface (Fowler *et al.*, 2001). In the urban environment the situation is more complicated due to the very heterogeneous nature of the canopy. Sufficient elevation of measurement sensors is required to ensure the small scale processes occurring at the surface blend into one homogenous net flux above the city. However, operating at the required heights can result in the de-coupling of the measurement location from the ground, especially at night time and during the early hours of the morning as was shown in

Chapter 4 by the lag time between the morning increase in traffic counts and the measured fluxes. In this case the measurement location was thought to be above the top of the nocturnal boundary layer and clearly was not representative of the true exchange occurring at the surface. In situations such as this applying the conservation equation in it's simplest form may not be justified as errors from storage and advection may occur. Investigating this effect goes beyond the scope of the current study. Nonetheless, it is felt that the use of daily averaged flux profiles should give a robust estimate of the surface exchange, as de-coupling was not observed on a daily basis.

6.8 Conclusions

Calculating the errors associated with VOC flux measurements is not trivial and requires careful consideration. The brief analysis of errors and uncertainty given in this chapter has highlighted some of the major sources of uncertainty surrounding measurements made by the DEC and vDEC systems and where possible an attempt was made to quantify these errors. Errors incurred due to flux attenuation of both low and high frequency eddies were highly site specific, but generally were not more than a few percent. In contrast, random errors associated with the PTR-MS count rates were found to be significant. It was shown that the precision of flux measurements made using both the DEC and vDEC techniques appear to depend upon two key factors, the length of disjunct sampling interval and the dwell time used for PTR-MS measurements, which in turn determine the level of noise in the cross correlation function. The former controls the number of data points used in the CC function, while the latter controls the random error of the individual measurements.

During the first application of the techniques in Manchester, the use of short dwell times for the vDEC of 20 ms resulted in the systematic over estimation of fluxes due to the high level of noise in the CC function if this technique was used to determine the time-lag. In London, as the technique was developed further, efforts were made to increase the precision of measurements by reducing the random count rate error through the increase of dwell times to 0.1 s. This step greatly reduced the noise of the CC function and allowed for the clear identification of lag times, calculation of individual measurement precision and the estimation of flux detection limits. During the Castelporziano measurements the dwell times were increased further to 0.2 s in an effort to further increase measurement precision, however the CC function remained very noisy which confounded the identification of lag times. The reason for the noise is unclear but it is thought to relate to the very low turbulence ($u^* < 0.25 \text{ m s}^{-1} \gg 80\%$) and poorly defined turbulence statistics that were observed throughout the study. In addition, the PTRMS used at Castelporziano had a significantly lower sensitivity than that used in London.

The analysis of the integral turbulent statistics and rotation angles suggests none of the three measurement sites chosen during this work to be ideal and all were very likely subject to some errors due to the effects of wake turbulence. However, turbulence characteristics proved to be satisfactory. Measuring over non-homogenous canopies requires sufficient elevation above the canopy to ensure the small scale fluxes blend into one homogenous net flux. Finding locations to meet this requirement is challenging, especially in the urban environment, where there are additional considerations such as building access and safety. For all measurement campaign, sampling sites were chosen very carefully and reflect the best possible balance between quality and practicality.

Chapter VII

7. Discussion and conclusions

The original aims of this thesis were threefold. First, a system capable of measuring surface layer fluxes of volatile organic compounds between the biosphere and atmosphere was to be designed, tested and validated. Secondly, the system was to be deployed over a range of terrain types, including both rural and urban locations. Finally, wherever possible, measured fluxes were to be compared to current bottom-up modelling techniques and evaluated. In the following sections the two flux measurement techniques developed will be discussed and the relative merits and limitations of each approach will be considered. Areas for improvement will be highlighted and possible future work and long term goals will be reviewed.

7.1 Disjunct eddy covariance

The disjunct eddy covariance technique has been explored both theoretically and experimentally and results have demonstrated the potential for this approach to give very detailed information on surface layer fluxes of volatile organic compounds. Theoretical appraisal of the disjunct eddy covariance (DEC) concept has highlighted the importance of selecting sample / analysis times which relate to the measurement height, with a clear need for faster measurement frequencies when operating close to the terrain surface. The field evaluation of the technique, where the disjunct flux sampler (DFS) was compared with the established eddy covariance technique, has validated the method, and importantly, highlighted the system limitations, which should be addressed before future work is carried out.

Many of these issues relate to the grab sampling system, which in its current configuration is bulky, heavy and difficult to mount. Although these problems could be addressed by replacing the stainless steel ISRs and pipe work with lightweight PTFE alternatives and the addition of mounting brackets, other problems persist. The most serious of these relates to the backpressure that is generated when drawing air from the ISR for analysis, which has been shown to alter the E/N ratio in the PTR-MS by up to 5 Td and could introduce a large systematic error to VOC mixing ratios. As explained in chapters 2 and 3, the backpressure occurs because of the separation distance between the DFS and PTR-MS, and is exacerbated when the distance is increased. In some situations, where the sonic anemometer and gas analyser are separated by tens of metres, as was the case at the Telecom Tower, the volume of air in the sample tube may exceed the total volume of the ISR, thus rendering the technique unusable. Furthermore, the mounting of the DFS to tall masts is difficult because of the weight of both the sampler and the lengths of heavy armoured cable which are needed to activate the mains operated solenoid valves. Although a solution for this problem is demonstrated in chapter 3, where the DFS was teed directly into the sampling line at the base of the mast, corrections are needed for the ISR concentrations, as an increase in ISR carry-over between samples is observed, and the technique loses its directness. As a consequence, one of the major advantages of the DFS system, which is the flagging of grab samples to allow for the pairing of corresponding PTR-MS and wind data, as demonstrated in chapter 2, is lost, resulting in the use of a cross-correlation function to identify lag times, which, when limited data are available, can become noisy and difficult to interpret.

Despite these drawbacks, the DEC technique should not be discarded. The increased analysis times afforded by the ISR chambers allow for much longer PTR-

MS dwell times, which can substantially increase the signal to noise ratio of the individual measurements and ultimately reduce the associated random error. A higher level of precision in flux measurements is very desirable as uncertainties surrounding them are often very large, as was demonstrated in chapter 6. Simple revisions to the current sampler configuration could greatly improve the system, such as reducing the length of tubing between ISR and the evacuation pump to curtail flow resistance and aid in the evacuation of sample canisters, or the widening of sample valve orifices to decrease the response time of the instrument. Ultimately, however, this technique is best suited to locations where separation between the DFS and PTR-MS can be kept to a minimum.

7.2 Virtual disjunct eddy covariance

In contrast to the DEC system, the vDEC technique is much simpler to install and operate, which is a major advantage, especially for deployment in locations such as Portland Tower (Manchester) or the Telecom Tower (London), where the mounting of equipment to the instrument mast is logistically difficult. The only technical difficulties are associated with the development of software capable of recording data from the PTR-MS and sonic anemometer simultaneously. Previously, some researchers have chosen to wire the output of the PTR-MS into the analogue channels of the sonic anemometer. However, it has been demonstrated here that this is unnecessary as the “DDE” protocol can be used to pass data between the Quadstar and LabVIEW software, thus allowing the concurrent storage of both 3D wind velocities and PTR-MS data to a single file.

The absence of a physical sampling system means the vDEC technique is not logistically limited in the same way as the DEC system. Firstly, sample lines can be

mounted very close to the sonic anemometer, causing only a minimal disruption to the wind flow. Secondly, no significant pressure drop is created as air is sub-sampled from the inlet line, allowing measurements to be made at a constant E/N ratio. Finally, sampling intervals are not limited by the time taken to evacuate the ISR, as in DEC, therefore many compounds can be measured during each duty cycle, using relatively short dwell times and thus minimising disjunct sample intervals, which consequently reduces the uncertainty associated with the use of a discontinuous data set. However, it is important to note that any increase in precision gained from the use of shorter sampling intervals may well be nullified by the increased random error which is associated with the use of shorter dwell times. Furthermore, the increased noise associated with short dwell times can hinder the determination of lag times when using cross-correlation functions to align the vertical wind velocity with PTR-MS count rates. The use of experimentally calculated lag times for files where no clear maximum in the CC function can be identified, as in Chapter 3, can introduce a systematic overestimation of the flux. Instead, it is recommended that data are rejected, resulting in a smaller but ultimately more precise data set, as shown in chapters 4 and 5.

7.3 System improvements

7.3.1 Compound identification

Compound identification is an issue whenever using the PTR-MS, consequently, both the vDEC and DEC techniques would benefit with improvements in this area. In the short term, improvements could be made by using a GC-MS system in conjunction with the PTR-MS, splitting the sampled air flow between the two instruments. Although the GC-MS has a much lower sampling resolution compared to

that of the PTR-MS, it would allow compound identification on a time scale of < 2 hrs, which would complement the PTR-MS measurements, particularly for VOCs such as acetone and isoprene which can suffer interference from other ion fragments.

In the medium-to-long term, time of flight-proton transfer reaction-mass spectrometry (TOF-PTR-MS) will allow for both the speciation and simultaneous measurement of the entire mass spectrum and thus allow the standard eddy covariance technique to be applied to VOC flux measurements. However, this kind of analytical system, which is already in place in some instruments, such as the aerosol mass spectrometer, brings with it the problem of data storage, as half hour, 10 Hz flux measurements can be as large as two gigabytes per file.

7.3.2 *Online calibration*

In chapter 5, the vDEC setup was altered, with the introduction of a 3-way Teflon switching valve to allow for the periodical measurement of the SEM voltage and calibration standards. This valve could be utilised further to make the calibration of the PTR-MS either fully automated or user controlled. This could be implemented using a series of mass flow controllers, each powered by the A/O of the PTR-MS and controlled by the Quadstar sequence file. Continued venting of the calibration gas would provide stable VOC concentrations (a particular problem for methanol), and the introduction of zero air through the mass flow controllers could dilute the standards to the desired concentrations. This system could then be made fully automated and configured to calibrate the PTR-MS once a week. Alternatively, calibrations could be performed at a touch of a button, using controls in the LabVIEW logging programme (such as a Boolean switch) to trigger events in the Quadstar sequence file (such as the calibration sequence). This latter procedure would require the bidirectional “poking”

of data between the PTR-MS and LabVIEW programme with each switching between client and server, in a process which currently has only had limited success.

7.3.3 *Padding of data for spectral analysis*

During this work, measured VOC fluxes were subjected to a stationarity test, as first proposed by Foken *et al* (1996). The test is particularly useful for disjunct data sets as it does not require vertical wind velocities and mixing ratios to be of the same temporal resolution. However, more sophisticated tests, such as ogives, can be performed using spectral analysis in the frequency domain. In order to transform the data from the time domain into the frequency domain a mathematical tool known as the Fast Fourier Transform (FFT) is used. Much as a prism allows us to deconstruct a beam of white light to see its component parts, the FFT allows us to do the same with turbulence data and ultimately calculate what portion of the flux is carried by a particular frequency (Stull, 1988). In order to apply the FFT to a data set, both the vertical wind velocity and scalar concentration must be of the same time resolution. While this is the case for EC data sets, for both DEC and vDEC this causes a problem as the resolution of the PTR-MS data is much less than that of the measurements of the vertical wind velocity. Previous groups have employed gap filling as a means of padding the PTR-MS data to allow for spectral analysis. In practice this is achieved by simply repeating the PTR-MS measurement until the next data point becomes available and therefore a single data point is considered to be representative of the total measurement cycle. While this may be true for data sets collected at high measurement heights, where low frequencies dominate the flux, at lower elevations a larger portion of the flux may be carried by the higher frequency eddies and these

contributions may become attenuated and lost. Consequently the benefits of spectral analysis of the data may not outweigh the cost of flux loss. In such cases there

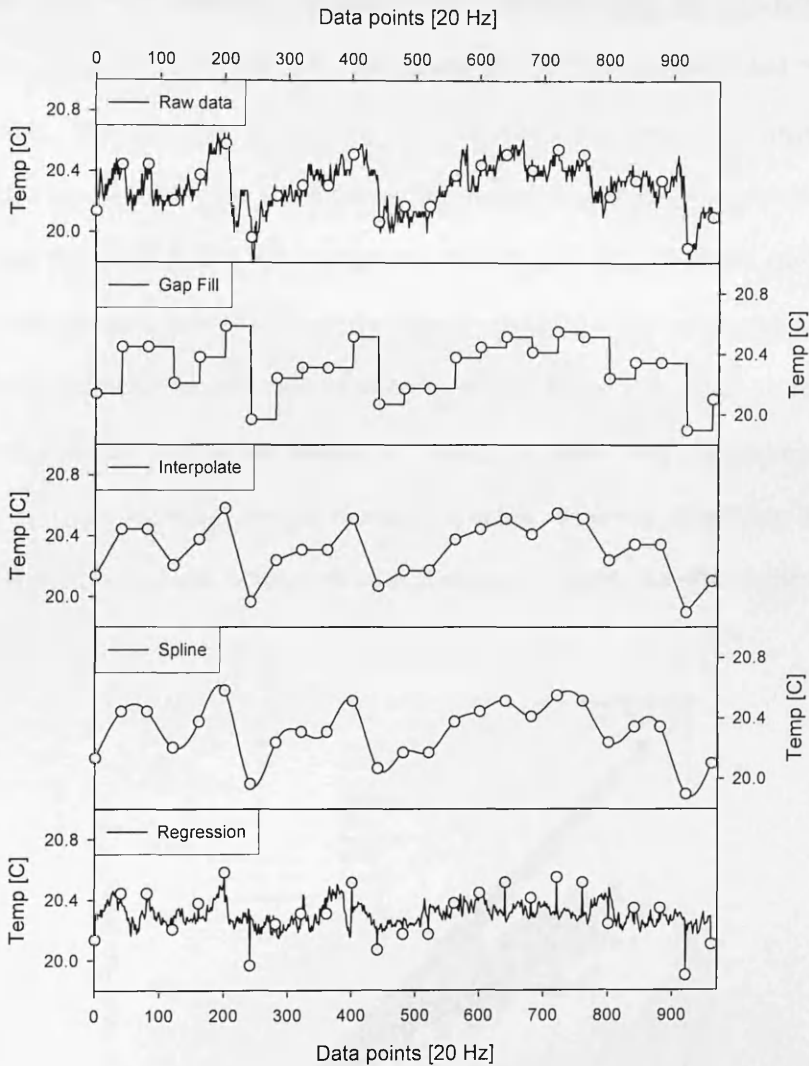


Figure 7.1 Graph showing alternative padding methodologies to the standard “Gap fill” approach for disjunct data sets. Increasing the resolution of the data in this way allows more robust quality checks to be imposed upon the data in the frequency domain.

is a need for alternative means of padding the data which reduce the attenuation of higher frequencies. Figure 7.1 shows the concept of data padding and demonstrates some simple alternatives which may help to reduce the flux loss. Each of these methods was tested using a week long set of sensible heat data collected at a height of

5 m to simulate a disjunct flux (2 s interval), which could then be compared back to the original EC data set. The results of the experiment (shown in Fig 7.2) showed the standard “Gap Fill” technique to perform worst, underestimating the cumulative flux by 36%, compared to 29 and 25% respectively for the “interpolation” and “spline” techniques. The least attenuation, 2%, was observed when using the “regression” method, a process where the w and χ data sets are first aligned to correct for temporal shifts and then correlated to give a regression line which is used to fill the gaps in the data. This approach means higher frequencies are retained in the covariance function and therefore much of the flux carried by higher frequency eddies is retained; however, it is not without its limitations. Firstly, lag times must be accounted for before using the technique, which eliminates a major advantage of padding disjunct data, which is a clearer cross-correlation function. Secondly, the effectiveness of

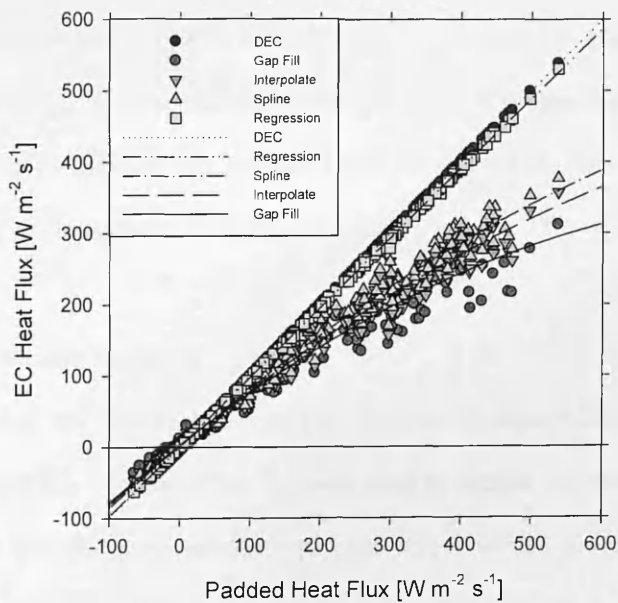


Figure 7.2 Regression plot of disjunct eddy covariance (DEC) heat fluxes (2 s disjunct sampling interval) against standard eddy covariance (EC) heat fluxes. Each DEC data set was padded using various gap filling methodologies to match the time resolution of the EC data. The data set labelled DEC was not gap filled in any way.

the padding depends on (i) how well the relationship between w and χ can be characterised and (ii) the relationship remaining stationary throughout the averaging period. Despite these drawbacks, the “regression” method illustrates how relatively simple steps can be taken to avoid attenuating the flux when padding disjunct data. There is obviously a large scope for further improvement in this area. Many of the techniques currently being used to gap fill missing data in long-term eddy covariance measurements of CO₂ could be applied to this problem and allow for a more comprehensive assessment of disjunct data sets in the frequency domain. For example, Stauch and Jarvis (2006) showed that by combining a multidimensional semi-parametric spline interpolation with independent variables such as light, temperature and time, gaps in CO₂ data could be filled. In chapter 5 it was shown that the biogenic VOCs measured were all strongly controlled by changes in either light, temperature or both. Similarly, when measuring over urban canopies as in chapters 3 and 4, it was clear that anthropogenic VOCs were strongly controlled by traffic density and temperature. Therefore, these variables could be used in a similar way to help pad the missing sections in disjunct data sets and allow for much more detailed analysis and quality testing of disjunct data in future campaigns.

7.3.4 *Improvements to logging software*

Recently, the manufacture's of the PTR-MS, Ionicon (GmbH, Innsbruck), have released a new version of the software used to operate the instrument. Rather than using the Quadstar programme, the new software is written entirely in LabVIEW. The major advantage of this, is that data from the PTR-MS are channelled directly into the LabVIEW programme via the serial interface, negating the need for the dynamic data exchange protocol, which is a less efficient means of data transfer.

Simple amendments to the software developed in this thesis could be made to include this new data transfer mechanism, or perhaps, more simply, global variables could be used to share data between the PTR-MS software and the vDEC logging software which could be run simultaneously. Upgrading the software in this way would mean only the LabVIEW software would be needed to run the system, which would free up system resources and potentially reduces random spikes in the data which are caused when the serial buffer becomes full.

7.4 “Top down” versus “Bottom up” emission inventory approach

During the course of this thesis, two “top-down” style approaches, DEC and vDEC, have been developed and applied for the measurement of VOC surface layer fluxes. In Manchester, measured fluxes of benzene were up-scaled to give an annual emission estimate for the city centre, which was subsequently compared to emission estimates from the NAEI. Despite the large degree of uncertainty surrounding the flux measurements, the “top-down” approach gave a figure that was in the same ballpark as estimates made using the “bottom-up” approach of the NAEI. In London, efforts were made to reduce the uncertainty of the flux measurements by increasing dwell times to enhance the precision of the VOC measurements. Again, fluxes of benzene were compared to emission estimates from the NAEI, but rather than simply extrapolating the 4 weeks of data as before, a parameterisation between VOC fluxes and traffic density was used. For a second time, estimates from the “top-down” measurement approach compared well with the “bottom-up” style of the NAEI and in addition, similar comparisons with CO flux data, showed even closer agreement with less than 35% difference between the two approaches. This demonstrates that, on an annual basis, the bottom-up approach adopted by the NAEI can provide emission

estimates of benzene and CO that are in the right ball park. The performance of the inventory with regards to other important VOCs is still unknown; nevertheless, as the majority of VOC within the city are emitted from vehicles, their emission from within the urban environment should be well characterised by the NAEI. However, in rural areas, the NAEI is not a suitable means for deriving VOC emission estimates as its primary focus is anthropogenic emissions. In these more remote locations where biogenic emissions dominate the total flux, models such as MEGAN (Guenther *et al.*, 2006) and the G95 algorithm (Guenther *et al.*, 1995) are better suited.

In chapter 5, fluxes of five biogenic volatile organic compounds were measured above a typical Mediterranean ecosystem type. Comparisons of monoterpenes and isoprene fluxes with those measured by the G95 algorithm showed the “bottom-up” modelling approach to give a very good approximation of the measured flux. Once more this suggests that bottom-up style techniques are very capable of providing emissions estimates from both urban and in this case rural locations.

Both “bottom-up” and “top-down” approaches have been shown to be effective, but in reality the “bottom-up” style emission inventory approach will always be favourable. They can be applied on much larger spatial scales, are cost effective and, depending on the variables supplied, can give information on both current and future emissions. Nonetheless, top-down measurement techniques such as those presented in this thesis will always be relevant as they provide a means with which to validate and constrain emission estimates made by bottom-up modelling approaches.

7.5 Future work

In the short term, there are plans to deploy the vDEC system as part of the NERC funded consortium project “Oxidant and particle photochemical processes (OP3) above a South-East Asian tropical rain forest”. The overall goal of this project is to increase our understanding of the interactions that exist between natural forests and the Earth’s climate system in the tropical regions. The vDEC system will be deployed on a 100 m tower to measure fluxes of a wide range of BVOCs from the forest canopy below. This activity will be complemented and verified by a series of finger print measurements of VOC mixing ratios made by GC-MS both above and below canopy. The work will be staged over two separate campaigns which will each last approximately 4 weeks during 2008.

In the longer term, research using these techniques should be focused on generating flux measurements over longer time periods, as a criticism often levelled at VOC flux measurements is their short duration. Typically, measurement campaigns last between two and four weeks, which only provides a snap-shot of the surface exchange occurring throughout the year. Although this may be enough to generate an appreciation of emission rates occurring at that given time, it does not consider how seasonality may impact upon emission rates. For example, in chapter 4, analysis of data from a long-term monitoring station showed strong seasonal trends in isoprene and toluene concentrations which could not have been resolved during a typical campaign of 4 weeks.

Since there is now an infrastructure at the Telecom Tower to support micrometeorological measurements, the site presents an excellent platform from which to make longer-term measurements of VOC fluxes from the city. In addition to resolving important temporal trends in emission rates, an extended campaign may well help to establish if the biogenic isoprene observed in chapter 4 originated from

locations within the flux footprint such as Regent's Park or Hyde Park, or was simply advected from sources situated further outside of central London. Quantifying the biogenic fraction of isoprene in London is important for two reasons. Firstly, as was demonstrated in chapter 4, the biogenic component can make up a significant fraction of the total observed isoprene during periods of elevated temperatures and secondly, due to its highly reactive nature, isoprene is an important precursor for photochemical pollution episodes. Given that the NAEI currently do not consider motor vehicle exhaust or evaporative sources of isoprene in their inventory (R.G. Derwent, personal comm) there is a real need to quantify and separate the three major sources (direct emissions from cars, evaporative emissions and biogenic emissions) of isoprene in the city.

In order to set about this task, a two-fold approach would be required. Firstly, deployment of the vDEC system at the Telecom Tower would be needed to provide direct flux measurements of isoprene emissions from the city centre. In addition, measurements of aromatic compounds such as benzene and ethylbenzene could be used as a marker for vehicle related emissions, which in turn could help to separate the biogenic isoprene fraction. Secondly, as was stated in chapter 4, the most likely source of the biogenic isoprene was thought to be the parkland situated to the south west of the Tower. Although Hyde Park may fall within the flux footprint (wind direction allowing), Richmond Park, which was thought to be the most likely source due to its extensive covering of oak trees, which are strong emitters of isoprene, would not. Therefore, any attempt to quantify the source of biogenic isoprene using flux measurements based at the Telecom Tower, should be supported by ancillary flux measurements made above canopy at Richmond Park.

7.6 Final remarks

The theoretical appraisal and field deployment of the DEC and vDEC systems have convincingly demonstrated their capacity to give very detailed information on VOC fluxes from both urban and rural canopies. This information has compared well with bottom-up style inventory approaches and may be further improved with longer term measurements and more detailed analysis of the flux footprint.

Evaluation of the DEC approach in the field, although convincing, has shown the technique to be logistically limited. Future applications should be restricted to measurement locations where the separation distance between the PTR-MS and sampling system can be kept short and pressure drops along sampling lines minimised. In contrast, the vDEC technique is practical and simple in its operation, but may suffer from decreased measurement precision when PTR-MS dwell times are very short. On this basis, it is recommended that dwell times are set to at least 0.2 s, with 0.5 s thought to be an optimum value.

In conclusion, the DEC and vDEC flux measurement techniques can be used to provide robust estimates for the surface exchange of a large number of VOCs from both urban and rural canopies and at length scales of 100 m^2 to 10^6 m^2 . The results generated can subsequently be used to feed into regional and global scale models such as MEGAN (Guenther *et al.*, 2006) or to validate and constrain emission inventories such as the NAEI.

References

- Ammann, C., Spirig, C., Neftel, A., Steinbacher, M., Komenda, M., and Schaub, A.: Application of PTR-MS for measurements of biogenic VOC in a deciduous forest, *International Journal of Mass Spectrometry*, 239, 87-101, 2004.
- Ammann, C., Brunner, A., Spirig, C., and Neftel, A.: Technical note: Water vapour concentration and flux measurements with PTR-MS, *Atmospheric Chemistry and Physics*, 6, 4643-4651, 2006.
- Anderson, L. G., Lanning, J. A., Barrell, R., Miyagishima, J., Jones, R. H., and Wolfe, P.: Sources and sinks of formaldehyde and acetaldehyde: An analysis of Denver's ambient concentration data, *Atmospheric Environment*, 30, 2113-2123, 1996.
- Anderson, D. E., and Farrar, C. D.: Eddy covariance measurement of CO₂ flux to the atmosphere from an area of high volcanogenic emissions, Mammoth Mountain, California, *Chemical Geology*, 177, 31-42, 2001.
- Atkinson, R.: Atmospheric chemistry of VOCs and NO_x, *Atmospheric Environment*, 34, 2063-2101, 2000.
- Aubinet, M., Chermanne, B., Vandenhaute, M., Longdoz, B., Yernaux, M., and Laitat, E.: Long term carbon dioxide exchange above a mixed forest in the Belgian Ardennes, *Agricultural and Forest Meteorology*, 108, 293-315, 2001.
- Aubinet, M., Grelle, A., Ibrom, A., Rannik, U., Moncrieff, J., Foken, T., Kowalski, A. S., Martin, P. H., Berbigier, P., Bernhofer, C., Clement, R., Elbers, J., Granier, A., Grunwald, T., Morgenstern, K., Pilegaard, K., Rebmann, C., Snijders, W., Valentini, R., and Vesala, T.: Estimates of the annual net carbon and water exchange of forests: The EUROFLUX methodology, in: *Advances in ecological research*, vol 30, *Advances in ecological research*, 113-175, 2000.
- Ayra, S. P.: *Unstable and convective boundary layers. Dynamics of Atmospheric Flows: Atmospheric Transport and Diffusion Processes*. M. P. Singh. Southampton, Computational Mechanics Publications. 18: 246, 1998.
- Baldocchi, D. D.: Assessing the eddy covariance technique for evaluating carbon dioxide exchange rates of ecosystems: Past, present and future, *Global Change Biology*, 9, 479-492, 2003.
- Baldocchi, D. D., Hicks, B. B., and Meyers, T. P.: Measuring biosphere-atmosphere exchanges of biologically related gases with micrometeorological methods, *Ecology*, 69, 1331-1340, 1988.
- Beauchamp, J., Wisthaler, A., Hansel, A., Kleist, E., Miebach, M., Niinemets, U., Schurr, U., and Wildt, J.: Ozone induced emissions of biogenic VOC from tobacco: Relationships between ozone uptake and emission of LOX products, *Plant Cell and Environment*, 28, 1334-1343, 2005.

- Berbigier, P., Bonnefond, J. M., and Mellmann, P.: CO₂ and water vapour fluxes for 2 years above EUROFLUX forest site, *Agricultural and Forest Meteorology*, 108, 183-197, 2001.
- Bertin, N., Staudt, M., Hansen, U., Seufert, G., Ciccioli, P., Foster, P., Fugit, J. L., and Torres, L.: Diurnal and seasonal course of monoterpene emissions from *Quercus ilex* (l.) under natural conditions - applications of light and temperature algorithms, *Atmospheric Environment*, 31, 135-144, 1997.
- Borbon, A., Fontaine, H., Veillerot, M., Locoge, N., Galloo, J. C., and Guillermo, R.: An investigation into the traffic-related fraction of isoprene at an urban location, *Atmospheric Environment*, 35, 3749-3760, 2001.
- Bowling, D. R., Turnipseed, A. A., Delany, A. C., Baldocchi, D. D., Greenberg, J. P., and Monson, R. K.: The use of relaxed eddy accumulation to measure biosphere-atmosphere exchange of isoprene and of her biological trace gases, *Oecologia*, 116, 306-315, 1998.
- Brunner, C. A., A. Neftel, C. Spirig.: Methanol exchange between grassland and the atmosphere. *Biogeosciences* 4: 395-410, 2007.
- Burnett, R. T., Brook, J. R., Yung, W. T., Dales, R. E., and Krewski, D.: Association between ozone and hospitalization for respiratory diseases in 16 Canadian cities, *Environmental Research*, 72, 24-31, 1997.
- Businger, J. A.: Evaluation of the accuracy with which dry deposition can be measured with current micrometeorological techniques, *Journal of Climate and Applied Meteorology*, 25, 1100-1124, 1986.
- Businger, J. A., and Oncley, S. P.: Flux measurement with conditional sampling, *Journal of Atmospheric and Oceanic Technology*, 7, 349-352, 1990.
- Cao, X., Hewitt, C. N.: The sampling and analysis of volatile organic compounds in the atmosphere. *Reactive hydrocarbons in the atmosphere*. C. N. Hewitt. London, Academic Press: 120-153, 1999.
- Caplain, I., Cazier, F., Nouali, H., Mercier, A., Dechaux, J. C., Nollet, V., Journard, R., Andre, J. M., and Vidon, R.: Emissions of unregulated pollutants from European gasoline and diesel passenger cars, *Atmospheric Environment*, 40, 5954-5966, 2006.
- Caruso, M. L., and Valentini, A. M.: Localization of p53 protein and human papillomavirus in laryngeal squamous lesions, *Anticancer Research*, 17, 4671-4675, 1997.
- Chiang, H. L., Hwu, C. S., Chen, S. Y., Wu, M. C., Ma, S. Y., and Huang, Y. S.: Emission factors and characteristics of criteria pollutants and volatile organic compounds (VOCs) in a freeway tunnel study, *Science of the Total Environment*, 381, 200-211, 2007.
- Christian, T. J., Kleiss, B., Yokelson, R. J., Holzinger, R., Crutzen, P. J., Hao, W. M., Shirai, T., and Blake, D. R.: Comprehensive laboratory measurements of

- biomass-burning emissions: 2. First intercomparison of open-path FTIR, PTR-MS, and GC-MS/FID/ECD, *Journal of Geophysical Research-Atmospheres*, 109, 2004.
- Ciccioli, P., Brancaleoni, E., Frattoni, M., Marta, S., Brachetti, A., Vitullo, M., Tirone, G., and Valentini, R.: Relaxed eddy accumulation, a new technique for measuring emission and deposition fluxes of volatile organic compounds by capillary gas chromatography and mass spectrometry, *Journal of Chromatography A*, 985, 283-296, 2003.
- Ciccioli, P., Fabozzi, C., Brancaleoni, E., Cecinato, A., Frattoni, M., Cieslik, S., Kotzias, D., Seufert, G., Foster, P., and Steinbrecher, R.: Biogenic emission from the Mediterranean pseudosteppe ecosystem present in Castelporziano, *Atmospheric Environment*, 31, 167-175, 1997.
- Cojocariu, C., Kreuzwieser, J., and Rennenberg, H.: Correlation of short-chained carbonyls emitted from *Picea Abies* with physiological and environmental parameters, *New Phytologist*, 162, 717-727, 2004.
- Cox, R. A., Eggleton, A. E. J., Derwent, R. G., Lovelock, J. E., and Pack, D. H.: Long-range transport of photochemical ozone in north-western Europe, *Nature*, 255, 118-121, 1975.
- Crawford, T. L., Dobosy, R. J., McMillen, R. T., Vogel, C. A., and Hicks, B. B.: Air-surface exchange measurement in heterogeneous regions: Extending tower observations with spatial structure observed from small aircraft, *Global Change Biology*, 2, 275-285, 1996.
- Dabberdt, W. F., Lenschow, D. H., Horst, T. W., Zimmerman, P. R., Oncley, S. P., and Delany, A. C.: Atmosphere-surface exchange measurements, *Science*, 260, 1472-1481, 1993.
- de Gouw, J., and Warneke, C.: Measurements of volatile organic compounds in the Earth's atmosphere using proton-transfer-reaction mass spectrometry, *Mass Spectrometry Reviews*, 26, 223-257, 2007.
- de Gouw, J., Warneke, C., Karl, T., Eerdeken, G., van der Veen, C., and Fall, R.: Sensitivity and specificity of atmospheric trace gas detection by proton-transfer-reaction mass spectrometry, *International Journal of Mass Spectrometry*, 223, 365-382, 2003.
- de Gouw, J. A., Howard, C. J., Custer, T. G., Baker, B. M., and Fall, R.: Proton-transfer chemical-ionization mass spectrometry allows real-time analysis of volatile organic compounds released from cutting and drying of crops, *Environmental Science & Technology*, 34, 2640-2648, 2000.
- Denmead, O. T., Dunin, F. X., Wong, S. C., and Greenwood, E. A. N.: Measuring water-use efficiency of eucalypt trees with chambers and micrometeorological techniques, *Journal of Hydrology*, 150, 649-664, 1993.
- Derwent, R. G.: The long-range transport of ozone within Europe and its control, *Environmental Pollution*, 63, 299-318, 1990.

- Derwent, R. G., Davies, T. J., Delaney, M., Dollard, G. J., Field, R. A., Dumitrean, P., Nason, P. D., Jones, B. M. R., and Pepler, S. A.: Analysis and interpretation of the continuous hourly monitoring data for 26 c²-c⁸ hydrocarbons at 12 United Kingdom sites during 1996, *Atmospheric Environment*, 34, 297-312, 2000.
- Derwent, R. G., Jenkin, M. E., Saunders, S. M., Pilling, M. J., Simmonds, P. G., Passant, N. R., Dollard, G. J., Dumitrean, P., and Kent, A.: Photochemical ozone formation in North West Europe and its control, *Atmospheric Environment*, 37, 1983-1991, 2003.
- Desjardins, R. L.: A study of carbon-dioxide and sensible heat fluxes using the eddy correlation technique. Cornell University. PhD, 1972.
- Dollard, G. J., Dumitrean, P., Telling, S., Dixon, J., and Derwent, R. G.: Observed trends in ambient concentrations of C²-C⁸ hydrocarbons in the United Kingdom over the period from 1993 to 2004, *Atmospheric Environment*, 41, 2559-2569, 2007.
- Dorsey, J. R., Nemitz, E., Gallagher, M. W., Fowler, D., Williams, P. I., Bower, K. N., and Beswick, K. M.: Direct measurements and parameterisation of aerosol flux, concentration and emission velocity above a city, *Atmospheric Environment*, 36, 791-800, 2002.
- Fairall, C. W.: Interpretation of eddy-correlation measurements of particulate deposition and aerosol flux, *Atmospheric Environment*, 18, 1329-1337, 1984.
- Falge, E., Baldocchi, D., Olson, R., Anthoni, P., Aubinet, M., Bernhofer, C., Burba, G., Ceulemans, G., Clement, R., Dolman, H., Granier, A., Gross, P., Grunwald, T., Hollinger, D., Jensen, N. O., Katul, G., Keronen, P., Kowalski, A., Lai, C. T., Law, B. E., Meyers, T., Moncrieff, J., Moors, E., Munger, J. W., Pilegaard, K., Rannik, U., Rebmann, C., Suyker, A., Tenhunen, J., Tu, K., Verma, S., Vesala, T., Wilson, K., and Wofsy, S.: Gap filling strategies for long term energy flux data sets, *Agricultural And Forest Meteorology*, 107, 71-77, 2001.
- Fall, R.: Abundant oxygenates in the atmosphere: A biochemical perspective, *Chemical Reviews*, 103, 4941-4951, 2003.
- Fall, R., and Benson, A. A.: Leaf methanol - the simplest natural product from plants, *Trends In Plant Science*, 1, 296-301, 1996.
- Fall, R., Karl, T., Hansel, A., Jordan, A., and Lindinger, W.: Volatile organic compounds emitted after leaf wounding: On-line analysis by proton-transfer-reaction mass spectrometry, *Journal of Geophysical Research-Atmospheres*, 104, 15963-15974, 1999.
- Filella, I., and Penuelas, J.: Daily, weekly, and seasonal time courses of VOC concentrations in a semi-urban area near Barcelona, *Atmospheric Environment*, 40, 7752-7769, 2006.

- Filella, I., Wilkinson, M. J., Llusia, J., Hewitt, C. N., and Penuelas, J.: Volatile organic compounds emissions in Norway spruce (*Picea abies*) in response to temperature changes, *Physiologia Plantarum*, 130, 58-66, 2007.
- Finnigan, J. J., Clement, R., Malhi, Y., Leuning, R., and Cleugh, H. A.: A re-evaluation of long-term flux measurement techniques - part i: Averaging and coordinate rotation, *Boundary-Layer Meteorology*, 107, 1-48, 2003.
- Foken, T., and Oncley, S.: Workshop on instrumental and methodical problems of land-surface flux measurements, *Bulletin of The American Meteorological Society*, 76, 1191-1193, 1995.
- Foken, T., and Wichura, B.: Tools for quality assessment of surface-based flux measurements, *Agricultural and Forest Meteorology*, 78, 83-105, 1996.
- Foken, T., Göckede, M., Mauder, M., Mahrt, L., Amiro, B., and Munger, W.: Post-field data quality control [IN] *Handbook of Micrometeorology: A guide for surface flux measurement and analysis*. W. M. X. Lee., B. Law. Dordrecht, Kluwer Academic Publishers. 29: 181-203, 2004.
- Fowler, D., Coyle, M., Flechard, C., Hargreaves, K., Nemitz, E., Storeton-West, R., Sutton, M., and Erisman, J. W.: Advances in micrometeorological methods for the measurement and interpretation of gas and particle nitrogen fluxes, *Plant And Soil*, 228, 117-129, 2001.
- Friedrich, R. and Obermeier, A.: *Anthropogenic Emissions of Volatile Organic Compounds. Reactive Hydrocarbons in the Atmosphere*. Hewitt, C. N. Academic Press, California pp 1-39, 1999.
- Fukui, Y., and Doskey, P. V.: Air-surface exchange of non-methane organic compounds at a grassland site: Seasonal variations and stressed emissions, *Journal of Geophysical Research-Atmospheres*, 103, 13153-13168, 1998.
- Gallagher, M. W., Clayborough, R., Beswick, K. M., Hewitt, C. N., Owen, S., Moncrieff, J., and Pilegaard, K.: Assessment of a relaxed eddy accumulation for measurements of fluxes of biogenic volatile organic compounds: Study over arable crops and a mature beech forest, *Atmospheric Environment*, 34, 2887-2899, 2000.
- Garratt, J. R.: *The atmospheric boundary layer*. Cambridge, Cambridge University Press, 1992.
- Geron, C. D., Guenther, A. B., and Pierce, T. E.: An improved model for estimating emissions of volatile organic-compounds from forests in the eastern united-states, *Journal of Geophysical Research-Atmospheres*, 99, 12773-12791, 1994.
- Grabmer, W., Graus, M., Lindinger, C., Wisthaler, A., Rappengluck, B., Steinbrecher, R., and Hansel, A.: Disjunct eddy covariance measurements of monoterpene fluxes from a Norway spruce forest using PTR-MS, *International Journal of Mass Spectrometry*, 239, 111-115, 2004.

- Grabmer, W., Kreuzwieser, J., Wisthaler, A., Cojocariu, C., Graus, M., Rennenberg, H., Steigner, D., Steinbrecher, R., and Hansel, A.: VOC emissions from Norway spruce (*picea abies* l. [karst]) twigs in the field - results of a dynamic enclosure study, *Atmospheric Environment*, 40, S128-S137, 2006.
- Greenberg, J. P., Guenther, A., Harley, P., Otter, L., Veenendaal, E. M., Hewitt, C. N., James, A. E., and Owen, S. M.: Eddy flux and leaf-level measurements of biogenic VOC emissions from Mopane woodland of Botswana, *Journal of Geophysical Research-Atmospheres*, 108, 2003.
- Grosjean, D., Grosjean, E., and Moreira, L. F. R.: Speciated ambient carbonyls in Rio de Janeiro, Brazil, *Environmental Science & Technology*, 36, 1389-1395, 2002.
- Grosjean, D.: Ambient pan and ppn in Southern California from 1960 to the scos97-narsto, *Atmospheric Environment*, 37, S221-S238, 2003.
- Grosjean, E., Grosjean, D., Fraser, M. P., and Cass, G. R.: Air quality model evaluation data for organics.2. C-¹-c-¹⁴ carbonyls in Los Angeles air, *Environmental Science & Technology*, 30, 2687-2703, 1996.
- Guenther, A., Hewitt, C. N., Erickson, D., Fall, R., Geron, C., Graedel, T., Harley, P., Klinger, L., Lerdau, M., McKay, W. A., Pierce, T., Scholes, B., Steinbrecher, R., Tallamraju, R., Taylor, J., and Zimmerman, P.: A global-model of natural volatile organic-compound emissions, *Journal of Geophysical Research-Atmospheres*, 100, 8873-8892, 1995.
- Guenther, A.: Trace gas emission measurements. *Environmental Monitoring Handbook*. F. R. Burden, McGraw Hill, 2002
- Guenther, A., Geron, C., Pierce, T., Lamb, B., Harley, P., and Fall, R.: Natural emissions of non-methane volatile organic compounds; carbon monoxide, and oxides of nitrogen from North America, *Atmospheric Environment*, 34, 2205-2230, 2000.
- Guenther, A.: The contribution of reactive carbon emissions from vegetation to the carbon balance of terrestrial ecosystems, *Chemosphere*, 49, 837-844, 2002.
- Guenther, A., Karl, T., Harley, P., Wiedinmyer, C., Palmer, P. I., and Geron, C.: Estimates of global terrestrial isoprene emissions using MEGAN (model of emissions of gases and aerosols from nature), *Atmospheric Chemistry And Physics*, 6, 3181-3210, 2006.
- Guenther, A. B., Zimmerman, P. R., Harley, P. C., Monson, R. K., and Fall, R.: Isoprene and monoterpene emission rate variability - model evaluations and sensitivity analyses, *Journal of Geophysical Research-Atmospheres*, 98, 12609-12617, 1993.
- Guenther, A. B., and Hills, A. J.: Eddy covariance measurement of isoprene fluxes, *Journal of Geophysical Research-Atmospheres*, 103, 13145-13152, 1998.

- Hansel, A., Jordan, A., Holzinger, R., Prazeller, P., Vogel, W., and Lindinger, W.: Proton-transfer reaction mass-spectrometry - online trace gas-analysis at the ppb level, *International Journal of Mass Spectrometry*, 150, 609-619, 1995.
- Haugen, D. A.: Effects of sampling rates and averaging periods on meteorological measurements in Proc., Fourth Symp. On Meteorological Observations and Instrumentation. Denver, CO, American Meteorological Society. 15-11, 1978.
- Hayward, S., Hewitt, C. N., Sartin, J. H., and Owen, S. M.: Performance characteristics and applications of a proton transfer reaction-mass spectrometer for measuring volatile organic compounds in ambient air, *Environmental Science & Technology*, 36, 1554-1560, 2002.
- Hayward, S., Tani, A., Owen, S. M., and Hewitt, C. N.: Online analysis of volatile organic compound emissions from Sitka spruce (*Picea Sitchensis*), *Tree Physiology*, 24, 721-728, 2004.
- Heath, J., Ayres, E., Possell, M., Bardgett, R. D., Black, H. I. J., Grant, H., Ineson, P., and Kerstiens, G.: Rising atmospheric CO₂ reduces sequestration of root-derived soil carbon, *Science*, 309, 1711-1713, 2005.
- Heeb, N. V., Forss, A. M., Bach, C., Reimann, S., Herzog, A., and Jackle, H. W.: A comparison of benzene, toluene and C²-benzenes mixing ratios in automotive exhaust and in the suburban atmosphere during the introduction of catalytic converter technology to the Swiss car fleet, *Atmospheric Environment*, 34, 3103-3116, 2000.
- Hewitt, C. N., Hayward, S., and Tani, A.: The application of proton transfer reaction-mass spectrometry (PTR-MS) to the monitoring and analysis of volatile organic compounds in the atmosphere, *Journal of Environmental Monitoring*, 5, 1-7, 2003.
- Hicks, B. B., and McMillen, R. T.: A simulation of the eddy accumulation method for measuring pollutant fluxes, *Journal of Climate And Applied Meteorology*, 23, 637-643, 1984.
- Hollinger, D. Y., and Richardson, A. D.: Uncertainty in eddy covariance measurements and its application to physiological models, *Tree Physiology*, 25, 873-885, 2005.
- Holzinger, R., Sandoval-Soto, L., Rottenberger, S., Crutzen, P. J., and Kesselmeier, J.: Emissions of volatile organic compounds from *Quercus ilex* l. Measured by proton transfer reaction mass spectrometry under different environmental conditions, *Journal of Geophysical Research-Atmospheres*, 105, 20573-20579, 2000.
- Holzinger, R., Jordan, A., Hansel, A., and Lindinger, W.: Methanol measurements in the lower troposphere near Innsbruck (047 degrees 16 ' n; 011 degrees 24 ' e), Austria, *Atmospheric Environment*, 35, 2525-2532, 2001.

- Horst, T. W., and Weil, J. C.: Footprint estimation for scalar flux measurements in the atmospheric surface-layer, *Boundary-Layer Meteorology*, 59, 279-296, 1992.
- Hurst, D. F., Griffith, D. W. T., and Cook, G. D.: Trace gas emissions from biomass burning in tropical Australian savannas, *Journal of Geophysical Research-Atmospheres*, 99, 16441-16456, 1994.
- Hwa, M. Y., Hsieh, C. C., Wu, T. C., and Chang, L. F. W.: Real-world vehicle emissions and VOCs profile in the Taipei tunnel located at Taiwan Taipei area, *Atmospheric Environment*, 36, 1993-2002, 2002.
- Jobson, B. T., Alexander, M. L., Maupin, G. D., and Muntean, G. G.: On-line analysis of organic compounds in diesel exhaust using a proton transfer reaction mass spectrometer (PTR-MS), *International Journal of Mass Spectrometry*, 245, 78-89, 2005.
- Johnson, E. S., Langard, S., and Lin, Y. S.: A critique of benzene exposure in the general population, *Science of the Total Environment*, 374, 183-198, 2007.
- Kanemasu, E. T., Wesely, M.L., Hicks, B.B., and Heilman, J.L.: Techniques for calculating energy and mass fluxes. Modification of the ariel environment of crops, *American Society of Agricultural Engineers - ASAE Monograph*:15 6-182, 1979.
- Karl, T., Guenther, A., Lindinger, C., Jordan, A., Fall, R., and Lindinger, W.: Eddy covariance measurements of oxygenated volatile organic compound fluxes from crop harvesting using a redesigned proton-transfer-reaction mass spectrometer, *Journal of Geophysical Research-Atmospheres*, 106, 24157-24167, 2001.
- Karl, T., Harley, P., Guenther, A., Rasmussen, R., Baker, B., Jardine, K., and Nemitz, E.: The bi-directional exchange of oxygenated VOCs between a Loblolly pine (*Pinus taeda*) plantation and the atmosphere, *Atmospheric Chemistry And Physics*, 5, 3015-3031, 2005.
- Karl, T. G., Spirig, C., Rinne, J., Stroud, C., Prevost, P., Greenberg, J., Fall, R., and Guenther, A.: Virtual disjunct eddy covariance measurements of organic compound fluxes from a subalpine forest using proton transfer reaction mass spectrometry, *Atmospheric Chemistry and Physics*, 2, 279-291, 2002.
- Kato, S., Miyakawa, Y., Kaneko, T., and Kajii, Y.: Urban air measurements using PTR-MS in Tokyo area and comparison with GC-FID measurements, *International Journal of Mass Spectrometry*, 235, 103-110, 2004.
- Kean, A. J., Grosjean, E., Grosjean, D., and Harley, R. A.: On-road measurement of carbonyls in California light-duty vehicle emissions, *Environmental Science & Technology*, 35, 4198-4204, 2001.
- Kesselmeier, J., Bode, K., Hofmann, U., Muller, H., Schafer, L., Wolf, A., Ciccioli, P., Brancaleoni, E., Cecinato, A., Frattoni, M., Foster, P., Ferrari, C., Jacob, V., Fugit, J. L., Dutaur, L., Simon, V., and Torres, L.: Emission of short

- chained organic acids, aldehydes and monoterpenes from *Quercus ilex* L. And *Pinus pinea* L. In relation to physiological activities, carbon budget and emission algorithms, *Atmospheric Environment*, 31, 119-133, 1997.
- Kesselmeier, J., and Staudt, M.: Biogenic volatile organic compounds (VOC): An overview on emission, physiology and ecology, *Journal of Atmospheric Chemistry*, 33, 23-88, 1999.
- King, K., Sturman, J., and Passant, P.: NAEI U.K Emission Mapping Methodology 2003.
- Kljun, N., Calanca, P., Rotachhi, M. W., and Schmid, H. P.: A simple parameterisation for flux footprint predictions, *Boundary-Layer Meteorology*, 112, 503-523, 2004.
- Kreuzwieser, J., Scheerer, U., and Rennenberg, H.: Metabolic origin of acetaldehyde emitted by poplar (*populus tremula* x *p-alba*) trees, *Journal of Experimental Botany*, 50, 757-765, 1999a.
- Kreuzwieser, J., Schnitzler, J. P., and Steinbrecher, R.: Biosynthesis of organic compounds emitted by plants, *Plant Biology*, 1, 149-159, 1999b.
- Kristensen, L., Mann, J., Oncley, S. P., and Wyngaard, J. C.: How close is close enough when measuring scalar fluxes with displaced sensors? *Journal of Atmospheric and Oceanic Technology*, 14, 814-821, 1997.
- Kulmala, M., Suni, T., Lehtinen, K. E. J., Dal Maso, M., Boy, M., Reissell, A., Rannik, U., Aalto, P., Keronen, P., Hakola, H., Back, J. B., Hoffmann, T., Vesala, T., and Hari, P.: A new feedback mechanism linking forests, aerosols, and climate, *Atmospheric Chemistry And Physics*, 4, 557-562, 2004.
- Langford, B., Davison, B., Nemitz, E., and Hewitt, C.N.: Mixing ratios and fluxes of volatile organic compounds from an urban canopy (Manchester U.K), *Atmospheric Chemistry and Physics Discussions*, 8, 245-284, 2008.
- Leclerc, M. Y., and Thurtell, G. W.: Footprint prediction of scalar fluxes using a markovian analysis, *Boundary-Layer Meteorology*, 52, 247-258, 1990.
- Lee, A., Schade, G. W., Holzinger, R., and Goldstein, A. H.: A comparison of new measurements of total monoterpene flux with improved measurements of speciated monoterpene flux, *Atmospheric Chemistry and Physics*, 5, 505-513, 2005.
- Lenschow, D. H., Mann, J., and Kristensen, L.: How long is long enough when measuring fluxes and other turbulence statistics, *Journal of Atmospheric And Oceanic Technology*, 11, 661-673, 1994.
- Lenschow, D. H.: Micrometeorological techniques for measuring biosphere-atmosphere trace gas exchange.[IN] *Biogenic Trace Gases: Measuring Emissions from Soil & Water*. P. A. Matson. London, Blackwell: 126-163, 1995.

- Lichtenthaler, H. K.: The 1-deoxy-d-xylulose-5-phosphate pathway of isoprenoid biosynthesis in plants, *Annual Review of Plant Physiology And Plant Molecular Biology*, 50, 47-65, 1999.
- Lindinger, W., Hansel, A., and Jordan, A.: Proton-transfer-reaction mass spectrometry (PTR-MS): On-line monitoring of volatile organic compounds at pptv levels, *Chemical Society Reviews*, 27, 347-354, 1998a.
- Lindinger, W., Hansel, A., and Jordan, A.: On-line monitoring of volatile organic compounds at pptv levels by means of proton-transfer-reaction mass spectrometry (PTR-MS) - medical applications, food control and environmental research, *International Journal of Mass Spectrometry*, 173, 191-241, 1998b.
- Lipari, F., Dasch, J. M., and Scruggs, W. F.: Aldehyde emissions from wood-burning fireplaces, *Environmental Science & Technology*, 18, 326-330, 1984.
- Loreto, F., and Sharkey, T. D.: A gas-exchange study of photosynthesis and isoprene emission in *quercus-rubra* l, *Planta*, 182, 523-531, 1990.
- Loreto, F., Fischbach, R. J., Schnitzler, J. P., Ciccioli, P., Brancaleoni, E., Calfapietra, C., and Seufert, G.: Monoterpene emission and monoterpene synthase activities in the Mediterranean evergreen oak *Quercus ilex* l. Grown at elevated CO₂ concentrations, *Global Change Biology*, 7, 709-717, 2001.
- Manes, F., Grignetti, A., Tinelli, A., Lenz, R., and Ciccioli, P.: General features of the Castelporziano test site, *Atmospheric Environment*, 31, 19-25, 1997.
- McMillen, R. T.: An eddy-correlation technique with extended applicability to non-simple terrain, *Boundary-Layer Meteorology*, 43, 231-245, 1988.
- Moncrieff J., Finnigan R. C., J., Meyers T.: Averaging, detrending, and filtering of eddy covariance time series. *Handbook of Micrometeorology: A guide for surface flux measurement and analysis*. W. M. X. Lee., B. Law. Dordrecht, Kluwer Academic Publishers. 29, 7-30, 2004.
- Moncrieff, J. B., Malhi, Y., and Leuning, R.: The propagation of errors in long-term measurements of land-atmosphere fluxes of carbon and water, *Global Change Biology*, 2, 231-240, 1996.
- Mudgett, M. B., and Clarke, S.: Characterization of plant l-isoaspartyl methyltransferases that may be involved in seed survival - purification, cloning, and sequence-analysis of the wheat-germ enzyme, *Biochemistry*, 32, 11100-11111, 1993.
- Nemitz, E., Gallagher, M. W., Duyzer, J. H., and Fowler, D.: Micrometeorological measurements of particle deposition velocities to moorland vegetation, *Quarterly Journal of the Royal Meteorological Society*, 128, 2281-2300, 2002a.

- Nemitz, E.: Surface-Atmosphere exchange of ammonia and chemically interacting species. Department of Physics. Manchester, University of Manchester Institute of Science and Technology. PhD, 1998.
- Nemitz, E., Hargreaves, K. J., McDonald, A. G., Dorsey, J. R., and Fowler, D.: Meteorological measurements of the urban heat budget and CO₂ emissions on a city scale, *Environmental Science & Technology*, 36, 3139-3146, 2002b.
- Nemitz, E., Jimenez, J.L., Huffman, J.A., Canagaratna, M.R., Worsnop, D.R., Guenther, A.B.: An eddy-covariance system for the measurement of surface / atmosphere exchange fluxes of submicron aerosol chemical species – first application above an urban area. *Aerosol Science Technology* [in press]
- Olofsson, M., Ek-Olausson, B., Ljungstrom, E., and Langer, S.: Flux of organic compounds from grass measured by relaxed eddy accumulation technique, *Journal of Environmental Monitoring*, 5, 963-970, 2003.
- Owen, S., Boissard, C., Street, R. A., Duckham, S. C., Csiky, O., and Hewitt, C. N.: Screening of 18 Mediterranean plant species for volatile organic compound emissions, *Atmospheric Environment*, 31, 101-117, 1997.
- Owen, S. M.: VOC emissions from vegetation in the Mediterranean region, PhD, Environmental Science Department, Lancaster University, Lancaster, 1998.
- Owen, S. M., Boissard, C., Hagenlocher, B., and Hewitt, C. N.: Field studies of isoprene emissions from vegetation in the northwest Mediterranean region, *Journal of Geophysical Research-Atmospheres*, 103, 25499-25511, 1998.
- Owen, S. M., Boissard, C., and Hewitt, C. N.: Volatile organic compounds (VOCs) emitted from 40 Mediterranean plant species: VOC speciation and extrapolation to habitat scale, *Atmospheric Environment*, 35, 5393-5409, 2001.
- Panofsky, H. A., Dutton, J. A.: *Atmospheric Turbulence – models and methods for engineering applications*, John Wiley and Sons, New York, 397pp, 1984.
- Pierce, T. E., and Waldruff, P. S.: Pc-beis - a personal-computer version of the biogenic emissions inventory system, *Journal of The Air & Waste Management Association*, 41, 937-941, 1991.
- Placet, M., Mann, C. O., Gilbert, R. O., and Niefer, M. J.: Emissions of ozone precursors from stationary sources: A critical review, *Atmospheric Environment*, 34, 2183-2204, 2000.
- Plantaz, M. A. H. G.: Surface/atmosphere exchange of ammonia over grazed pasture. PhD, 1998.
- Possanzini, M., Dipalo, V., Petricca, M., Fratarcangeli, R., and Brocco, D.: Measurements of lower carbonyls in rome ambient air, *Atmospheric Environment*, 30, 3757-3764, 1996.

- Raupach, M. R., Thom, A. S., and Edwards, I.: A wind-tunnel study of turbulent-flow close to regularly arrayed rough surfaces, *Boundary-Layer Meteorology*, 18, 373-397, 1980.
- Rinne, H. J. I., Delany, A. C., Greenberg, J. P., and Guenther, A. B.: A true eddy accumulation system for trace gas fluxes using disjunct eddy sampling method, *Journal of Geophysical Research-Atmospheres*, 105, 24791-24798, 2000.
- Rinne, H. J. I., Guenther, A. B., Warneke, C., de Gouw, J. A., and Luxembourg, S. L.: Disjunct eddy covariance technique for trace gas flux measurements, *Geophysical Research Letters*, 28, 3139-3142, 2001.
- Rinne, J., Taipale, R., Markkanen, T., Ruuskanen, T. M., Hellen, H., Kajos, M. K., Vesala, T., and Kulmala, M.: Hydrocarbon fluxes above a Scots Pine forest canopy: Measurements and modeling, *Atmospheric Chemistry And Physics*, 7, 3361-3372, 2007.
- Rinne, J.: Application and development of surface layer flux techniques for measurement of volatile organic compound emissions from vegetation. Academic dissertation, University of Helsinki, Department of Physical Sciences, 2001.
- Roth, M.: Review of atmospheric turbulence over cities, *Quarterly Journal of The Royal Meteorological Society*, 126, 941-990, 2000.
- Schade, G. W., and Goldstein, A. H.: Seasonal measurements of acetone and methanol: Abundances and implications for atmospheric budgets, *Global Biogeochemical Cycles*, 20, 2006.
- Schuepp, P. H., Macpherson, J. I., and Desjardins, R. L.: Adjustment of footprint correction for airborne flux mapping over the fife site, *Journal of Geophysical Research-Atmospheres*, 97, 18455-18466, 1992.
- Seufert, G., Bartzis, J., Bomboi, T., Ciccioli, P., Cieslik, S., Dlugi, R., Foster, P., Hewitt, C. N., Kesselmeier, J., Kotzias, D., Lenz, R., Manes, F., Pastor, R. P., Steinbrecher, R., Torres, L., Valentini, R., and Versino, B.: An overview of the Castelporziano experiments, *Atmospheric Environment*, 31, 5-17, 1997.
- Shao, M., Czapiewski, K. V., Heiden, A. C., Kobel, K., Komenda, M., Koppman, R., and Wildt, J.: Volatile organic compound emissions from Scots Pine: Mechanisms and description by algorithms, *Journal of Geophysical Research-Atmospheres*, 106, 20483-20491, 2001.
- Shao, M., and Wildt, J.: Quantification of acetone emission from pine plants, *Science In China Series B-Chemistry*, 45, 532-540, 2002.
- Sigsby, J. E., Tejada, S., Ray, W., Lang, J. M., and Duncan, J. W.: Volatile organic-compound emissions from 46 in-use passenger cars, *Environmental Science & Technology*, 21, 466-475, 1987.
- Sillman, S.: The relation between ozone, nox and hydrocarbons in urban and polluted rural environments, *Atmospheric Environment*, 33, 1821-1845, 1999.

- Singh, H. B., Ohara, D., Herlth, D., Sachse, W., Blake, D. R., Bradshaw, J. D., Kanakidou, M., and Crutzen, P. J.: Acetone in the atmosphere - distribution, sources, and sinks, *Journal of Geophysical Research-Atmospheres*, 99, 1805-1819, 1994.
- Singsaas, E. L., Laporte, M. M., Shi, J. Z., Monson, R. K., Bowling, D. R., Johnson, K., Lerdau, M., Jasentuliytana, A., and Sharkey, T. D.: Kinetics of leaf temperature fluctuation affect isoprene emission from Red Oak (*quercus rubra*) leaves, *Tree Physiology*, 19, 917-924, 1999.
- Spirig, C., Neftel, A., Ammann, C., Dommien, J., Grabmer, W., Thielmann, A., Schaub, A., Beauchamp, J., Wisthaler, A., and Hansel, A.: Eddy covariance flux measurements of biogenic VOCs during echo 2003 using proton transfer reaction mass spectrometry, *Atmospheric Chemistry and Physics*, 5, 465-481, 2005.
- Stauch, V. J., and Jarvis, A. J.: A semi-parametric gap-filling model for eddy covariance CO₂ flux time series data, *Global Change Biology*, 12, 1707-1716, 2006.
- Steiner, A., Luo, C., Huang, Y., and Chameides, W. L.: Past and present-day biogenic volatile organic compound emissions in East Asia, *Atmospheric Environment*, 36, 4895-4905, 2002.
- Stiener, A., and Goldstein, A.: Biogenic VOCs [IN] Koppmann, R.: Volatile organic compounds in the atmosphere. Blackwell publishing, Oxford, 2007.
- Stewart, H. E., Hewitt, C. N., Bunce, R. G. H., Steinbrecher, R., Smiatek, G., and Schoenemeyer, T.: A highly spatially and temporally resolved inventory for biogenic isoprene and monoterpene emissions: Model description and application to Great Britain, *Journal of Geophysical Research-Atmospheres*, 108, 2003.
- Stull, R., B.: An introduction to boundary layer meteorology. Kluwer academic publishers, London, 1988.
- Tani, A., Hayward, S., and Hewitt, C. N.: Measurement of monoterpenes and related compounds by proton transfer reaction-mass spectrometry (PTR-MS), *International Journal of Mass Spectrometry*, 223, 561-578, 2003.
- Tani, A., Hayward, S., Hansel, A., and Hewitt, C. N.: Effect of water vapour pressure on monoterpene measurements using proton transfer reaction-mass spectrometry (PTR-MS), *International Journal of Mass Spectrometry*, 239, 161-169, 2004.
- Taucher, J., Hansel, A., Jordan, A., and Lindinger, W.: Analysis of compounds in human breath after ingestion of garlic using proton-transfer-reaction mass spectrometry, *Journal of Agricultural And Food Chemistry*, 44, 3778-3782, 1996.
- Thomas, R.: Measurement of Speciated Aerosol Fluxes. Ph.D. Thesis, University of Manchester, 2007.

- UN ECE, 1991. Protocol to the 1979 Convention on Long-Range Transboundary Air Pollution Concerning the Control of Emissions of Volatile Organic Compounds on their Transboundary Fluxes. ECE/EB.AIR/30. United Nations Economic Commission for Europe, Geneva, Switzerland.
- UN ECE, 1999. Protocol to the 1979 Convention on Long-range Transboundary Air Pollution to Abate Acidification, Eutrophication and Ground-level Ozone. United Nations Economic Commission for Europe, Geneva, Switzerland.
- Velasco, E., Lamb, B., Pressley, S., Allwine, E., Westberg, H., Jobson, B. T., Alexander, M., Prazeller, P., Molina, L., and Molina, M.: Flux measurements of volatile organic compounds from an urban landscape, *Geophysical Research Letters*, 32, 2005.
- Warneke, C., Karl, T., Judmaier, H., Hansel, A., Jordan, A., Lindinger, W., and Crutzen, P. J.: Acetone, methanol, and other partially oxidized volatile organic emissions from dead plant matter by biological processes: Significance for atmospheric HO_x chemistry, *Global Biogeochemical Cycles*, 13, 9-17, 1999.
- Warneke, C., van der Veen, C., Luxembourg, S., de Gouw, J. A., and Kok, A.: Measurements of benzene and toluene in ambient air using proton-transfer-reaction mass spectrometry: Calibration, humidity dependence, and field intercomparison, *International Journal of Mass Spectrometry*, 207, 167-182, 2001.
- Warneke, C., Luxembourg, S. L., de Gouw, J. A., Rinne, H. J. I., Guenther, A. B., and Fall, R.: Disjunct eddy covariance measurements of oxygenated volatile organic compounds fluxes from an alfalfa field before and after cutting, *Journal of Geophysical Research-Atmospheres*, 107, 2002.
- Wesely, M. L. and Hart, R. L.: Variability of short term eddy-covariance estimates of mass exchange, in: *The forest atmosphere interactions*, (eds) Hutchison, B. and Hicks, B., D. Reidel publishing Company, Dordrecht, the Netherlands, 591-612, 1985
- Wilkinson, M. J., Owen, S. M., Possell, M., Hartwell, J., Gould, P., Hall, A., Vickers, C., and Hewitt, C. N.: Circadian control of isoprene emissions from Oil Palm (*elaeis guineensis*), *Plant Journal*, 47, 960-968, 2006.
- Wilkinson, M. J.: Circadian control of isoprene emissions from Oil Palm. Ph.D. Thesis, Lancaster University, 2006.
- Wilson, K. B., and Meyers, T. P.: The spatial variability of energy and carbon dioxide fluxes at the floor of a deciduous forest, *Boundary-Layer Meteorology*, 98, 443-473, 2001.
- Wyngaard, J. C.: The effects of probe-induced flow distortion on atmospheric-turbulence measurements, *Journal of Applied Meteorology*, 20, 784-794, 1981.

Zhang, Y., Huang, J. P., Henze, D. K., and Seinfeld, J. H.: Role of isoprene in secondary organic aerosol formation on a regional scale, *Journal of Geophysical Research-Atmospheres*, 112, 2007.

Zhao, J., and Zhang, R. Y.: Proton transfer reaction rate constants between hydronium ion (H_3O^+) and volatile organic compounds, *Atmospheric Environment*, 38, 2177-2185, 2004.

List of URLs:

http://www.naei.org.uk/datachunk.php?t_datachunk_id=174

<http://www.airquality.co.uk>

<http://www.arl.noaa.gov/ready/hysplit4.html>

Appendix I

The sequence file used to perform SEM voltage checks is shown below. This sequence was written for the testing of Pfeiffer SEMs, hence the higher voltage range (2000 – 3500 v), when using a Mascom SEM, this range is lowered to 1400-2500 V.

```
// SEM Check

// Start Voltage = 2000 [V]
// End Voltage = 3500 [V]

// Entering the start voltage
SetVar( i[0]=2000 )
SetAO( 8=10000 )

// This loop increases the SEM voltage by 50 volts every time it
iterates. The 1500, is the total number of volts to be added to the
2000 starting volts
Loop( i[1]=0;1500;50 )
Begin

    // adds initial SEM voltage to the incremented loop voltages
    Calculate( i[2] = i[0]+i[1] )
    // sets SEM to new voltage, and turns it on
    SetQMS( CommSEM=i[2], SEM=on )
    // This pauses the check for 5 s to allow everything to settle
after the change of voltage
    Delay( Time=5, Disp=off )
    // The second loop controls the number of cycles per voltage -
default is 10 cycles
    Loop( i[3]=0;9 )
    Begin
        DDEInit( Service="QUADSTAR" )
        Message( Text="SEM check now in progress.....please
wait.....SEM voltage is currently ";i[2] )
        MID(
Par="c:\progra~1\qs422\workpl~1\sequence\ec\sem.mip", SaveGfa=0,
SaveCyc=gs[0] )
        DDEPoke( Service="labview", Topic="PTR-MS", Item="mass0",
Data=gfa[0][0] )
        DDEPoke( Service="labview", Topic="PTR-MS", Item="mass1",
Data=gfa[0][1] )
        DDEPoke( Service="labview", Topic="PTR-MS", Item="mass2",
Data=gfa[0][2] )
        DDEPoke( Service="labview", Topic="PTR-MS", Item="mass3",
Data=gfa[0][3] )
        DDEPoke( Service="labview", Topic="PTR-MS", Item="mass4",
Data=gfa[0][4] )
        DDEPoke( Service="labview", Topic="PTR-MS", Item="mass5",
Data=gfa[0][5] )
        DDEPoke( Service="labview", Topic="PTR-MS", Item="mass6",
Data=gfa[0][6] )
    End
End
```

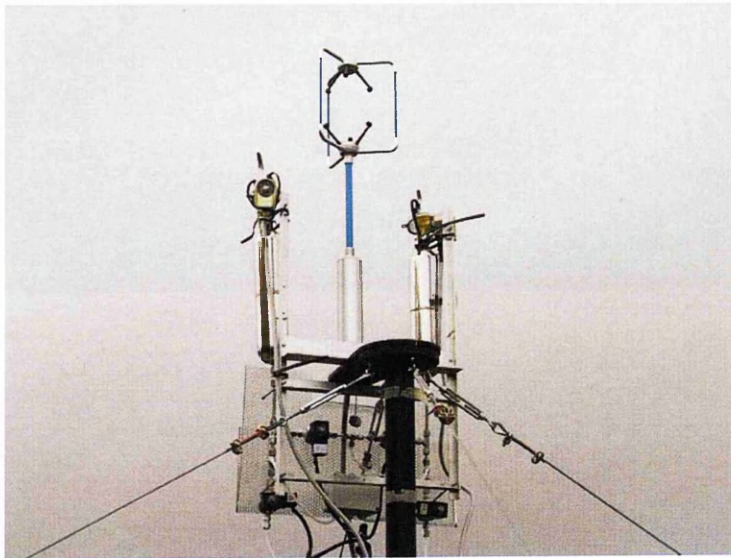
```
        DDEPoke( Service="labview", Topic="PTR-MS", Item="mass7",
Data=gfa[0][7] )
        DDEPoke( Service="labview", Topic="PTR-MS", Item="mass8",
Data=gfa[0][8] )
        DDEPoke( Service="labview", Topic="PTR-MS", Item="mass9",
Data=gfa[0][9] )
        SetVar( gi[1]=1 )
        DDEPoke( Service="labview", Topic="PTR-MS",
Item="newdata", Data=gi[1] )

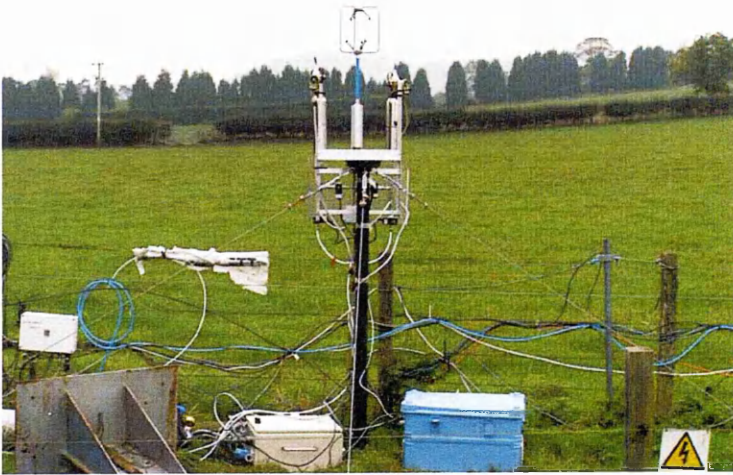
    End
End
SetQMS( CommSEM=0, SEM=off )

SetAO( 8=0 )
```

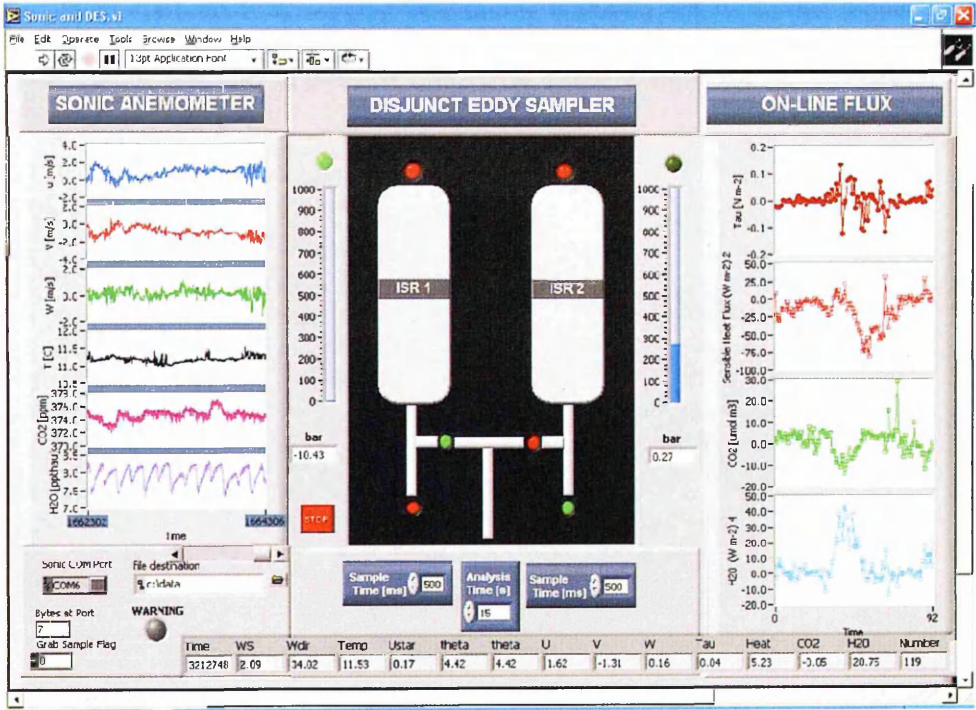
* * *

Below are photos of the disjunct flux sampler during the validation study where CO₂ and H₂O flux measurements were compared with those measured by the standard eddy covariance technique.





Screen shot of the DFS logging software, showing the operation of sample valves, ISR pressures, sonic anemometer and IRGA data and preliminary online flux calculations.



Appendix II

The sequence file used to control the DDE protocol and transfer data from the PTR-MS to the LabVIEW logging programme is shown below. In this sequence the PTR-MS mode was altered from DEC to vDEC every 30 minutes.

```
// i[0]      main loop counter
// i[1] year
// i[2] month
// i[3] day
// i[4] hours of current time
// i[5] minutes of current time
// gi[0] global mode flag (0=Scan; 1=MID)
// gi[1] global data flag (1=new available)
// gfa[0]...gfa[9] data

SetPar( BarWidth=15, ColorMode=single, Cycles=50, DispOpt=last,
LineType=solid, Marker=on, YRaster=on )
DDEInit( Service="QUADSTAR" )
Loop( i[0]=0;200000000 )
Begin
    GetDate( Day=i[3], Month=i[2], Year=i[1] )
    GetTime( Hour=i[4], Min=i[5] )
    SetString( gs[0] = "####" )
    SetString( gs[0] = gs[0];i[1] )
    SetString( gs[0] = gs[0];i[2] )
    SetString( gs[0] = gs[0];i[3] )
    SetString( gs[0] = gs[0];i[4] )
    //Repeat MID measurement for at least 25 minutes

    IfVar( i[5] < 4 )
    Begin
        SetVar( gi[0]=0 )
        DDEPoke( Service="labview", Topic="PTR-MS",
Item="ptrmsmode", Data=gi[0] )
        ScanBar(
Par="c:\progra~1\qs422\workpl~1\sequence\ec\portland.sbp",
Disp=on, SaveCyc=gs[0] )

    End
    Else
        IfVar( i[5] < 30 )
        Begin
            SetVar( gi[0]=1 )
            DDEPoke( Service="labview", Topic="PTR-MS",
Item="ptrmsmode", Data=gi[0] )
            MID(
Par="c:\progra~1\qs422\workpl~1\sequence\ec\ec.mip", SaveGfa=0,
SaveCyc=gs[0] )
        End
    End
End
```

```

        DDEPoke( Service="labview", Topic="PTR-MS",
Item="mass0", Data=gfa[0][0] )
        DDEPoke( Service="labview", Topic="PTR-MS",
Item="mass1", Data=gfa[0][1] )
        DDEPoke( Service="labview", Topic="PTR-MS",
Item="mass2", Data=gfa[0][2] )
        DDEPoke( Service="labview", Topic="PTR-MS",
Item="mass3", Data=gfa[0][3] )
        DDEPoke( Service="labview", Topic="PTR-MS",
Item="mass4", Data=gfa[0][4] )
        DDEPoke( Service="labview", Topic="PTR-MS",
Item="mass5", Data=gfa[0][5] )
        DDEPoke( Service="labview", Topic="PTR-MS",
Item="mass6", Data=gfa[0][6] )
        DDEPoke( Service="labview", Topic="PTR-MS",
Item="mass7", Data=gfa[0][7] )
        DDEPoke( Service="labview", Topic="PTR-MS",
Item="mass8", Data=gfa[0][8] )
        DDEPoke( Service="labview", Topic="PTR-MS",
Item="mass9", Data=gfa[0][9] )
        DDEPoke( Service="labview", Topic="PTR-MS",
Item="mass10", Data=gfa[0][10] )
        DDEPoke( Service="labview", Topic="PTR-MS",
Item="mass11", Data=gfa[0][11] )
        SetVar( gi[1]=1 )
        DDEPoke( Service="labview", Topic="PTR-MS",
Item="newdata", Data=gi[1] )
    End
    Else
        IfVar( i[5] < 34 )
        Begin
            SetVar( gi[0]=0 )
            DDEPoke( Service="labview", Topic="PTR-MS",
Item="ptrmsmode", Data=gi[0] )
            ScanBar(
Par="c:\progra-1\qs422\workpl-1\sequenze\ec\portland.sbp",
Disp=on, SaveCyc=gs[0] )

            End
            Else
            Begin
                SetVar( gi[0]=1 )
                DDEPoke( Service="labview", Topic="PTR-MS",
Item="ptrmsmode", Data=gi[0] )

                MID(
Par="c:\progra-1\qs422\workpl-1\sequenze\ec\disjunct.mip",
SaveGfa=0, SaveCyc=gs[0] )
                DDEPoke( Service="labview", Topic="PTR-MS",
Item="mass0", Data=gfa[0][0] )
                DDEPoke( Service="labview", Topic="PTR-MS",
Item="mass1", Data=gfa[0][1] )
                DDEPoke( Service="labview", Topic="PTR-MS",
Item="mass2", Data=gfa[0][2] )
                DDEPoke( Service="labview", Topic="PTR-MS",
Item="mass3", Data=gfa[0][3] )
                DDEPoke( Service="labview", Topic="PTR-MS",
Item="mass4", Data=gfa[0][4] )

```

```

DDEPoke( Service="labview", Topic="PTR-MS",
Item="mass5", Data=gfa[0][5] )
DDEPoke( Service="labview", Topic="PTR-MS",
Item="mass6", Data=gfa[0][6] )
DDEPoke( Service="labview", Topic="PTR-MS",
Item="mass7", Data=gfa[0][7] )
DDEPoke( Service="labview", Topic="PTR-MS",
Item="mass8", Data=gfa[0][8] )
DDEPoke( Service="labview", Topic="PTR-MS",
Item="mass9", Data=gfa[0][9] )
DDEPoke( Service="labview", Topic="PTR-MS",
Item="mass10", Data=gfa[0][10] )
DDEPoke( Service="labview", Topic="PTR-MS",
Item="mass11", Data=gfa[0][11] )

SetVar( gi[1]=1 )
DDEPoke( Service="labview", Topic="PTR-MS",
Item="newdata", Data=gi[1] )

End
DDEClose( )
End.

```

Photos of taken during the City Flux campaign in Manchester. Picture A shows a view of Portland tower taken from the east at street level.



Photo by Claire Martin

Picture B shows the instrument mast which extended 15 m above the roof surface.

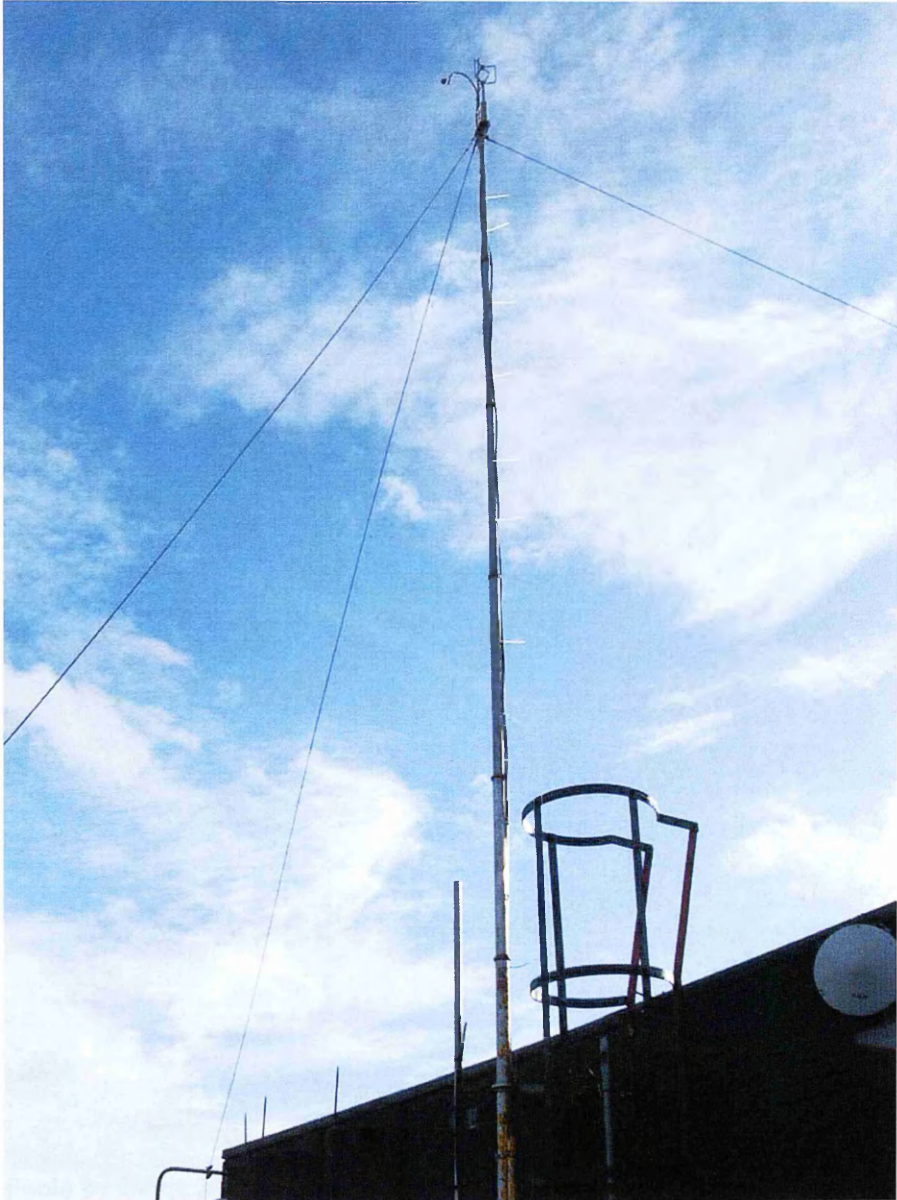


Photo by Claire Martin

Picture C gives a view from the roof of Portland Tower looking North. In this wind vector both the City Tower and Arndale centre can be clearly seen.



Photo by Claire Martin

Graph illustrating intermittent spikes in the VOC concentrations. This was caused by the thermal trip of the sample pump. Averaging periods affected were filtered and removed and were not included in the final data analysis.

Appendix III

Laboratory testing of disjunct flux sampler

The DFS was setup under “normal” operating conditions; intake valve switching set for 0.5 s opening (the minimum time required for an evacuated ISR to be pressurised to ambient level), and sample analysis time (disjunct interval) set to 12-15 s. A Tedlar® bag filled with breath isoprene was attached to the intake valve of one channel, the other left open to ambient air. A short length of ¼” PTFE tubing connected the bag to a manually operated 2-way solenoid valve (Swagelok, Manchester Fluid Systems), with a further inlet line connected directly to the DFS and the other line to the PTR-MS instrument. Such a setup allowed the PTR-MS to switch freely between analysing the air within the Tedlar® bag and the air from the DFS (Fig. 1).

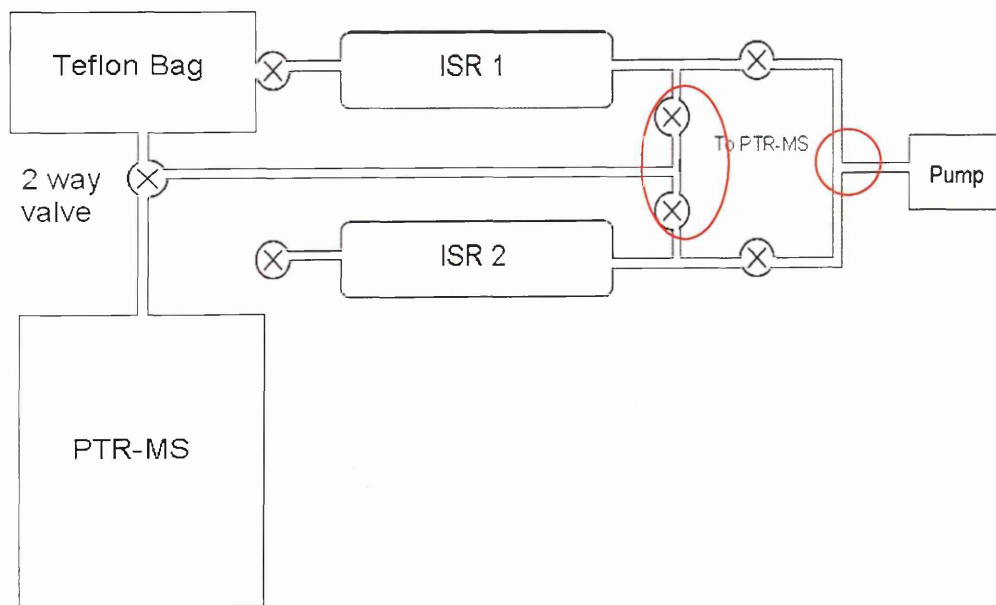


Figure 1. Schematic of the disjunct eddy sampler and experimental setup. Crossed circles represent computer automated switching valves and red circles areas of the system where the two independent channels converge.

Assuming the system is airtight and there is no dilution occurring from inter-channel mixing, concentrations recorded in the bag should be the same as those sampled by the DFS. Any discrepancies between the two monitored sources would indicate system leakages. The experiment was then repeated with the bag placed upon the second inlet valve with the previous valve now open to ambient air.

Results

Channel 1 testing:

The results from Channel 1 testing initially indicated a serious discrepancy between the measured concentrations from the channel and the bag. The concentration of isoprene within the bag was measured at a stable 70 ppb, such stability indicating a

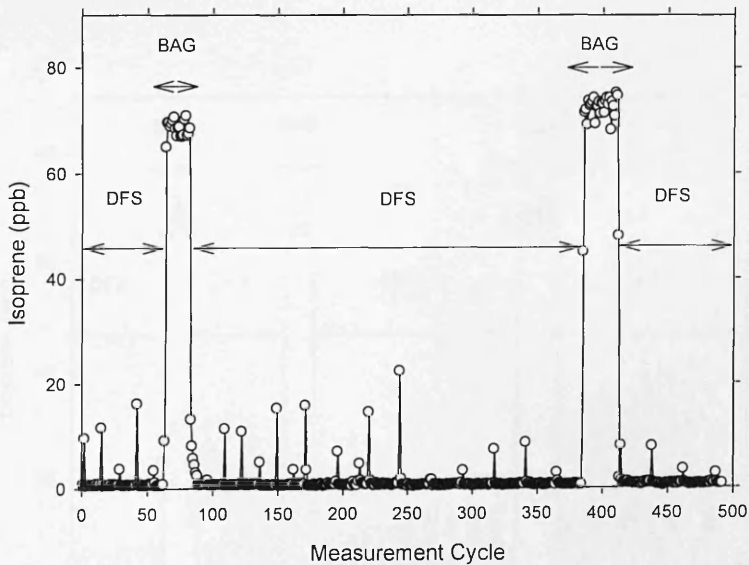


Figure 2. Graph showing the results for Channel 1. The plot indicates isoprene concentrations to differ between the bag (large peaks), Channel 1 (intermediate peaks) and Channel 2 (baseline) which was left open to ambient air. Irregular isoprene concentrations observed within channel 1 indicate multiple leakages within the system.

good seal around the intake valve and outlet tubing. The isoprene concentration from channel 1 was markedly lower, at an average of 10 ppb, 14 % of that of the bag (Fig. 2). Channel 1 concentrations showed no evidence of stability, ranging from as low as 1 ppb to 23 ppb. Such irregularities within the recorded concentrations indicate more than one source of leakage within that channel.

Channel 2 testing:

Further discrepancies between the bag isoprene and DFS channel isoprene concentrations were observed when Channel 2 was investigated. Again concentrations were in the region of 14% of the measured bag concentration of 70 ppb. This figure rose to approximately 21% when the PTR-MS intake flow rate was increased from 250 ml min^{-1} to $> 350 \text{ ml min}^{-1}$. Unlike channel 1, stability was observed in channel 2 concentrations, possibly indicating just one leak within this region of the DFS system (Fig. 3).

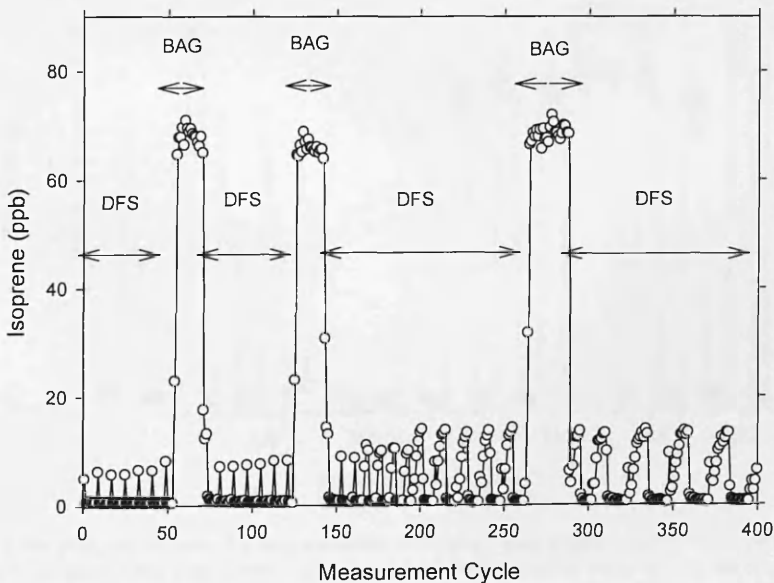


Figure 3. Graph showing the results of Channel 2 testing. The graph indicates how isoprene concentrations differed between the bag (large peaks), Channel 2 (intermediate peaks) and Channel 1 (baseline) which was left open to ambient air. Channel 2 concentrations show

regularity when compared to channel 1 (Fig. 2). PTR-MS intake flow rate was increased to $>350 \text{ ml min}^{-1}$ at 200 cycles, which saw an increase of $\sim 5 \text{ ppb}$ in concentration.

When the deficit between the two channels and bag concentrations are considered it is noticeable that both channels are underestimating by $\sim 86\%$. Such agreement between the two independent channels indicates the primary source of leakage to occur at such a point where the two channels converge (Fig. 1).

Leak testing of DFS

In order to locate the source of dilution occurring within the DFS the two channels were separated, ensuring total independence. Repeating the experiment outlined above on each channel saw excellent agreement with concentrations directly measured from the bag. The connection between the two channels along the

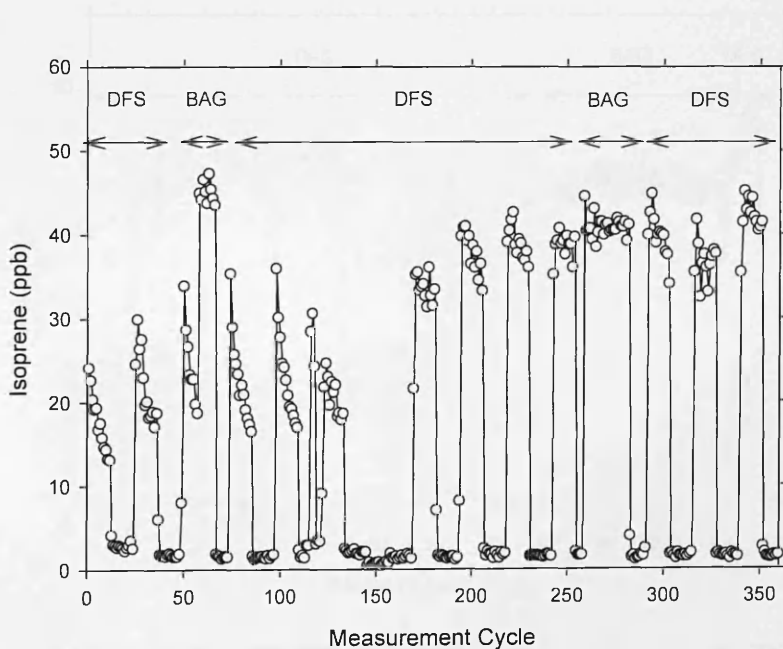


Figure 4 the plot shows how the reorientation of valves 3 and 6 saw isoprene concentrations rise from 14% of that in the bag to 60%. The decline in concentration observed in the first few peaks is indicative of leakages. Tightening of piping joints took place at around 200 cycles which had an immediate impact.

evacuation pump tubing (Fig 1) was first eliminated by reassembling the DFS and installing separate pumps for each channel. This saw concentrations in both channels drop to the levels seen in Figs. 2 and 3, thus indicating valves 3 and 6 on the DFS to be at fault.

Testing of valves 3 and 6 revealed them to maintain a pressure better in one direction compared with the other. Thus in their present orientation, when each canister was undergoing evacuation, air was drawn from the opposite canister, disrupting the measured concentration. A simple reorientation of both valves 3 and 6 saw immediate success as concentrations rose to that of the bag (Fig. 4 and 5). In the case of Channel 1, which had previously been suspected of having more than one leak due to the irregularity

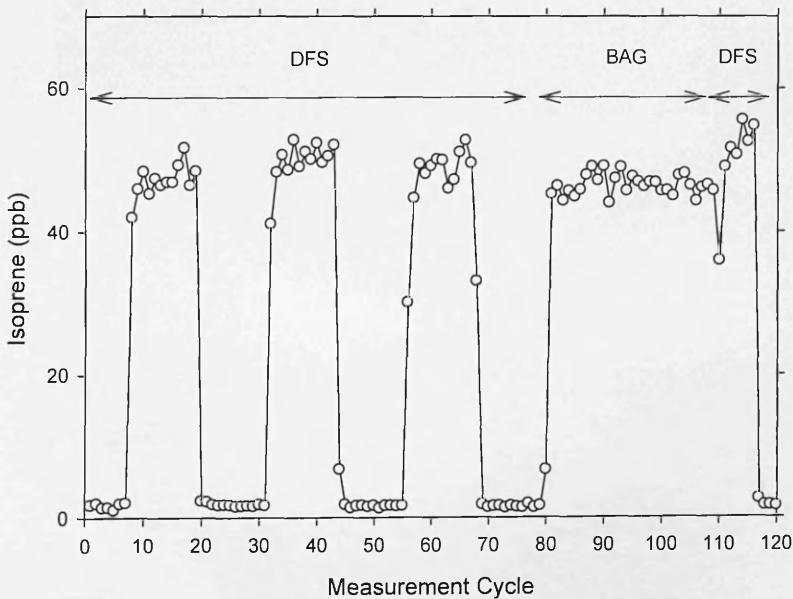


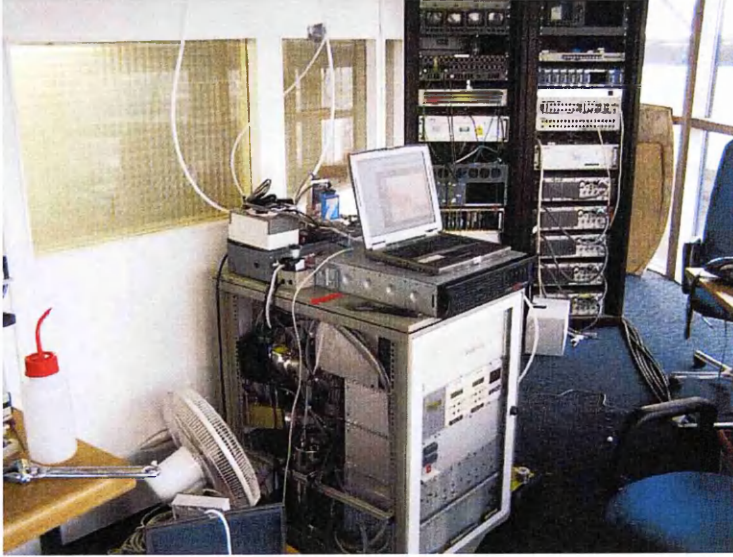
Figure 5. Plot showing the results from the leak testing of Channel 2 after the reorientation of valves 3 and 6. Concentrations now being representative of that of the bag indicate an air tight system.

of measured concentrations, isoprene levels were still approximately 40% below that in the bag. When the data from Channel 1 was analysed it was clear to see a decline in

concentration with each 3 second PTR-MS cycle, such a drop off is indicative of a leak within the system. All jointing within Channel 1 was tightened, which resulted in the immediate rise of concentrations equivalent to those seen in the bag.

Appendix IV

Photos of the vDEC setup during the REPARTEE campaign, the Telecom Tower and views of the surrounding areas.





Appendix V

The sequence file used during the Castelporziano field campaign is shown below. The sequence has been modified to allow the automated switching of valves, which enables the PTR-MS to switch freely between the sample line and the zero air source.

```
// i[0]    main loop counter
// i[1] year
// i[2] month
// i[3] day
// i[4] hours of current time
// i[5] minutes of current time
// gi[0] global mode flag (0=Scan; 1=MID)
// gi[1] global data flag (1=new available)
// gfa[0]...gfa[9] data

SetPar( BarWidth=15, ColorMode=single, Cycles=50, DispOpt=last,
LineType=solid, Marker=on, YRaster=on )
DDEInit( Service="QUADSTAR" )
Loop( i[0]=0;200000000 )
Begin

    GetDate( Day=i[3], Month=i[2], Year=i[1] )
    GetTime( Hour=i[4], Min=i[5] )
    SetString( gs[0] = "@@@@" )
    SetString( gs[0] = gs[0];i[1] )
    SetString( gs[0] = gs[0];i[2] )
    SetString( gs[0] = gs[0];i[3] )
    SetString( gs[0] = gs[0];i[4] )
    //Repeat MID measurement for at least 25 minutes

    IfVar( i[5] < 5 )

        Begin
            SetAO( 9=10000 )
            SetVar( gi[0]=1 )
            DDEPoke( Service="labview", Topic="PTR-MS",
Item="ptrmsmode", Data=gi[0] )
            MID( Par="c:\qs422\workpl~1\sequenze\ec\ec_italy.mip",
SaveGfa=0, SaveCyc=gs[0] )
            DDEPoke( Service="labview",Topic="PTR-MS",
Item="mass0",Data=gfa[0][0])
            DDEPoke( Service="labview", Topic="PTR-MS",
Item="mass1", Data=gfa[0][1] )
            DDEPoke( Service="labview", Topic="PTR-MS",
Item="mass2", Data=gfa[0][2] )
```

```

DDEPoke( Service="labview", Topic="PTR-MS",
Item="mass3", Data=gfa[0][3] )
DDEPoke( Service="labview", Topic="PTR-MS",
Item="mass4", Data=gfa[0][4] )
DDEPoke( Service="labview", Topic="PTR-MS",
Item="mass5", Data=gfa[0][5] )
DDEPoke( Service="labview", Topic="PTR-MS",
Item="mass6", Data=gfa[0][6] )
DDEPoke( Service="labview", Topic="PTR-MS",
Item="mass7", Data=gfa[0][7] )
DDEPoke( Service="labview", Topic="PTR-MS",
Item="mass8", Data=gfa[0][8] )
DDEPoke( Service="labview", Topic="PTR-MS",
Item="mass9", Data=gfa[0][9] )
DDEPoke( Service="labview", Topic="PTR-MS",
Item="mass10", Data=gfa[0][10] )
DDEPoke( Service="labview", Topic="PTR-MS",
Item="mass11", Data=gfa[0][11] )
SetVar( gi[1]=1 )
DDEPoke( Service="labview", Topic="PTR-MS",
Item="newdata", Data=gi[1] )
End
Else
IfVar( i[5] < 30 )
Begin
SetAO( 9=0 )
SetVar( gi[0]=1 )
DDEPoke( Service="labview", Topic="PTR-MS",
Item="ptrmsmode", Data=gi[0] )
MID(
Par="c:\qs422\workpl-1\sequence\ec\ec_italy.mip", SaveGfa=0,
SaveCyc=gs[0] )
DDEPoke( Service="labview", Topic="PTR-MS",
Item="mass0", Data=gfa[0][0] )
DDEPoke( Service="labview", Topic="PTR-MS",
Item="mass1", Data=gfa[0][1] )
DDEPoke( Service="labview", Topic="PTR-MS",
Item="mass2", Data=gfa[0][2] )
DDEPoke( Service="labview", Topic="PTR-MS",
Item="mass3", Data=gfa[0][3] )
DDEPoke( Service="labview", Topic="PTR-MS",
Item="mass4", Data=gfa[0][4] )
DDEPoke( Service="labview", Topic="PTR-MS",
Item="mass5", Data=gfa[0][5] )
DDEPoke( Service="labview", Topic="PTR-MS",
Item="mass6", Data=gfa[0][6] )
DDEPoke( Service="labview", Topic="PTR-MS",
Item="mass7", Data=gfa[0][7] )
DDEPoke( Service="labview", Topic="PTR-MS",
Item="mass8", Data=gfa[0][8] )
DDEPoke( Service="labview", Topic="PTR-MS",
Item="mass9", Data=gfa[0][9] )
DDEPoke( Service="labview", Topic="PTR-MS",
Item="mass10", Data=gfa[0][10] )
DDEPoke( Service="labview", Topic="PTR-MS",
Item="mass11", Data=gfa[0][11] )
SetVar( gi[1]=1 )

```

```

DDEPoke( Service="labview", Topic="PTR-MS",
Item="newdata", Data=gi[1] )
End
Else
  IfVar( i[5] < 35 )
  Begin
    SetVar( gi[0]=1 )
    DDEPoke( Service="labview", Topic="PTR-MS",
Item="ptrmsmode", Data=gi[0] )
    MID(
Par="c:\qs422\workpl~1\sequence\ec\masscan.mip", SaveGfa=0,
SaveCyc=gs[0] )
    DDEPoke( Service="labview", Topic="PTR-MS",
Item="mass0", Data=gfa[0][0] )
    DDEPoke( Service="labview", Topic="PTR-MS",
Item="mass1", Data=gfa[0][1] )
    DDEPoke( Service="labview", Topic="PTR-MS",
Item="mass2", Data=gfa[0][2] )
    DDEPoke( Service="labview", Topic="PTR-MS",
Item="mass3", Data=gfa[0][3] )
    DDEPoke( Service="labview", Topic="PTR-MS",
Item="mass4", Data=gfa[0][4] )
    DDEPoke( Service="labview", Topic="PTR-MS",
Item="mass5", Data=gfa[0][5] )
    DDEPoke( Service="labview", Topic="PTR-MS",
Item="mass6", Data=gfa[0][6] )
    DDEPoke( Service="labview", Topic="PTR-MS",
Item="mass7", Data=gfa[0][7] )
    DDEPoke( Service="labview", Topic="PTR-MS",
Item="mass8", Data=gfa[0][8] )
    DDEPoke( Service="labview", Topic="PTR-MS",
Item="mass9", Data=gfa[0][9] )
    DDEPoke( Service="labview", Topic="PTR-MS",
Item="mass10", Data=gfa[0][10] )
    DDEPoke( Service="labview", Topic="PTR-MS",
Item="mass11", Data=gfa[0][11] )
    SetVar( gi[1]=1 )
    DDEPoke(
Service="labview", Topic="PTR-MS",
Item="newdata", Data=gi[1] )
  End
Else

  Begin
    SetVar( gi[0]=1 )
    DDEPoke( Service="labview", Topic="PTR-MS",
Item="ptrmsmode", Data=gi[0] )
    MID(
Par="c:\qs422\workpl~1\sequence\ec\ec_italy.mip", SaveGfa=0,
SaveCyc=gs[0] )
    DDEPoke( Service="labview", Topic="PTR-MS",
Item="mass0", Data=gfa[0][0] )
    DDEPoke( Service="labview", Topic="PTR-MS",
Item="mass1", Data=gfa[0][1] )
    DDEPoke( Service="labview", Topic="PTR-MS",
Item="mass2", Data=gfa[0][2] )

```

```

DDEPoke( Service="labview", Topic="PTR-MS",
Item="mass3", Data=gfa[0][3] )
DDEPoke( Service="labview", Topic="PTR-MS",
Item="mass4", Data=gfa[0][4] )
DDEPoke( Service="labview", Topic="PTR-MS",
Item="mass5", Data=gfa[0][5] )
DDEPoke( Service="labview", Topic="PTR-MS",
Item="mass6", Data=gfa[0][6] )
DDEPoke( Service="labview", Topic="PTR-MS",
Item="mass7", Data=gfa[0][7] )
DDEPoke( Service="labview", Topic="PTR-MS",
Item="mass8", Data=gfa[0][8] )
DDEPoke( Service="labview", Topic="PTR-MS",
Item="mass9", Data=gfa[0][9] )
DDEPoke( Service="labview", Topic="PTR-MS",
Item="mass10", Data=gfa[0][10] )
DDEPoke( Service="labview", Topic="PTR-MS",
Item="mass11", Data=gfa[0][11] )

SetVar( gi[1]=1 )
DDEPoke( Service="labview", Topic="PTR-MS",
Item="newdata", Data=gi[1] )

End
DDEClose( )
End

```

Calibration graphs for methanol, acetaldehyde and acetone. The slope of the fit gives the instrument sensitivity which is used for the calculation of mixing ratios.

